

For Reference

NOT TO BE TAKEN FROM THIS ROOM

Ex libris
UNIVERSITATIS
ALBERTAENSIS





Digitized by the Internet Archive
in 2019 with funding from
University of Alberta Libraries

<https://archive.org/details/El-Nahhas1980>

THE UNIVERSITY OF ALBERTA

RELEASE FORM

NAME OF AUTHOR: FATHALLA EL-NAHHAS
TITLE OF THESIS: THE BEHAVIOUR OF TUNNELS IN STIFF SOILS
DEGREE FOR WHICH THESIS WAS PRESENTED: DOCTOR OF PHILOSOPHY
YEAR THIS DEGREE GRANTED: SPRING, 1981

Permission is hereby granted to THE UNIVERSITY OF ALBERTA LIBRARY to reproduce single copies of this thesis and to lend or sell such copies for private, scholarly or scientific research purposes only.

The author reserves other publication rights, and neither the thesis nor extensive extracts from it may be printed or otherwise reproduced without the author's written permission.

THE UNIVERSITY OF ALBERTA

THE BEHAVIOUR OF TUNNELS IN STIFF SOILS

by



FATHALLA EL-NAHHAS

A THESIS

SUBMITTED TO THE FACULTY OF GRADUATE STUDIES AND RESEARCH
IN PARTIAL FULFILMENT OF THE REQUIREMENTS FOR THE DEGREE
OF DOCTOR OF PHILOSOPHY

IN

GEOTECHNICAL ENGINEERING

DEPARTMENT OF CIVIL ENGINEERING

EDMONTON, ALBERTA

DECEMBER, 1980

THE UNIVERSITY OF ALBERTA
FACULTY OF GRADUATE STUDIES AND RESEARCH

The undersigned certify that they have read, and recommend to the Faculty of Graduate Studies and Research, for acceptance, a thesis entitled THE BEHAVIOUR OF TUNNELS IN STIFF SOILS submitted by FATHALLA EL-NAHHAS in partial fulfilment of the requirements for the degree of DOCTOR OF PHILOSOPHY in GEOTECHNICAL ENGINEERING.

TO NANY AND HESHAM

ABSTRACT

Utilizing the measurements drawn from an extensive field monitoring program, the characteristic elements of the behaviour of tunnels in stiff soils are identified, described and discussed. The three dimensional displacement field around a tunnel is used to identify the main sources of ground loss which are found to occur around the drilling machine and up to 2.5 to 3 diameters behind the face. It is apparent that the soil displacement can be minimized by reducing the size of the drilling machine's overcut and expanding the lining into contact with the soil directly behind the tail of the mole as soon as possible.

The in-situ behaviour of two lining systems, precast concrete segments and rib-lagging were studied. In the case of the rib and lagging system, the ultimate radial component of the soil pressure was found to be uniform and equal to 12% of the overburden stress. For the relatively stiffer segmented concrete lining, the distribution of radial soil pressure was elliptical. At the crown the magnitude of soil pressure varied between 45 and 59% of the overburden stress while the springline values ranged between 27 and 36%.

The measured soil displacements were used to drive the strain field within the soil mass. The mode of shear strength mobilization was studied and the failure zones around the tunnel were defined. These zones do not form the uniform circular ring, commonly predicted by two dimensional

closed form analyses. However, there are some similarities to such zones observed in model tests and obtained from elasto-plastic finite element analyses.

The development of failure zones and the mobilization of shear strength, as described in this thesis, agrees with the mode of failure of a tunnel roof observed ten years ago in an unsupported portion of a tunnel in the same soil. The mobilization process has also confirmed the occurrence of the arching of soil stresses around the tunnel which consequently results in the relatively low pressures transmitted to the linings.

ACKNOWLEDGEMENT

This research project was funded jointly by the National Research Council of Canada and by the City of Edmonton. This support is gratefully acknowledged.

This thesis was conducted under the direct supervision of Professor Z. Eisenstein. In addition to his vigorous efforts to arrange for funding of the project, Dr. Eisenstein provided continuous encouragement and helpful guidance. This support made working under his supervision a very rewarding and pleasant experience.

The author is also grateful for the advice and help given by Dr. S. Thomson, a wonderful mentor. He willingly spent long hours in discussion, especially during preparation of the final draft of this thesis. The stimulating comments by and discussion with Dr. N. Morgenstern on several occasions are greatly appreciated. The writer also wishes to thank Drs. E. Cording, B. Stimpson and S. Simmons for their very interesting comments during the final oral examination. Thanks are also due to Drs. R. May, P. Kaiser and D. Sego.

The cooperation and help of the Edmonton Water and Sanitation Department in allowing access to the experimental tunnel during construction is gratefully acknowledged. Particularly appreciated is the assistance provided by Messrs. R. Oster and G. Emmanuel.

The author is grateful to Mr. D. Morse of Supercrete Alberta Ltd., the manufacturers of the precast concrete segments, and to Mr. K. Morrison of R.V. Anderson Associates, the designers of these segments. Their assistance during installation of the lining instruments was very helpful.

The success of the instrumentation program, which forms the main part of this thesis, would have been very difficult to achieve without the sincere help provided by my colleagues. Their enthusiasm and invaluable assistance made the most difficult stages of this project an enjoyable, rewarding experience. In particular, I would like to thank Oldrich Hungr, John Simmons, Bryan Watts, Kevin Sterne, Don Sargent and Howard Plewes.

Special thanks are due to John Sobkowicz and Alan Gale for the many hours they spent proofreading various drafts of the thesis and trying to understand my puzzling English.

The author also wishes to acknowledge the helpful technical assistance provided by O. Wood, during installation of the soil instruments, and by L. Burden and G. Cyre during installation of the lining instruments. Some of the devices were built at the University of Alberta. A. Muir and T. Brown were very helpful in machining and assembling them. S. Gamble and D. Fushtey spent many hours in the cold taking the field measurements with me. S. Rogers provided the photographic assistance and R. Howels helped with computing. Lorraine Iwaskow did an excellent job in

entering the text of the thesis in the computer. To all of you my sincere thanks.

I was lucky to have the opportunity to meet and develop real friendships with a remarkable group of graduate students. We shared many hours; not only in hard work and discussion but also socially (especially playing soccer!). In particular, I would like to sincerely acknowledge the friendship of Alan Gale, Sergio da Fontoura, Luciano Medeiros, Erman Evgin and Jean Marie Konrad.

The author also wishes to express his appreciation to the staff of the Edmonton office of Thurber Consultants Ltd. for their understanding and encouragement.

My utmost gratitude is due to my wife Nany and son Hesham. Their love and understanding made this thesis possible. Nany also proved that a dentist's hands could be as good in drafting as they are in pulling teeth!

Finally, the author wishes to acknowledge the financial assistance provided by the Natural Sciences and Engineering Council of Canada and the Department of Civil Engineering of the University of Alberta in the form of operational research grants and teaching assistantships respectively.

Table of Contents

Chapter	Page
1. <u>INTRODUCTION</u>	1
1.1 GENERAL	1
1.2 SCOPE AND ORGANIZATION OF THE THESIS	2
2. <u>DESIGN OF TUNNELS IN SOILS</u>	6
2.1 INTRODUCTION	6
2.2 DESIGN OF LINING IN SOIL TUNNELS	7
2.2.1 METHODS BASED ON EARTH PRESSURE THEORIES	7
2.2.2 METHODS BASED ON SUBGRADE REACTION THEORY ...	10
2.2.3 GROUND AND SUPPORT REACTION CURVES	14
2.2.4 ANALYSES BASED ON CONTINUUM MECHANICS	18
2.2.5 FINITE ELEMENT ANALYSES	26
2.3 SOIL MOVEMENTS DUE TO TUNNELING	31
2.3.1 GROUND SURFACE MOVEMENTS	31
2.3.2 SUBSURFACE SOIL MOVEMENTS	41
2.3.3 FINITE ELEMENT ANALYSES	45
2.4 SUMMARY	45
3. <u>THE EXPERIMENTAL TUNNEL</u>	48
3.1 INTRODUCTION	48
3.2 GEOLOGY OF EDMONTON AREA	51
3.3 SOIL PROFILE ALONG THE EXPERIMENTAL TUNNEL	56
3.4 CONSTRUCTION DETAILS	60
3.4.1 CONVENTIONAL LINING SYSTEM	62
3.4.2 PRECAST SEGMENTED LINING	67
3.5 FIELD TEST SECTIONS	72
3.5.1 TEST SECTION 1	74

3.5.2	TEST SECTION 2	74
3.5.3	TEST SECTION 3	77
4.	<u>MEASUREMENTS OF SOIL DISPLACEMENTS AROUND THE</u> <u>EXPERIMENTAL TUNNEL</u>	79
4.1	INTRODUCTION	79
4.2	SOIL INSTRUMENTATION	80
4.2.1	SETTLEMENT POINT	82
4.2.2	SINGLE POINT EXTENSOMETER	84
4.2.3	MULTIPOINT EXTENSOMETER	85
4.2.3.1	MAGNETIC MULTIPOINT EXTENSOMETER	86
4.2.3.2	INSTALLATION PROCEDURE	91
4.2.3.3	MEASUREMENT PROCEDURE	94
4.2.3.4	REPRODUCIBILITY	94
4.2.3.5	COST	98
4.2.4	SLOPE INDICATOR	98
4.3	FIELD MEASUREMENTS OF SOIL DISPLACEMENT	104
4.3.1	TEST SECTION 1	104
4.3.2	TEST SECTION 2	108
4.3.3	TEST SECTION 3	115
4.4	DISCUSSION OF THE MEASUREMENTS	127
4.4.1	DEVELOPMENT OF SOIL DISPLACEMENTS WITH TUNNEL ADVANCE	127
4.4.2	VARIATION OF SOIL DISPLACEMENTS WITH DEPTH .	131
4.4.3	EFFECT OF DIFFERENT LINING SYSTEMS ON SOIL DISPLACEMENTS	131
4.5	SUMMARY	134
5.	<u>BEHAVIOUR OF TWO SYSTEMS OF TUNNEL LINING</u>	136
5.1	INTRODUCTION	136

5.2	ALTERNATES TO THE CONVENTIONAL LINING SYSTEM	138
5.3	LINING INSTRUMENTATION	145
5.3.1	PRESSURE CELLS	145
5.3.2	STRAIN GAUGES	145
5.3.3	LOAD CELLS	151
5.3.4	TAPE EXTENSOMETER	152
5.4	FIELD MEASUREMENTS FROM LINING INSTRUMENTS	156
5.4.1	TEST SECTION 1	156
5.4.2	TEST SECTION 2	160
5.4.3	TEST SECTION 3	166
5.5	STRENGTH OF LONGITUDINAL JOINTS OF SEGMENTS	179
5.5.1	DESCRIPTION OF SAMPLES AND TEST RESULTS	179
5.5.2	DISCUSSION OF TEST RESULTS	181
5.6	DISCUSSION ON LINING BEHAVIOUR	184
5.6.1	RIB-LAGGING SYSTEM	184
5.6.2	PRECAST SEGMENTED LINING	191
5.6.2.1	STRAINS AND STRESSES IN THE LINING .	191
5.6.2.2	LINER THRUST AND SOIL PRESSURE	194
5.6.2.3	DISTORTION OF LINING	195
5.6.2.4	GAPS BETWEEN LINING AND SOIL	197
5.6.2.5	STRENGTH OF LONGITUDINAL JOINTS	199
5.7	PRESSURE-DEFORMATION RELATIONS OF THE TWO LINING SYSTEMS	199
5.8	SUMMARY	202
6.	<u>STRAIN FIELDS AROUND A TUNNEL ADVANCING IN A STIFF SOIL</u>	205
6.1	INTRODUCTION	205
6.2	SURFACE II GRAPHICS SYSTEM	206

6.3	THE DISPLACEMENT FIELD AROUND AN ADVANCING TUNNEL	210
6.3.1	DISPLACEMENTS AT SECTION A	213
6.3.2	DISPLACEMENTS AT SECTION B	216
6.3.3	DISPLACEMENTS AT SECTION C	223
6.4	STRAIN FIELDS AROUND AN ADVANCING TUNNEL	223
6.4.1	CALCULATION OF STRAINS FROM DISPLACEMENTS ..	223
6.4.2	STRAINS AT SECTION A	230
6.4.3	STRAINS AT SECTION B	236
6.4.4	STRAINS AT SECTION C	236
6.5	MOBILIZATION OF SHEAR STRENGTH	244
6.5.1	CONTOUR MAPS OF MAXIMUM SHEAR STRAINS	244
6.5.2	RESULTS OF LABORATORY TESTS ON TILL	246
6.5.3	MECHANISM OF SHEAR STRENGTH MOBILIZATION ...	250
6.6	SUMMARY	261
7.	<u>CONCLUSIONS AND RECOMMENDATIONS FOR FURTHER STUDIES</u> ..	264
7.1	THE BEHAVIOUR OF TUNNELS IN STIFF SOILS	264
7.1.1	SOIL RESPONSE TO TUNNELING	265
7.1.2	BEHAVIOUR OF LINING SYSTEMS	267
7.1.3	STRAIN FIELDS AROUND TUNNELS	269
7.1.4	MOBILIZATION OF SHEAR STRENGTH AROUND TUNNELS	270
7.2	GENERAL CONCLUSIONS	271
7.3	RECOMMENDATIONS FOR FURTHER STUDIES	274
	REFERENCES	277
APPENDIX A	MULTIPOINT EXTENSOMETER MEASUREMENTS OF TEST SECTION 3	286
APPENDIX B	SLOPE INDICATOR MEASUREMENTS AT TEST SECTION 3	297

List of Tables

TABLE		PAGE
2.1	Comparison between field measurements and analytical results using Anders Bull method (after Mathis, 1974).....	13
2.2	Stiffness ratios of tunnel liners.....	20
2.3	Equations of theoretical volume of ground loss due to unsupported tunnels in clay (after Peck et al., 1969).....	33
3.1	Quaternary geology of Edmonton area (after May and Thomson, 1978).....	52
3.2	Geotechnical properties of Edmonton till (after Thomson and El-Nahhas, 1980).....	55
3.3	Specification of the tunnel boring machine.....	64
3.4	Mix design of the concrete used for casting the segments.....	69
4.1	Details of multipoint extensometers used in the experimental tunnel.....	105
4.2	Details of slope indicators used in the experimental tunnel.....	106
4.3	Details of settlement points and single point extensometers used in the experimental tunnel....	107
5.1	Cost of tunnels in Edmonton (Data courtesy of City of Edmonton).....	143
5.2	Strength of longitudinal joints.....	182

TABLE		PAGE
5.3	Soil pressure on the primary lining in Edmonton tunnels.....	189
6.1	Strain-Displacement relationships.....	228
6.2	Strains in triaxial test samples under different stress paths.....	249
6.3	Maximum shear strains from laboratory tests.....	253

List of Figures

FIGURE		PAGE
2.1	Pressure distribution and statical system used for the design of tunnel lining (after Hewett and Johannesson, 1922).....	8
2.2	Anders Bull method (after Bull, 1944).....	11
2.3	Reaction curve for ideal elastic continuum (after Deere et al., 1969).....	15
2.4	Reaction curves for soil tunnels (after Peck, 1969).....	17
2.5	Variation of bending moment with flexibility ratio (after Peck et al., 1972).....	21
2.6	Variation of thrust with compressibility ratio (after Peck et al., 1972).....	22
2.7	Effect of liner flexibility on the diameter changes (after Peck et al., 1972).....	23
2.8	Bending moments in the lining as calculated by different methods (after Ebaid and Hammad, 1978).....	25
2.9	Calculated stresses in steel ribs using the field measurements of lining deformation (after El-Nahhas, 1977).....	29
2.10	Effect of tunnel face on liner thrust (after Ranken and Ghaboussi, 1975).....	30
2.11	Comparison between calculated and measured volume of ground loss (after Peck et al., 1969)...	34

FIGURE		PAGE
2.12	The Gaussian distribution function used for describing subsidence profiles (after Peck et al., 1969).....	36
2.13	Trough width, subsidence over tunnels in clay (after Peck et al., 1969).....	38
2.14	Trough width, subsidence over tunnels in different soils (Peck, 1969).....	38
2.15	Maximum surface settlement related to depth and diameter for tunnels in stiff clay (after Attewell and Farmer, 1975).....	40
2.16	Soil displacement around Washington metro tunnels (after Hansmire, 1975).....	42
2.17	Subsurface soil displacement measured around tunnels in U.K. (after Craig and Muir Wood, 1978).....	44
3.1	Location of the experimental tunnel.....	50
3.2	Subsurface soil profile along 125 Avenue.....	57
3.3	Subsurface soil provile along 122 Street.....	59
3.4	Tunnel drilling machine (Lovat M-100 Series 1900).....	63
3.5	Conventional lining system.....	66
3.6	Precast segmented lining.....	68
3.7	Location of the test sections.....	73
3.8	Layout of Test Section 1.....	75

FIGURE		PAGE
3.9	Layout of soil instruments at Test Section 2.....	76
3.10	Layout of Test Section 3.....	78
4.1	Details of settlement point and single point extensometer.....	83
4.2	Magnetic multipoint extensometers.....	87
4.3	Details of magnetic ring.....	89
4.4	Magnetic fields around the ring.....	90
4.5	Installation of multipoint extensometers.....	92
4.6	Micrometer head.....	96
4.7	Field data sheet for multipoint extensometer.....	97
4.8	Installation of slope indicators.....	101
4.9	Vertical displacement measured using extensometer MX11.....	109
4.10	Vertical displacement vs. tunnel advance (MX11)..<	110
4.11	Vertical displacement vs. tunnel advance (MX12)..<	111
4.12	Settlement trough at Test Section 1.....	112
4.13	Horizontal displacement measured using slope indicator SI11.....	113
4.14	Horizontal displacement (Direction A) vs. tunnel advance (SI11).....	114

FIGURE	PAGE
4.15	Vertical displacement measured using extensometer MX22.....116
4.16	Vertical displacement vs. tunnel advance (MX22)..117
4.17	Vertical displacement vs. tunnel advance (MX21)..118
4.18	Settlement trough at Test Section 2.....119
4.19	Horizontal displacement at the tunnel face.....120
4.20	Final settlement measured at Test Section 3 (MX31-MX35).....122
4.21	Final settlement measured at Test Section 3 (MX36-MX310).....123
4.22	Final settlement measured at Test Section 3 using single point extensometers.....124
4.23	Final settlement trough at Test Section 3.....125
4.24	Final horizontal displacement in direction A measured at Test Section 3.....126
4.25	Final horizontal displacement in direction B measured at Test Section 3.....128
4.26	Vertical displacement vs. tunnel advance.....130
4.27	Soil displacement around different lining systems.....132
5.1	Development of segmented lining in the United Kingdom (McBean and Harries, 1970).....141
5.2	Strain gauges used in the experimental tunnel....147

FIGURE		PAGE
5.3	Installation of concrete strain gauges.....	150
5.4	Design and installation of load cells.....	153
5.5	Details of tape extensometer.....	155
5.6	Instrumented steel rib of Test Section 1.....	157
5.7	Strains in the steel rib vs. time (Test Section 1).....	158
5.8	Strain distribution in steel sections.....	159
5.9	Change in horizontal and vertical diameters, 170 Street tunnel (after El-Nahhas, 1977).....	161
5.10	Level change of tunnel invert, 170 Street tunnel (after El-Nahhas, 1977).....	162
5.11	Details of Test Section 2 (lining instruments)...	163
5.12	Measured strains in the concrete at the crown and springline of the tunnel (Test Section 2)....	165
5.13	Measurements of lining thrust at Test Section 2..	167
5.14	Details of Test Section 3 (lining instruments)...	169
5.15	Measurements of liner thrust (Section 3 - Ring 1).....	170
5.16	Measurements of liner thrust (Section 3 - Ring 2).....	171
5.17	Measurements of liner thrust (Section 3 - Ring 3).....	172

FIGURE		PAGE
5.18	Measurements of liner thrust (Section 3 - Ring 5).....	173
5.19	Size of gap between lining and soil (Ring 1).....	174
5.20	Size of gap between lining and soil (Ring 2).....	175
5.21	Size of gap between lining and soil (Ring 3).....	176
5.22	Size of gap between lining and soil (Ring 4).....	177
5.23	Size of gap between lining and soil (Ring 5).....	178
5.24	Details of longitudinal joint samples.....	180
5.25	Modes of failure of reinforced and unreinforced joints.....	185
5.26	Strains at neutral axes in the steel rib of Section 1.....	187
5.27	Stresses at the neutral axis of segmented lining (Test Section 2).....	192
5.28	Estimated pressure distribution on segmented lining (Test Section 2).....	193
5.29	Variation of soil pressure on the lining systems.....	196
5.30	Reaction curves for the two lining systems.....	201
6.1	Slope projection procedure (after Sampson, 1978).....	208
6.2	Distance weighting functions (after Sampson, 1978).....	209

FIGURE	PAGE
6.3	Sections chosen for the contour maps.....212
6.4	Location of data points of vertical displacement in Section A.....214
6.5	Location of data points of horizontal displacement in Section A.....215
6.6	Contour map of vertical displacement (Section A).....217
6.7	Contour map of horizontal displacement (Section A).....218
6.8	Location of data points of vertical displacement in Section B.....219
6.9	Location of data points of horizontal displacement in Section B.....220
6.10	Contour map of vertical displacement (Section B).....221
6.11	Contour map of horizontal displacement (Section B).....222
6.12	Location of data points of lateral and longitudinal displacements in Section C.....224
6.13	Contour map of lateral displacement (Section C)..225
6.14	Contour map of longitudinal displacement (Section C).....226
6.15	First derivative at a nodal point using SURFACE II.....229
6.16	Flow chart of calculation of strains from displacements.....231

FIGURE	PAGE
6.17	Contour map of major principal strains (Section A).....232
6.18	Contour map of minor principal strains.....233
6.19	Strain rosette plot (Section A).....234
6.20	Contour map of volumetric strains (Section A)....235
6.21	Contour map of longitudinal strains (Section B)..237
6.22	Contour map of vertical strains (Section B).....238
6.23	Contour map of shear strains (Section B).....239
6.24	Contour map of lateral strains (Section C).....240
6.25	Contour map of longitudinal strains (Section C)..241
6.26	Contour map of shear strains (Section C).....243
6.27	Contour map of maximum shear strains (Section A).....245
6.28	Bilinear stress-strain relationship.....248
6.29	Results of triaxial drained test on Edmonton Till.....251
6.30	Results of triaxial undrained test on Edmonton Till.....252
6.31	Zones of mobilized shear strength.....255
6.32	Failure zones in model test on overconsolidated Kaolin (after Atkinson and Potts, 1977).....256

FIGURE	PAGE
6.33	Shear strains from finite element simulation of a model test (after Ghaboussi et al., 1978).....257
6.34	Failure zone of unsupported section of tunnel roof (after Matheson, 1970).....259

List of Photographic Plates

PLATE		PAGE
3.1	Skip hoist at the main shaft of the experimental tunnel.....	61
3.2	Tunnel drilling machine (Lovat-Model M-100 Series 1900).....	61
3.3	Conventional lining system.....	65
3.4	Steel forms used to cast the secondary concrete lining.....	65
3.5	Top segment wedged in place.....	71
3.6	Ring expander.....	71
5.1	Embedded vibrating wire strain gauge during casting.....	148
5.2	Surface vibrating wire strain gauge.....	148
5.3	Weldable vibrating wire strain gauge.....	148
5.4	Lining instruments at Test Section 2.....	164
5.5	Failutre of unreinforced longitudinal joint.....	183
5.6	Failure of reinforced longitudinal joint.....	183

CHAPTER 1

INTRODUCTION

1.1 GENERAL

The 1970's were characterized by a realization of the shortage in available hydrocarbon energy, a mounting concern over disturbance of the environment, a rapid growth of urban centres, and a sharp increase in the cost of land, particularly in large cities. The petroleum shortage made unconventional energy sources, such as oilsand, seem feasible and attractive. Many of the possible schemes for in-situ extraction of the deeper deposits would be greatly enhanced by the construction of shafts and tunnels around and within the oilsand deposits. The environmental restrictions and the continuous increase in the cost of land especially in city centres directed attention to the development of underground space for subway systems, storage, and other purposes. Construction of tunnels for storm and sanitary sewer systems also increased concurrent with the rapid growth of these cities, and the development of vast areas for new subdivisions. As a result of these factors, a large number of tunneling projects have been planned and constructed in the last 10 years.

The search for more efficient and economical tunneling methods resulted in the introduction and testing of new tunneling technologies, which in turn created a powerful

thrust for efforts to increase our knowledge concerning the behaviour of tunnels in different ground conditions. Field trials and in-situ monitoring of tunnels under construction have played a major role in the assessment of new technologies and the verification of new design concepts. Such tunnel monitoring programs will continue to fulfill this important role until reliable analytical techniques are established and confirmed by case histories. Such development can lead, eventually, to the development of a general design theory.

The design of tunnels in soils consists of two major parts: the dimensioning of the lining, and the prediction of soil movement associated with tunnel advance and lining installation. In soft soils, additional problems such as ground water control and stabilization of the tunnel face would require special attention in design and construction. The control of ravelling ground is another important element which must be considered in the design of tunnels in cohesionless soils.

1.2 SCOPE AND ORGANIZATION OF THE THESIS

This thesis investigates the main elements of the behaviour of tunnels in stiff soils. The soil mass response to tunnel advance and the in-situ performance of two lining systems were monitored in an experimental tunnel located in northwest Edmonton. The tunnel was advanced through an overconsolidated silty clay using a shielded drilling

machine. Conventional rib and lagging lining, and precast segmented lining, were used as support systems in separate portions of the tunnel. This is the first time precast concrete segments have been used to line a tunnel in the overconsolidated soils and soft rocks of Western Canada.

The in-situ performance of the two lining systems was compared, and the behaviour of the precast segmented lining was studied in detail utilizing field measurements and laboratory testing. Extensive measurements of soil displacement were used to identify the characteristic trends of ground response to tunnel advance. Field measurements were also employed to investigate the spatial deformation and strain fields around the tunnel.

The investigation was extended to include a study of the mode of mobilization of shear strength in the immediate vicinity of the tunnel. The manner in which this mobilization occurred reveals important factors concerning a possible failure mechanism of the soil, and the extent of the arching of stresses around the tunnel.

Chapter 2 of this thesis contains a review of the methods discussed in the literature which deal with the design of tunnel linings and the estimation of associated soil movements. The methods were classified according to the processes assumed and/or the techniques used. One or more examples of each group was discussed in some detail to illustrate the advantages and shortcomings of the methods in that group.

Details of the experimental tunnel are given in Chapter 3 which includes an overview of the geology of the Edmonton area, a description of the subsurface soil profile along the tunnel, and the construction procedures employed. The layout of the instrumentation program implemented in this project is also described.

Chapter 4 contains a summary of various soil instruments that may be used to monitor the behaviour of tunnels in stiff soils. A detailed description of the particular instruments chosen for this experimental tunnel is given. The measurements obtained from each test section are presented and discussed to identify the trends and characteristics of the soil displacements associated with this tunnel.

Chapter 5 is devoted to the investigation of the in-situ behaviour of the conventional support system and the precast segmented lining. A discussion of possible alternatives to the conventional lining system, and also a summary of the instrumentation required to monitor the performance of linings in soil tunnels is considered. The results obtained from the lining instrumentation in the experimental tunnel are presented and used together with the results of laboratory tests on the longitudinal joints of the concrete segments to evaluate the performance of the lining systems.

Based on the measurements of soil displacements given in Chapter 4, contour maps of the spatial displacement and

strain fields were constructed using a computer graphical system (SURFACE II). These maps are presented in Chapter 6. The maximum shear strains around the tunnel and the results of laboratory tests on the till were used to investigate the mobilization of shear strength in the vicinity of the tunnel. The results and implications of this investigation are discussed.

Finally, the conclusions and recommendations for further studies are summarized in Chapter 7.

CHAPTER 2

DESIGN OF TUNNELS IN SOILS

2.1 INTRODUCTION

The design of a tunnel in soil for Civil Engineering purposes can be divided into a number of steps. For example, determination of the size of a tunnel depends on its purpose. For a subway system, a medium size twinned tunnel or a large single tunnel may be required, while for sewer tunnels the size varies according to the class of the sewer-line and the maximum volume of discharge. Similar consideration usually determine the route, depth, geometry and grade of the tunnel.

Geotechnically, the design of a tunnel in a stiff soil consists of two major tasks. First, the design of the lining and second, the estimate of soil movement associated with the tunnel construction. Although these two tasks are interrelated, they are usually dealt with separately to simplify the analysis.

This chapter discusses the different methods described in the literature for the analysis of lining behaviour and soil deformations, due to tunneling. Limitations and shortcomings of the various design methods are pointed out.

2.2 DESIGN OF LINING IN SOIL TUNNELS

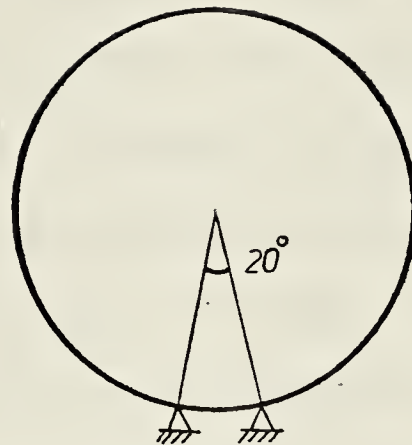
The design of a tunnel lining usually starts with the determination of the soil pressure acting on it and extends to the calculation of the accompanying normal forces and bending moments. A complete design should also examine the deformation of the lining as an important criterion governing its structural dimensions.

This section contains a review of the different methods of tunnel lining design. The methods are classified according to the concepts and techniques employed in each analysis. At least one method of each group is discussed in some detail to show the advantages and limitations of the concepts and/or the techniques employed.

2.2.1 Methods Based on Earth Pressure Theories

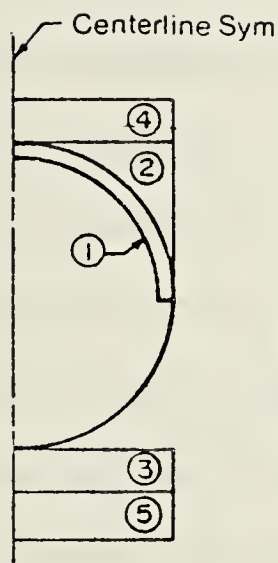
These methods assume hypothetical or empirical pressure distribution on the lining which are used to determine the internal forces and deformations of the lining (Szechy, 1966). An example of these methods is the analysis proposed by Hewett and Johannesson (1922). Figure 2.1 shows the pressure distribution assumed for this method under short and long term conditions. Hewett and Johannesson (op. cit.) have derived formulas for the normal forces and bending moments in the tunnel lining due to these pressure distributions. Their analysis was based on the assumption that the lining is a continuous rigid elastic structure.

For the analysis of a real tunnel lining, they



Under weight of lining only

SHORT TERM



LOADS

- ① The weight of the upper half of the tunnel.
- ② The weight of the earth within the area marked 2.
- ③ A uniform upward force balancing 1 and 2.
- ④ The weight of the loading above the top of the tunnel.
- ⑤ A uniform upward reaction balancing 4.
- ⑥ The horizontal pressure due to the water above the top of the tunnel.
- ⑦ The horizontal pressure due to the water from top to bottom of the tunnel.
- ⑧ The horizontal pressure due to the earth above the top of the tunnel equal to the product of the weight of earth (buoyant unit weight if submerged) above the top of the tunnel and the factor K .
- ⑨ The horizontal pressure due to the earth between the top and the bottom of the tunnel. At any point, the pressure is the product of the weight of soil between that point and the top of the tunnel and the factor K . Soil weighed as in 8.

LONG TERM

Figure 2.1 Pressure distribution and statical system used for the design of tunnel lining (after Hewett and Johannesson, 1922)

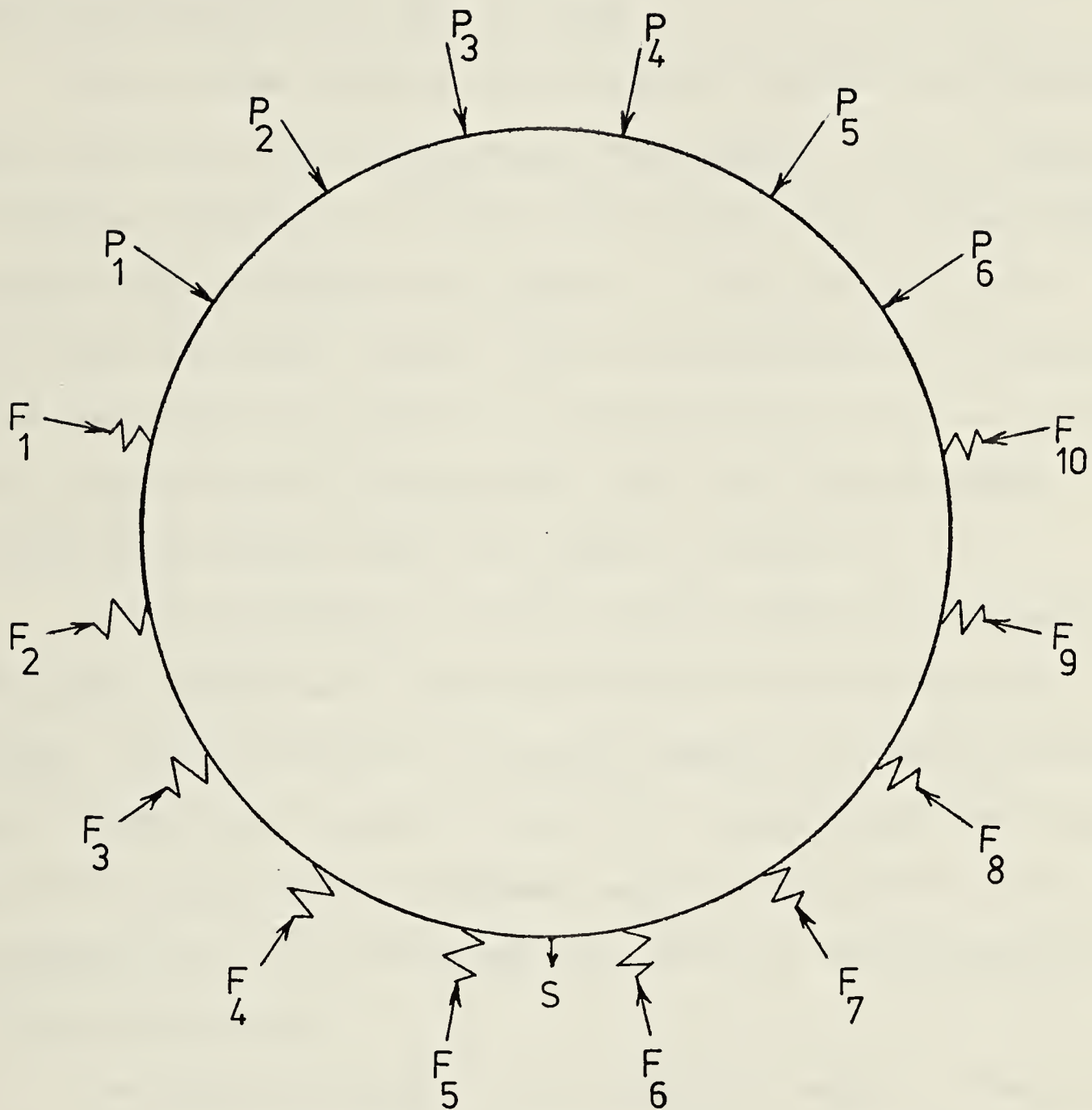
suggested that the unknown earth pressure coefficient be assigned a value greater than the active earth pressure coefficient but less than the passive coefficient. The lining is assumed to adjust its center line to coincide with the thrust line. Hence, the exact value of the earth pressure coefficient is chosen to satisfy this condition, which implies that no bending moments are developed in the lining. For the construction stage (short-term), they suggested the analysis of an isolated ring of the tunnel lining under its own weight while being supported on two knife-edges as shown in Figure 2.1.

The Hewett-Johannesson method has several weak points. First, the assumption of a lining which is rigid and yet allowed to adjust its center line to eliminate bending moments is inconsistent. Second, the procedure suggested for the determination of the coefficient of earth pressure could result in values lower than K_a or higher than K_p . The use of one of the extreme values, in these cases, would result in the development of bending moments in the lining. Third, the proposed analysis for the short term case is unrealistic and archaic with respect to the tunneling technologies presently in use. Fourth, the soil pressure distribution suggested in this method does not take into consideration the redistribution and arching of soil stresses which take place before the soil lining interaction starts.

2.2.2 Methods Based on Subgrade Reaction Theory

Unlike the previous group, the methods based on subgrade reaction theory consider the dependency of the soil pressure on lining deformation (Bull, 1944; Wissmann, 1968). Soil behaviour is assumed to be given by Winkler's subgrade reaction coefficient (Terzaghi, 1955), which is simplified by introducing single springs at the nodes of the framework representing the lining.

In the method proposed by Bull (1944), the lining periphery is divided into sixteen segments which are radially supported by springs to simulate the effect of the elastic soil reactions as shown in Figure 2.2. Bull derived the influence values of thrust, bending moment and deflection of mid-points of the sixteen segments. The active pressure on the lining (for points moving inward) is estimated and replaced by equivalent point loads. The magnitude of these loads can be reduced empirically to account for the arching effect. A deformation compatibility equation is formed for each of the remaining points as a function of the unknown soil reactions at these points and an unknown settlement of the tunnel invert. One additional equation is formed by introducing the condition of equilibrium in the vertical direction. By solving these equations simultaneously, the passive forces acting on the lining and the settlement of the tunnel invert are determined. Finally the internal forces and deformation of the lining are calculated. If the pattern of calculated



P_1 to P_6 : Estimated active forces

F_1 to F_{10} : Unknown passive reactions

S : Unknown invert settlement

Figure 2.2 Anders Bull method (after Bull, 1944)

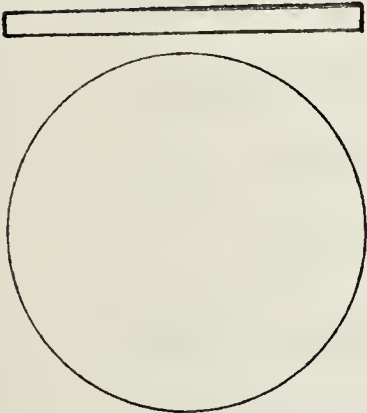
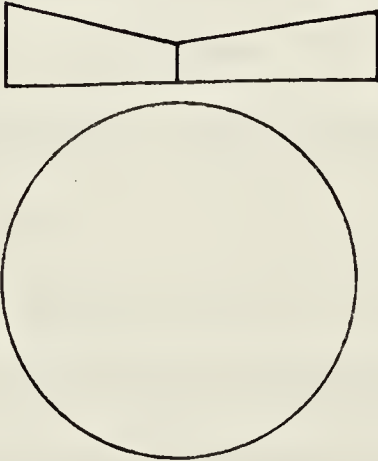
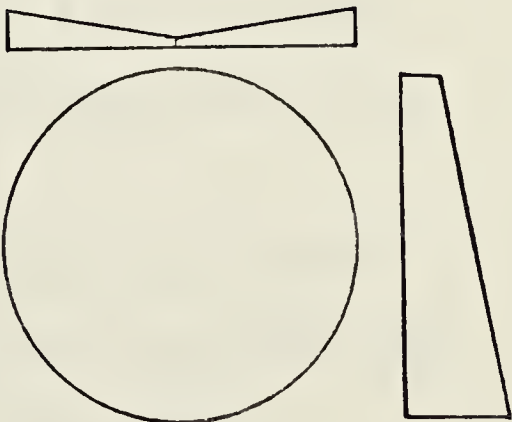
deformation is inconsistent with the assumed zones of active and passive pressure, the calculations have to be repeated with modified active point loads.

Due to the tedious calculations involved in forming and solving the simultaneous equations, Mathis (1974) prepared a computer program to perform the analysis for linings under symmetrical loading with respect to the vertical axis through the tunnel center line. He analyzed the lining of the Garrison Dam tunnels for three possible active loadings. The results were compared with the field measurements reported by Burke (1957) as shown in Table 2.1.

It was concluded that the thrust loads calculated by the Bull method were about 12% lower than the measured loads. The difference in bending moments and deformations were much larger. Mathis (op. cit.) postulated that the initial construction stresses, and the possibility of asymmetrical soil pressures were the main contributors to these differences.

The methods based on the subgrade reaction theory avoid some of the weak points encountered in the methods using earth pressure theory. However, they still have some shortcomings. First, the coefficient of subgrade reaction is not independent of the magnitude of the pressure and it does not have the same value along the contact area between the lining and the excavated surface of the soil. For the case of a footing, for example, Terzaghi (1955) indicated that this coefficient varies with the size, shape and depth of

Table 2.1 Comparison between field measurements and analytical results using Anders Bull method (after Mathis, 1974)

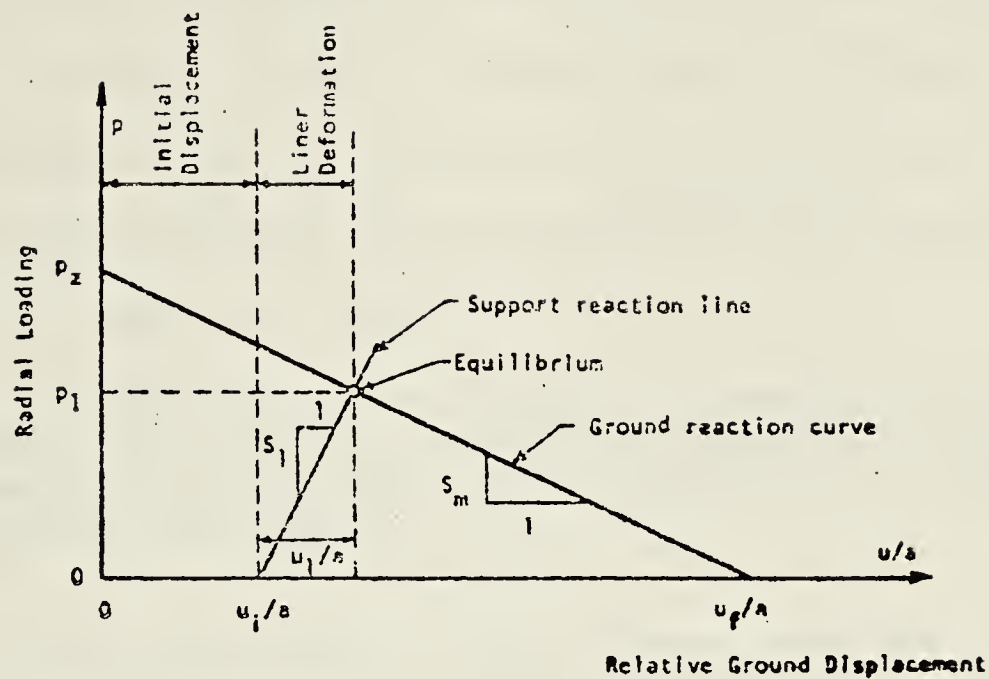
		<u>Measured Data</u>	<u>Loading (1)</u>	<u>Loading (2)</u>	<u>Loading (3)</u>
Thrust (Kips)	invert	111.3	108.35	111.41	114.95
	springline	96.0, 118.5	106.63	109.69	113.04
	crown	115.8	103.87	107.21	111.45
Moments (ft.Kips)	invert	+43.6	-0.4846	-0.4990	+0.0149
	springline	-38.8, -47.7	-0.0030	-0.0816	-2.9021
	crown	-73.1	-19.0305	-13.6541	0.2485
Horizontal diameter change (ft)		0.0750	0.0014	0.0014	-0.0020
Vertical diameter change (ft)		-0.0920	-0.0035	-0.0031	+0.0011
Maximum stress (psi)			8,700 -5,260	-4,900 -4,490	
					
Loading (1)		Loading (2)		Loading (3)	
$\sigma_v = 1 \text{ tsf}$		$\sigma_v = \gamma \cdot h = 1.576 \text{ tsf}$ (centre)		$\sigma_v = \gamma \cdot Z = 0.492 \text{ tsf}$ (centre)	
$\sigma_h = 0$		$\sigma_h = 0$		$\sigma_h = k_o \cdot \sigma_v$ ($k_o = 0.667$)	

the surface of contact. Second, these analyses require some judgment with respect to the magnitude and distribution of active loading, and the areas of active and passive reaction. Third, the methods do not consider the effect of construction procedures, which in some cases account for a significant portion of the stresses in the lining. Fourth, although these analyses do not put any restrictions on the rigidity of the lining, they fail to consider the effect of the joints in the lining on the tunnel behaviour.

2.2.3 Ground and Support Reaction Curves

A ground reaction curve shows the relationship between the radial deformation of a tunnel wall and the radial loading necessary to restrain further deformation. A support reaction curve shows the relationship between the ring thrust and the radial deformation of the lining. The two curves can be coupled, as shown in Figure 2.3 for an ideal elastic soil, to determine the equilibrium condition of the soil-lining interaction.

This method was described for rock tunnels by Pacher (1964) and was introduced as a design tool for the NATM (New Austrian Tunneling Method) by Rabcewicz (1964, 1965). Factors affecting the ground and support reaction curves were examined analytically by Lombardi (1970, 1973). Ladanyi (1974) derived a closed-form solution of the ground reaction curve for a circular tunnel in an isotropic rock mass under an isotropic state of in-situ stress for different



Lining Compressibility $S_l = t \cdot E_l / (a - t/2)$

Medium Stiffness $S_m = 2 \cdot E_m / ((1 + K_o) \cdot (1 + \nu))$

where :

E_l & E_m : Young's Modulus of
Lining & Medium

t : Lining Thickness

a : Exterior Radius

p_z : Average Radial Pressure

u : Radial Displacement

ν : Poisson's Ratio

Figure 2.3 Reaction curve for ideal elastic continuum
(after Deere et al., 1969)

stress-strain models.

The use of reaction curves for soft ground tunnels was examined and discussed by Deere et al. (1969) and Peck (1969). Curves similar to those shown in Figure 2.4 were approximated in a few instances on the basis of field observations combined with theoretical considerations. Peck (op. cit.) concluded that:

" . . . The results, although extremely tentative, suggest that the procedure is reasonable and could serve as a basis for improved design if supported by adequate field data"

The reaction curves offer a more realistic representation of the interaction sequence of the lining with the surrounding soil. They are of great value when used as a tool for qualitative discussions on some of the parameters involved in the design of linings for tunnels in soil. However, some points must be resolved before their use can be extended to quantitative design.

First, the concept of reaction curves assumes an axisymmetrical behaviour of both the soil and the lining which does not take into account the development of bending moments in the lining. Field measurements in many tunnels have shown that most tunnels, even at great depths, do not behave axisymmetrically. Field studies of the behaviour of tunnel linings have also illustrated that bending moments account for a significant portion of the stresses in the lining.

Second, the doming of stresses around the tunnel face,

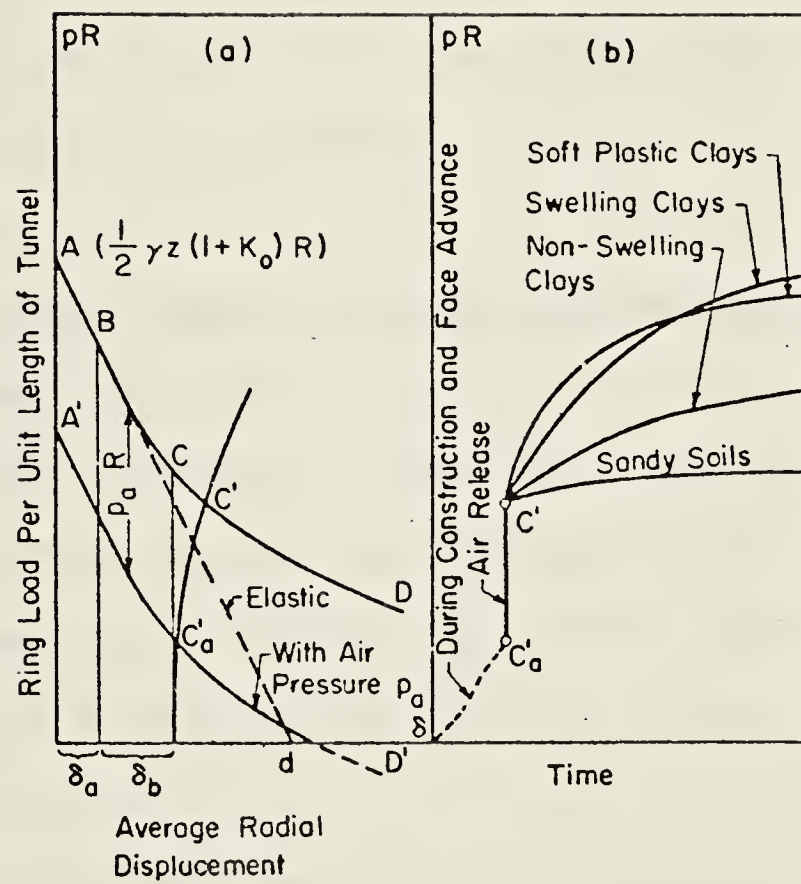


Figure 2.4 Reaction curves for soil tunnels (after Peck, 1969)

and its effect on ground behaviour, would be included more realistically if the gap between actual measurements and predictions based on theoretical curves was to be reduced. A simplified analytical treatment of this point was attempted by Lombardi (1973).

Third, it should be noted that this method deals with the soil-lining interaction in the vicinity of the tunnel. It does not provide any indication, however, of the development of soil displacement profiles near the ground surface, which constitute the second important element in the design of soil tunnels.

2.2.4 Analyses Based on Continuum Mechanics

Closed-form solutions for the interaction of an elastic medium with a buried cylinder were derived by Burns and Richard (1964) and by Hoeg (1968). These analyses were made through the use of extensional shell theory for the shell, and Michell's formulation of Airy's stress function for the soil medium.

Although these analyses were originally developed to study the behaviour of culverts, Peck et al. (1972) used them to calculate the internal forces and deformation of a tunnel lining of intermediate flexibility. They assumed that the case of full slippage between the lining and the soil would approximate more nearly the behaviour of soft ground tunnel lining. The lining stiffness was considered to be divided into two separate and distinct types. The first is

an extensional stiffness, represented by the Compressibility Ratio "C", which is a measure of the equal all-around uniform pressure necessary to cause a unit diametrical strain of the lining with no change in shape. The second is a flexural stiffness, represented by the Flexibility Ratio "F", which is a measure of the magnitude of the non-uniform pressure necessary to cause a unit diametrical strain which results in a change in shape or an ovaling of the lining. The derived formulas for these coefficients are given in Table 2.2.

The variation of bending moment with Flexibility Ratio, and the variation of thrust with Compressibility Ratio are given in dimensionless form in Figures 2.5 and 2.6 respectively. The effect of liner flexibility on the diameter changes of the lining is illustrated in Figure 2.7. In general, the plots indicate that the lining behaves as a flexible lining if the Flexibility Ratio is greater than 10.

A similar attempt to analyze the behaviour of a tunnel lining, using the Airy stress function, is given by Morgan (1961). His analysis was based on the assumption that the lining deforms in an elliptical mode. This analysis was corrected and extended to more realistic conditions by Muir Wood (1975). Formulas for bending moments and deformation of the lining were derived, and the effect of shear forces between the ground and the lining was examined. For the analysis of a real tunnel, it was suggested that upper and lower limits on the reduction of in-situ stresses due to

Table 2.2 Stiffness ratio for tunnel liners

Compressibility Ratio

$$C = \frac{\frac{E}{(1+\nu)(1-2\nu)}}{\frac{E_\ell t}{(1-\nu_\ell^2)}} \frac{1}{R}$$

Flexibility Ratio

$$F = \frac{\frac{E}{(1+\nu)}}{\frac{6 E_\ell I_\ell}{(1-\nu_\ell^2)}} \frac{1}{R^3}$$

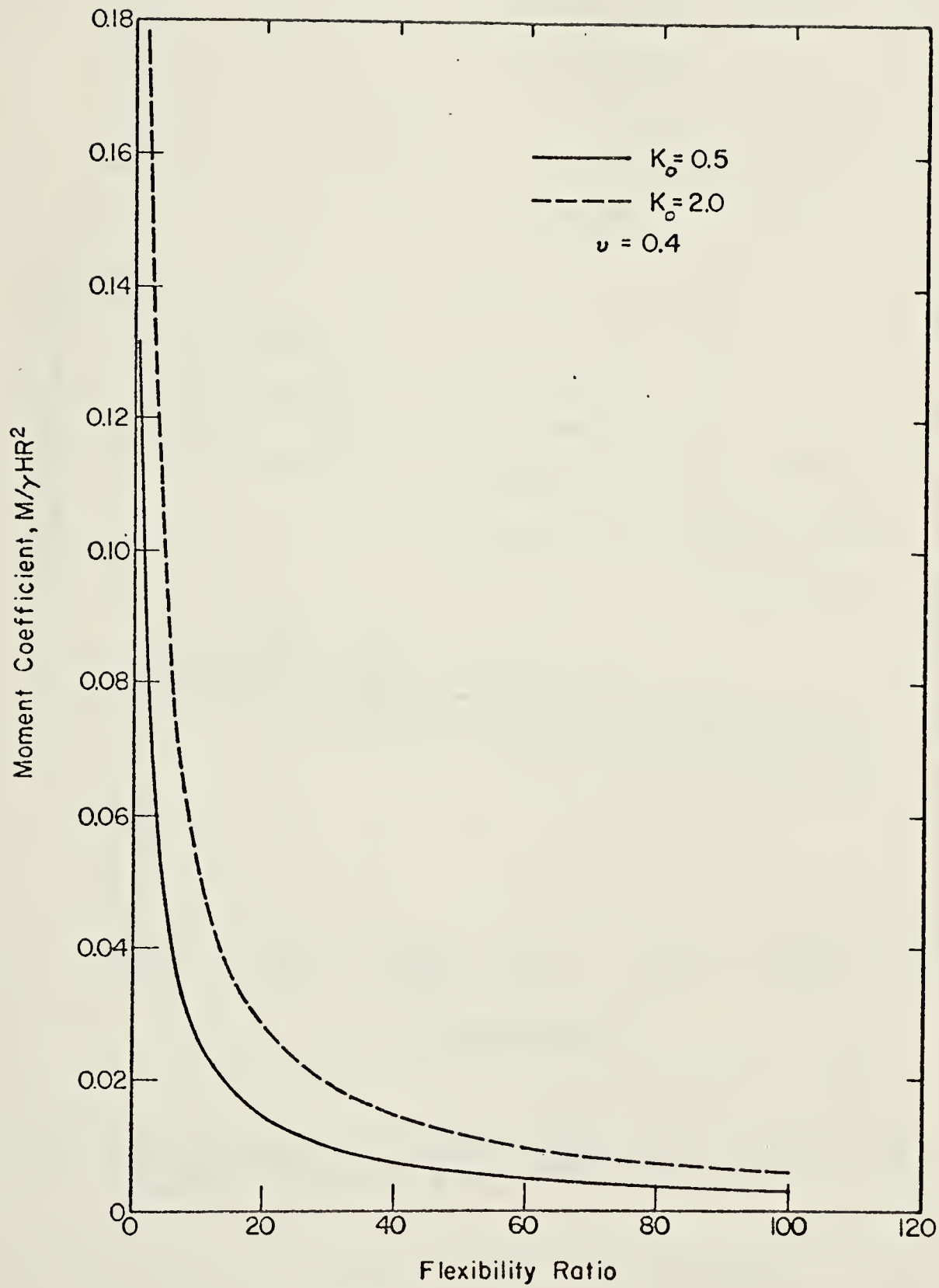


Figure 2.5 Variation of bending moment with flexibility ratio (after Peck et al., 1972)

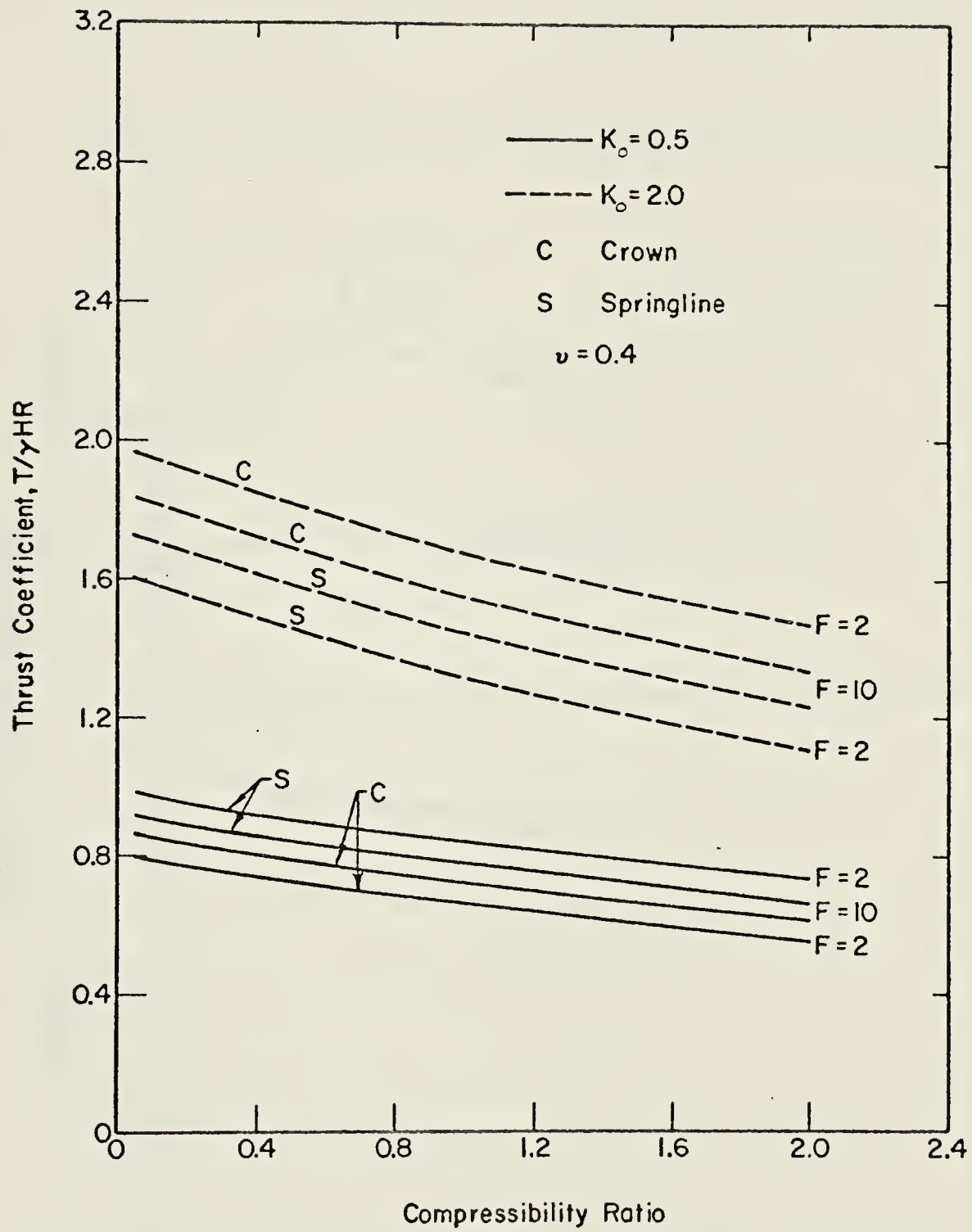


Figure 2.6 Variation of thrust with compressibility ratio (after Peck et al., 1972)

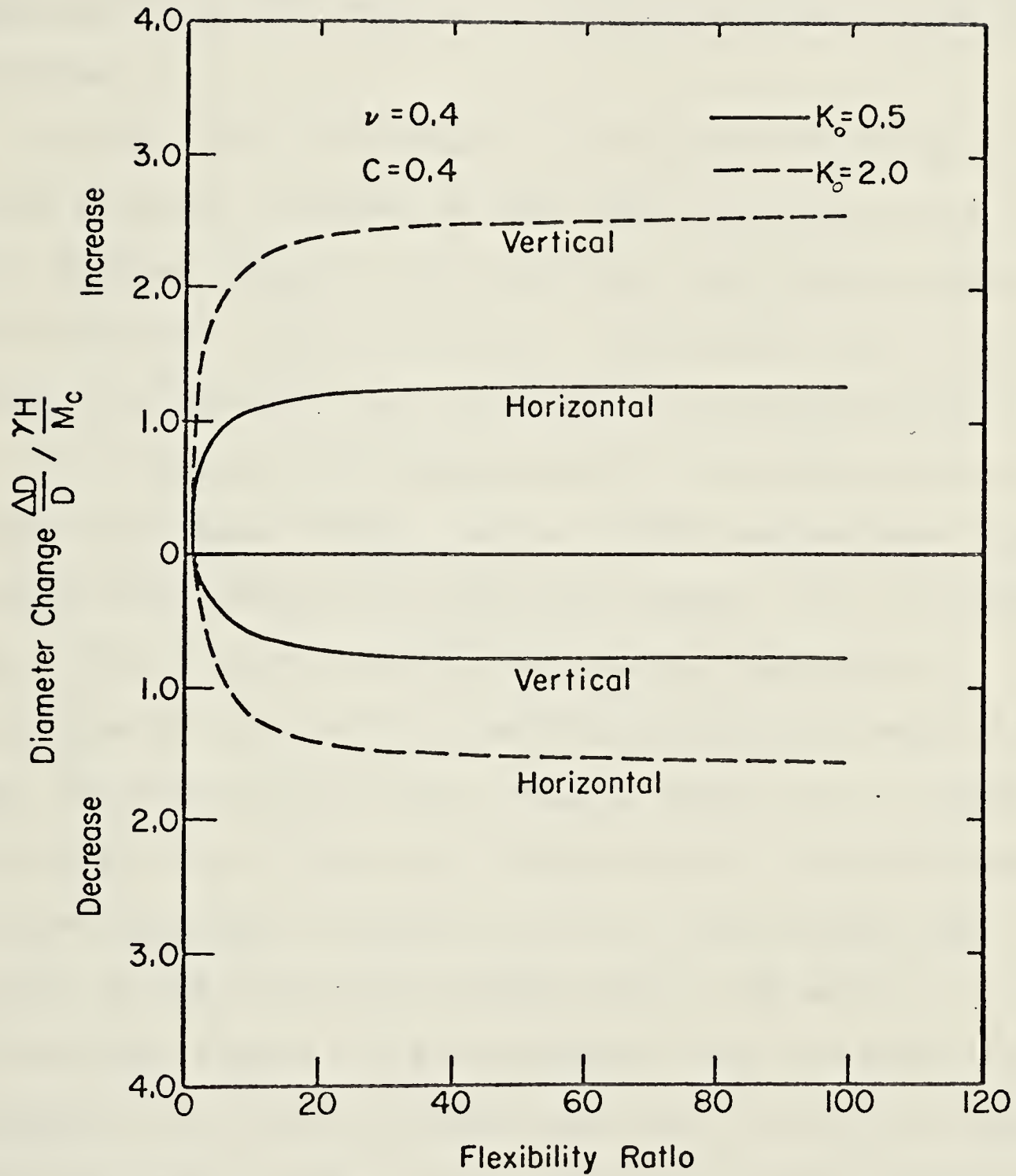


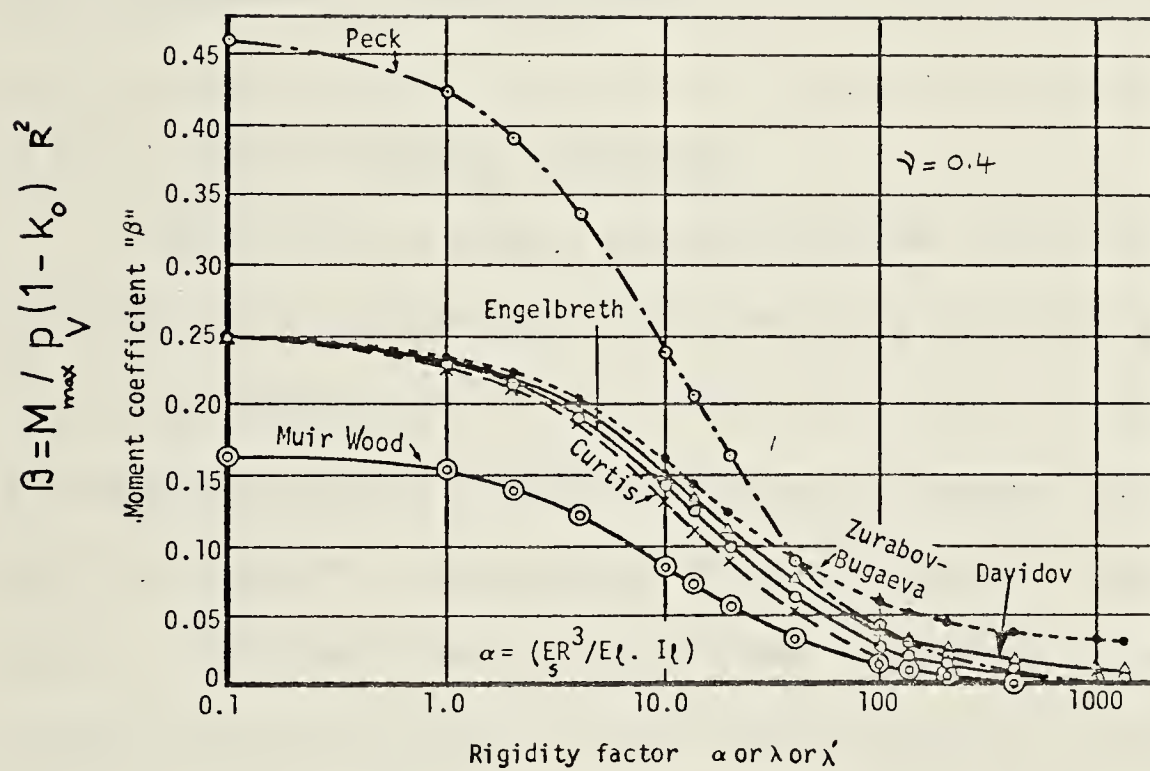
Figure 2.7 Effect of liner flexibility on the diameter changes (after Peck et al., 1972)

arching should be investigated. A simple formula was proposed to calculate an equivalent stiffness of the segmented lining taking into account the effect of the joints. The equivalent moment of inertia of an expanded and articulating lining which consists of eight segments is suggested to be 25% that of a solid lining having the same thickness.

Curtis (1976) discussed this analysis pointing out the effect of shear stresses on the radial deformation of the soil. He gave formulas for the thrust and bending moments in the lining for cases of no shear interaction and full shear interaction between the lining and the surrounding soil.

The formulas for bending moment obtained by Peck et al. (1972), Muir Wood (1975), Curtis (1976) and another three methods were compared by Ebaid and Hammad (1978) as shown in Figure 2.8. They indicated that the bending moments calculated by Peck et al.'s method are in the range of 2.4-3 times those obtained by Muir Wood's method, for a range of Poisson's ratio of the soil between 0-0.5. The difference in the bending moments calculated by the two methods was related to the different assumptions of the mode of lining deformation. Figure 2.8 also suggests that the modification proposed in the Curtis method resulted in slightly higher bending moments in the lining compared to those calculated by Muir Wood's method.

The methods based on continuum mechanics have introduced a few factors which were overlooked by some of



$$\lambda = \frac{EI}{R^4} \cdot \frac{z}{E_s}$$

$$\lambda = \frac{EI}{C R^4}$$

$$C = \frac{E_s}{(1+\nu) R}$$

Figure 2.8 Bending moments in the lining as calculated by different methods (after Ebaid and Hammad, 1978)

the preceding methods. The assumptions of continuum mechanics analyses however, limit their use to deep tunnels in a homogeneous, isotropic, elastic ground. The derivation of similar formulas for different boundary conditions or for advanced stress-strain models of soil behaviour would be tedious and formidable. It should also be noted that these methods leave some important factors, such as arching of soil stresses and the effect of construction procedures, to the judgment of the designer.

2.2.5 Finite Element Analyses

The finite element method assumes that the continuum is divided into elements interconnected only at a finite number of nodal points at which some fictitious forces, representative of the distributed stresses actually acting on the element boundaries, are introduced (Zienkiewicz, 1971). Such an idealization made the analysis of many complicated problems in continuum mechanics possible. The significant implications of introducing this method into Geotechnical Engineering practice was described by Morgenstern (1975):

" . . . While less than ten years ago a review of the complexity of soil behaviour would invariably have observed how difficult it is to apply well known aspects of soil behaviour to problems of practical interest, this is no longer true"

The use of the finite element method in analyzing tunneling problems has been replacing closed-form analysis whenever the boundary conditions or soil behaviour model

become complicated. Analysis of unlined shallow tunnels in sensitive and insensitive soft ground were studied by Hoyaux and Ladanyi (1970). Peck et al. (1972) used the finite element method to extend their study (of the behaviour of tunnel lining of intermediate flexibility) to the case of shallow tunnels. An extensive parametric study using plane strain finite element analysis was conducted by Kulhawy (1974, 1975) to evaluate the different factors affecting the behaviour of unlined underground openings. Hanafy (1976) presented a finite element simulation of the time-dependent behaviour of tunnels excavated in rocks. The use of finite element analysis in the New Austrian Tunneling Method has been discussed by many authors, including Swoboda (1979) and Wanninger (1979).

A two dimensional finite element analysis of a lined tunnel usually over-estimates the stresses in the lining. This is a result of the unrealistic assumption that the lining is placed before any release of in-situ stresses in the soil due to the tunnel excavation occurs. A modified plane strain analysis, taking into consideration (empirically) the release of a portion of the in-situ stresses before the interaction starts, could yield more realistic results (see for example: Sakurai, 1977). Another procedure which can circumvent this problem in determining the stresses in a tunnel lining is the coupling of a finite element analysis with field measurements. El-Nahhas (1977) measured the displacement of the internal surface of a

lining and imposed it as a boundary condition in a 2-D finite element mesh. The stresses in the lining were calculated using the deformed shape measured 16 and 134 days after lining installation in the tunnel. The results are shown in Figure 2.9.

The analysis of stresses and deformations around an advancing tunnel using axisymmetrical finite elements was investigated by Ranken and Ghaboussi (1975). They performed a parametric study for the behaviour of lined and unlined tunnels in elastic and elasto-plastic mediums. They showed, as illustrated in Figure 2.10, the importance of including the effect of the tunnel face on the value of liner thrust. A similar analysis for tunnels in soils whose behaviour are time dependent is given by Ghaboussi and Gioda (1976). The simulation of tunnel advance in different soils using axisymmetrical finite elements but with non-symmetrical radial loadings was carried out by Hanafy and Emery (1979).

With the significant improvement in computer efficiency in the past few years, the cost of a true three dimensional analysis is becoming more reasonable. Ghaboussi et al. (1978) suggested that three dimensional analyses may be feasible for the study of underground structures on a case by case basis, but not for parametric studies.

The use of the finite element method as a tool for tunnel design seems very promising. However, its reliability is governed by its ability to model the stress-strain behaviour of soils and the excavation and lining response in

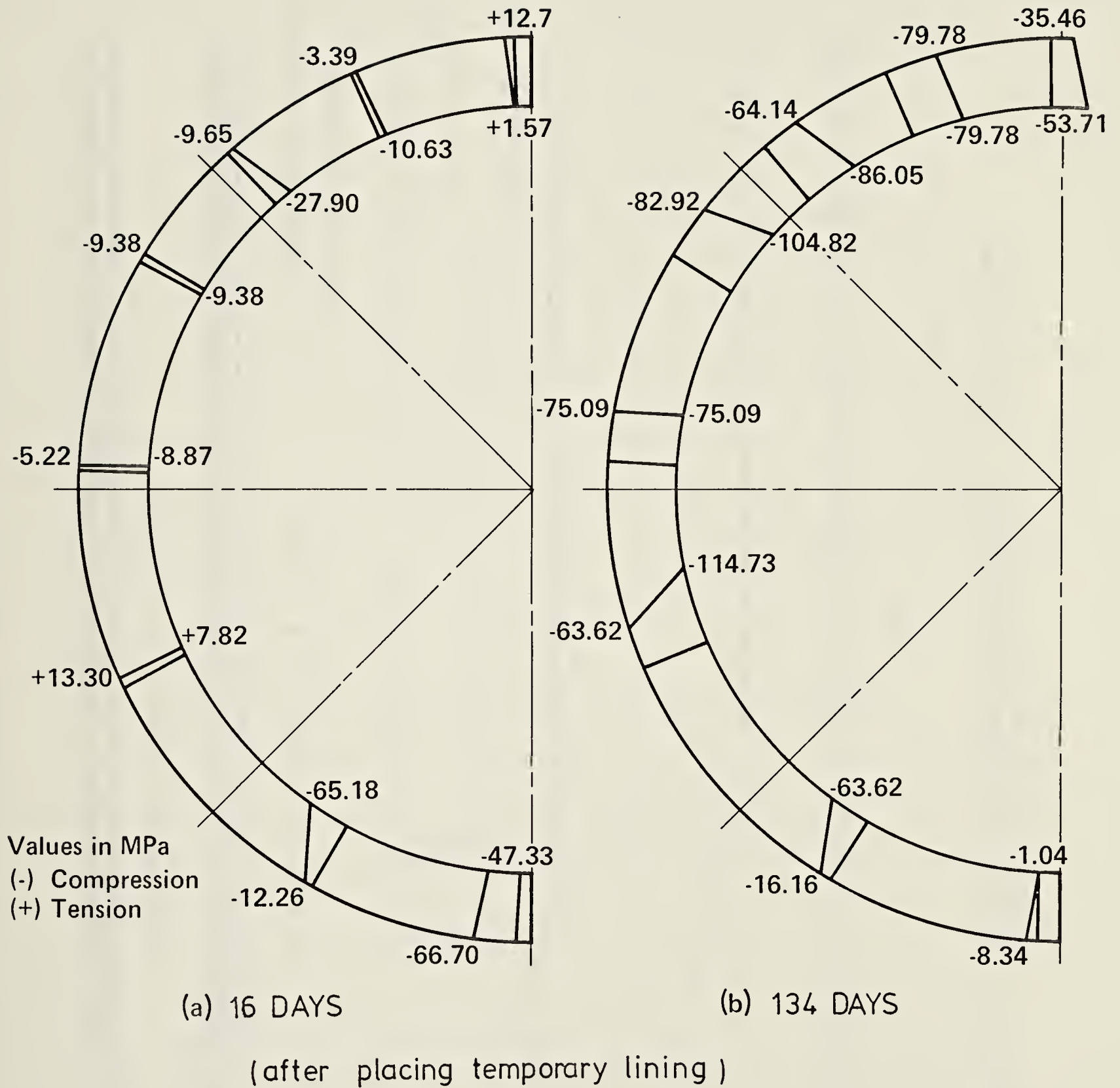


Figure 2.9 Calculated stresses in steel ribs using the field measurements of lining deformation (after El-Nahhas, 1977)

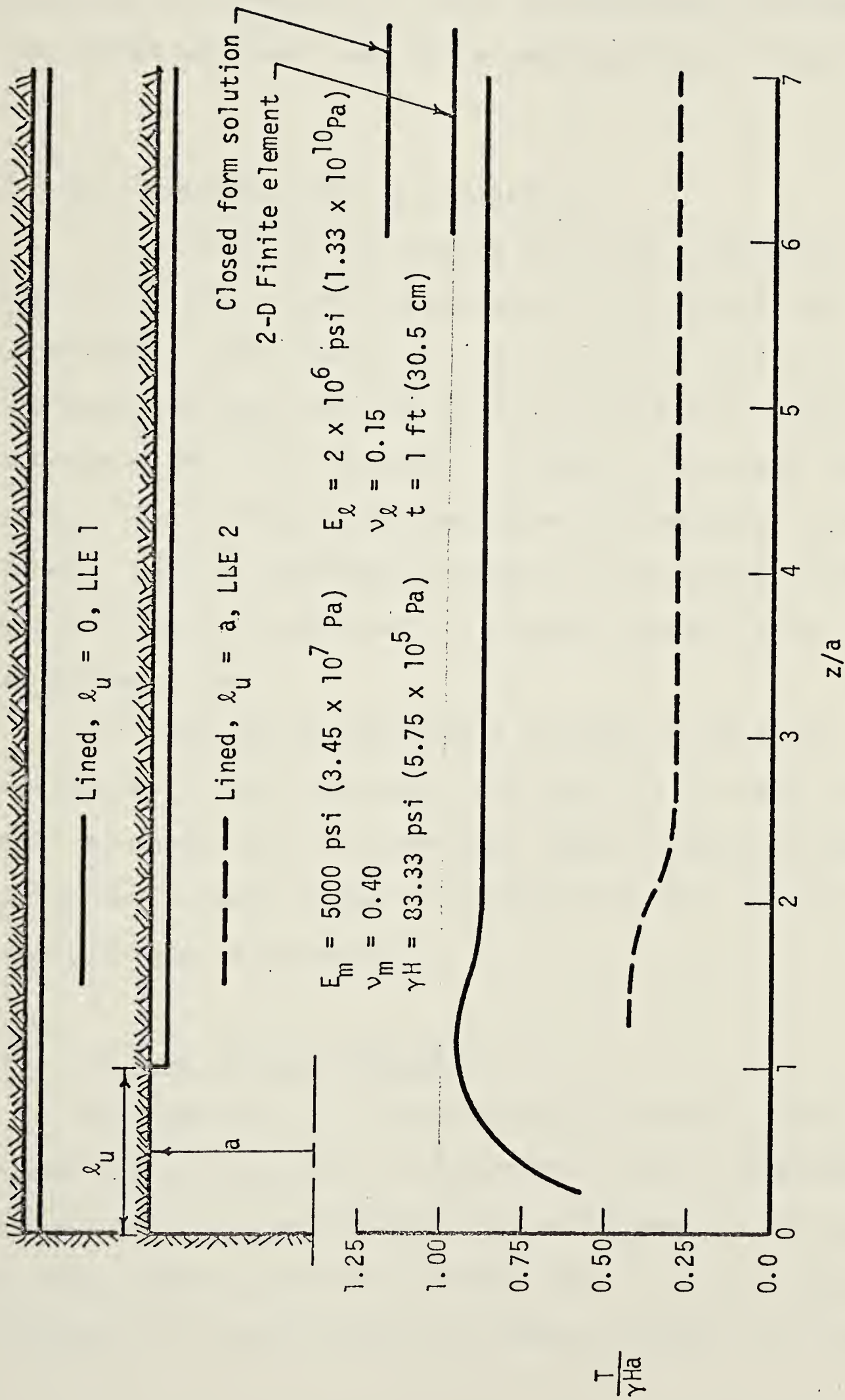


Figure 2.10 Effect of tunnel face on liner thrust (after Ranken and Ghaboussi, 1975)

tunnels. The growing number of case histories that compare the results of finite element analyses with actual field behaviour of tunnels will help introduce more refinement into these analyses, and hence improve their reliability.

2.3 SOIL MOVEMENTS DUE TO TUNNELING

The evaluation and prediction of soil movements associated with tunneling represents the second task undertaken by the designer. The prediction must include both the magnitude and the mode of the surface and subsurface movements, which are essential elements for examining the safety of existing structures above and adjacent to the tunnel. Such an assessment requires an estimate of the total and differential settlement along and perpendicular to an advancing tunnel.

This section of the thesis reviews the methods available in the literature which deal with prediction of soil movements due to tunneling. Some of these methods are described in detail and a discussion of their merits and shortcomings is presented.

2.3.1 Ground Surface Movements

The feasibility of constructing a tunnel under urban areas and city centres is governed by how the expected amount of total and differential settlement of the ground surface compares with that which the existing structures may tolerate. If the expected settlement exceeds the allowable

movements, expensive measures, such as underpinning and soil improvement techniques, must be utilized. The Canadian Foundation Engineering Manual (1978) provides guidelines for the allowable total and differential settlement for different types of buildings. Similar recommendations are given by Bjerrum (1963).

One of the procedures commonly used to estimate the ground surface settlement associated with tunneling is the method described by Schmidt (1969) and Peck (1969). This method is supported by extensive field measurements, which have been accumulated during a period of three decades. It separates the prediction of the settlement trough perpendicular to the direction of tunnel advance into two components; the first is an estimate of the ground loss incurred during tunneling, from which the volume of the settlement trough may be estimated, and the second is a prediction of the distribution of the subsidence, or the shape of the settlement trough, (Peck et al., 1969).

For tunnels in clay, the volume of ground loss (V_1) above unsupported tunnels, (volume of soil displaced across the perimeter of the tunnel), is related theoretically to the overload factor (OFS) as indicated by the equations given in Table 2.3. A comparison between these theoretical relationships and the volume of ground loss reported in different case histories is illustrated in Figure 2.11. Almost invariably, the measurements of ground loss are much less than the theoretical values. This is partly due to the

Table 2.3 Equations of theoretical volume of ground loss above unsupported tunnels in clay. (after Peck et al. 1969)

a) For $\text{OFS} \geq 1$

$$V_1 = \frac{A}{1 + A} \approx A \dots \dots \dots 2.1$$

where $A = 3 \frac{C}{E} \exp (\text{OFS}-1)$

b) For $\text{OFS} \leq 1$

$$V_1 = 3(P_z - P_i)/E = 3 \text{ OFS } C/E \dots 2.2$$

where

$$\text{OFS} = \text{overload factor} = (P_z - P_i)/C$$

C = undrained shear strength

E = elastic modulus

P_z = overburden pressure

P_i = internal pressure (air pressure)

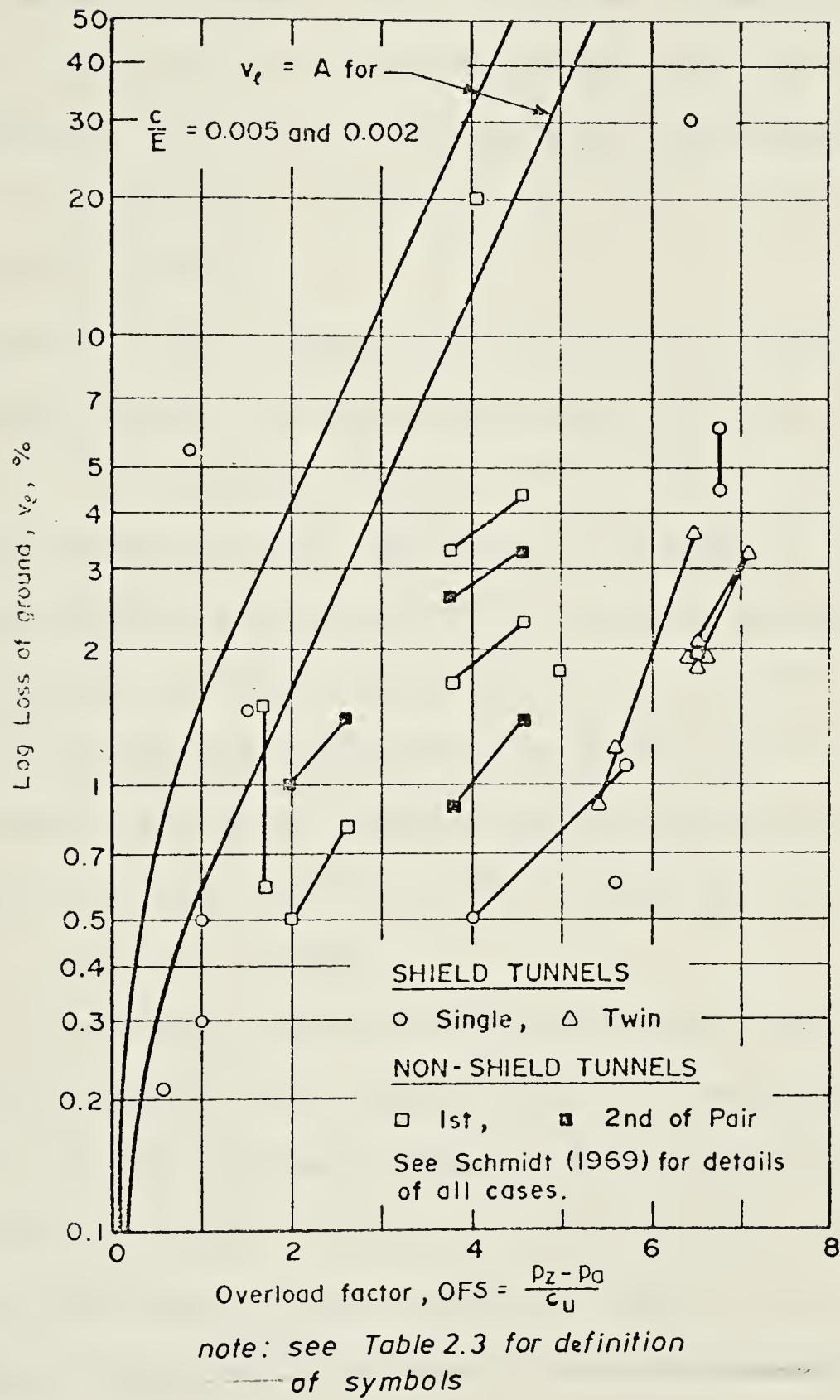


Figure 2.11 Comparison between calculated and measured volume of ground loss (after Peck et al., 1969)

fact that in almost all the case histories used in this comparison, the tunnels are supported at an early stage of construction. If measurements of liner thrust in these tunnels were available, they could be introduced as an internal pressure for calculating the overload factor. Consequently, the points representing the measurements in Figure 2.11 could be shifted to the left, closer to the theoretical values.

Schmidt (1969) suggested that the settlement trough of the ground surface be approximated by the Gaussian error function. The important properties of this function as used for subsidence profiles are given in Figure 2.12. The choice of this function was based partly on some theoretical justification, but more importantly on its very close fit to most of the measured subsidence profiles. The volume of a unit length of the settlement trough (V_s) can be obtained by integration. This results in the following expression:

$$V_s = 2.5 i \underline{S_{max}} \quad 2.3$$

' V_s ' and $\underline{S_{max}}$ are functions of ground loss, but ' i ', (which represents the trough width), is dependent on the geometry of the problem. Based on both theoretical stochastic processes (see Litviniszyn, 1956), elastic analyses and model tests, Schmidt (1969) fitted the following relationship between i and the geometry of the tunnel for clays:

$$i/a = (Z/2a)^{0.8} \quad 2.4$$

where ' Z ' and ' a ' are the depth of the tunnel center line

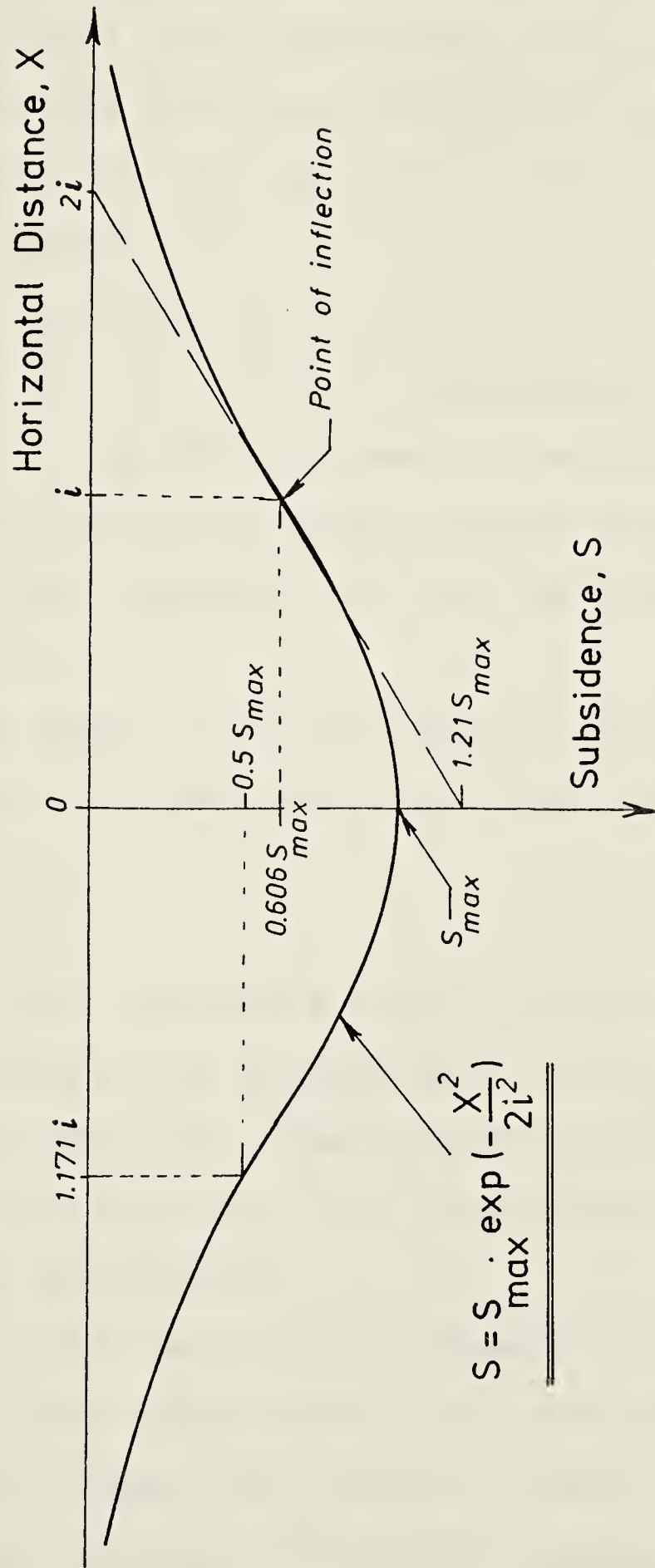


Figure 2.12 The Gaussian distribution function used for describing subsidence profiles (after Peck et al., 1969)

and its radius respectively.

A comparison between this relationship and actual measurements over tunnels in clay is illustrated in Figure 2.13. Similar relationships for different types of soils are given by Peck (1969), as illustrated on Figure 2.14.

For predicting the ground surface settlement above a tunnel excavated in clay, Peck et al. (1969) suggested the following procedure:

1. Estimate the volume of lost ground from Figure 2.11.
2. Use Figure 2.13 to estimate trough width.
3. Calculate the maximum settlement from equation 2.3.
4. Adjust the results for volume changes within the soil.
(However, they suggested that such adjustment is negligible.)
5. The trough shape can be obtained by substituting in the equation for the Gaussian distribution function given on Figure 2.12.

Peck et al. (1972) considered that the volume of the settlement trough can be assumed equal to 1% of the tunnel volume. They pointed out, however, that this value could be as little as half this amount for exceptionally good soil conditions and workmanship.

Attewell and Farmer (1974a) stated that the estimate of a settlement trough based on an error curve profile tends to overestimate settlement for tunnels in rocks, hard clays, and sands above the water table, and to underestimate in the

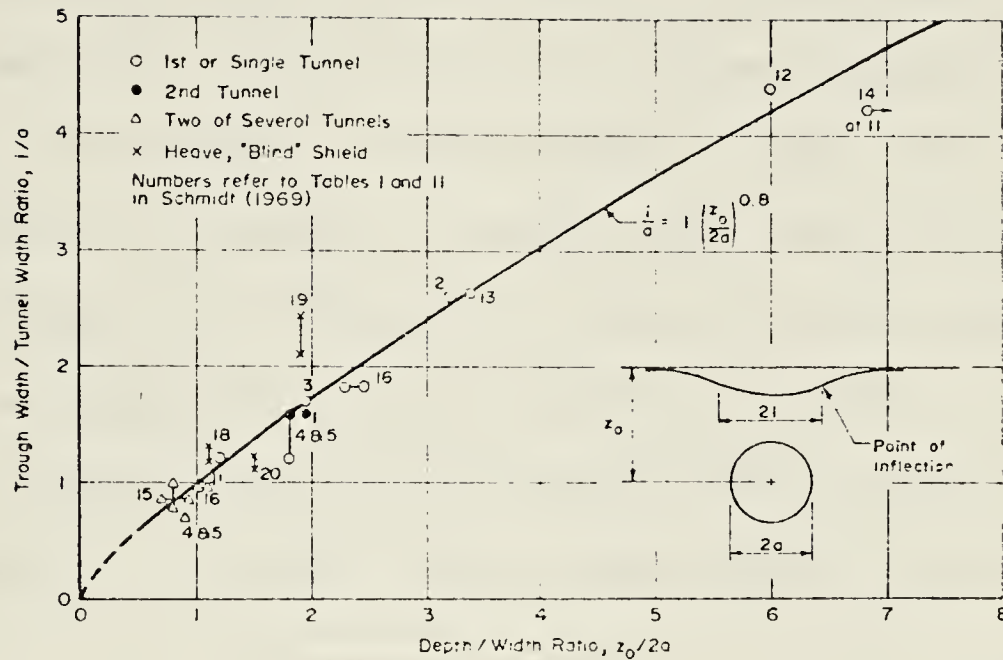


Figure 2.13 Trough width, subsidence over tunnels in clay (after Peck et al., 1969)

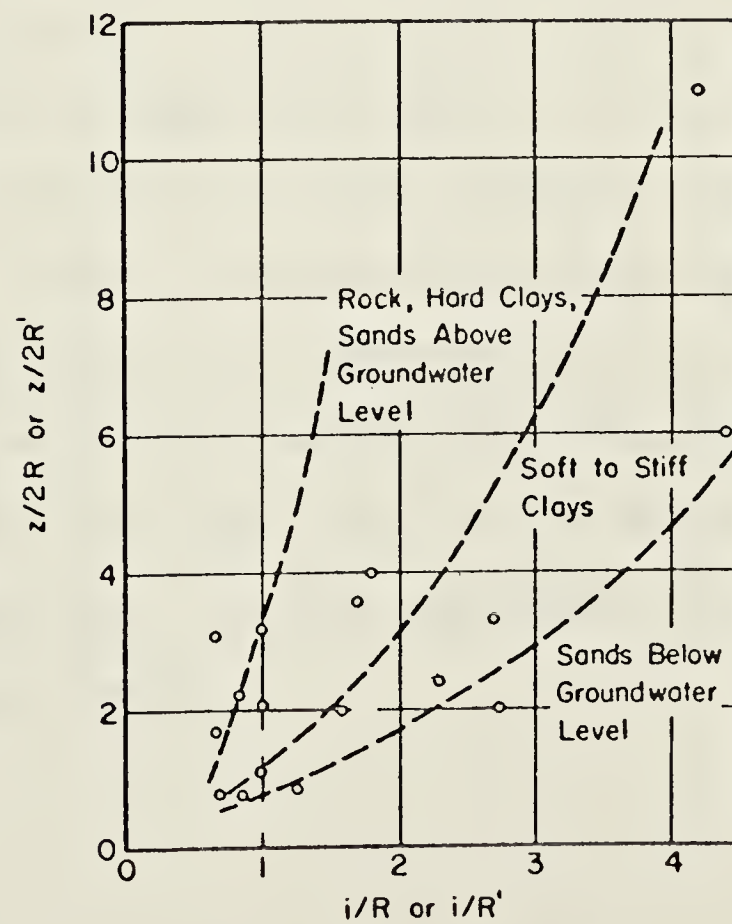


Figure 2.14 Trough width, subsidence over tunnels in different soils (Peck, 1969)

case of cohesionless ravelling materials. They also pointed out that high lateral in-situ stresses (in overconsolidated stiff fissured clays) could result in settlement troughs wider than that calculated by the above procedure. For instance, the width of a settlement trough due to the excavation of a tunnel in London clay, where $K_0=1.65$, was underestimated by 50% when the above procedure was used. They also suggested that the exponent of 0.8 (in equation 2.4) be replaced by 1.0. This modification was supported by the results of a model test as reported by Hudson et al. (1976).

By replotting the data given by Peck (1969) and Attewell and Farmer (1974-b) as shown in Figure 2.15, Attewell and Farmer (1975) demonstrated that an empirical relationship might exist between S_{max} , D and Z . They suggested that such a relationship could provide at least a first estimate of S_{max} for tunnels in clay.

Atkinson and Potts (1977) compared the results of plane strain model tests on sand and overconsolidated kaolin with the field measurements of Washington Metro tunnels and the tunnels constructed in London clay. They suggested the following empirical equations for the standard deviation of the error function, i , which represents the width of the ground surface trough:

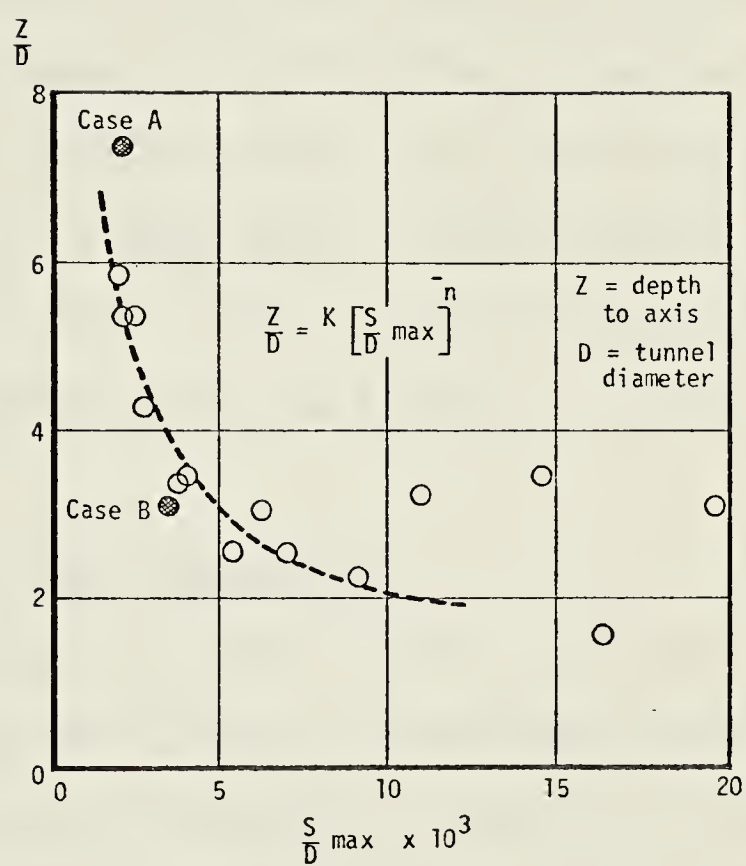


Figure 2.15 Maximum surface settlement related to depth and diameter for tunnels in stiff clay (after Attewell and Farmer, 1975)

for tunnels in sand $i = 0.25 (Z + 0.5 D)$ 2.5

for tunnels in
overconsolidated clays $i = 0.25 (1.5 Z + 0.25 D)$ 2.6

where Z = Depth of tunnel center line

D = Tunnel diameter

In addition to the limitations mentioned above, it should be noted that the use of the error function provides an estimate of settlements for the final transverse section only. The method does not give any indication of the mode of the development or the gradient of settlement in the longitudinal direction which could be more critical to the existing structures above the tunnel.

2.3.2 Subsurface Soil Movements

Designers use estimates of the settlement at the ground surface to assess the safety of buildings above tunnels. Utilization of these estimates to identify the source of lost ground or to study the behaviour of the soil and the safety of structures in the vicinity of the tunnels can be misleading. Realizing this fact, most of the recent tunnel instrumentation programs have employed slope indicators and single and/or multipoint extensometers to monitor subsurface displacements. For example, Hansmire (1975) monitored the soil displacements around Washington Metro tunnels while they advanced through layers of sand, gravel and silty clay. The development of these displacements with the tunnel advance is shown in Figure 2.16. Many field measurements of

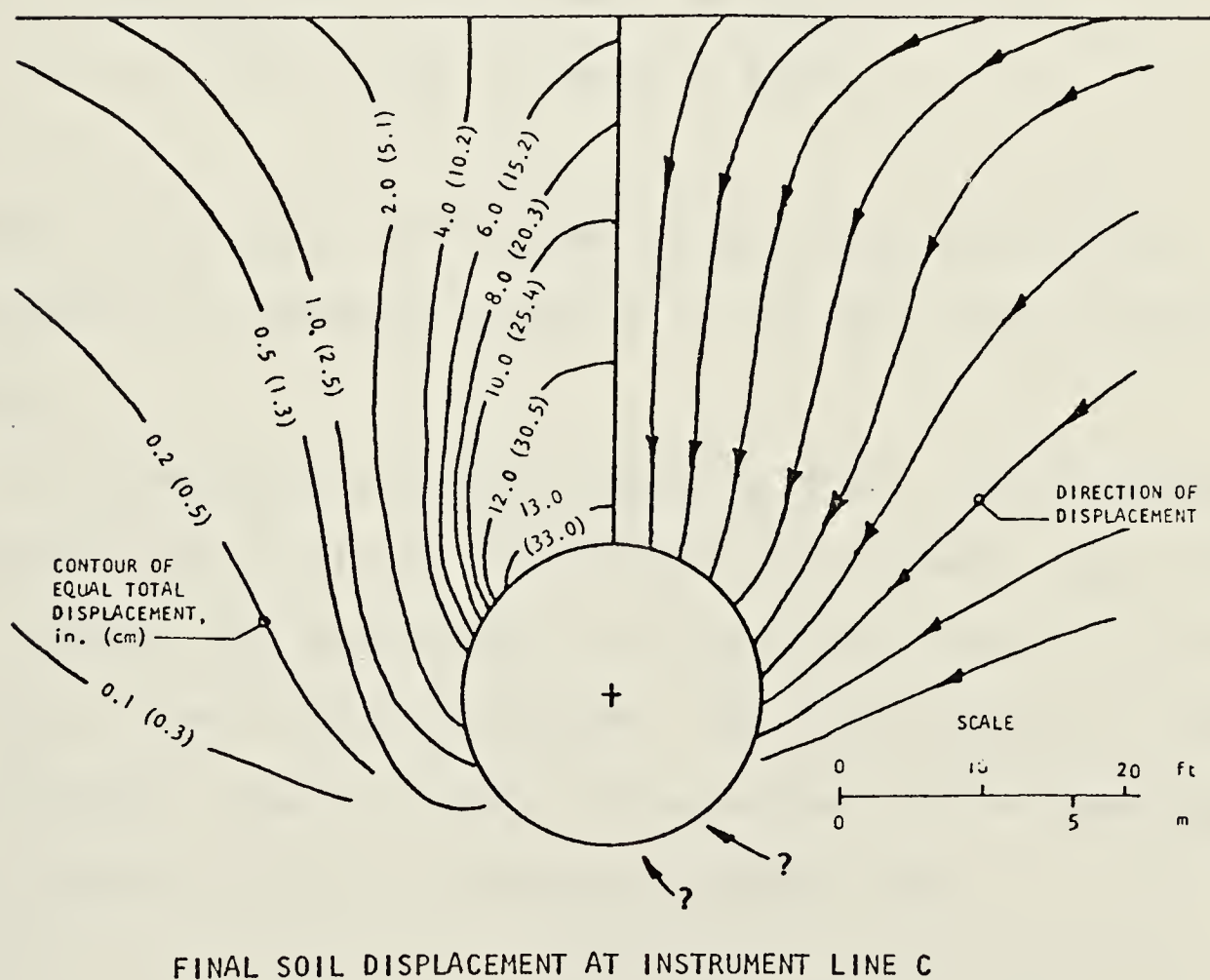
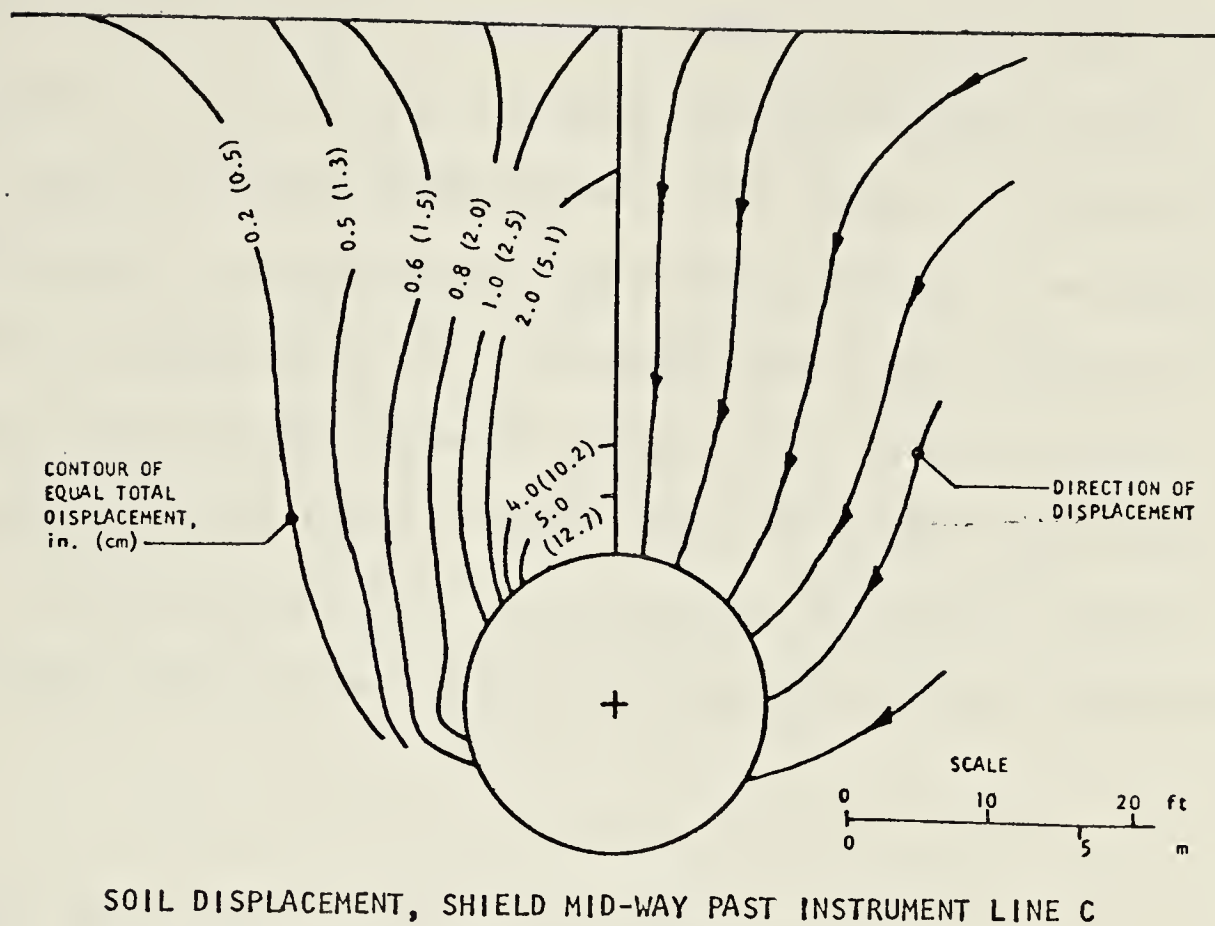


Figure 2.16 Soil displacement around Washington metro tunnels (after Hansmire, 1975)

subsurface soil movements were obtained during the construction of tunnels through London clay and other soil formations in the United Kingdom (Craig and Muir Wood, 1978). Some of these measurements are shown in Figure 2.17.

Attempts to develop an empirical method to estimate the profile of subsurface soil movement has been limited to relating the maximum ground surface settlement (S_s) to settlement at the tunnel crown (S_c). Atkinson and Potts (1977) investigated this relationship using the results of model tests and a few field measurements. They suggested that:

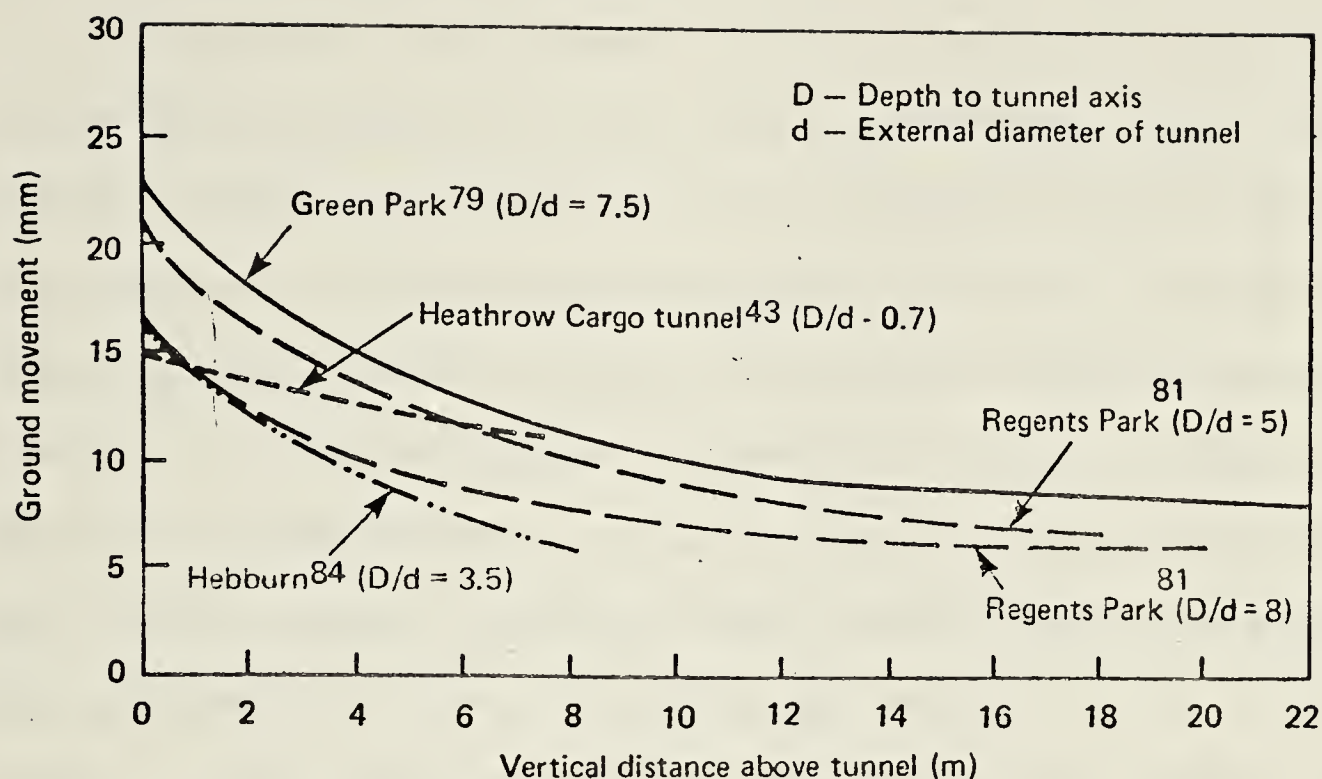
$$S_s / S_c = 1.0 - n (Z - 0.5 D) / D \quad > 0 \quad 2.7$$

where $n = 0.13$ for tunnels in clay

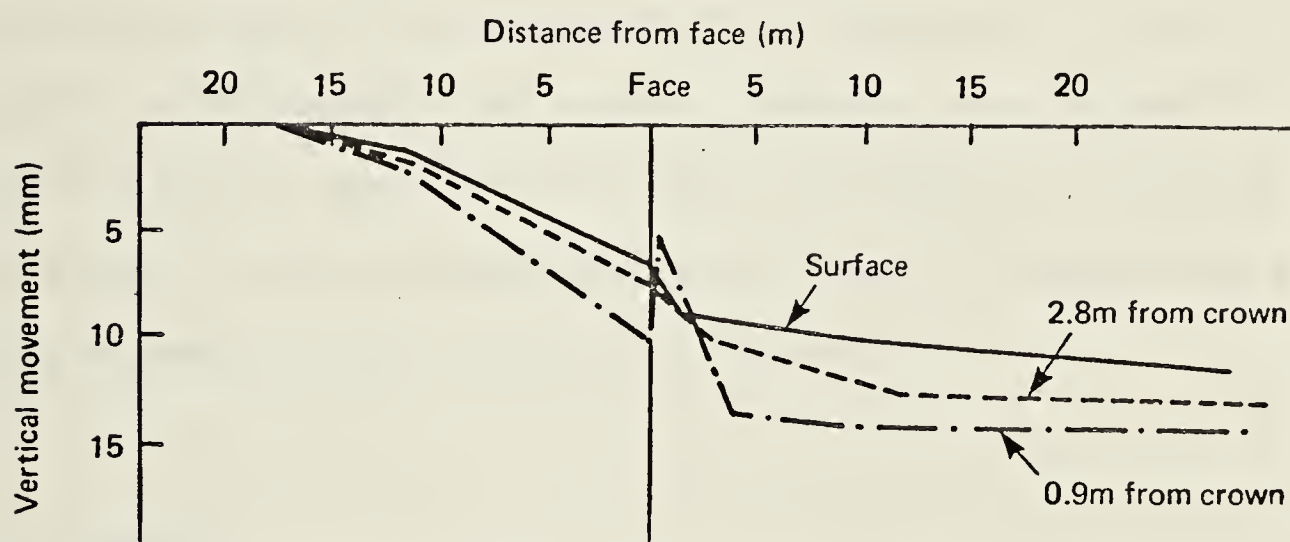
$n = 0.4$ for tunnels in sand

A comparison between this equation and many more field measurements is essential before it can be used for design purposes.

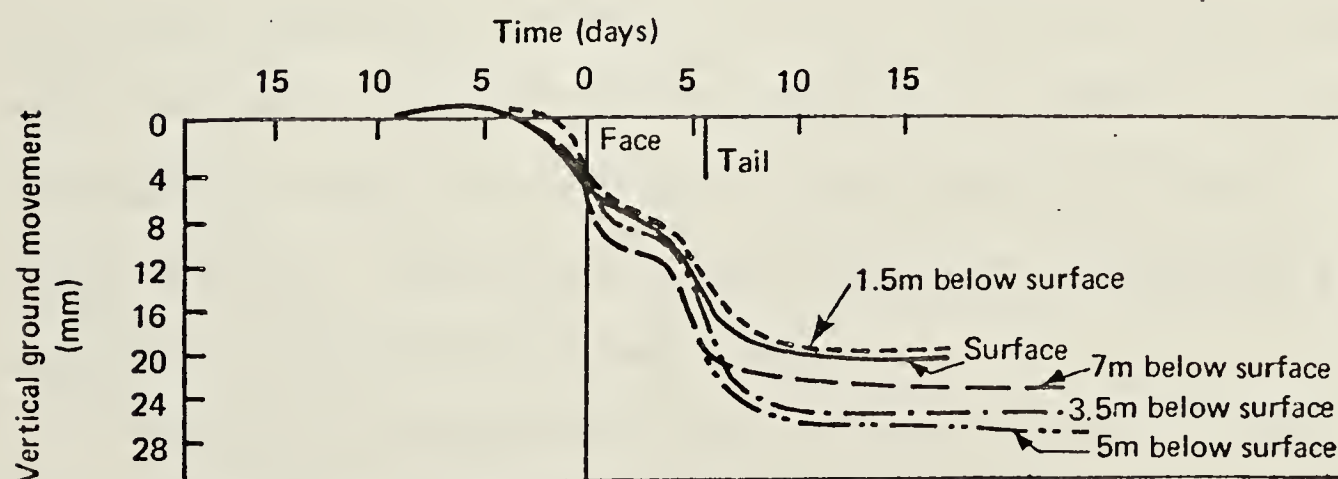
On a few occasions, the subsurface soil displacements measured in the field or those measured in model tests were used to study the development of the strain field in the vicinity of the tunnel (Atkinson, 1973 and Hansmire, 1975). These studies, however, were not extended to the development of the spatial strains around the tunnel face.



(a) Ground movements on vertical section through tunnel centreline



(b) Ground movements for Heathrow Cargo tunnel



(c) Ground movements at LTE running tunnel at New Cross

Figure 2.17 Subsurface soil displacement measured around tunnels in U.K. (after Craig and Muir Wood, 1978)

2.3.3 Finite Element Analyses

Since the finite element method treats the soil and the lining simultaneously in one consistent model, most of the studies reported in section 2.2.5 consider the analysis of deformations, strains and stresses in the soil around the tunnel as well as the lining. Of special interest here, however, is the work given by Ghaboussi et al. (1978) on the analysis of subsidence over soil tunnels. They showed that the finite element analyses often overestimate the width of the settlement trough. It was suggested that this is the result of the incapability of linearly elastic models (and even most of the elasto-plastic material models) of producing high shear strains which develop in the soil mass in the vicinity of the tunnel. Despite this present limitation of the finite element analysis, the method seems to offer the most promising technique for analyzing soil displacements associated with tunnels.

2.4 SUMMARY

This chapter presents a review and discussion of the different methods available in the literature which deal with the main elements of the design of tunnels in soil including an analysis of the lining and an estimate of soil deformations. The methods were classified according to the concepts and techniques employed.

From the discussion of the lining design, it was pointed out that the methods based on earth pressure

theories and the subgrade reaction theory suffer some serious drawbacks regarding the applicability of their basic assumptions to the actual behaviour of the tunnel lining and the surrounding soil. The ground and support reaction curves offer a more realistic representation of the interaction sequence of the lining with the surrounding soil. The merit of these curves is as a tool for qualitative discussions of some of the parameters involved in the design of linings for soil tunnels. However, some of their shortcomings must be dealt with before their use can be extended to quantitative design.

The assumptions employed in the tunnel lining design methods based on continuum mechanics limit their use to deep tunnels in homogenous, isotropic, elastic ground only. The derivation of similar analyses for different boundary conditions or for advanced stress-strain models of soil behaviour would be tedious and formidable. These methods leave some important factors, such as arching of soil stresses and effect of construction procedures, to the judgment of the designer.

The use of the finite element method as a tool for tunnel design seems promising. However, its reliability is governed by its ability to predict the behaviour and performance of real tunnels. The growing number of case histories comparing the results of finite element analyses to actual field measurements will help to refine the method and hence improve its reliability.

Available methods of predicting soil movements associated with tunneling in soils were reviewed. The empirical use of the error function for approximating the final lateral profile of the settlement trough was described and its limitations were discussed. The lack of similar empirical evaluations for the settlement of the ground surface in the longitudinal direction, and for the subsurface settlement profile, was pointed out. The prospect of using the finite element method to fill this gap seems the most promising.

CHAPTER 3

THE EXPERIMENTAL TUNNEL

3.1 INTRODUCTION

Tunnel construction in the City of Edmonton began in 1955 when a system of interceptor sewers and storm drains was installed (Beaulieu, 1972). Tunneling activity has been continuous since then, concurrent with the growth of the city.

Edmonton Water and Sanitation Department builds about five kilometers of tunnels annually using its own crews and equipment. Their past experience has been mainly with a two-phase lining system which involves a temporary lining followed by a cast-in-place permanent support. The geotechnical performance of the Edmonton Rapid Transit tunnels, which were constructed using this technique, was investigated and reported by Eisenstein and Thomson (1978). The results of a modest instrumentation program implemented in two sewer tunnels constructed using the same technology during 1977 are given by Thomson and El-Nahhas (1980).

In 1978, a new tunnel construction method using a precast segmented concrete lining was introduced on an experimental basis in Edmonton. The construction started on a tunnel in early 1979 in which the segmented lining was used in a section of construction. This is the first time precast concrete segments have been used to line a tunnel in

the overconsolidated soils of the Prairies.

The conventional two-phase support system and the precast segmented lining were used in two separate parts of the tunnel. In order to compare the performance of the two lining systems and, in particular to study the performance of the new lining, a field instrumentation program was implemented to monitor the stresses induced in the two types of lining upon installation and to observe the accompanying deformation of the surrounding soil mass.

The experimental tunnel was constructed under 125 Avenue, north of the Edmonton Municipal Airport (Figure 3.1). This tunnel will be used as a main storm sewer for a new freeway (Yellowhead-Trail) which is presently under construction. The tunnel now extends south under 122 Street to 111 Avenue, where it joins a main sewer line. On average the tunnel is 27 meters below ground surface and has an excavated diameter of 2.56 metres.

Since the behavior of tunnels is highly dependent on both the construction technology and ground condition, careful examination of these two factors constitute an essential part of any tunnel instrumentation program. This chapter summarizes the general geology of Edmonton area and presents the subsurface soil condition along the experimental tunnel in detail. It also contains a description of the construction procedures employed in this tunnel.

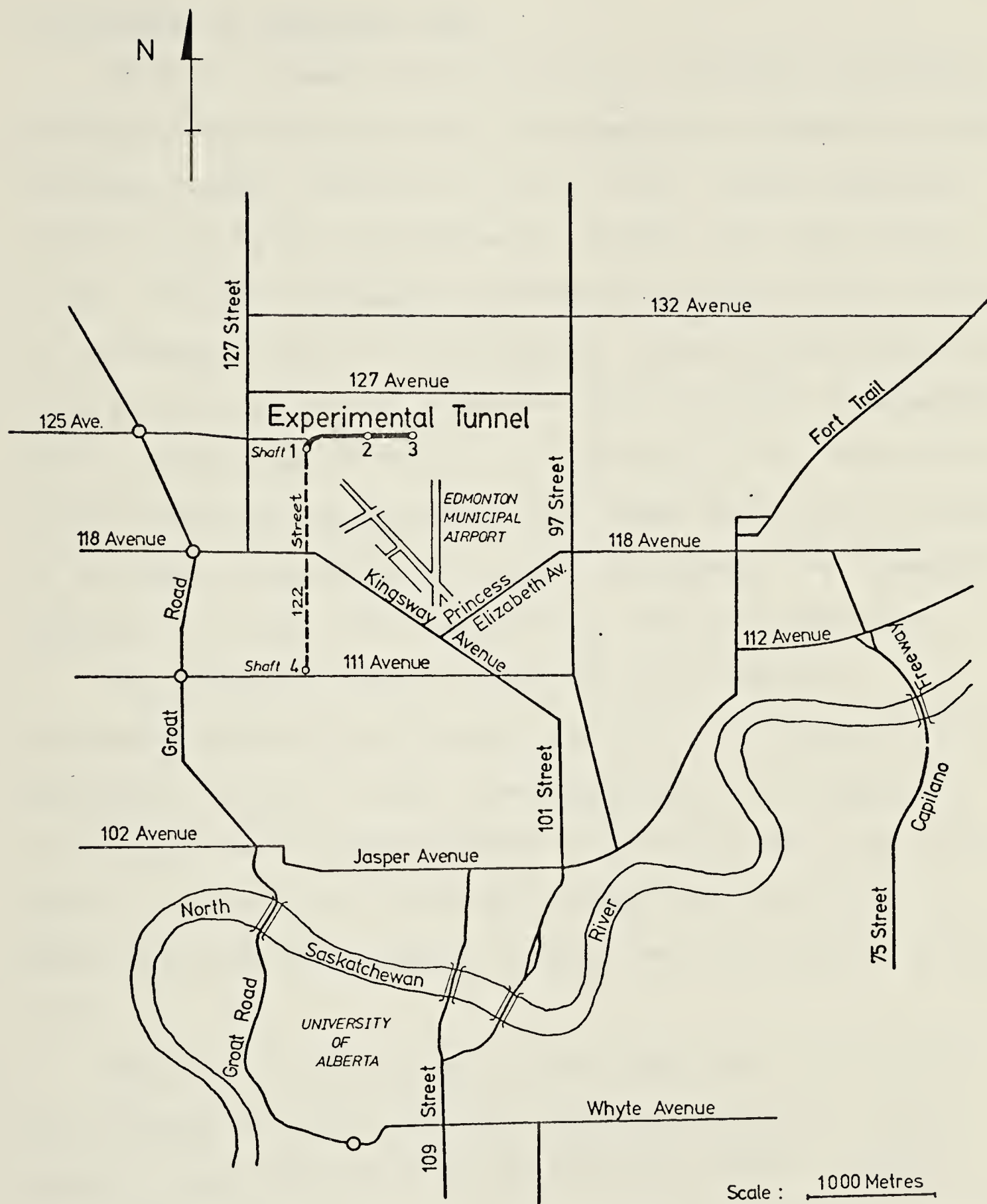


Figure 3.1 Location of the experimental tunnel

3.2 GEOLOGY OF EDMONTON AREA

Table 3.1 summarizes the currently accepted Quaternary geology of the Edmonton area. The bedrock in Edmonton is the Horseshoe Canyon Formation (Irish, 1970) (termed Edmonton Formation by Kathol and McPherson (1975)) and consists of strata of Upper Cretaceous age which, within the city, vary in thickness from 140 to 190 metres. These strata consist of fine-grained bentonitic sandstone and siltstone interbedded with, and grading vertically and laterally into, bentonitic silty claystone and mudstone. Coal seams and bentonite beds of variable thicknesses are common throughout the formation together with beds of claystone and sideritic sandstone.

The Horseshoe Canyon Formation has a regional northwest-southeast strike and a dip of 3 to 4 m/km to the southwest (Carlson, 1967). The topography of the upper surface of the Horseshoe Canyon Formation shows a series of dendritic preglacial drainage systems dominated by the Beverly Valley which passes through the north-center of the city.

Most of the preglacial valleys and their tributaries are floored with late Tertiary sands and gravels. These deposits were derived from conglomerates which, in turn, were derived from the Cordilleran region to the west which, in preglacial times, covered extensive uplands areas (Westgate, 1969). The conglomerates have been reworked and deposited in the early Pleistocene forming what is now known as Saskatchewan Sands and Gravels. Their depositional

Table 3.1

Quaternary geology of Edmonton area (after May and Thomson, 1978)

Cenozoic	Quaternary	Holocene	Alluvium, Organic deposits, recent lake deposits.
		Pleistocene	Lacustrine sand, silt and clay, organic deposits, aeolian sand and silt, river Alluvium
			Till
			Sand and sandy gravel, some silt and clay
			Till
	Tertiary (undivided)	Saskatchewan gravels and sands	

environment was established by the many preglacial structures observed in exposures in a gravel pit (Westgate and Bayrock, 1964). In some locations the Saskatchewan Sands and Gravels are saturated and the water may be under pressure. This could cause tunneling problems if a tunnel advancing through bedrock intersects or passes very close to but under a preglacial valley (Oster, 1975).

Westgate (1969) has considered that the Edmonton area has experienced at least two different glacial advances resulting in two distinct glacial till sheets. The first ice advance invaded the area more than 40,000 years ago and deposited the lower till, which directly overlies the Saskatchewan Sands and Gravels or bedrock. The lower till is characterized by its grayish color and rectangular joint system. The pebbles in this till are oriented NW-SE, which indicates the direction of glacial movement. In some areas large blocks of bedrock were found embedded in this till sheet.

Pebble orientation in the upper till and sole markings at the base of this sheet show that the second ice advance invaded the area from the northeast. This till has a brownish color and is columnar jointed. The tills are separated in places by a layer of yellowish, clean, moderately sorted sand, which is termed the Tofield Sand which may vary in thickness from 1 to 10 metres.

Despite the apparently different physical characteristics of the upper and lower tills, their

geotechnical behavior is similar. The geotechnical properties of the Edmonton tills, as reported by various authors, is summarized in Table 3.2. Both tills contain sand lenses which vary in size and shape from irregularly contorted inclusions less than 10 cm in size to more lenticular shaped bodies continuous over distances in excess of 50 metres (May and Thomson, 1978). Most of these lenses are saturated and the water may be under pressure. Similar tunneling problems may be encountered, as when tunneling close to preglacial valleys, although these aquifers are much less extensive.

The two till sheets contain large boulders, up to 2 metres in diameter. These boulders are smooth, semirounded and of Canadian shield origin. The tunnel advance is usually delayed, from a few hours to a day or so, when the drilling machine encounters a boulder larger than the opening in the face of the mole. In most cases the boulders must be removed manually, using jackhammers, before the mole can advance again.

The till sheets are overlain by clays and silty-clays of a buff to dark brown color. These sediments were deposited in glacial Lake Edmonton, which was originally formed as a superglacial lake (Hughes, 1958). It then enlarged into a proglacial lake when the drainage to the northeast became blocked as a result of the southward advance of a later glacier that did not enter the Edmonton area. The lake deposits are covered in some areas with fill,

Table 3.2 Geotechnical Properties of Edmonton Till (After Thomson and El-Nahas, 1980)

Reference	Morgenstern and Thomson (1970)	DeJong and Harris (1971)	Thomson and Yacyshyn (1977)	El-Nahas (1977)	Eisenstein and Thomson (1978)
Density (kN/m ³)	-	19-22	-	22	20.6-21.2
Natural Moisture Content %	12-22	11-19	15	12	12-20
Liquid Limit %	28-48	22-42	40	31	20-40
Plastic Limit %	12-22	9-20	20	15	12-20
% Clay	20-30	20	20-30	42	20-30
% Silt	-	38	25-35	31	25-35
% Sand	-	42	40-50	27	40-50
Void Ratio	-	0.35-0.4	-	0.36	-
Degree of Saturation %	-	75-95	-	89	-
Undrained Strength (kPa)	345-828	140-240	140-245	-	140-245
Peak Angle of Shearing Resistance	-	-	37°	-	-
Peak Cohesion (kPa)	-	28	-	-	-
Standard Penetration (blows/0.3 m)	-	60-150	-	-	40-60 some over 100

organic material or alluvial deposits.

3.3 SOIL PROFILE ALONG THE EXPERIMENTAL TUNNEL

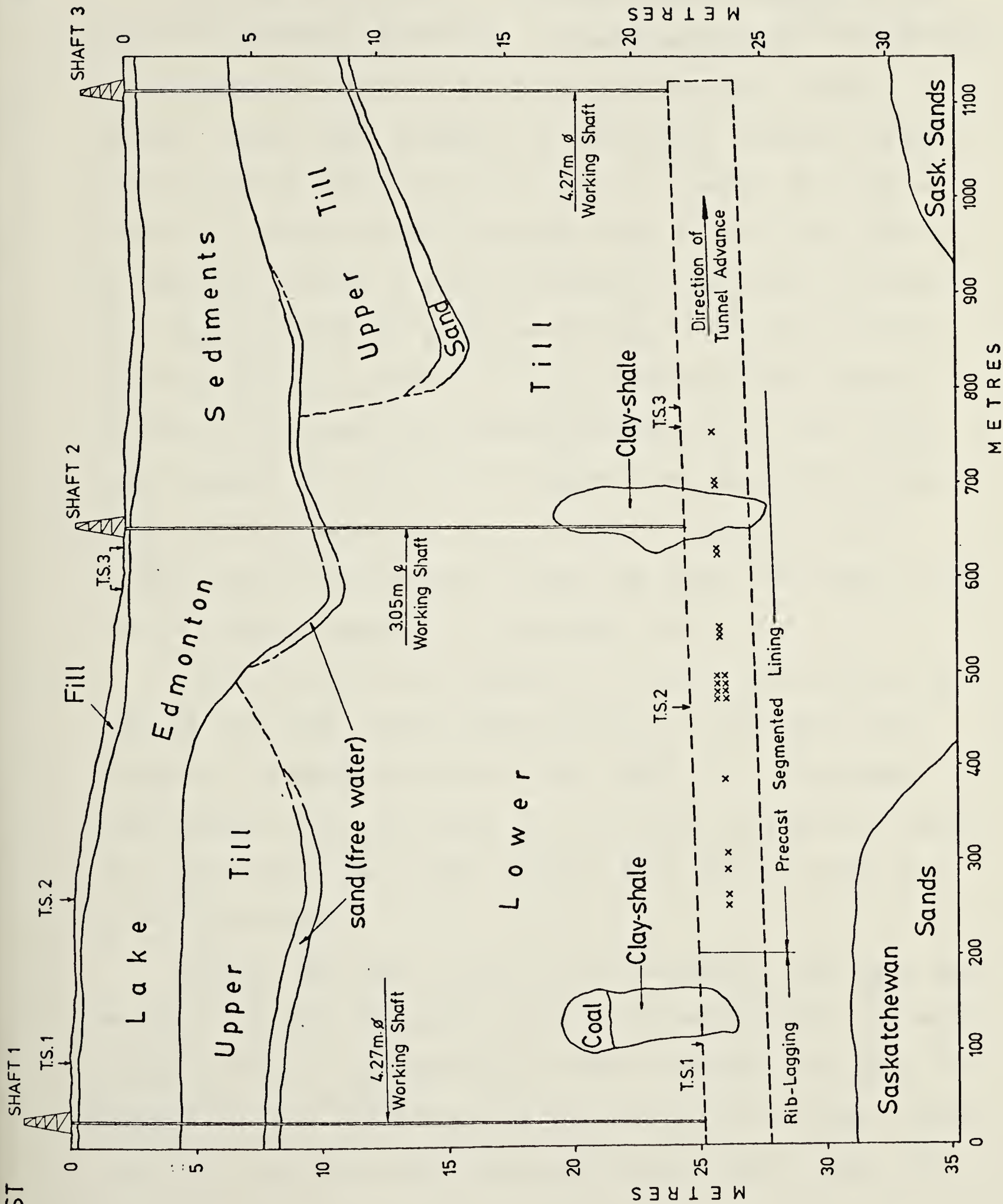
The subsurface soil profile along the experimental tunnel is given in Figure 3.2, based on borehole logs provided by the City of Edmonton and augmented by data gathered by the author during the installation of soil instrumentation.

The tunnel drilling machine passed through two large intra-till bedrock blocks, which consisted of weathered layers of coal and clayshale relatively dryer than the glacial till. The location of large boulders encountered during the tunnel advance and which delayed construction for a few hours are marked along the tunnel center line in Figure 3.2. The mole encountered only a few small sand lenses filled with water which caused minor problems. The free water in the Tofield sand and at the bottom of the lake deposits caused some problems during the installation of soil instruments at the test sections, and during the sinking of construction shafts.

The extension of the experimental tunnel under 122 Street was constructed using the conventional rib and lagging lining. Power holes, about 1 m diameter, were drilled from the surface at a spacing of 250 metres to provide an access for ventilation and electric power. Disturbed samples and undisturbed shelby tubes, 10 cm diameter, were obtained during the sinking of these holes.

WEST

EAST



x: Boulder encountered
by the mole

T.S.: Test Section

Figure 3.2 Subsurface soil profile along 125 Avenue

The soil profile along the 122 Street based on this information is given on Figure 3.3.

The large diameter of the power holes, compared with the 15 cm diameter boreholes, allowed additional information to be gathered concerning presence of boulders in the till sheets. These rocks stopped the sinking of a power access hole 80 metres south of 118 Avenue at a depth 16.5 metres below the ground surface. The drilling of this hole had to be restarted twice, 2 and 12 metres to the south, to avoid this large boulder or group of boulders. The same problem was encountered at depths 18 and 22 metres below ground surface at the new two locations respectively. One large rock stopped the tunnel drilling machining about 400 metres north of 118 Avenue for about a week. In general, the boulders were encountered in both the upper and lower tills, with a higher frequency in the lower till.

The soil profiles (Figures 3.2 and 3.3) also show that some of the sand lenses actually exist in the low-lying areas of the upper surface of the lower till. The number of sand pockets near the crown of the tunnel extension (Figure 3.3) were relatively high; however they did not cause any serious problems.

Neither the power holes nor the borehole logs were deep enough to locate the upper surface of the bedrock. The maps given by Kathol and McPherson (1975) indicate the depth of bedrock in this area to be in the order of 53 metres. These maps also indicate that the experimental tunnel under 125

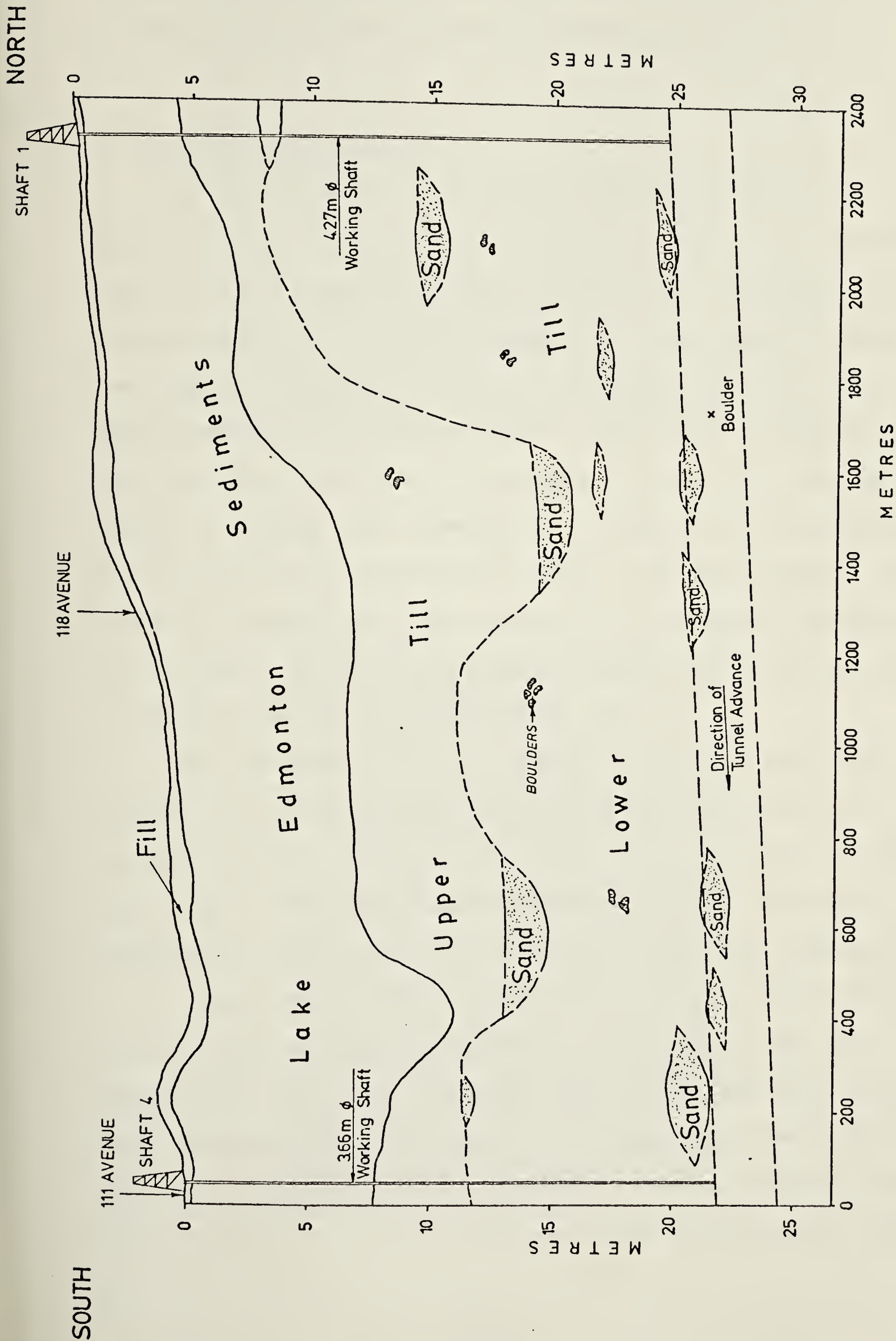


Figure 3.3 Subsurface soil profile along 122 Street

Avenue is located near the base of the northern valley wall of the main preglacial channel (Beverly Valley).

3.4 CONSTRUCTION DETAILS

The construction of a 2.56 m diameter tunnel in Edmonton usually starts with the sinking of a construction shaft, 4.25 m diameter, using hand methods. The shaft is lined, during sinking, with steel ribs and timber lagging. The lagging is wedged to the soil outside the ribs. When the shaft reaches the required depth, the tunnel is advanced a short distance horizontally by hand mining. This part of the tunnel is termed the 'undercut'. It usually has a horseshoe shape with overall dimensions larger than the diameter of the drilling machine. The undercut is extended on both sides of the shaft, with a wide space to allow the installation of a double track for switching mine cars.

The main shaft is usually provided with a skip hoist (Plate 3.1) on the ground surface, which controls the elevator used to move materials and crews into and out of the tunnel. The tunnel boring machine is then lowered through the shaft and starts advancing from the undercut.

In the experimental tunnel (Figure 3.1), shaft #1 which is located near the intersection of 122 Street and 125 Avenue was sunk first and provided with an undercut. The mole advanced southward under 122 Street, and then removed upon reaching shaft #4 on 111 Avenue. It was lowered again through shaft #1 in late 1978 and advanced northward into

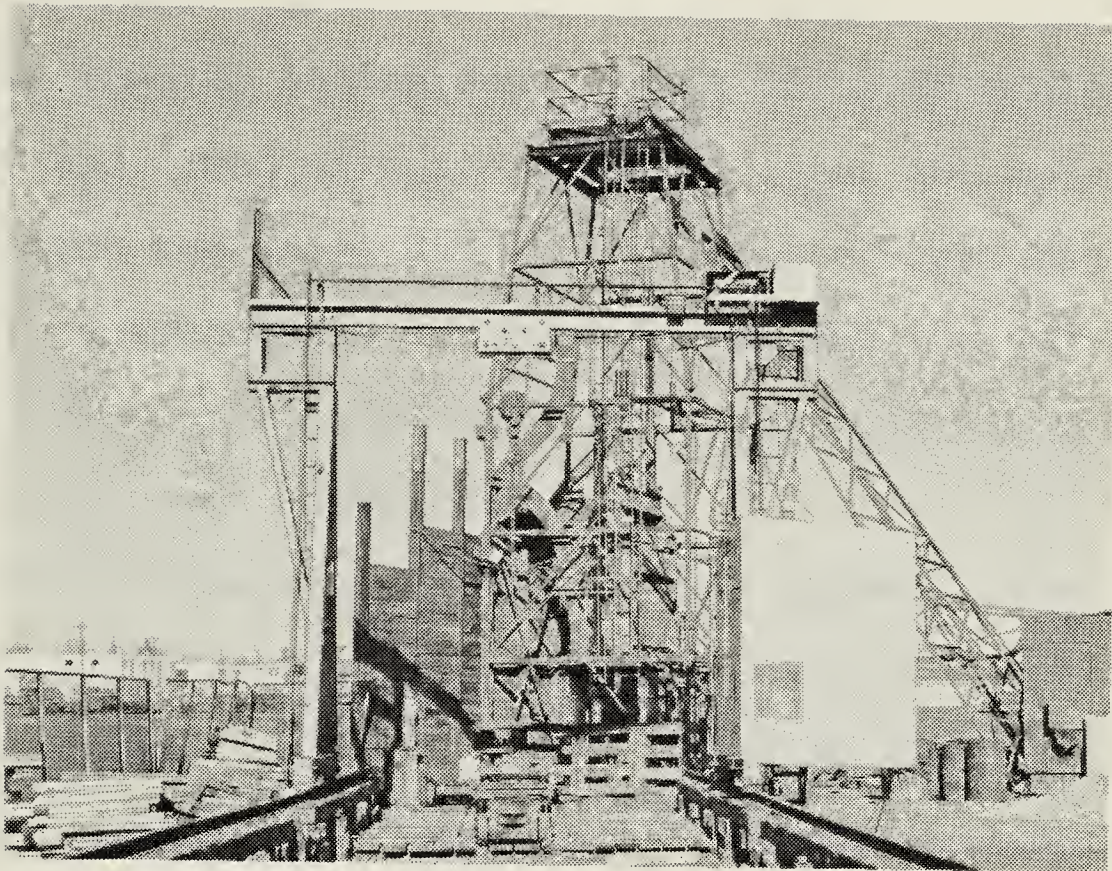


Plate 3.1 Skip hoist at the main shaft of the experimental tunnel

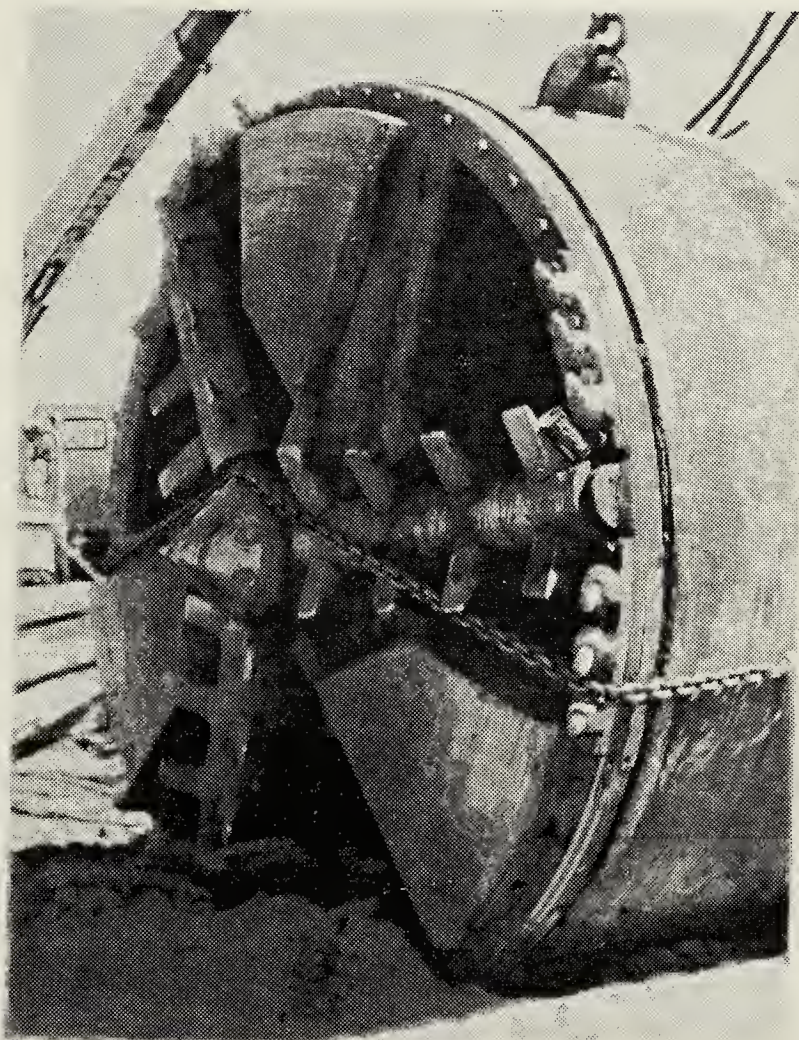


Plate 3.2 Tunnel drilling machine (Lovat model M-100 series 1900)

the curve turning to the east. Shaft #2, 3.05 m diameter, was sunk and lined with steel plates after the mole passed its location and shaft #3, 4.27 m diameter, was dug when the tunnel face approached its location during the period between November and December 1979. The mole was finally taken out through shaft #3.

The mole used in excavating this tunnel, shown in Plate 3.2, was built by Lovat Tunnel Equipment Inc., Ontario (Model M-100 Series 1900) and is owned by the City of Edmonton. Figure 3.4 shows a longitudinal section through this machine and its specifications are given in Table 3.3.

The conventional lining and precast segmented lining systems were used in two separate parts of this tunnel. The segmented lining was used for 920 metres west of shaft #3 and the remainder of the tunnel was lined with the conventional lining.

3.4.1 Conventional Lining System

This system is a two-phase lining; a primary, or temporary, and a secondary, or final lining (Plate 3.3). As shown in Figure 3.5, the primary lining comprises segmented steel ribs (WF100 x 19), 1.5 metre center to center, and 5 x 20 cm timber lagging placed between the webs of successive ribs. The secondary lining is a shell of cast-in-place, plain concrete, 20 cm thick.

The rib and lagging system is assembled within the shield of the mole. The drilling machine is then advanced by

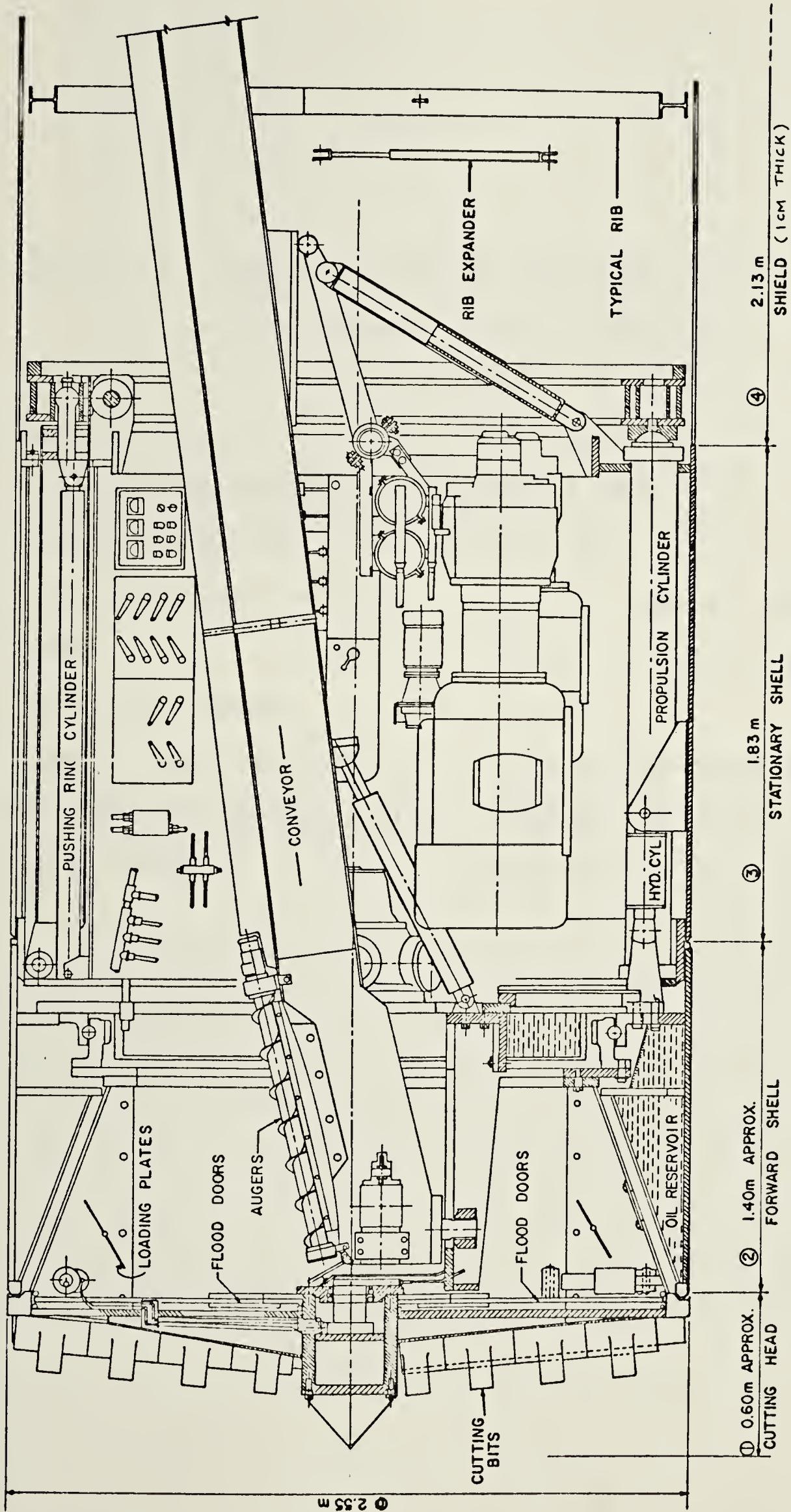


Figure 3.4 Tunnel drilling machine (Lovat M-100 Series 1900)

Table 3.3 Specifications of the tunnel boring machine
(Lovat Model M-100 Series 1900)

Bore	: 2.56 m
Cutting head torque	: 268.8 KN.m
Propulsion thrust	: 5.91 MN
Front Unitized Conveyor	: 0.61 m. wide x 7.62 m. long
Power	: 150 HP (112 KW) Electric motor
Rotational speed	: 10 rpm
Length (four sections)	: 5.94 m (approximate)
Maximum advance per thrust	: 1.68 m
Total weight	: 418 KN

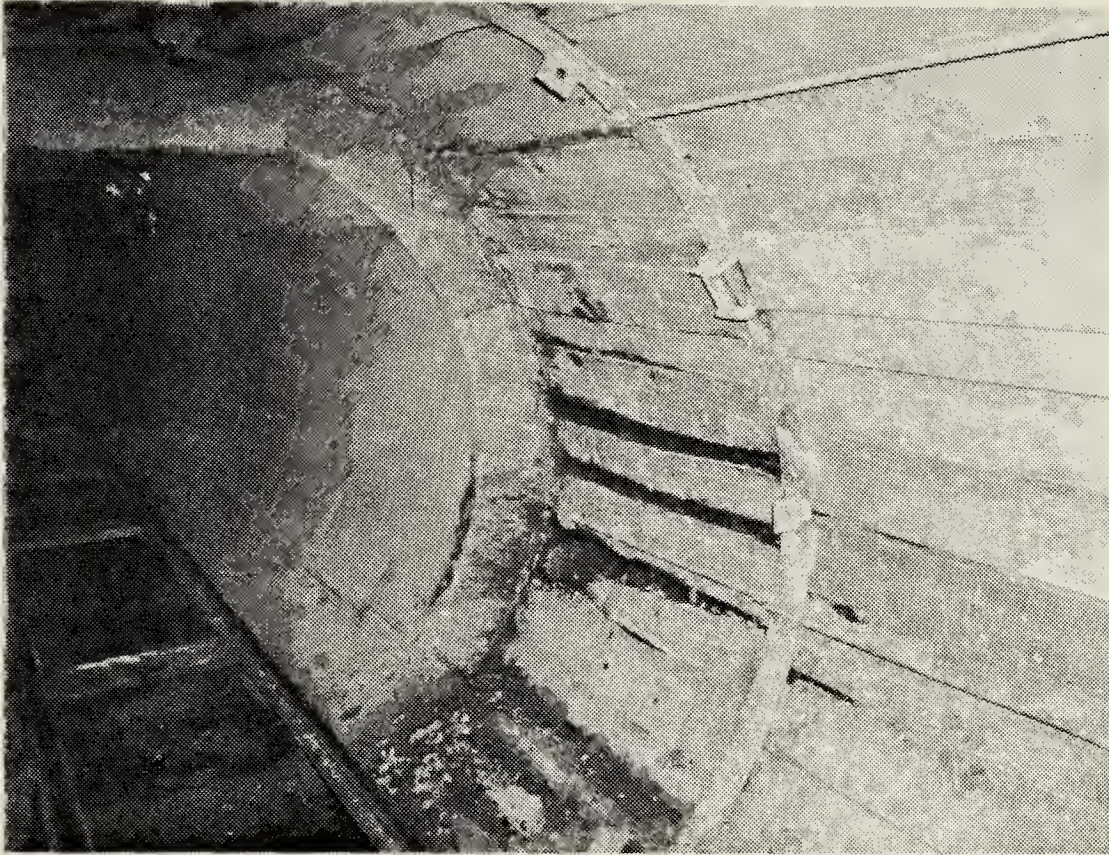


Plate 3.3 Conventional lining system

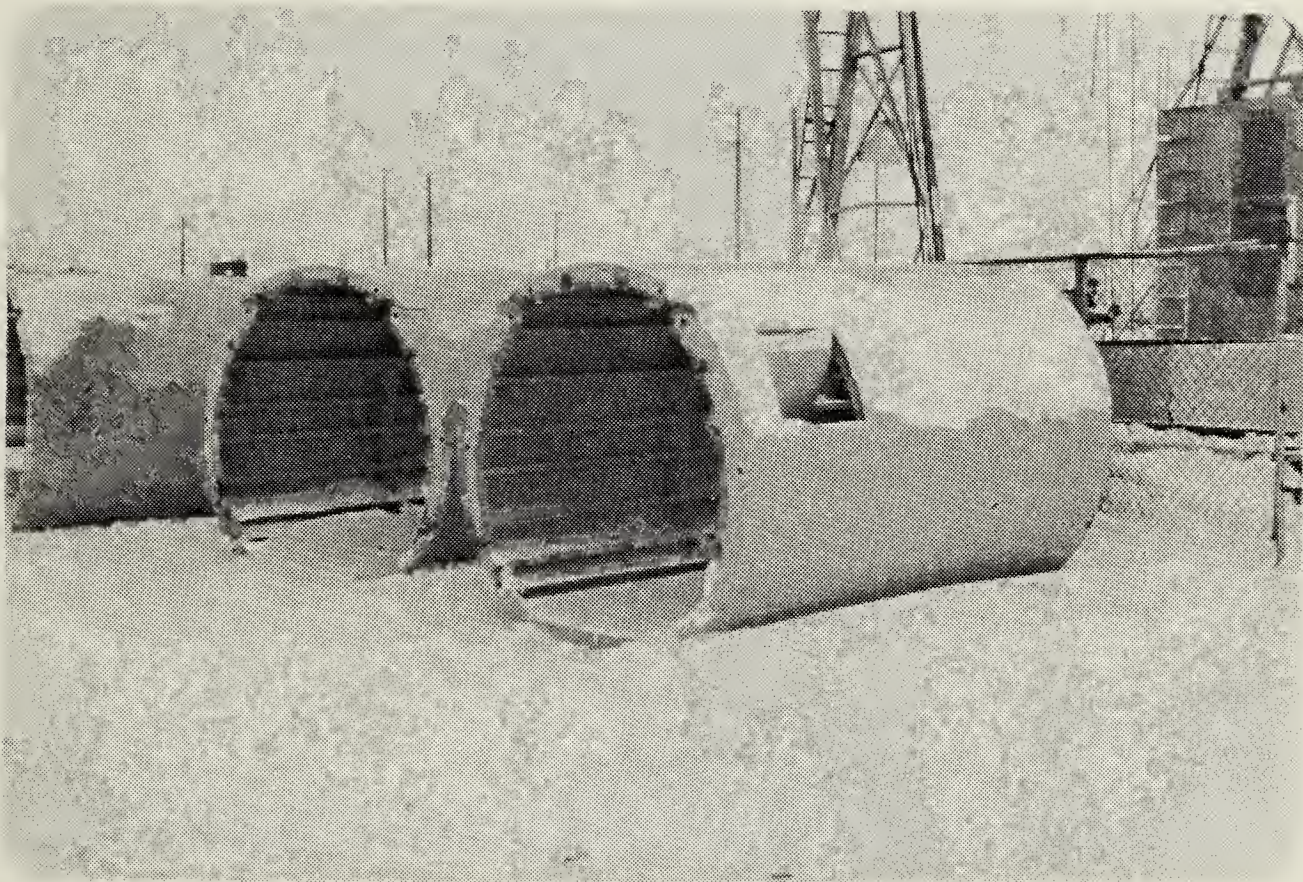
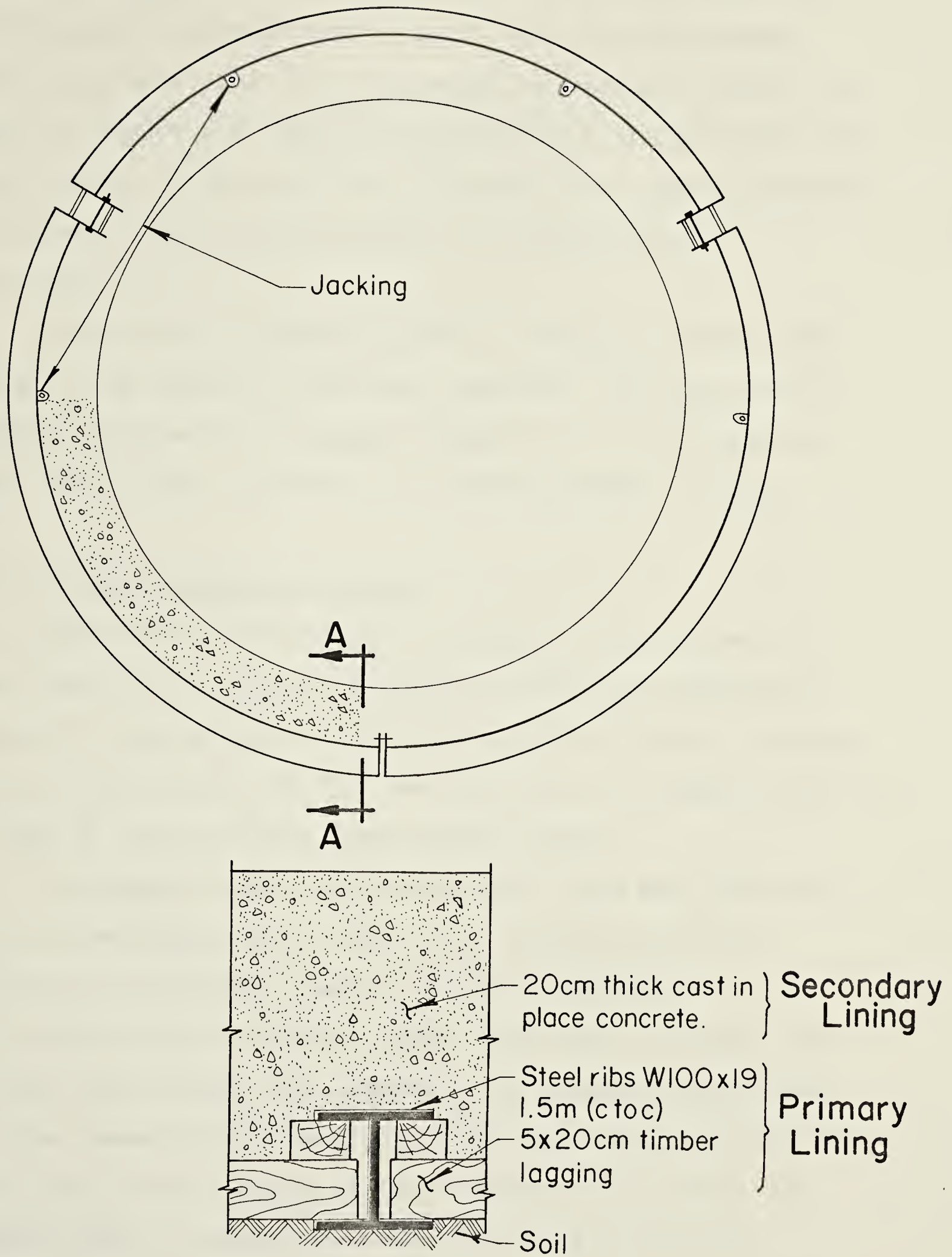


Plate 3.4 Steel forms used to cast the secondary concrete lining



Section A-A

Figure 3.5 Conventional lining system

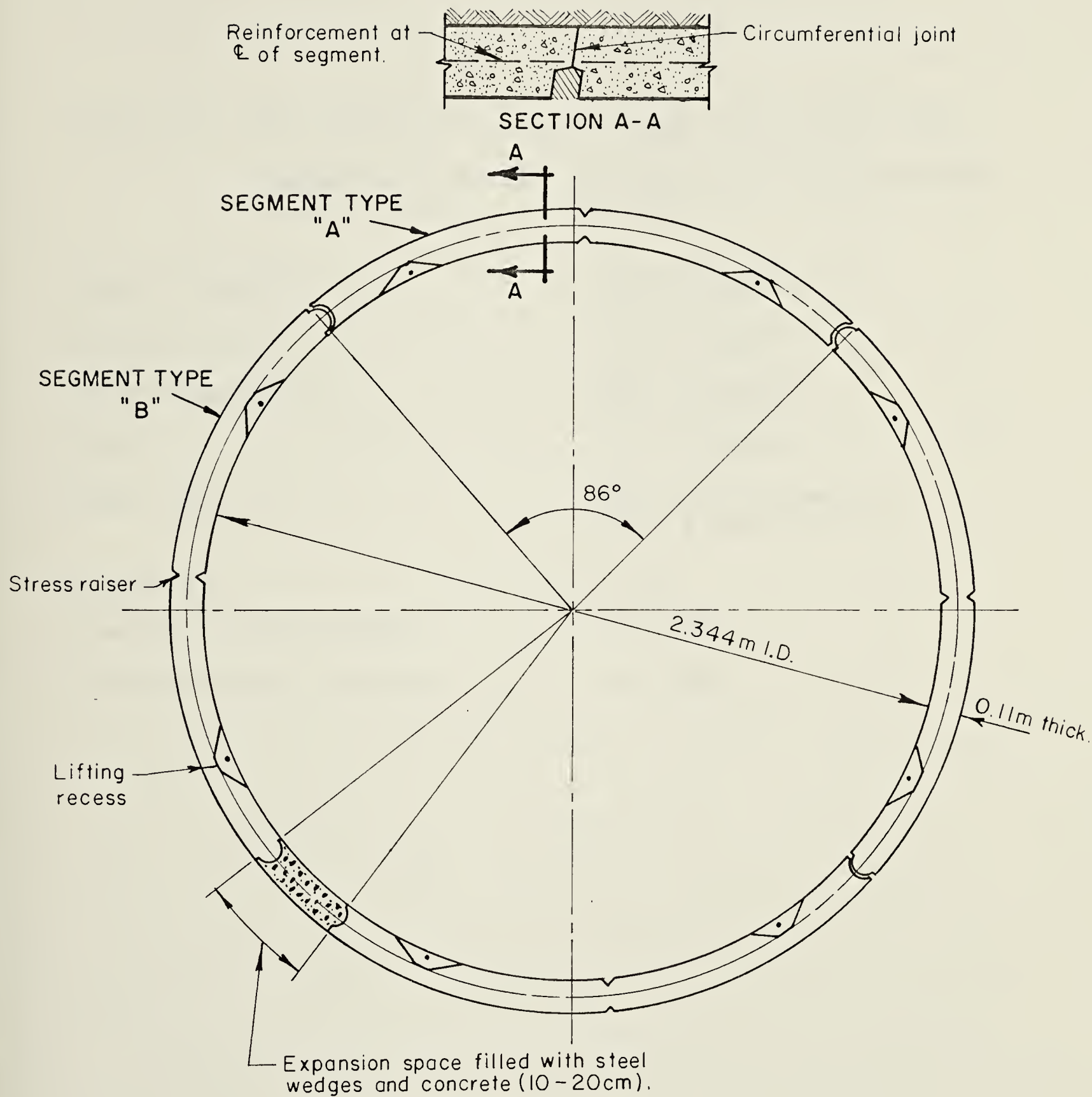
jacking against the rib of the temporary lining. When the mole has been advanced sufficiently that the rib emerges from the shield, the rib is expanded by hydraulic jacks, as shown in Figure 3.5, and 10 cm spacers are placed in the two upper joints of the steel rib. The next rib-lagging assembly is placed in the shield and the drilling operation continued.

The secondary concrete lining is usually placed after the drilling operation has been completed. The concrete is pumped into the annular space between a circular moveable steel form, shown in Plate 3.4, and the primary lining.

3.4.2 Precast Segmented Lining

Each metre of the precast concrete lining, shown in cross section in Figure 3.6, consists of four trapezoidal segments. The top and bottom segments are of type A, having concave longitudinal joints, and the two side segments are of type B, having convex longitudinal joints.

The segments were designed by R.V. Anderson Associates Ltd. and manufactured by Supercrete (Alberta) Ltd. Mix design of the concrete used is given in Table 3.4. Forty-eight concrete molds, twenty-four each of type A and B, were used to cast the segments. The segments were cured at room temperatures overnight. They were then taken off the molds and stored in sets of four at Supercrete yards. The segments were transported to the site in sets as the construction required.



I.D. : 2.344m
O.D. : 2.564m

Figure 3.6 Precast segmented lining

Table 3.4 Mix design of concrete used for casting the segments (Courtesy of Supercrete Incorporated)

Cement Type 30	400 Kilograms
Concrete Sand	705 Kilograms
10 mm Aggregate	1080 Kilograms
Water	154 Kilograms
Admix MBAE10	480 ml/45 kg adjust for 6% air \pm 1%
W/C ratio	0.38
Average 7 day strength	37.2 MPa
Average 28 day strength	42.2 MPa

Each segment is provided with a longitudinal stress raiser and two lifting recesses. The stress raiser acts as a section of low moment resistance which increases the flexibility of the lining and reduces the bending moment in the segments. The lifting recesses are used during assembly of the lining rings. All segments are provided with a light reinforcement mesh located at their center line. This reinforcement prevents cracking of the concrete upon temperature changes and increases the shear strength of the segment in the areas around the stress raiser and lifting recesses. All circumferential joints are coated with a layer of sealant just before their assembly.

During construction, a complete ring composed of four segments (two of type A and two of type B) is assembled within the shield using an erector arm mounted on the axle of the mole. The bottom segment is placed within the shield first followed by the side segments. Two 10 cm steel wedges are placed in one of the lower longitudinal joints then the fourth segment is wedged in place to form a full ring as shown on Plate 3.5. Two tie rods are temporarily used to secure the top segment to the lifting recesses of the side segments.

The entire drilling machine is advanced by jacking against the free circumferential joint. Every ring is expanded radially, to the excavated surface of the soil, as soon as the shield has advanced beyond that ring. The lower longitudinal joint, which is left open during the assembly

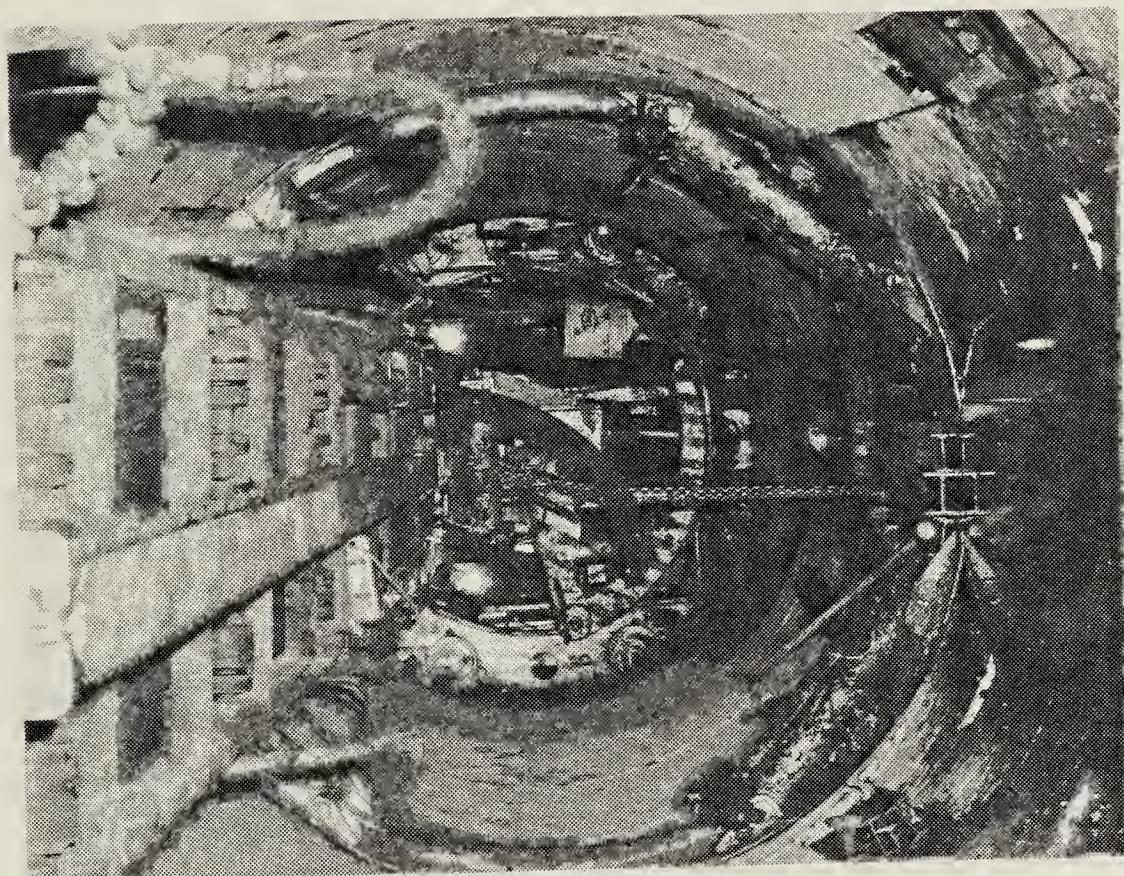


Plate 3.6 Ring expander

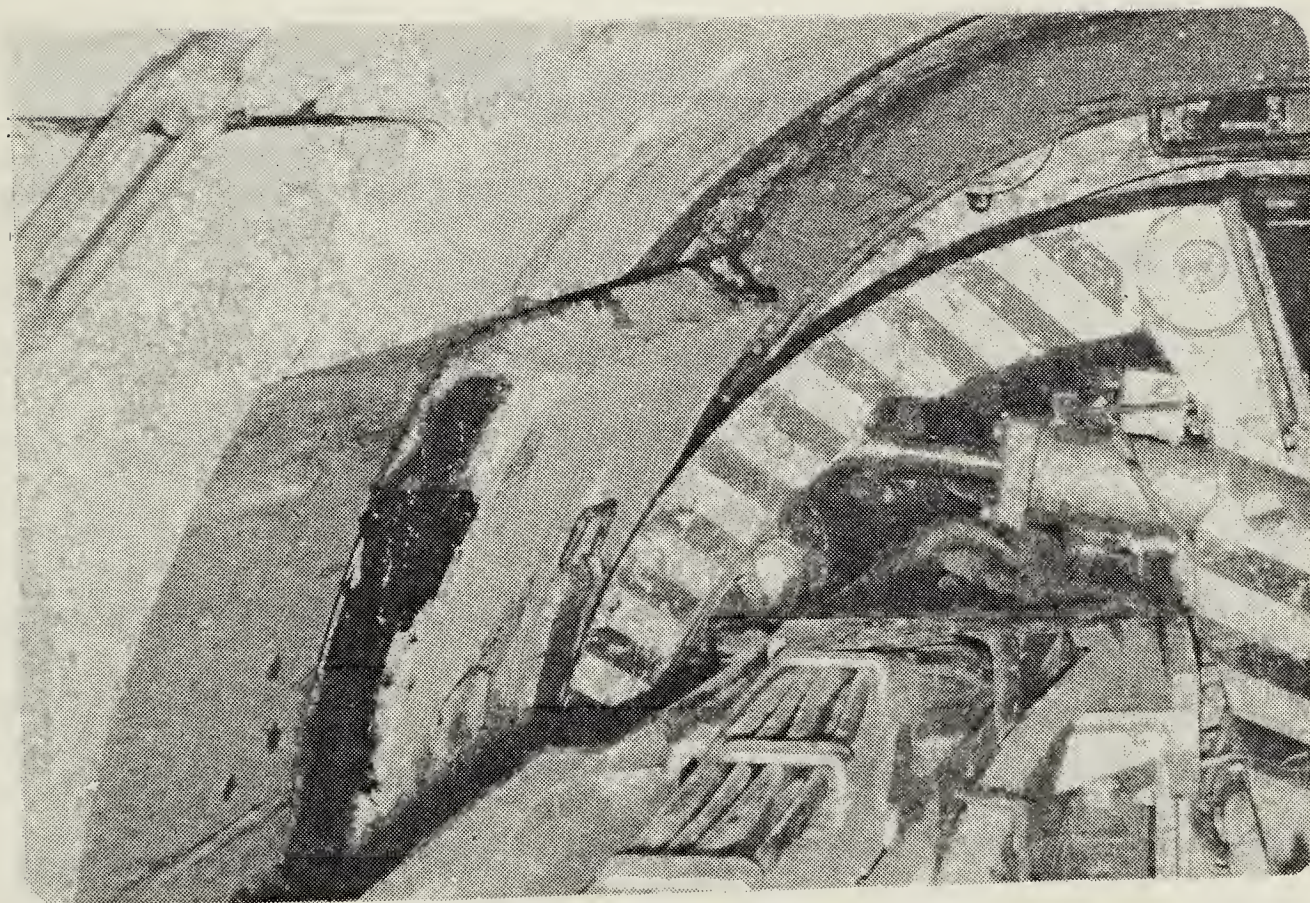


Plate 3.5 Top segment wedged in place

of the ring, is opened further using the ring expander shown on Plate 3.6. It is kept open by steel spacers (up to 20 cm long) and later filled with concrete. In successive rings, the longitudinal joint opening is alternated (Plate 3.6) thus forming a staggered pattern leading to an overall symmetry of lining behavior. This radial expansion minimizes the annular space between the lining and the soil and hence the need for grouting.

3.5 FIELD TEST SECTIONS

In order to compare the performance of the two lining systems and, in particular, to study the performance of the new lining, a field instrumentation program was implemented to monitor the stresses induced in the two types of lining upon installation and the accompanying deformation of the surrounding soil.

Instrumentation was concentrated in three sites referred to as Section 1, Section 2 and Section 3 (Figure 3.7). Section 1 is located on the old lining system and Section 2 was placed at an early stage of construction using the segmented lining. Both of these sections have a limited number of instruments, whose purpose was to indicate the general trends of lining and soil behaviour. Section 3, the main test section, is the site of a large number of instruments installed in both the soil and lining. It is located near the middle of the tunnel length. It should be noted that the lining instruments of Sections 2 and 3 were

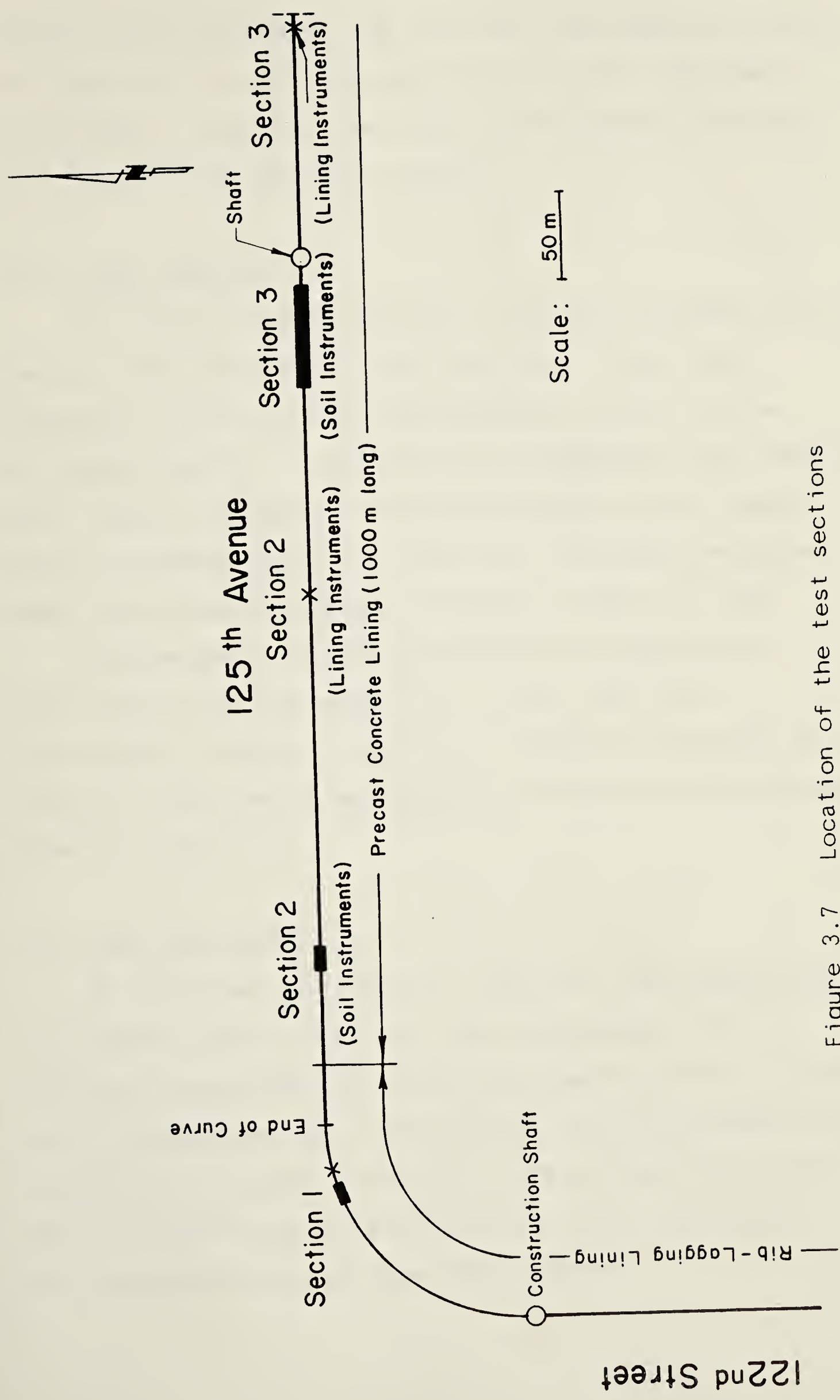


Figure 3.7 Location of the test sections

installed at a distance from the soil instruments as shown in Figure 3.7. A detailed description of the instruments installed in these test sections and the results obtained will be given in Chapters 4 and 5.

3.5.1 Test Section 1

The layout of Test Section 1 is given in Figure 3.8. The soil instrumentation used consisted of one slope indicator, two multipoint extensometers, eight shallow settlement points, a single point extensometer and a bench mark. These instruments were installed during the second week of November 1978. The tunnel drilling machine passed under their location between February 14 and 16, 1979.

Four weldable vibrating wire strain gauges were installed on the top segment of a steel rib. The instrumented rib was placed in the tunnel on February 19, 1979 at a location 23 metres west of the end of the curve as shown in Figure 3.8.

3.5.2 Test Section 2

As indicated in Figure 3.9, the soil instrumentation of this section consists of two slope indicators, two multipoint extensometers, seven settlement points, a single point extensometer and a datum point. Soil instruments were installed on November 29 and 30, 1978 and March 26 and 27, 1979. During the period May 28 to 31, 1979, the tunnel drilling machine passed under the section.

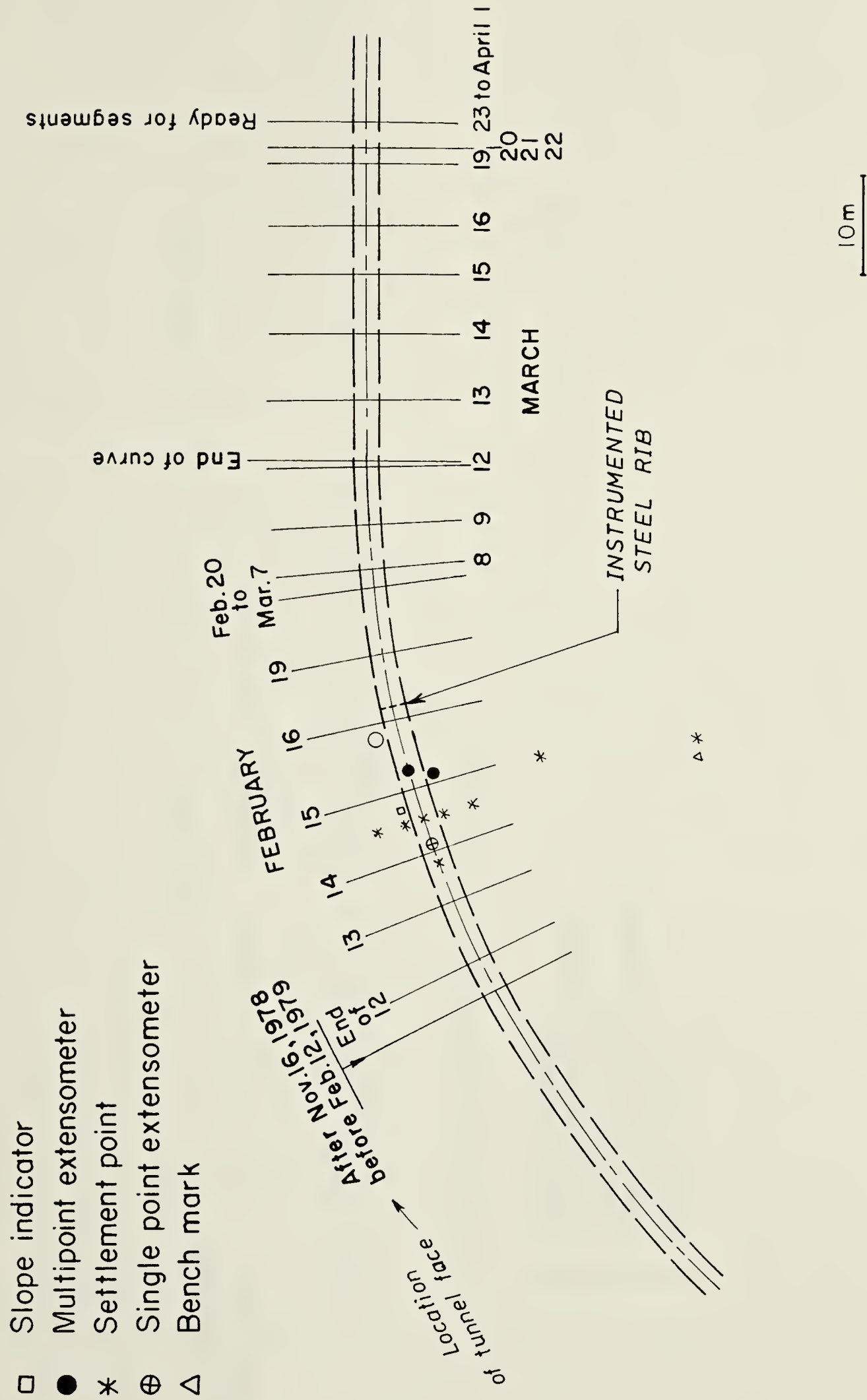
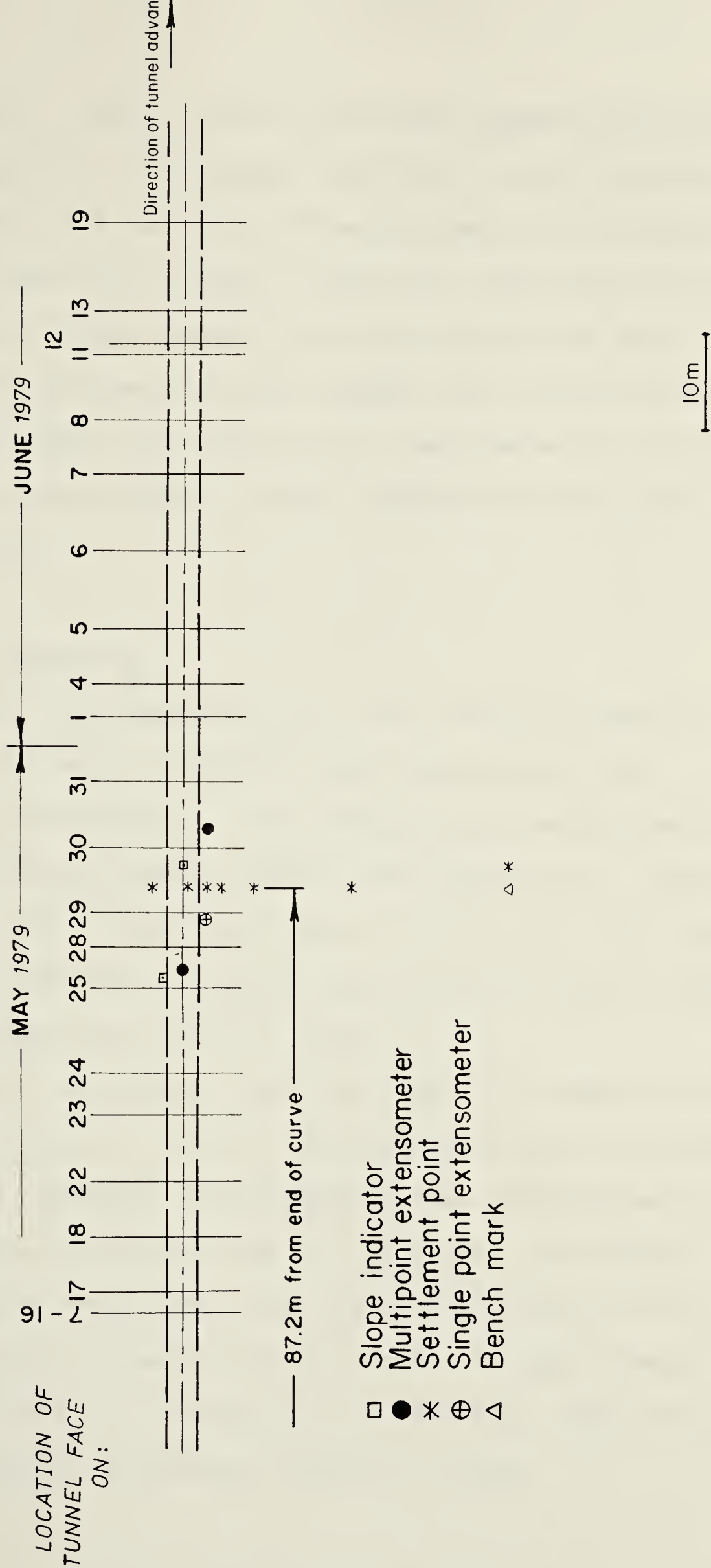


Figure 3.8 Layout of Test Section 1



- Slope indicator
- Multipoint extensometer
- * Settlement point
- ⊕ Single point extensometer
- △ * Bench mark

Figure 3.9 Layout of Test Section 2 (soil instruments)

On June 7, 1979, a set of concrete segments were cast for Test Section 2. They were installed in the tunnel on July 18, 1979 at a location 300 metres east of the end of the curve (about 200 m east of the soil instruments of this test section). These segments were provided with two embedded vibrating wire strain gauges, two surface vibrating wire strain gauges, two load cells, two eye-bolts for tape extensometer measurements, eight inspection holes and a set of Demec points.

3.5.3 Test Section 3

The soil instrumentation of this section, shown in Figure 3.10, consists of four slope indicators, ten multipoint extensometers, five single point extensometers, twenty shallow settlement points and a bench mark. These instruments were installed from April 2 to 19, 1979. The tunnel drilling machine passed under them during an eight day period beginning July 31, 1979.

Five sets of special concrete rings (20 segments) were cast on September 13, 1979. These segments were provided with special recesses to accommodate two vibrating wire load cells to be positioned at one of the lower longitudinal joints of each ring. Each ring was provided with twelve inspection holes to measure the size of any gap between the lining and the soil, and eye-bolts which were used with the tape extensometer to measure diameter change.

CHAPTER 4

MEASUREMENTS OF SOIL DISPLACEMENTS AROUND THE EXPERIMENTAL TUNNEL

4.1 INTRODUCTION

Prediction of soil displacements due to tunneling is one of the major questions to be answered in the design of a tunnel in soil. This prediction includes the determination of the expected amount and mode of movement of any existing structures above or adjacent to the tunnel. If these movements are intolerable, measures must be taken either to reduce the soil displacement or to strengthen the structures by underpinning. For such purposes, prediction of differential settlement along and perpendicular to an advancing tunnel, rather than just the ultimate settlement (after completion of the tunnel), is required.

As discussed in Chapter 2, in view of the present state of knowledge, a complete generalized method of such prediction does not exist. There is a general agreement in the recent state of-the-art reports (Peck, 1969; Cording and Hansmire, 1975; and Ward, 1978) that full scale field observations in tunnels are of outstanding urgency to help to fill the gaps in our knowledge of tunneling. These measurements have been considered as the most reliable means of predicting soil movements, for guiding construction through uncharted ground conditions, and when new

construction techniques are introduced. Nevertheless, the ultimate goal of tunneling research would be to develop a comprehensive theoretical concept or model which could be used to predict tunnel behavior.

Although tunneling in the Edmonton area was started in 1955, only a few observational programs have been carried out to measure soil movements (Eisenstein and Thomson, 1978; Thomson and El-Nahhas, 1980). The introduction of a precast segmented lining as a new technology in an experimental tunnel provided an excellent opportunity to monitor soil displacements around both the conventional and new lining systems. Details of the experimental tunnel have been given in the preceding chapter. In this chapter, the instruments used for measuring soil displacements around the experimental tunnel are described in detail. The field measurements from the three test sections are presented and discussed to establish the general trends and characteristics of soil displacements around a tunnel advancing through stiff glacial till using a shielded drilling machine. Additional analysis of the measurements are included in Chapter 6.

4.2 SOIL INSTRUMENTATION

Excavation of a tunnel results in a spatial displacement field. Displacement vectors can be resolved into three mutually perpendicular components, one vertical and two horizontal, the latter being parallel and

perpendicular to the tunnel center line. Choosing soil instruments to measure these components in the experimental tunnel was based on two criteria. First, was the reliability of an instrument which was assessed by taking into consideration the expected order of magnitude of displacements compared to the instrument sensitivity, reproducibility and accuracy, as well as its capability of functioning in the local soil and climatic conditions. Second, the availability and cost of the instrument was considered.

A literature search, focussing on the advantages, limitations, and practical experiences with various instruments, provided valuable information in the initial assessment and planning phases of the field instrumentation program. Some of the instruments were especially designed, built and calibrated at the University of Alberta to avoid the shortcomings of those commercially available and to reduce the overall cost of the instrumentation program.

Details of the soil instruments used in the experimental tunnel are presented in this section and some published references are given for each instrument. In general, the reports prepared by Cording et al. (1975) and Schmidt and Dunnicliff (1974), as well as the catalogues of different geotechnical instrumentation companies, cover a wide range of tunneling field instruments and were of value in the assessment and selection process.

For each of the instruments field data sheets and

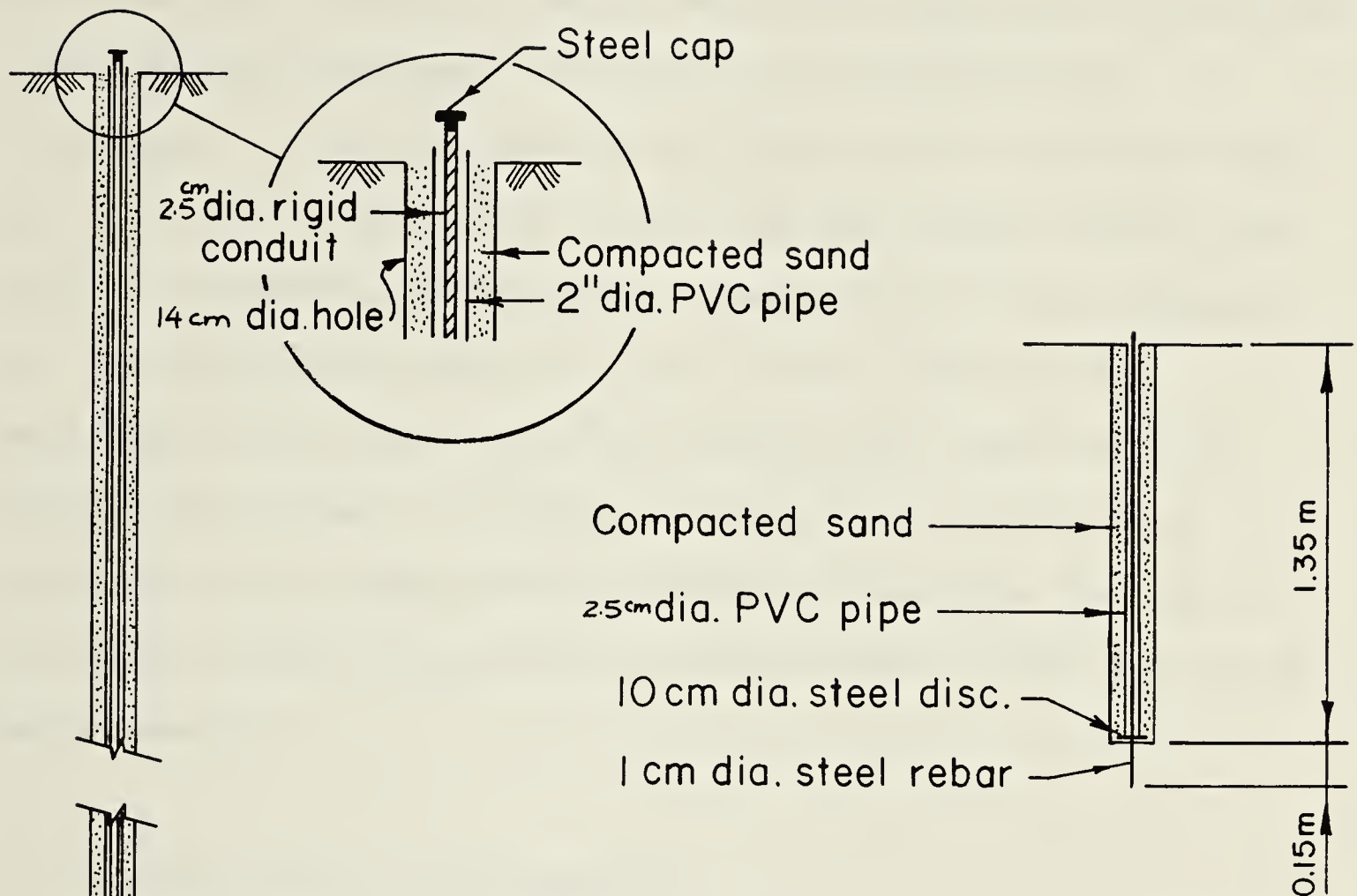
computer programs provided with plotting subroutines, were prepared in advance to reduce the data and plot the final results as soon as practically possible after the measurements were obtained.

4.2.1 Settlement Point

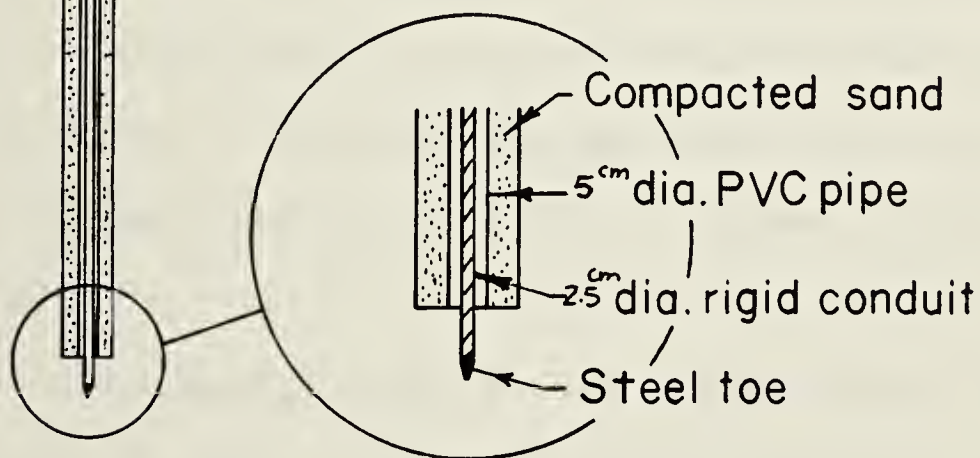
This instrument is commonly used to measure the vertical displacement of soil near the ground surface. The settlement is measured by surveying the level change of the top of a steel rod inserted in the soil to a shallow depth. Different designs for settlement points are given by Burland and Moore (1973), Marsland (1973), Hansmire (1975), Cording et al. (1975); and Barratt and Tyler (1976).

Figure 4.1(a) shows the details of the settlement points used in the experimental tunnel. A borehole, (15 cm diameter), is drilled to a depth 1.35 metres, which is deeper than frost penetration in this area. A steel reinforcing rod, (1 cm diameter having a 10 cm diameter steel disc 0.15 m from the end), is driven into the bottom of the borehole. A pvc pipe, (2.5 cm diameter), is placed around the upper part of the reinforcing rod before the hole is backfilled with sand. The pvc pipe eliminates any friction between the rod and the sand.

Optical levelling was carried out using a Geotec AL-23 surveying instrument, and a special surveying rod which is provided with a vertical level bubble and which can be read to the nearest 0.5 mm. Since a ground surface movement on



(a) Settlement Point



(b) Single Point Extensometer

Figure 4.1 Details of settlement point and single point extensometer

the order of 10 mm was expected, measurements were taken to ensure accuracy and repeatability to within ± 1 mm. The sight distance was limited to seven metres or less with a balanced foresight and backsight. Movement of the surveying instrument to tie the settlement points with the bench mark was kept to a minimum and one of the settlement points was used as a stable turning point. These precautions reduced the surveying closing errors to ± 1 mm or less. One settlement point was installed beside each bench mark to examine the effect of change in temperature and ground moisture on the measurements. However, readings indicated that such effects were within the accuracy of the surveying measurements.

4.2.2 Single Point Extensometer

This instrument is used to measure the vertical displacement of the soil at one deep point. It is also used as a bench mark if installed outside the zone affected by tunneling. Different designs for this instrument are given by Burland and Moore (1973), Cheney (1973) and Hansmire (1975).

The design used in the experimental tunnel is given in Figure 4.1(b). A hole, (15 cm diameter), is bored to the required depth. A rigid conduit pipe, (2.5 cm diameter), having a conical toe, is hammered into the bottom of the borehole. It is then surrounded with a 5 cm diameter pvc pipe. The space between the borehole wall and the pvc pipe

is filled with compacted sand. A steel cap is then placed on the pipe. Surveying of the level change of the center of this cap is carried out using the same precautions noted previously to guarantee accuracy and repeatability within ± 1 mm.

4.2.3 Multipoint Extensometer

Due to the high cost of drilling, (\$500 per day at the time of installation), there is a definite advantage in measuring vertical displacements at several depths in the same borehole, using a multipoint extensometer. The principle of this instrument is to install anchored measuring points in a predrilled hole at different depths, and to monitor the change of each anchor position which corresponds directly to the soil movement. Different types of extensometer employ different forms of anchors and/or use different methods for monitoring the anchor movement.

Wire multipoint extensometers were used by Shannon and Strazer (1968), Judd and Perloff (1971), and Hansmire (1975). The anchor for this type of extensometer is either grouted or wedged to the borehole wall. Each anchor is attached to a stainless steel wire (1.2 mm diameter). A constant tension is applied to each wire in a junction box at the ground surface and movement of the wires is monitored using dial gauges or electrical transducers.

Hedley (1969) indicated that this type of extensometer suffers significant hysteresis in holes deeper than 10

metres due to friction between the wire and the casing, or the wire and the guides. Hansmire (1975) indicated that such errors were overstated when the ground surface was settling more than the anchors.

In rod multipoint extensometers, the wires are replaced by aluminum alloy tubing. The maximum number of rods and anchors is limited by the size of the borehole. Solinst (1975) recommends not more than six rods per hole.

4.2.3.1 Magnetic Multipoint Extensometer

The magnetic multipoint extensometer was developed and used in different types of soil by the Building Research Establishment, U.K. (Burland et al. 1972; Burland and Moore 1973; Marsland and Quarterman 1974; and Smith and Burland 1976). It was first tried in Edmonton by Medeiros (1979) and in the Saline Creek Tunnel near Fort McMurray, Alberta by Chatterji et al. (1979).

This extensometer has two basic components, viz., anchored permanent magnets and an access tube. Axially magnetized circular magnets are fixed to a rigid pvc housing (Figure 4.2). These magnet assemblies are either embedded in the soil or inserted and fixed to the wall of a predrilled hole at different depths. The access tube consists of flush jointed pvc pipes installed in the center of the borehole. It is used as a guide for the movement of the magnet points during installation and provides an access to the probe of the readout unit.

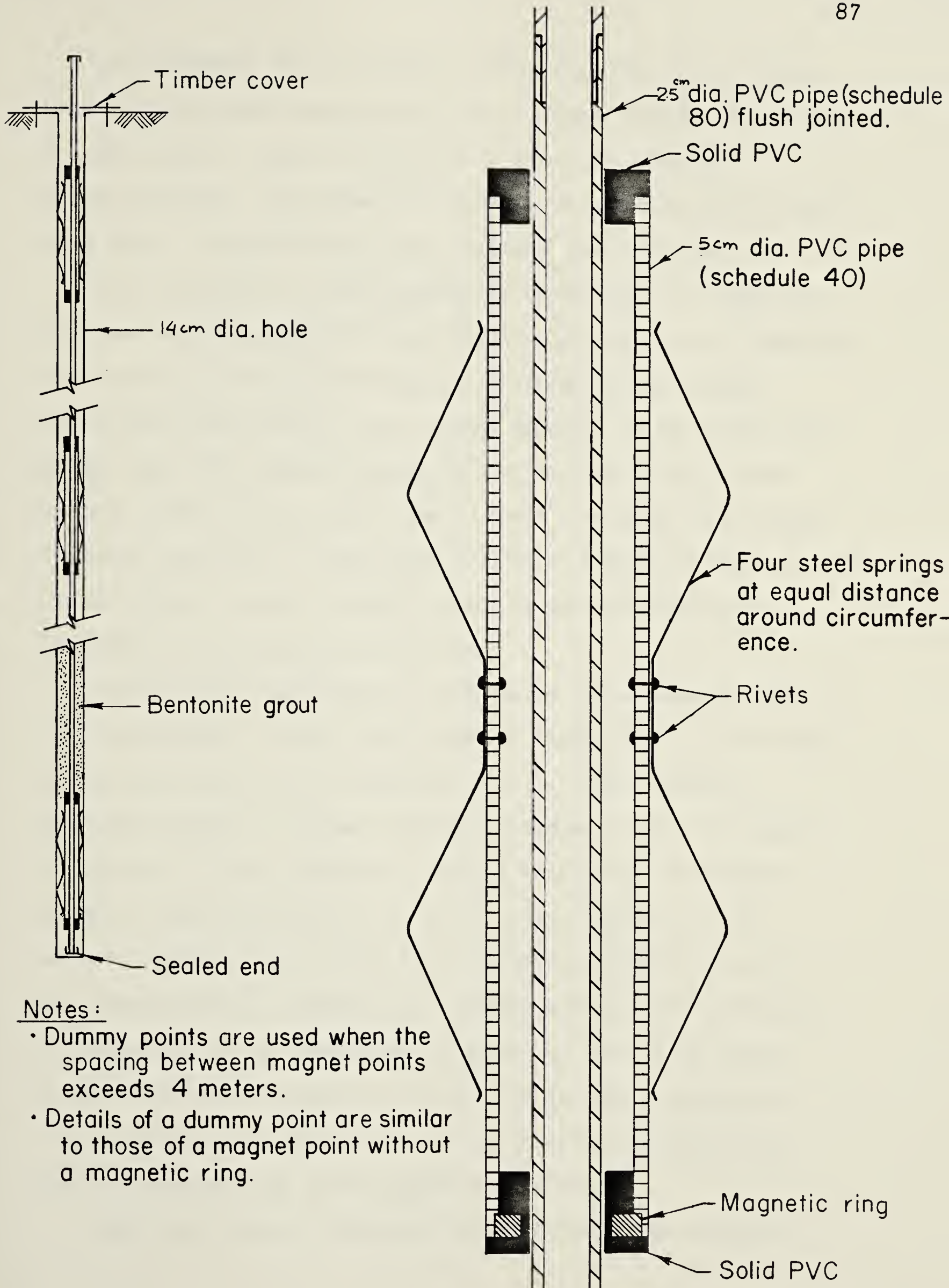


Figure 4.2 Magnetic multipoint extensometers

The readout unit (Solinst, 1975) consists of a single reed switch probe encapsulated in silicone rubber in a brass housing, with a head fitting for a steel or plastic measuring tape. The probe is fitted with braided cable wound on a drum, incorporating a dry battery and a buzzer.

The location of the magnets is determined by lowering the reed switch probe through the access tube. As it reaches the central field of the magnet, it snaps shut thereby activating the buzzer. This system appears to be simple and cheap since any number of points can be monitored in one hole at little extra cost, and without the need of a large diameter borehole. It has also proven reliable if the installation is done properly and the measurements are recorded by an experienced person.

Details of the magnetic multipoint extensometer used in the experimental tunnel are shown in Figure 4.2. It follows the principles given by Burland et al. (1972) using a modified design of magnet assembly (Ryzuk, 1977). As shown in Figure 4.3, the magnetic ring is formed of 14 ceramic magnets inserted between two split steel washers. The ceramic magnets have consistent magnetic properties which are independent of temperature change and are not affected by hammering or by immersion in water or bentonite grout. Three distinctive magnetic fields are formed around each ring as shown in Figure 4.4. The split steel washers are used to concentrate these magnetic fields.

When the probe intersects each of the three magnetic

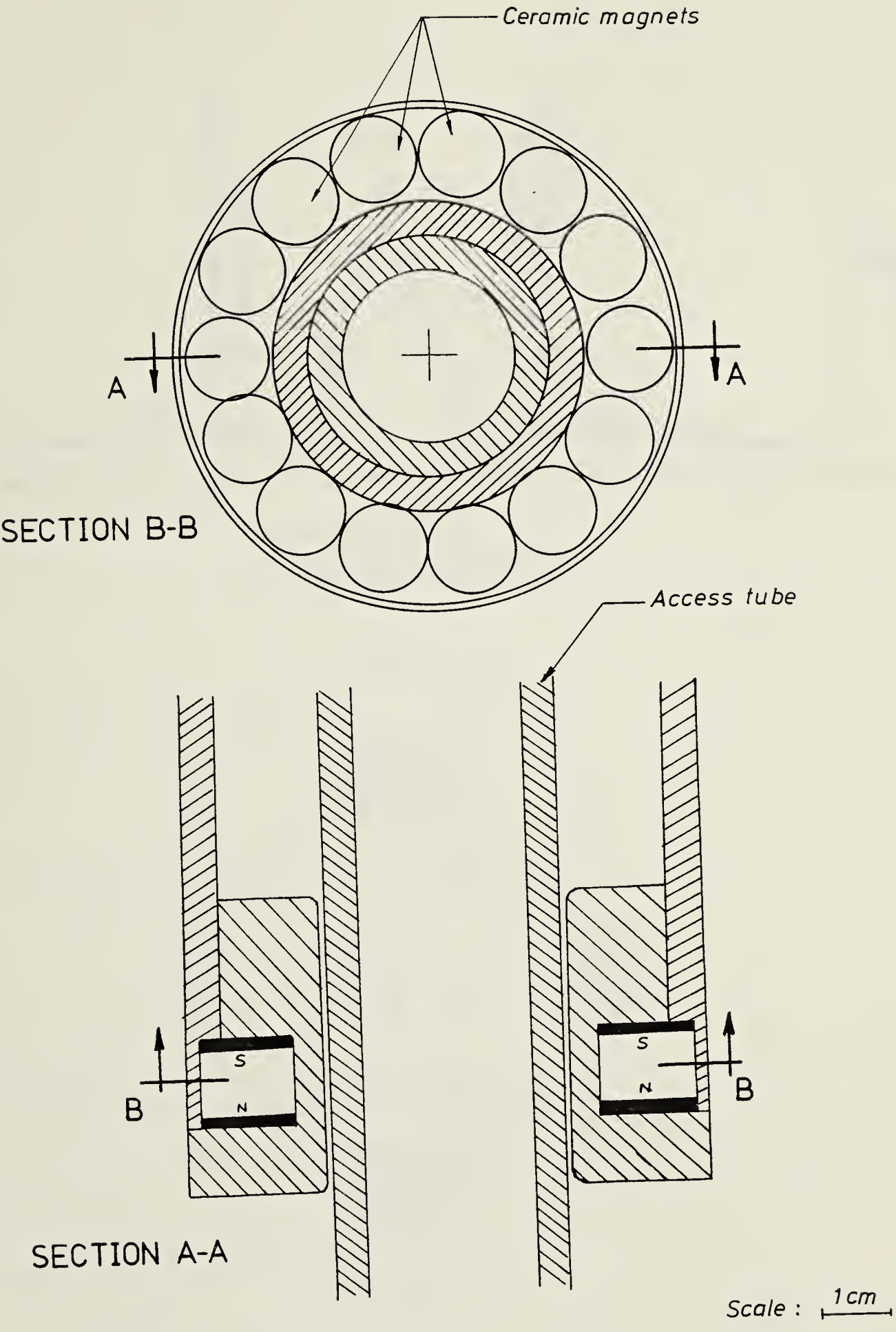


Figure 4.3 Details of magnetic ring

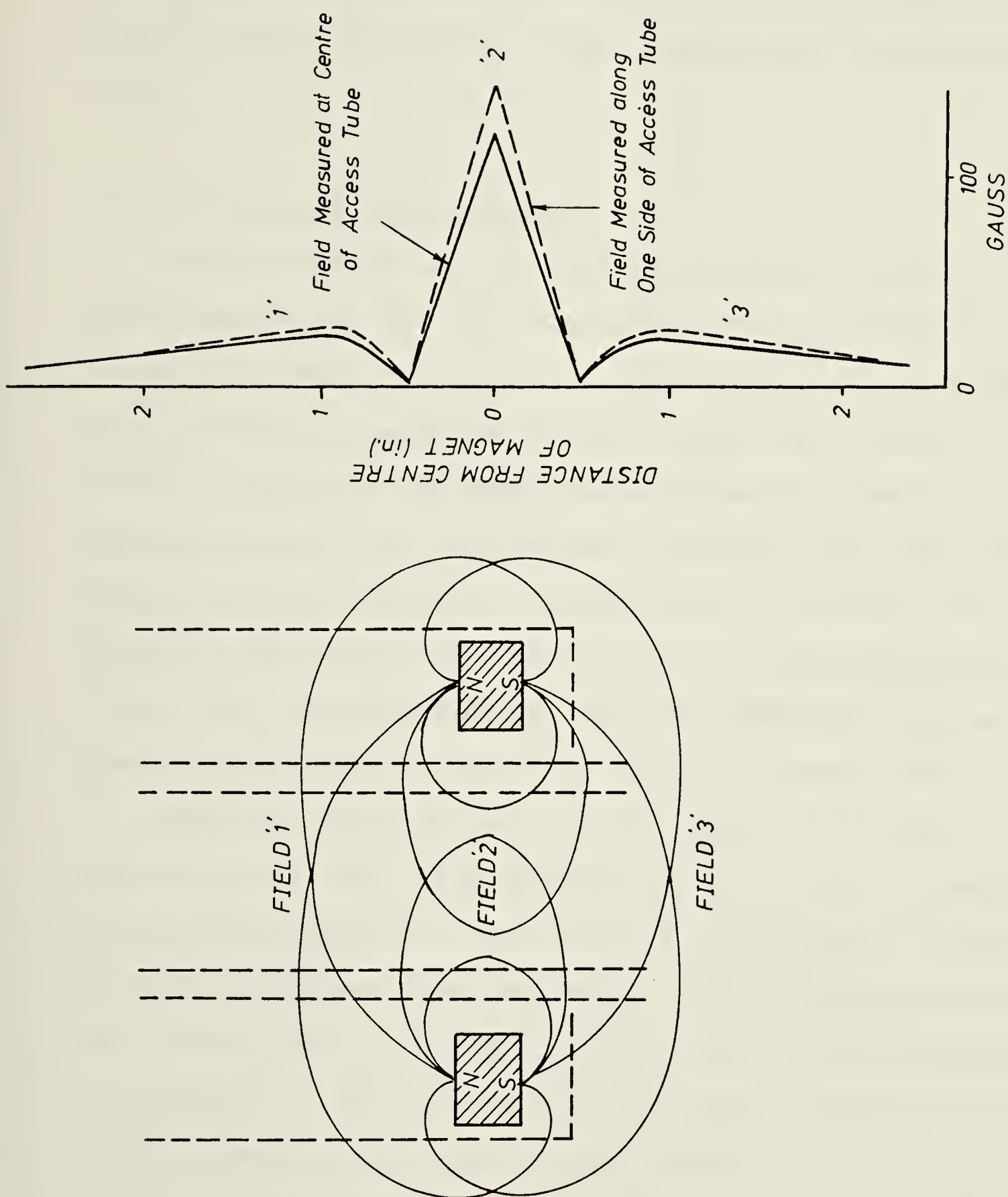


Figure 4.4 Magnetic fields around the ring

fields the buzzer is activated. Each assembly of magnetic rings was checked for the presence of three magnetic fields (three buzzes). The absence of any of these fields indicates that at least two of the ceramic magnets were placed upside down.

4.2.3.2 Installation Procedure

The procedure used in installing the multipoint extensometers in the test sections of the experimental tunnel is given in Figure 4.5. A continuous-flight solid auger mounted on a B61 drilling rig was used to drill the holes. As soon as the auger was withdrawn and while the bentonite grout was being mixed, the access pvc tube and the grouting plastic tube were assembled and inserted into the borehole. The joints of both tubes were cemented using water tight fast setting adhesive. The same adhesive was used to cement an end cap to the first length of access tube.

Wherever the hole was filled or partly filled with ground water, the access tube had to be filled with water during its placement in the hole to balance uplift forces. Filling the access tube with water could be delayed until the access tube is completely installed, but before grouting is started, if the hole is dry. The top two metres of all access tubes were filled with antifreeze.

A bentonite grout, (0.5 m^3 water mixed with 2.27 kg bentonite), was pumped into the hole from the bottom through the 2.5 cm diameter plastic tube. This tube was withdrawn

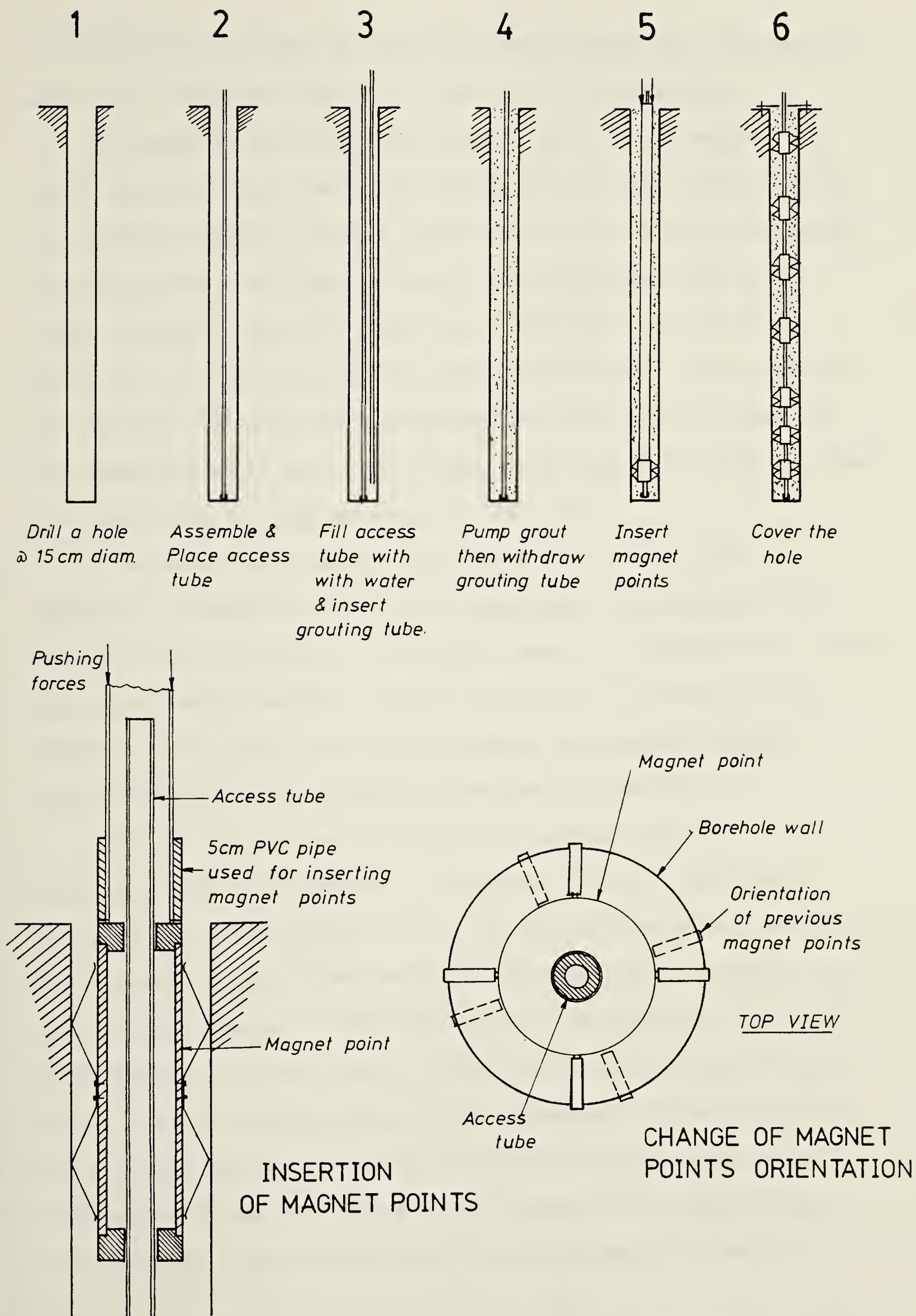


Figure 4.5 Installation of multipoint extensometers

from the hole as soon as grouting was completed. The magnets were then inserted one at a time into the borehole.

A group of threaded pvc pipes, (6.35 cm diameter - 3 and 6 metres long), were connected with couplings and used to push the magnets (see Figure 4.4) to the required depths. In some holes, the magnets had to be hammered with these pipes to force them through very tight portions of the borehole. The orientation of each magnet point was changed so that the springs were anchored on undisturbed areas of the borehole wall as illustrated in Figure 4.5. This ensured the tightness of the springs to the soil.

The steel springs of the shallowest two or three magnets in each hole had to be expanded, increasing their diameter by 0.5 cm, for the same reason. A dummy point, with the same design as the magnetic anchors but without the magnetic ring, was installed between successive magnet points wherever the spacing exceeded four metres.

The installation of the first two multipoint extensometers was checked a few days later by pushing or pulling the access tube about 0.5 cm and comparing readings of the magnet positions before and after this movement. A consistent change in the readings of the magnets indicates that they are sufficiently fixed to the borehole wall and free to slide on the access tube whenever the surrounding soil starts moving. The top of each hole was covered by timber, as shown in Figure 4.5, allowing the access tube free movement and protecting the extensometer from the

dropping of soil lumps or foreign bodies into the hole.

4.2.3.3 Measurement Procedure

To read the multipoint extensometer, the reed switch probe (with the tape attached) is lowered through the access tube. The depth at which the second buzz of each magnet point starts and where it ends is recorded to the nearest 0.5 mm. The difference between these two readings, i.e. the length of the second magnetic field, is used as an immediate check of the readings and to avoid transcribing mistakes. The average of the two readings is used to denote the location of the magnet point (see Figure 4.4). Since all these readings are related to a marked point on the tip of access tube, the elevation of this point is determined by a level survey immediately after each set of readings. This allows a computation of the absolute movement of each magnet point in the extensometer.

4.2.3.4 Reproducibility

Chatterji et al. (1979) reported that the reproducibility of this type of extensometer varies between 2 and 10 mm, although the tape can be read to the nearest 0.5 mm. Since the expected soil displacements at shallow depth above the experimental tunnel were expected to be in the order of 10 mm, different measures were examined at the planning stage to improve the reproducibility of the instrument.

A reading procedure was arranged to allow recording the location of the magnets twice for each set of readings, once while lowering the probe and again while taking it out. In both cases the probe was moved downward while taking the readings at the magnet levels. This specific procedure was followed until confidence in the instrument reproducibility was established. The special surveying rod, as well as the surveying precautions described in section 4.2.1 were used to ensure that the accuracy of the extensometer measurements would not be masked by surveying errors. Also, a micrometer head similar to that described by Burland et al. (1972) was designed to fit the top of the access tube (Figure 4.6). Replacement of the reed switch by a gaussmeter was examined but the results obtained in the laboratory were not satisfactory.

These alternatives were tried as soon as the first two extensometers were installed. The use of a micrometer head could improve both the sensitivity and repeatability of the instrument, but its operation, especially in sub zero temperatures, was time consuming and impractical. Reproducibility of 1 mm or less was obtained by following a consistent reading procedure with accurate surveying of the top of the access tube.

Field data sheets, shown in Figure 4.7, and a computer program were prepared to record, reduce the data, and plot the measurements as soon as practically possible after the readings were obtained.

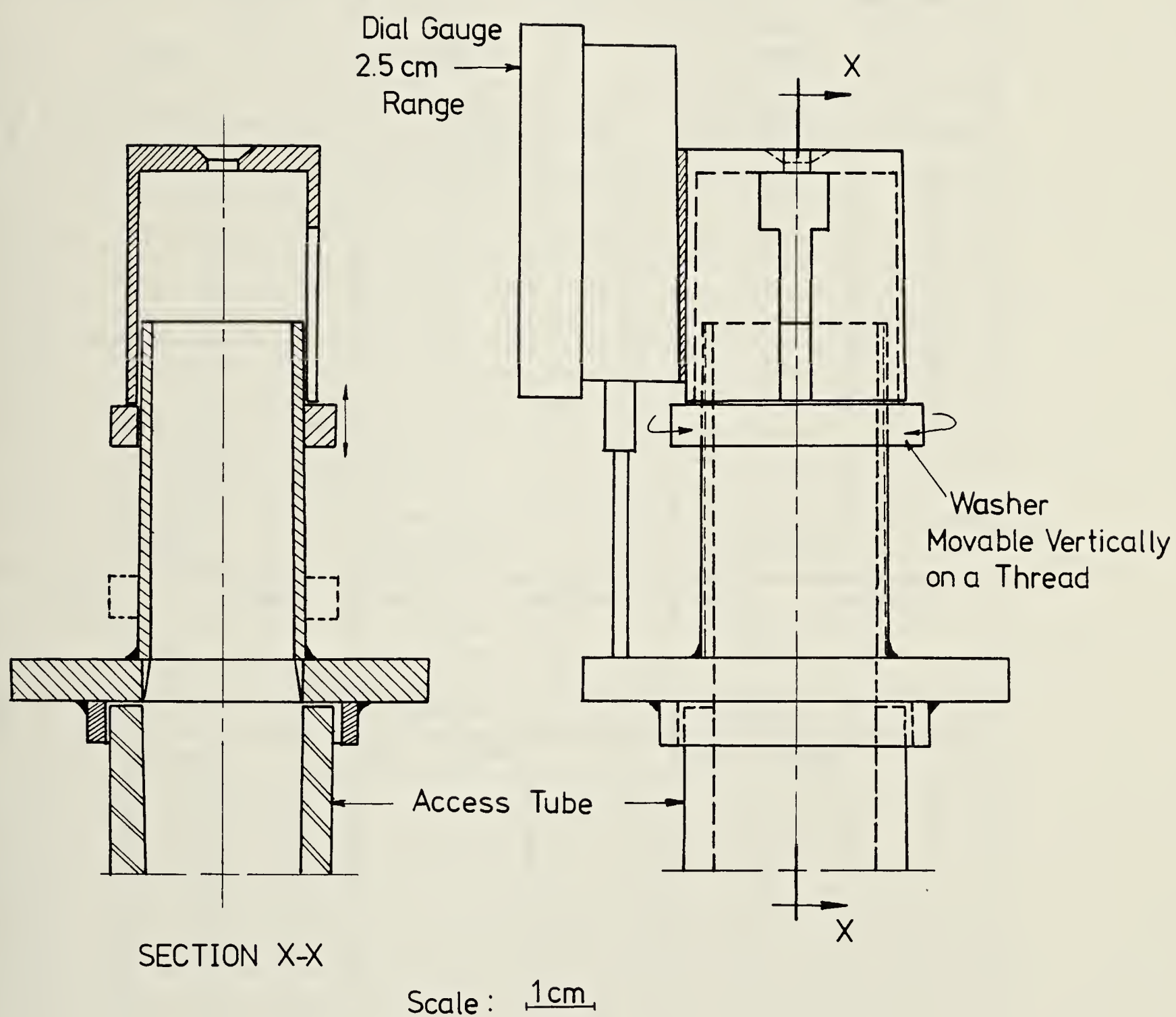


Figure 4.6 Micrometer head

UNIVERSITY OF ALBERTA DEPT. OF CIVIL ENGINEERING GEOTECHNICAL INSTRUMENTATIONS MULTIPOINT EXTENSOMETER FIELD SHEET										PROJECT : 125 th AVE TUNNEL DATE : TEST SECTION : READ BY: RECORDED BY:														
GENERAL COMMENTS :																				DAYS:				
Magnet No.	MX# MOLE LOC.:					MX# MOLE LOC.:					MX# MOLE LOC.:													
	TIME		TO			TIME :		TO			TIME :		TO											
	TEMP. :		°C			TEMP. :		°C			TEMP. :		°C											
	READINGS		CENTER	check		READINGS		CENTER	check		READINGS		CENTER	check										
	TOP	BOTTOM				TOP	BOTTOM				TOP	BOTTOM				TOP	BOTTOM							
1																								
2																								
3																								
4																								
5																								
6																								
7																								
8																								
Surveying Corr: cms					Surveying Corr: cms					Surveying Corr.: cms														
Magnet No.	MX# MOLE LOC.:					MX# MOLE LOC.:					MX# MOLE LOC.:													
	TIME :		TO			TIME :		TO			TIME :		TO											
	TEMP. :		°C			TEMP. :		°C			TEMP. :		°C											
	READINGS		CENTER	check		READINGS		CENTER	check		READINGS		CENTER	check										
	TOP	BOTTOM				TOP	BOTTOM				TOP	BOTTOM				TOP	BOTTOM							
1																								
2																								
3																								
4																								
5																								
6																								
7																								
8																								
Surveying Corr.: cms					Surveying Corr.: cms					Surveying Corr.: cms														

Figure 4.7 Field data sheet for multipoint extensometer

4.2.3.5 Cost

The magnet points used in the experimental tunnel were built at the University of Alberta. Total cost of one magnet point was \$35. The reed switch probe and tape were purchased from Solinst Canada Ltd.

The boreholes were drilled by a B61 drilling rig equipped with a pump for mixing the bentonite grout and a water tank. The drilling rig was also used during the installation of the magnet points. The average time required for drilling and installing one 30 metre deep extensometer, having 12 magnets and dummy points, was seven hours. A two man crew can record the magnet positions in 10 minutes.

4.2.4 Slope Indicator

This instrument is widely used to measure the profile of horizontal displacement with depth in a borehole. It comprises three components: casing, sensor and readout unit.

The casing consists of lengths of plastic or aluminum tubing, provided with four longitudinal grooves equally spaced around the inside circumference. It is placed and grouted in a predrilled borehole. Specifications for the dimensions of different available casings are given in manuals of the Slope Indicator Company and Soil Instrument Ltd.

The slope indicator sensor is a probe incorporating two fixed and two spring loaded wheels which are compatible in their size with the internal dimensions of the casings and

the grooves. The probe contains one or two pendulums. The deviation of these pendulums from the vertical is measured using different principles by different instrument manufacturers, as described by Dunnicliff (1971) and Hanna (1973). The probe is connected to the readout unit by a reinforced electrical cable. The indicator (readout unit) is a portable unit with a digital display of the tilt, and an optional magnetic tape recorder.

The casing is installed with its grooves oriented in the direction of expected principal deformation. The probe moves inside the casing with its wheels located in the grooves. The inclination of the casing from the vertical in two directions perpendicular to the tube axis is measured by the inclination of pendulums. Two sensing elements, (strain gauges or accelerometers), transform the tilt into an electrical signal, which is transmitted to the readout unit through the electric cable. The inclination of the casing is measured at intervals of 0.6 m (2 feet). Typical results from slope indicators which were used in tunnel test sections are given by Peck (1969), Kuesel (1972), Hansmire (1975), Belshaw and Palmer (1978) and DeLory et al. (1979).

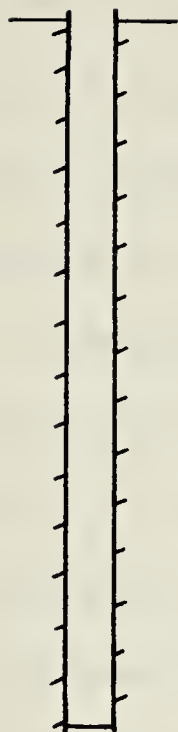
In the experimental tunnel, ABS plastic casing (70 mm O.D. x 59 mm I.D.), was assembled in 3 metre tube lengths. A biaxial probe, SINCO model 50320, was used with a digital readout unit (SINCO model 50306). The probe has two 1.0 g servo-accelerometers. One accelerometer has its sensing axis in the plane of the spring-loaded wheels, and the other

accelerometer has its sensing axis at 90° to the first. Hence the angle of inclination of the probe and the casing is measured in two orthogonal direction, (usually referred to as the A and B directions).

The procedure followed during the installation of slope indicators in the experimental tunnel is illustrated in Figure 4.8. A hole was first advanced using a hollow stem auger mounted on B61 drilling rig. The casing was then assembled, installed inside the hollow stem auger, and filled with water. As soon as the auger was withdrawn, a 6.35 cm pvc pipe was inserted beside the casing. Sand-cement grout was pumped into the hole at three equidistant depths. One quarter of the grouting pipe length was withdrawn and cut after each interval. The sand:cement weight ratio in the grout was 3:1 with a water/cement ratio of 0.8. This mix was determined from laboratory tests to model the stiffness of the soil.

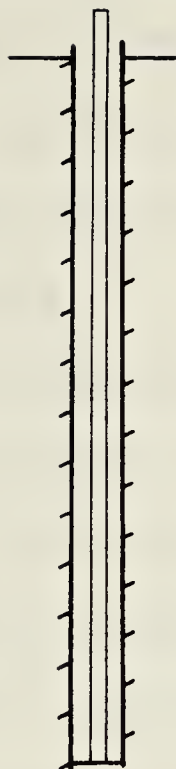
The installation of slope indicators in the three test sections followed the procedure outlined above though occasionally with minor changes. Only one major change was necessary during the installation of the slope indicators of test section 3. A sudden labour strike in most of the concrete companies made the delivery of a small amount of the sand-cement grout (1 m^3) for one hole every day very difficult. The hole drilled for slope indicator SI31 was left open more than five hours before the grout was delivered to the site by an independent concrete supplier.

1



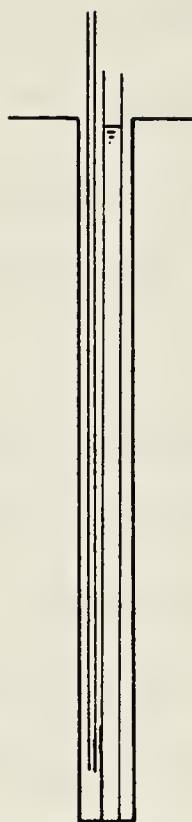
*Drilling a hole
20 cm diam.
using hollow stem
auger.*

2



*Insert the casing
inside the hollow
stem and fill it
with water.*

3



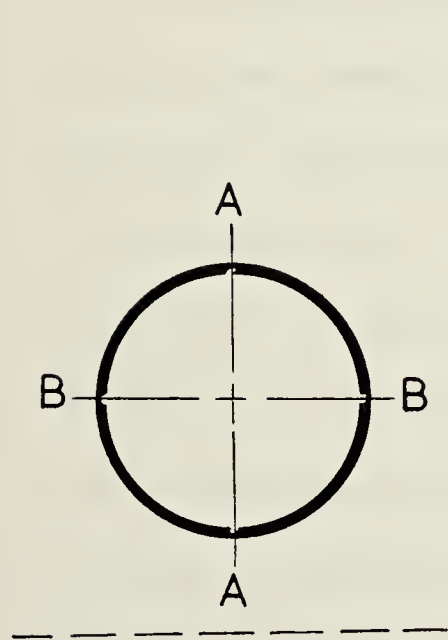
*Withdraw the
auger and insert
grouting tube.*

4

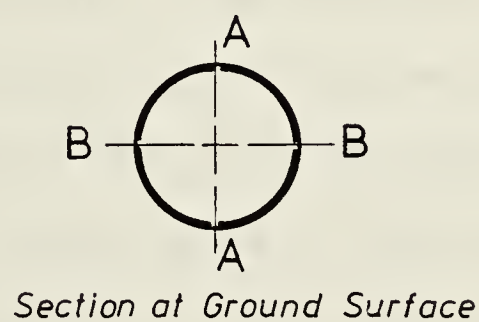


*Pump the grout
in three intervals.
Withdraw $\frac{1}{4}$ grouting
tube after each
interval.*

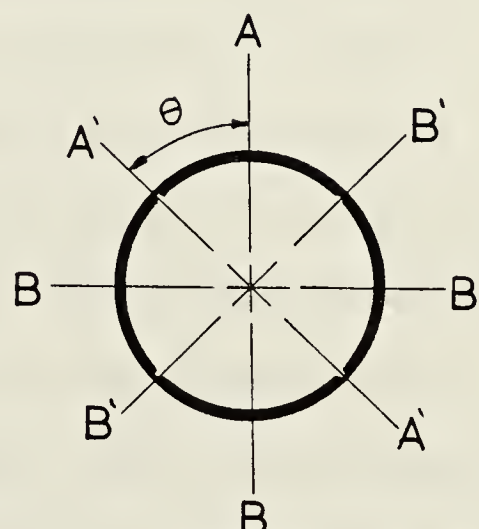
INSTALLATION STEPS (a)



(b)



SPIRAL DISTORTION
(c)



*A', B' : Measurement Axes
A, B : Preferred Axes*

ANGULAR ROTATION
(d)

Figure 4.8 Installation of slope indicators

This delay resulted in plugging of the grouting tube, which stuck in the hole. Therefore, the grout was pumped into the hole through a ten-metre long pipe. The small amount of grout pumped into the hole indicated that the hole was not completely grouted.

Because of these problems, it was decided to install the other three slope indicators initially with a bentonite grout, to keep the hole open. The bentonite grout was displaced, in the three holes on the same day, with sand-cement grout using one large delivery. This system worked very well and it was possible to pump the grout into each hole on three intervals. A quarter of the grouting tube length was withdrawn and cut after each interval to ensure the complete displacement of bentonite grout.

Plastic casing was preferred to aluminum casing because of the effective water tightness of its joints, which prevented cement particles from being washed into the casing. Grouting of the hole through N-size drill rods controlled by a check valve at the bottom of the casing (see Schmidt and Dunnicliff, 1974) was considered at the planning stage of the instrumentation program. This grouting method requires pumping of water at the end of the operation to displace the grout from the rods before their withdrawal. However, the method was not used in order to avoid the risk of discharging part of the grout inside the casing. Such a problem would require cleaning the casing with a stiff brush to remove grit from the casing tracks (Burland and Moore,

1973).

An ideal installation of a slope indicator results in an orientation of the casing grooves in the direction of principal displacements. For example, in a slope indicator installed beside a tunnel, directions A and B are chosen perpendicular and parallel to the tunnel center line respectively, as shown in Figure 4.8(b). In practice, however, the slope indicator casing usually has an angular displacement, as shown in Figure 4.8(d). In such a case, some additional calculations are required to rotate the axes of the measured displacements to the preferred axes.

Spiral distortion of the grooves in the casing is another possible irregularity which might occur during manufacture and installation of the casing. It results in a rotation of deep sections of the casing about its vertical axis relative to its top (see Figure 4.8(c)). A spiral checking instrument was rented from Slope Indicator Company and used to check the amount of this distortion in all the slope indicators installed in the experimental tunnel.

Investigations into the performance of slope indicators are given by Green (1973) and Savigny (1980). Repeatability and accuracy of the instrument used in the experimental tunnel were checked regularly by taking readings in a slope indicator casing located at far distance from the tunnel face. Similar repeatability tests were performed by Savigny (op. cit.) on the same inclinometer prope and readout unit used in the experimental tunnel. The results of these tests

indicate that the average performance is up to 10 times better than the manufacturers specifications, and even the poorest repeatability exceeded the specifications by approximately a factor of two. No obvious sensor axis rotation was observed in the measurements.

4.3 FIELD MEASUREMENTS OF SOIL DISPLACEMENT

As indicated in section 3.5, the instrumentation is concentrated in three test sections along the tunnel. The layout of these test sections is given in Figures 3.8, 3.9 and 3.10. The results from the soil instruments of each of the test sections are presented here. Tables 4.1, 4.2 and 4.3 should be consulted for details on the instruments under discussion.

4.3.1 Test Section 1

This test section is located on the portion of the tunnel with the conventional lining as shown in Figure 3.7. Its layout is given in Figure 3.8. The subsurface vertical displacement of the soil was monitored using two multipoint extensometers. Extensometer MX11 was installed above the tunnel center line and extensometer MX12 was placed beside the tunnel. The vertical movement of the soil at the tunnel crown was monitored using a single point extensometer (SPX). Eight shallow settlement points (SP1-SP8) were used to monitor the settlement of the ground surface. The profile of horizontal displacement with depth was monitored using one

Table 4.1 Details of multipoint extensometers used in the experimental tunnel

Test Section No.	Multipoint Extensometer	No. of Magnet Points	No. of Dummy Points	Location from Center-line (m)	Range of Depth of Magnets Points (m)	Date of Installation	Date the Mole Passed by	No. of Readings Taken	No. of Magnets Mal-functioned	Date of Most Recent Reading	Notes
1	MX11	8	2	00	4.8 -24.11	Nov. 10/78	Feb. 16/79	16	2	July 31/79	Damaged Aug. 1/79
	MX12	8	2	2.75 S	6.08-27.25	Nov. 13/78	Feb. 16/79	13	1	July 3/79	Damaged Aug. 1/79
	MX21	8	2	2.3 S	2.07-23.21	Nov. 29/78	May 31/79	30	3	June 22/79	Damaged June 22/79
	MX22	8	2	00	3.93-22.17	Mar. 26/79	May 28/79	22	3	Aug. 10/79	
3	MX31	10	2	4.6 N	3.72-26.26	Apr. 2/79	July 31/79	12	2	Nov. 16/79	
	MX32	10	2	2.3 N	4.04-27.28	Apr. 3/79	July 31/79	12	1	Nov. 16/79	
	MX33	8	2	00	2.55-20.88	Apr. 5/79	July 31/79	12	0	Nov. 16/79	
	MX34	10	2	2.1 S	2.39-28.27	Apr. 6/79	July 31/79	12	1	Nov. 16/79	
	MX35	10	2	4.5 S	4.19-27.31	Apr. 4/79	July 31/79	12	0	Nov. 16/79	
	MX36	10	2	3.2 N	2.72-27.00	Apr. 18/79	Aug. 2/79	10	0	Nov. 15/79	
	MX37	10	2	1.9 N	2.50-27.10	Apr. 18/79	Aug. 2/79	10	2	Nov. 15/79	
	MX38	8	2	00	2.47-20.86	Apr. 19/79	Aug. 2/79	10	3	Nov. 15/79	
	MX39	10	2	3.3 S	3.47-27.32	Apr. 17/79	Aug. 2/79	10	2	Nov. 15/79	
	MX310	10	2	5.0 S	2.24-26.77	Apr. 16/79	Aug. 2/79	10	0	Nov. 15/79	

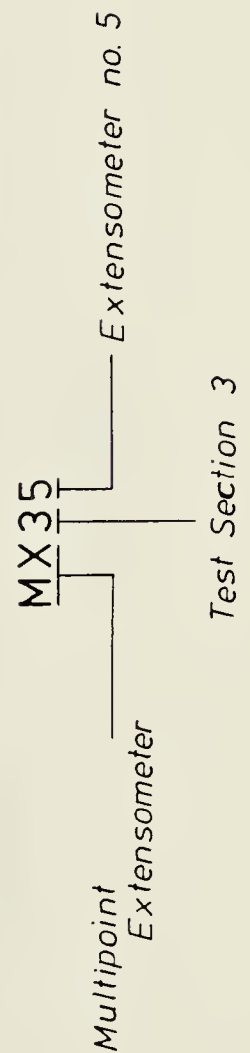


Table 4.2 Details of slope indicators used in the experimental tunnel

Test Section No.	Slope Indicator	Depth of Deepest Reading (m)	No. of Reading Points	Location from Tunnel Centerline (m)	Maximum Spiral Correction	Date of Installation	Date the Mole Passed-by	No. of Readings Taken	Date of Most Recent Reading	Notes
1	SI11	29.41	48	1.89 North	-12.8°	Nov. 14/78	Feb. 15/79	16	July 31/79	(Damaged Aug. 1)
2	SI21	32.46	53	00	-	Nov. 30/78	May 30/79	21	June 22/79	(Damaged June 22)
	SI22	31.85	52	1.74 North	10.5°	Mar. 27/78	May 28/79	19	June 22/79	
3	SI31	32.23	53	2.40 North	15.9°	Apr. 9/79	July 31/79	12	Nov. 16/79	
	SI32	32.00	52	5.06 North	16.7°	Apr. 10/78	July 31/79	10	Nov. 16/79	
	SI33	32.17	53	2.33 South	17.6°	Apr. 12/79	Aug. 2/79	10	Nov. 15/79	
	SI34	31.67	52	4.60 North	15.6°	Apr. 11/78	Aug. 2/79	9	Nov. 16/79	

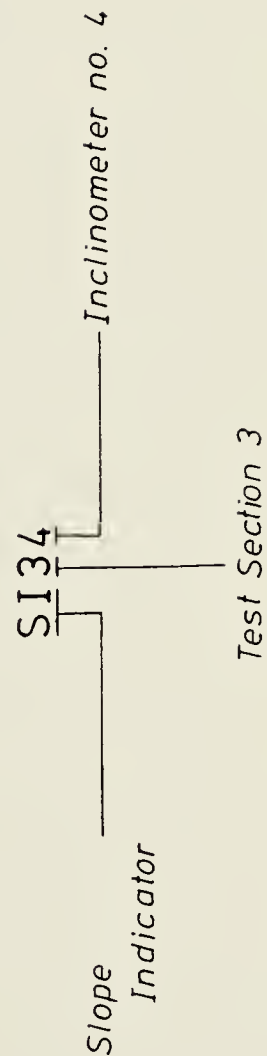


Table 4.3 Details of settlement points and single point extensometers used in the experimental tunnel

Test Section No.	Instrument	Depth from C.L. (m)	Location (m)
1	SP1	1.35	5.0 S
	SP2	1.35	1.3 S
	SP3	1.35	00
	SP4	1.35	1.3 N
	SP5	1.35	5.0 N
	SP6	1.35	00
	SP7	1.35	13.0 S
	SP8	1.35	30.0 S
	SPX	24.5	00
2	SP1	1.35	7.0 S
	SP2	1.35	3.5 S
	SP3	1.35	2.0 S
	SP4	1.35	0.5 S
	SP5	1.35	3.0 N
	SP6	1.35	20.5 S
	SP7	1.35	37.0 S
	SPX	24.0	2.0 S
3	SP1	1.35	4.2 N
	SP2	1.35	1.8 N
	SP3	1.35	00
	SP4	1.35	2.8 S
	SP5	1.35	5.5 S
	SP6	1.35	10.0 N
	SP7	1.35	5.3 N
	SP8	1.35	2.5 N
	SP9	1.35	0.5 N
	SP10	1.35	2.5 S
	SP11	1.35	5.0 S
	SP12	1.35	8.5 S
	SP13	1.35	6.0 N
	SP14	1.35	3.0 N
	SP15	1.35	0.2 N
	SP16	1.35	2.0 S
	SP17	1.35	4.5 S
	SP18	1.35	12.5 N
	SP19	1.35	12.9 N
	SP20	1.35	26.0 N
	SPX1	21.9	00
	SPX2	17.0	00
	SPX3	11.1	00
	SPX4	5.50	00
	SPX5	27.0	4.7 N

Note: SP: Settlement Point
SPX: Single Point Extensometer

slope indicator (SI11) installed beside the tunnel.

Subsurface vertical displacement, as measured using three magnet points in extensometer MX11, is given in Figure 4.9. Figure 4.10 shows vertical displacement vs. tunnel advance as measured using MX11 and SP6. A similar diagram (Figure 4.11) was constructed using the data obtained from MX12 and SP2. The profile of the trough of final settlement as measured using the shallow settlement points is given in Figure 4.12.

Horizontal displacements perpendicular (direction A) and parallel (direction B) to the tunnel center line were measured by slope indicator SI11 and the results are given in Figure 4.13. The displacement in direction A at depths "1", "2" and "3" (shown in Figure 4.13) is given in Figure 4.14 as a function of the advance of the tunnel face.

4.3.2 Test Section 2

Test Section 2 was placed at an early stage of construction (Figure 3.7) using the new segmented lining. Its layout is given in Figure 3.9. The subsurface vertical displacement of the soil was monitored using two multipoint extensometers and a single point extensometer. Extensometer MX21 and SPX were installed above the edge of the tunnel while MX22 was placed above the tunnel center line. Seven settlement points (SP1-SP7) were used to measure the settlement of the ground surface.

Two slope indicators were installed to measure the

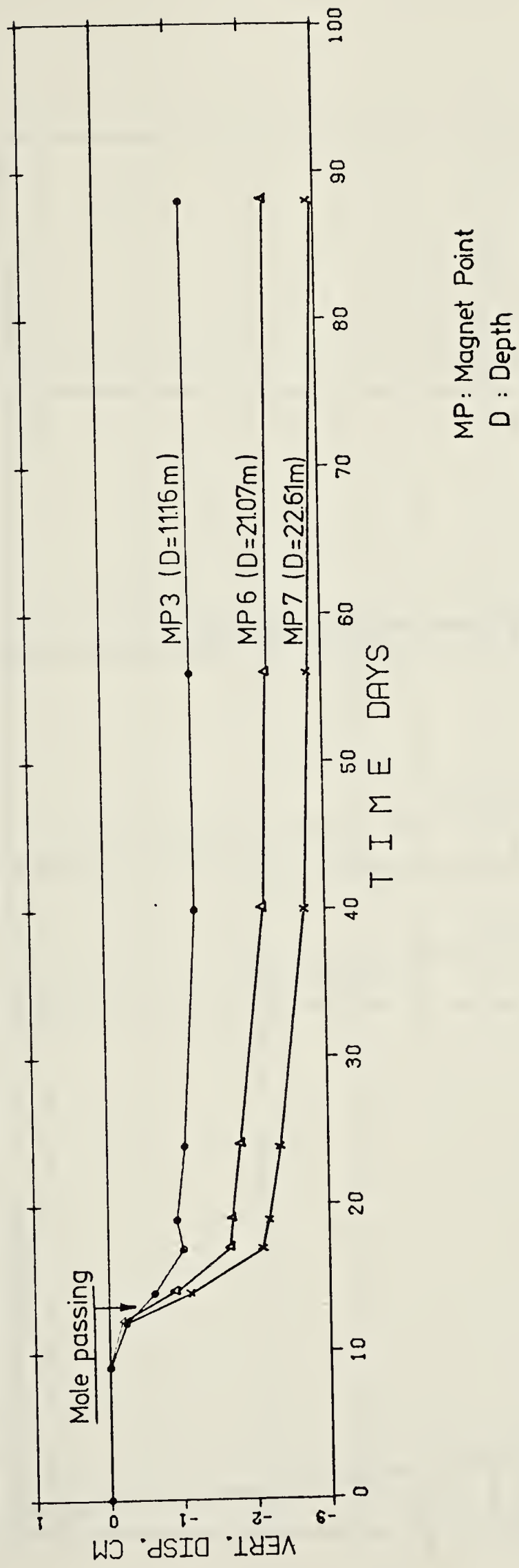


Figure 4.9 Vertical displacement measured using extensometer MX11

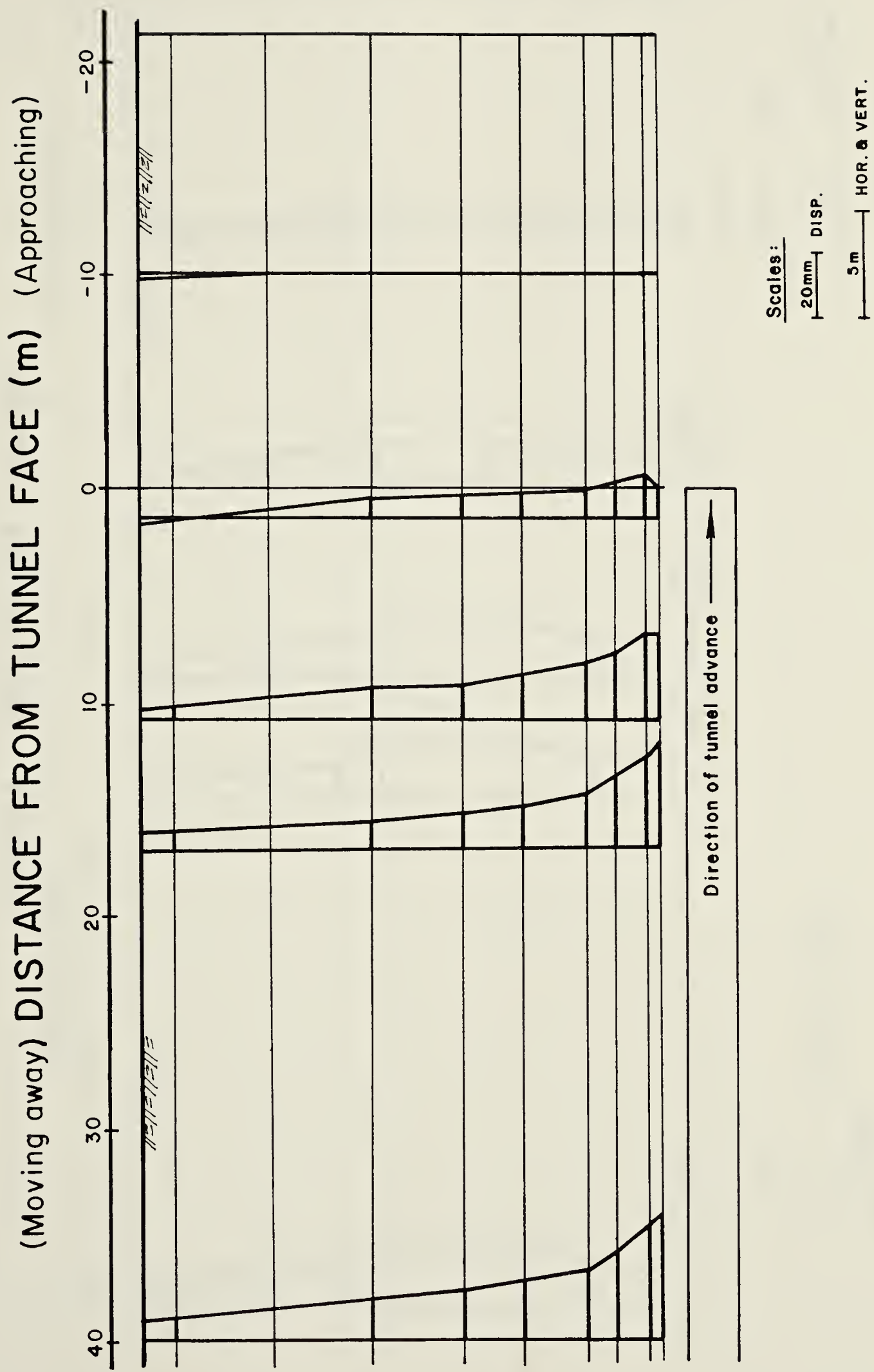


Figure 4.10 Vertical displacement vs. tunnel advance (MX11)

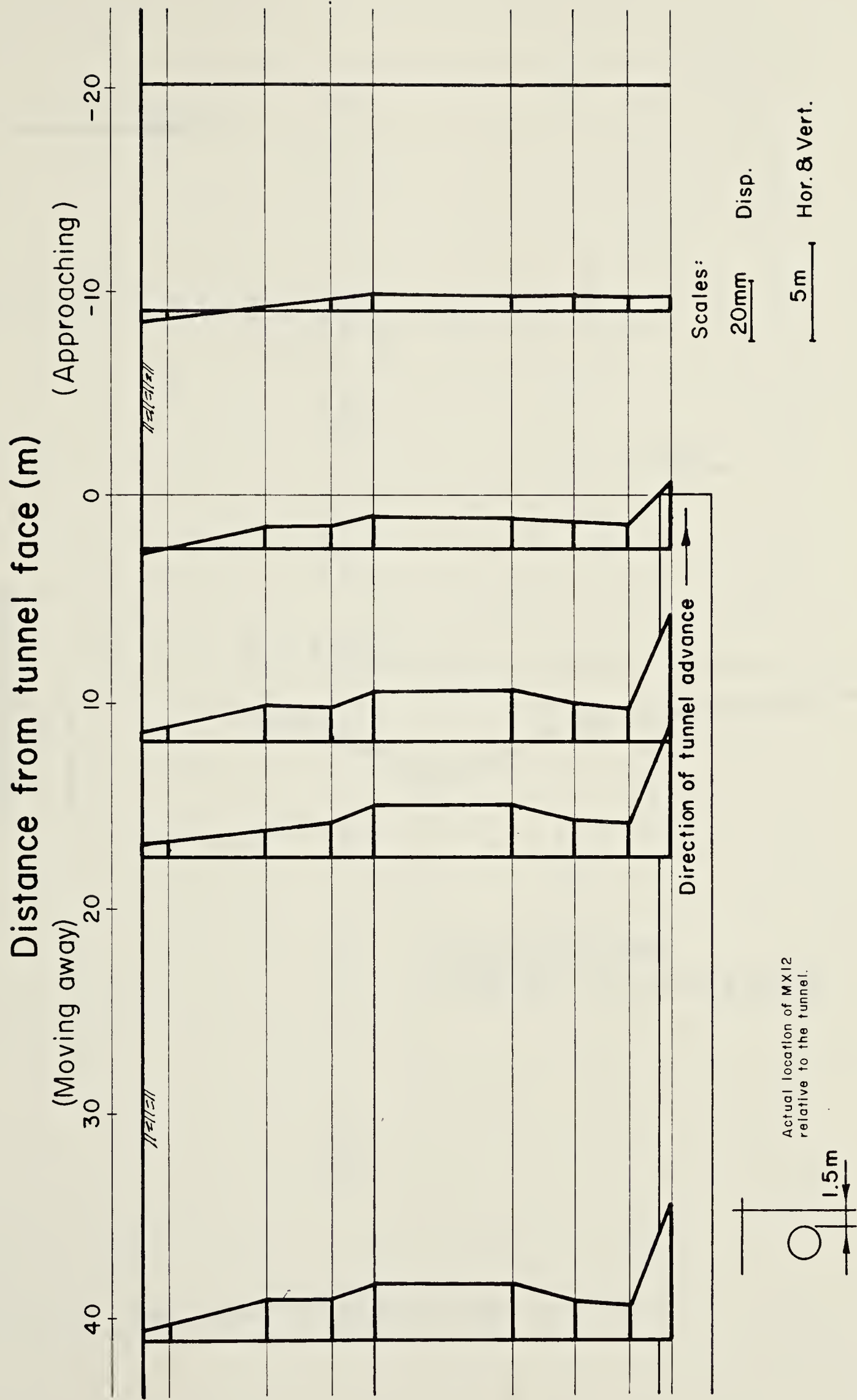


Figure 4.11 Vertical displacement vs. tunnel advance (MX12)

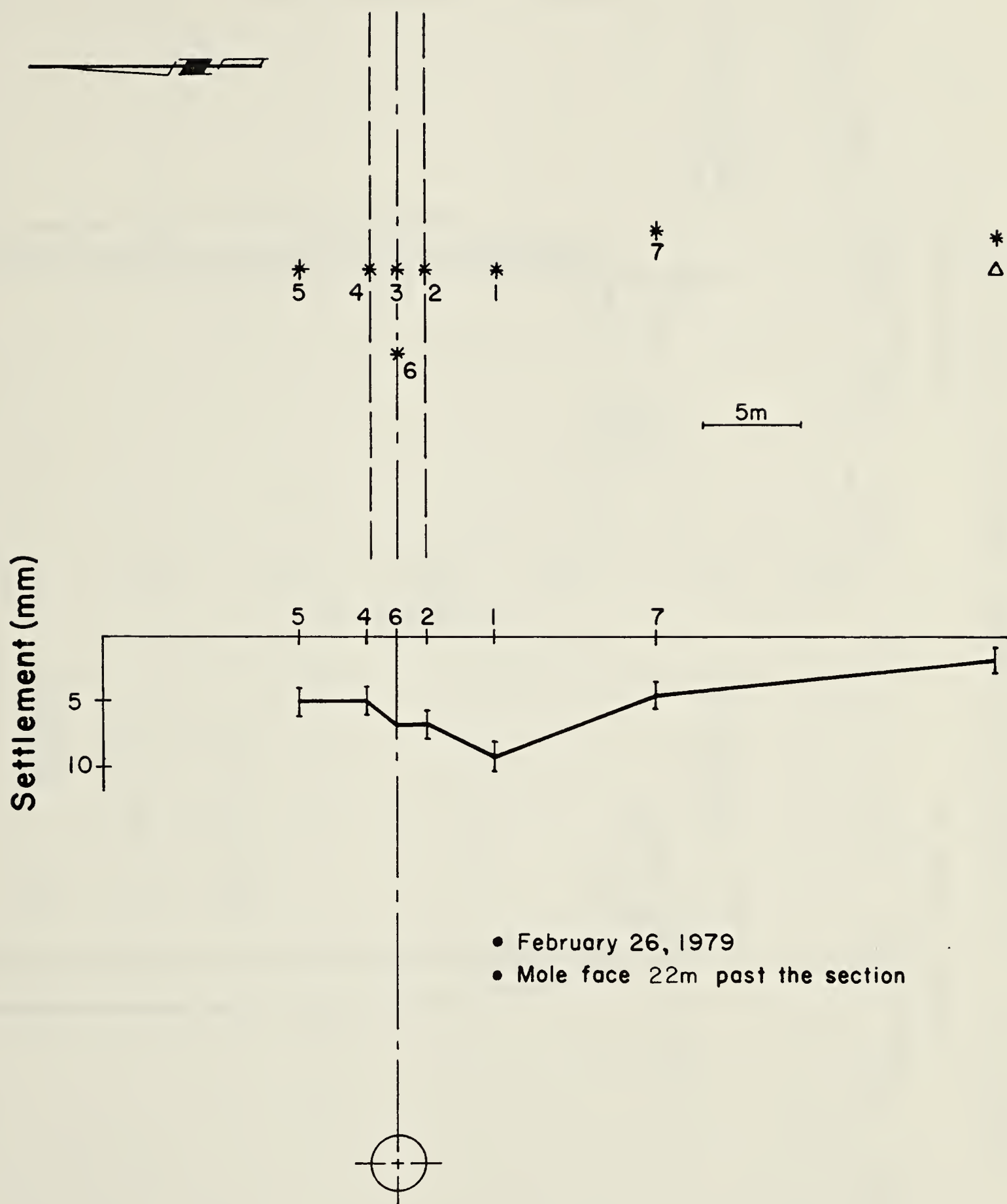


Figure 4.12 Settlement trough at Test Section 1

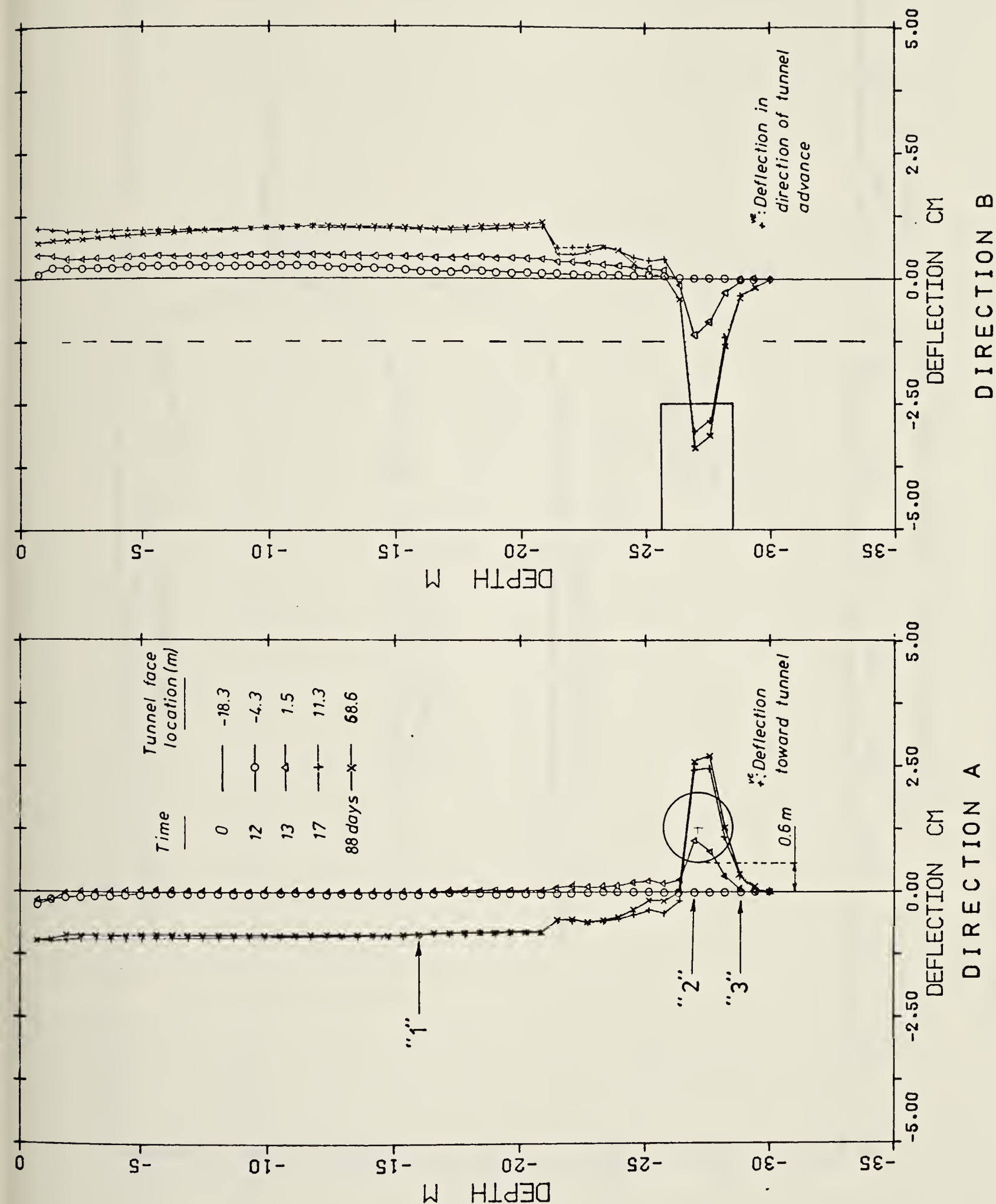


Figure 4.13 Horizontal displacement measured using slope indicator SI11

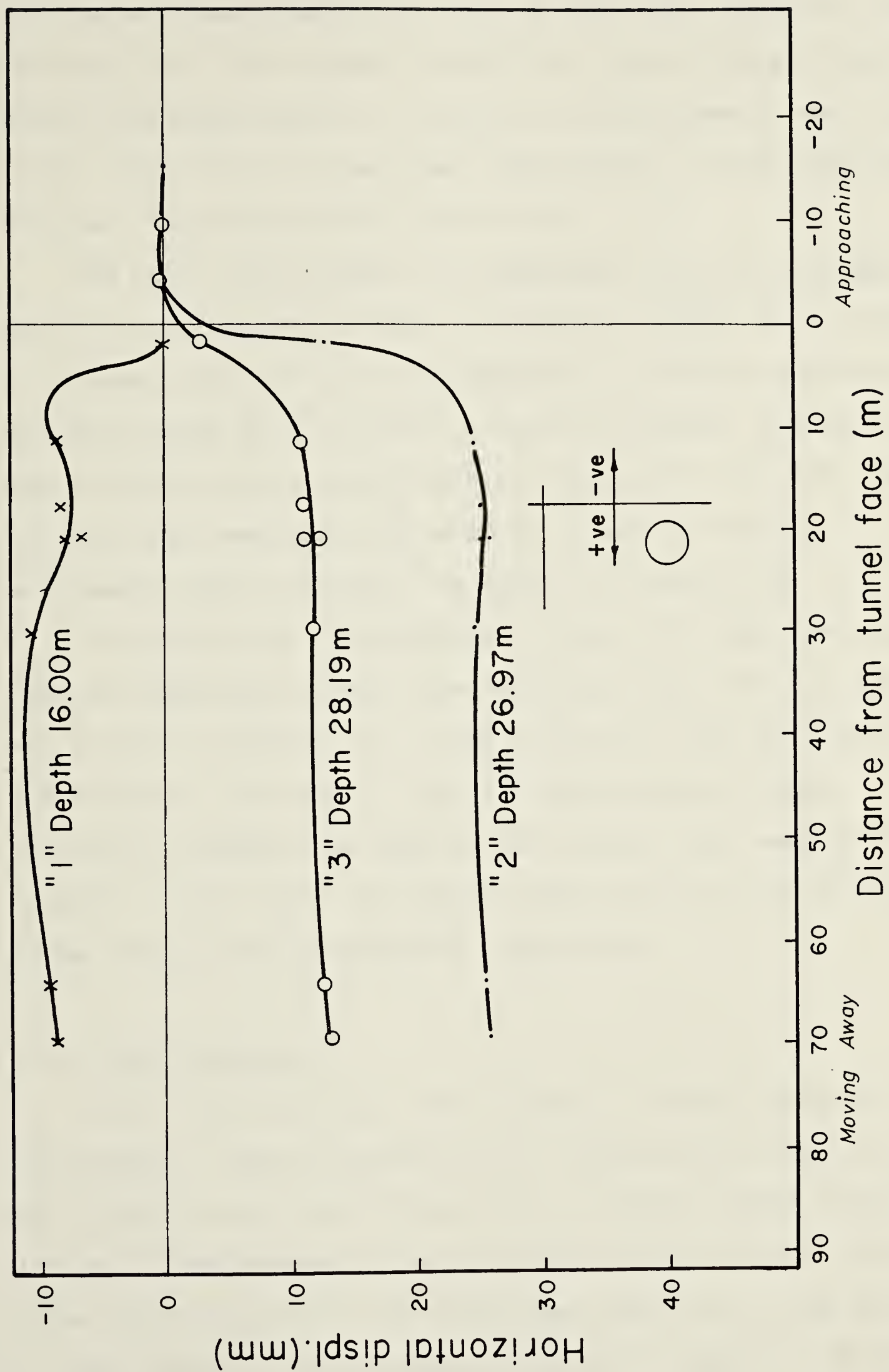


Figure 4.14 Horizontal displacement (Direction A) vs. tunnel advance (SI11)

horizontal displacement profiles in this test section. Slope indicator SI21 was placed through the tunnel center line to enable the measurement of horizontal displacement near the tunnel face while the mole was approaching. Slope indicator SI22 was installed beside the tunnel.

Vertical displacement, as measured using three magnet points in extensometer MX22, is given in Figure 4.15. Figure 4.16 shows vertical soil displacement vs. tunnel advance as measured using MX22 and SP4. A similar diagram (Figure 4.17) was plotted using the data obtained from MX21 and SP3. The ultimate settlement trough profile, based on shallow settlement point readings, is given in Figure 4.18.

The horizontal displacement of the soil near the tunnel face was measured using slope indicator SI21 and the results are given in Figure 4.19. Slope indicator SI22 was installed too close to the tunnel. Thus it experienced a large horizontal movement as soon as the tunnel face reached its location. This large deformation made insertion of the probe below crown level practically impossible.

4.3.3 Test Section 3

Both Test Sections 1 and 2 have a limited number of instruments, whose purpose was to indicate the trends of soil behavior and provide data for a general comparison of the soil displacement around the two lining systems. On the other hand, Section 3 (the main test section) is the site of a large number of instruments as shown in Figure 3.10. The

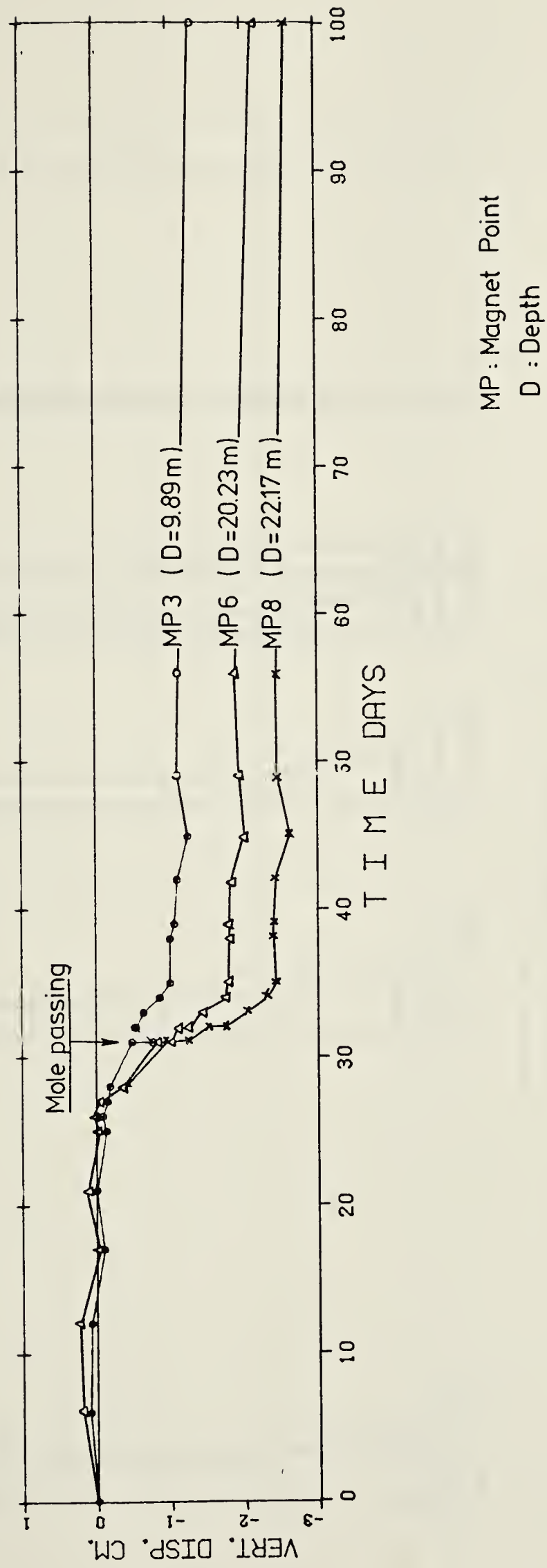


Figure 4.15 Vertical displacement measured using
extensometer MX22

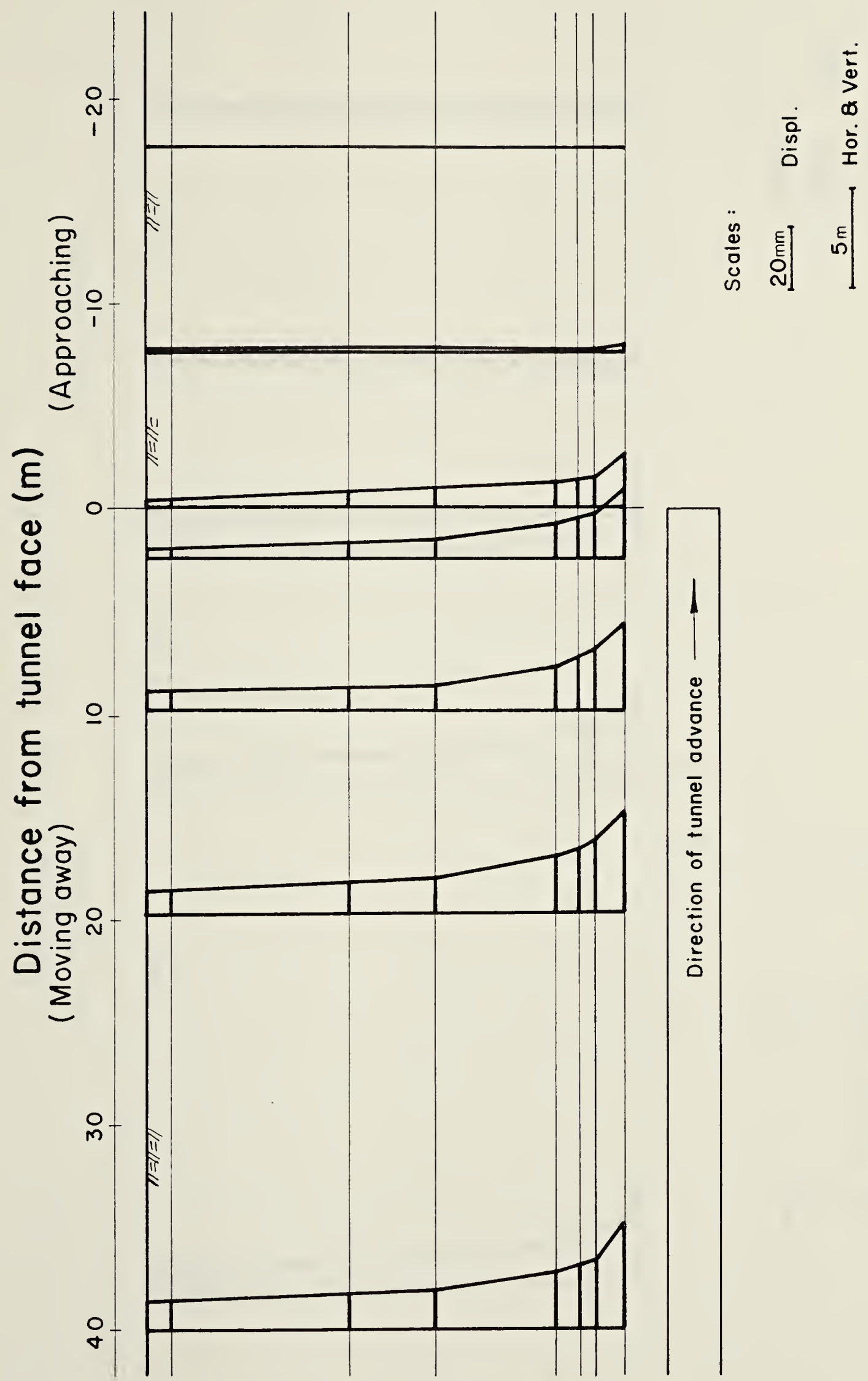


Figure 4.16 Vertical displacement vs. tunnel advance (MX22)

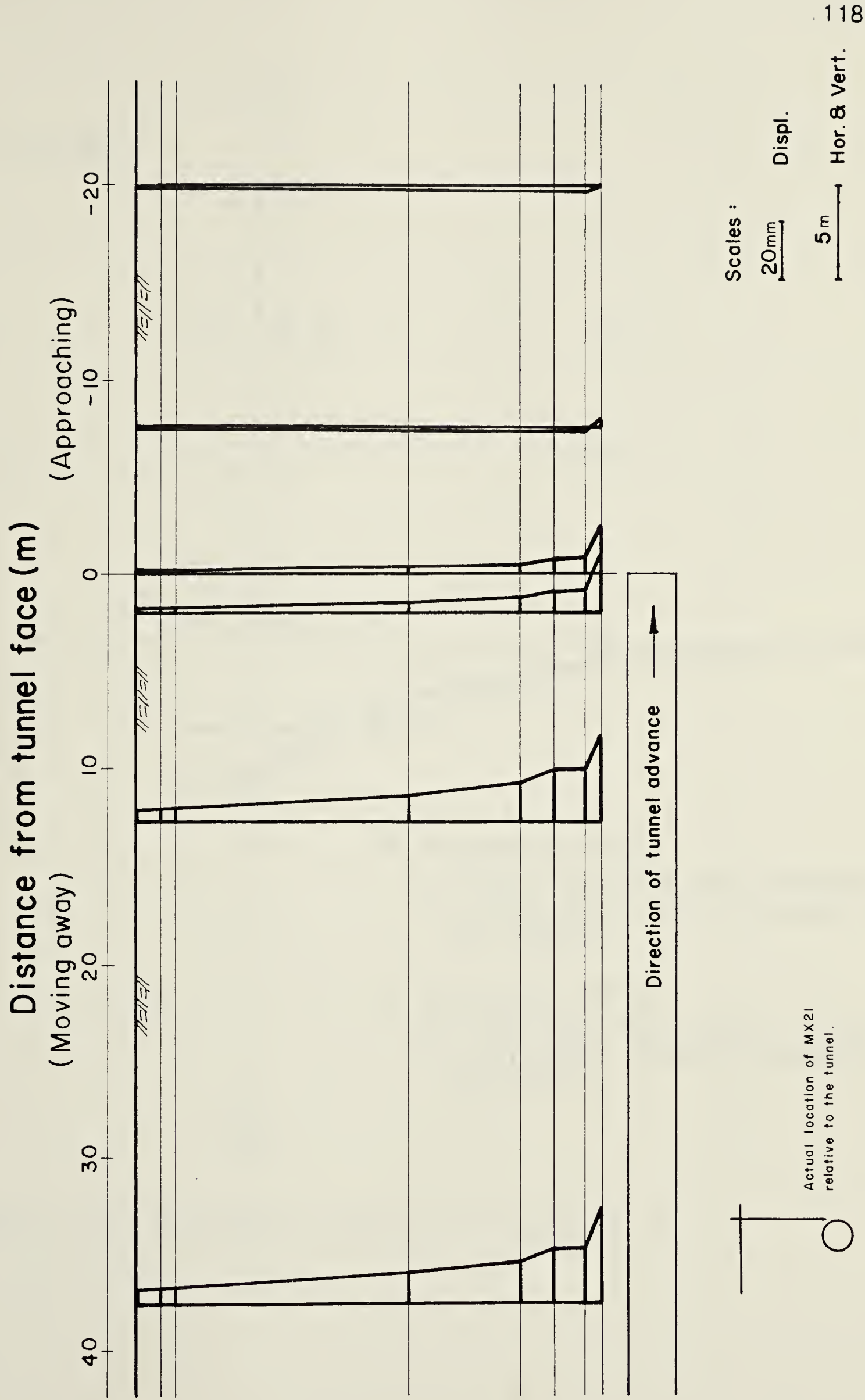


Figure 4.17 Vertical displacement vs. tunnel advance (MX21)

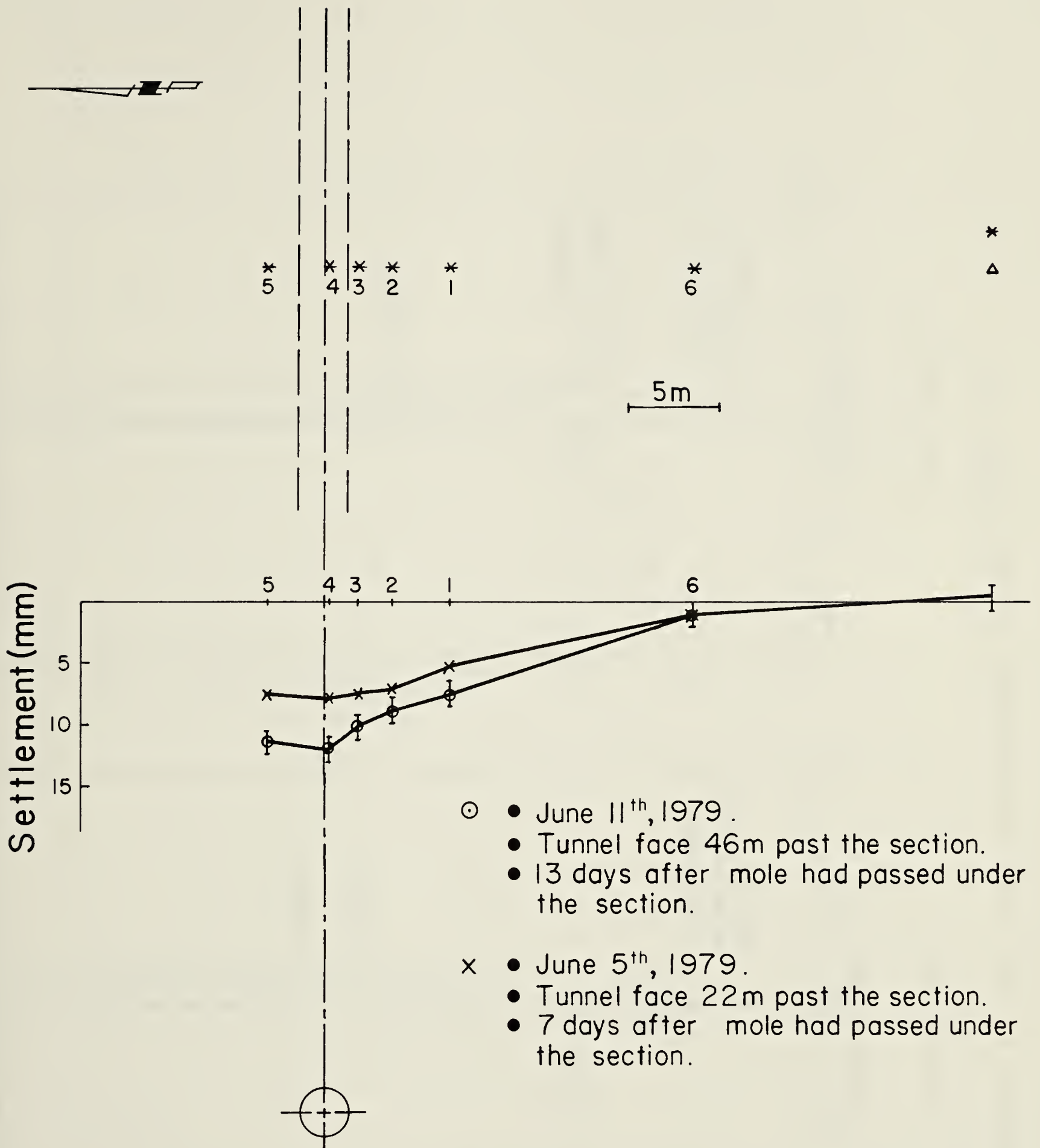


Figure 4.18 Settlement trough at Test Section 2

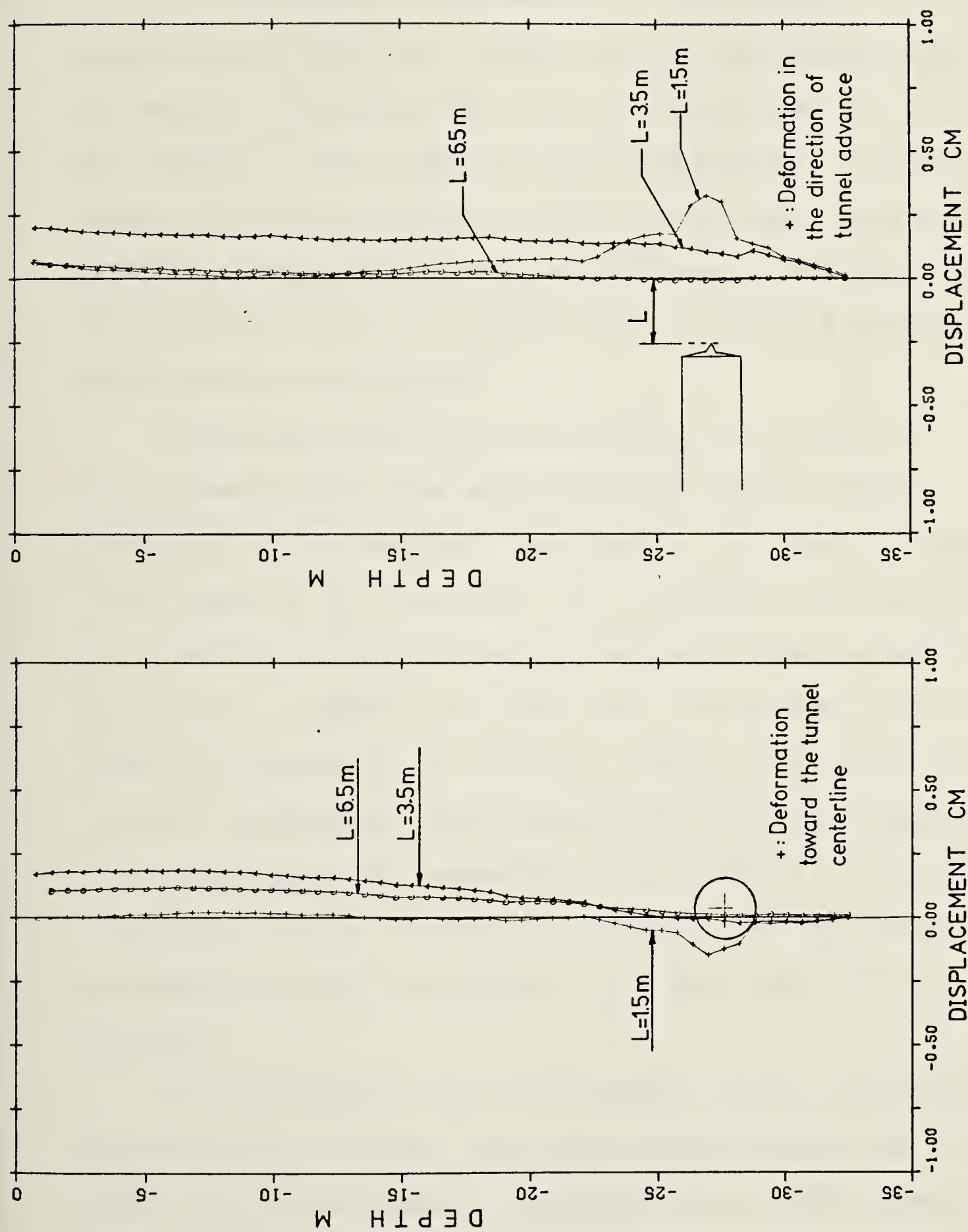


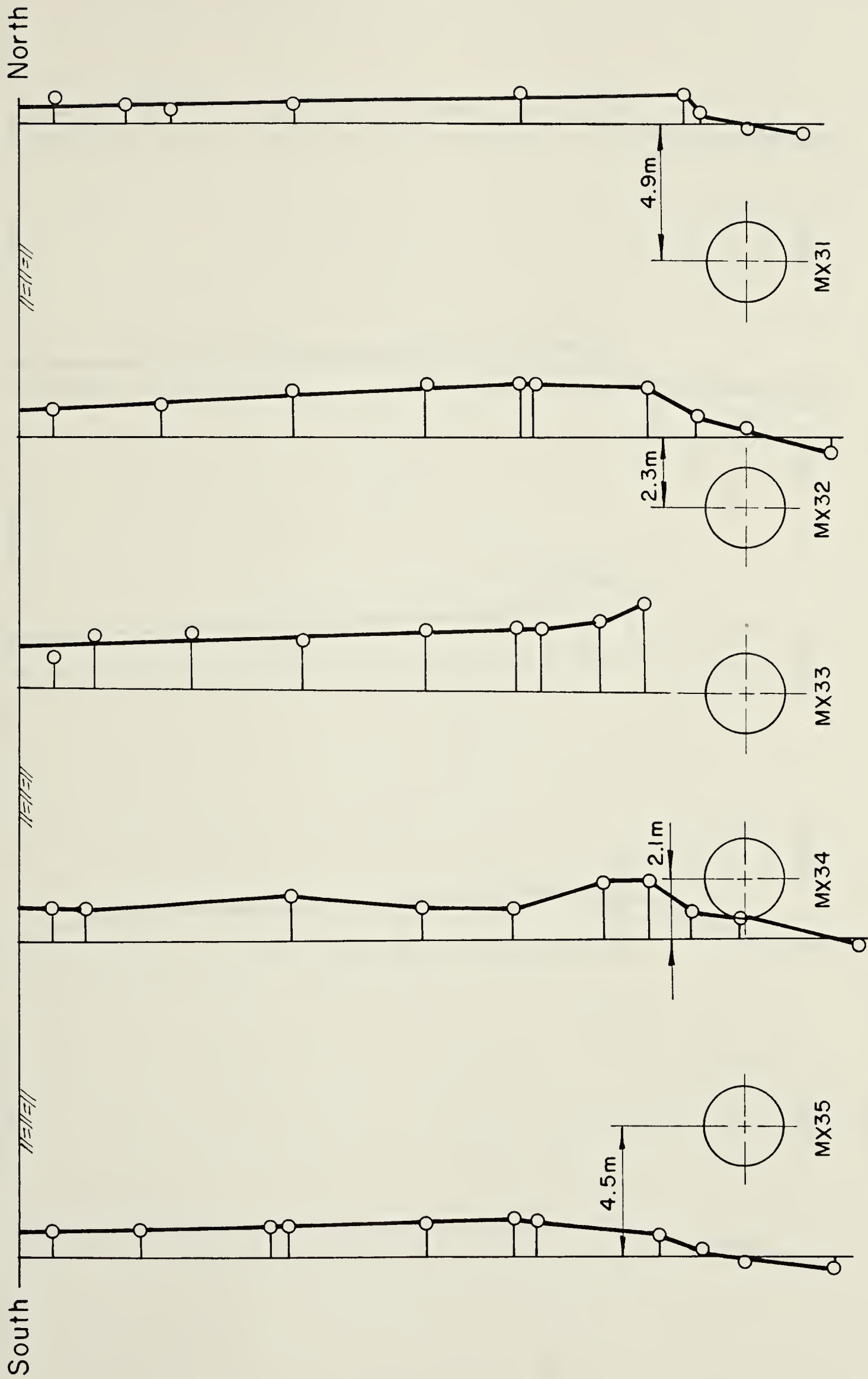
Figure 4.19 Horizontal displacement at the tunnel face

main objective of this test section was to measure the spatial pattern of soil displacement around the advancing tunnel.

Ten multipoint extensometers, containing ninety-six magnet points and five single point extensometers were used to measure the subsurface vertical displacement. The settlement of the ground surface was obtained by observing twenty shallow settlement points. Four slope indicators were installed beside the tunnel at different distances from the tunnel center line to measure the profile of horizontal displacements with depth.

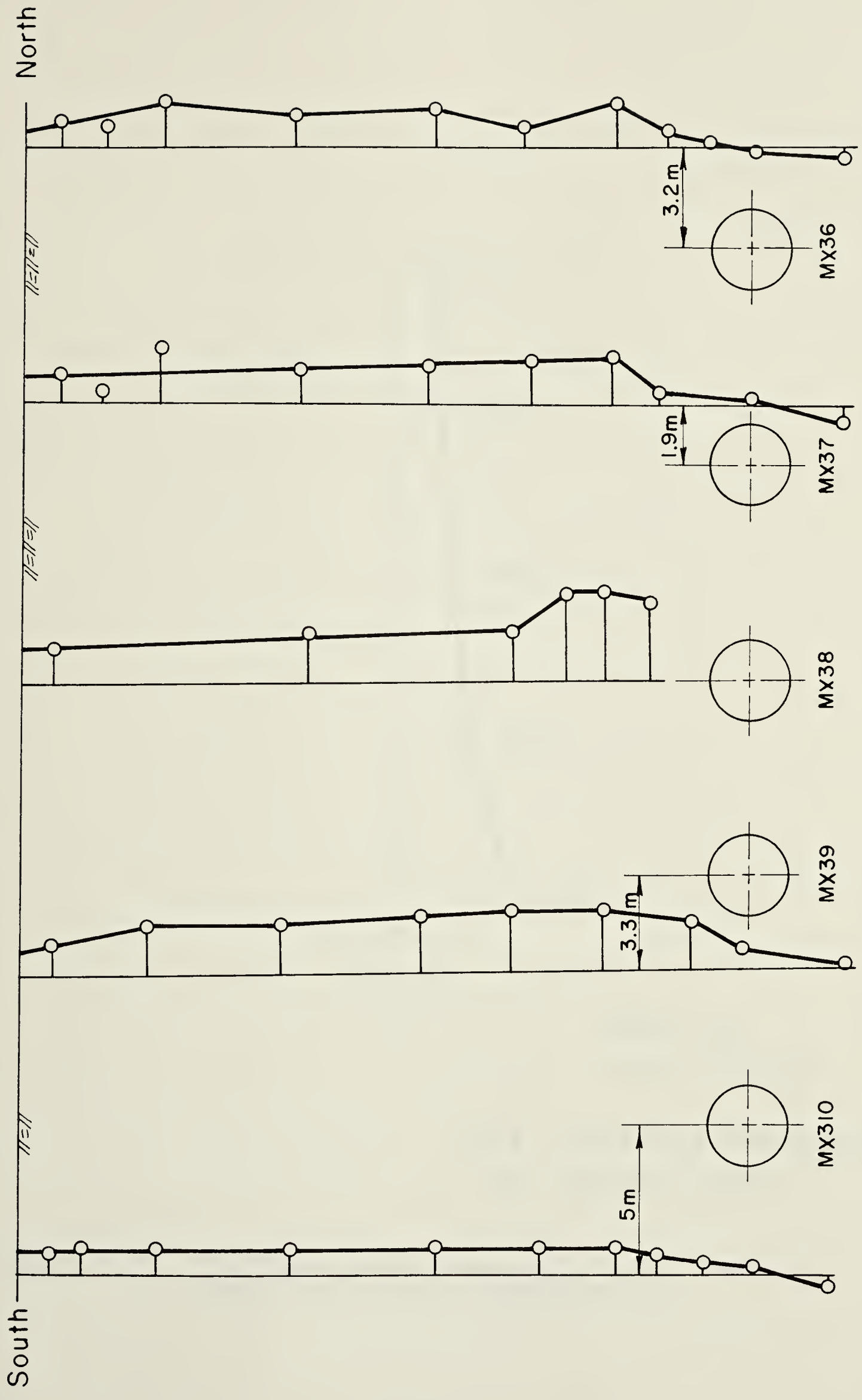
Graphs portraying the development of vertical displacement with time and with tunnel face advance, observed in this section, are similar to those of Section 2 (see Figure 4.15, 4.16 and 4.17). Complete records of the measurements obtained from the ten multipoint extensometers are given in Appendix A. The final displacement indicated by these extensometers is given in Figures 4.20 and 4.21. A similar diagram was constructed using the data obtained from the single point extensometers and is given in Figure 4.22. Figure 4.23 shows the profile of the final settlement trough as measured using the shallow settlement points in this section.

The horizontal soil displacement at this section was measured as the tunnel face approached, passed and moved away. Final displacement, perpendicular to the tunnel center line, is shown in Figure 4.24 as measured by the four slope



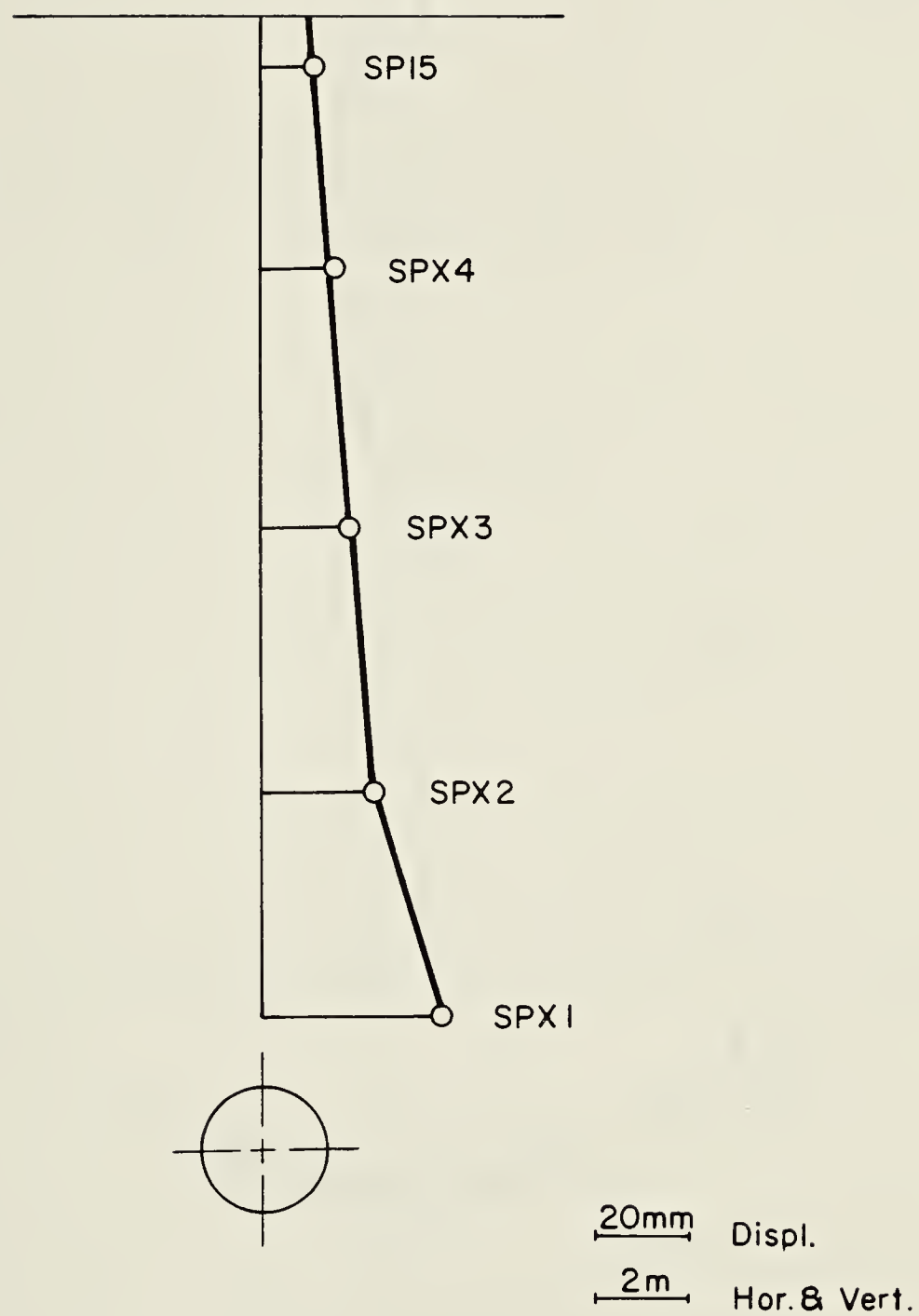
August 8, 1979.
8 days after mole passed the section

Figure 4.20 Final settlement measured at Test Section 3
(MX31-MX35)



August 10, 1979
8 days after mole passed the section

Figure 4.21 Final settlement measured at Test Section 3 (MX36-MX310)



SPX : Single point extensometer
SP : Settlement point

Figure 4.22 Final settlement measured at Test Section 3 using single point extensometers

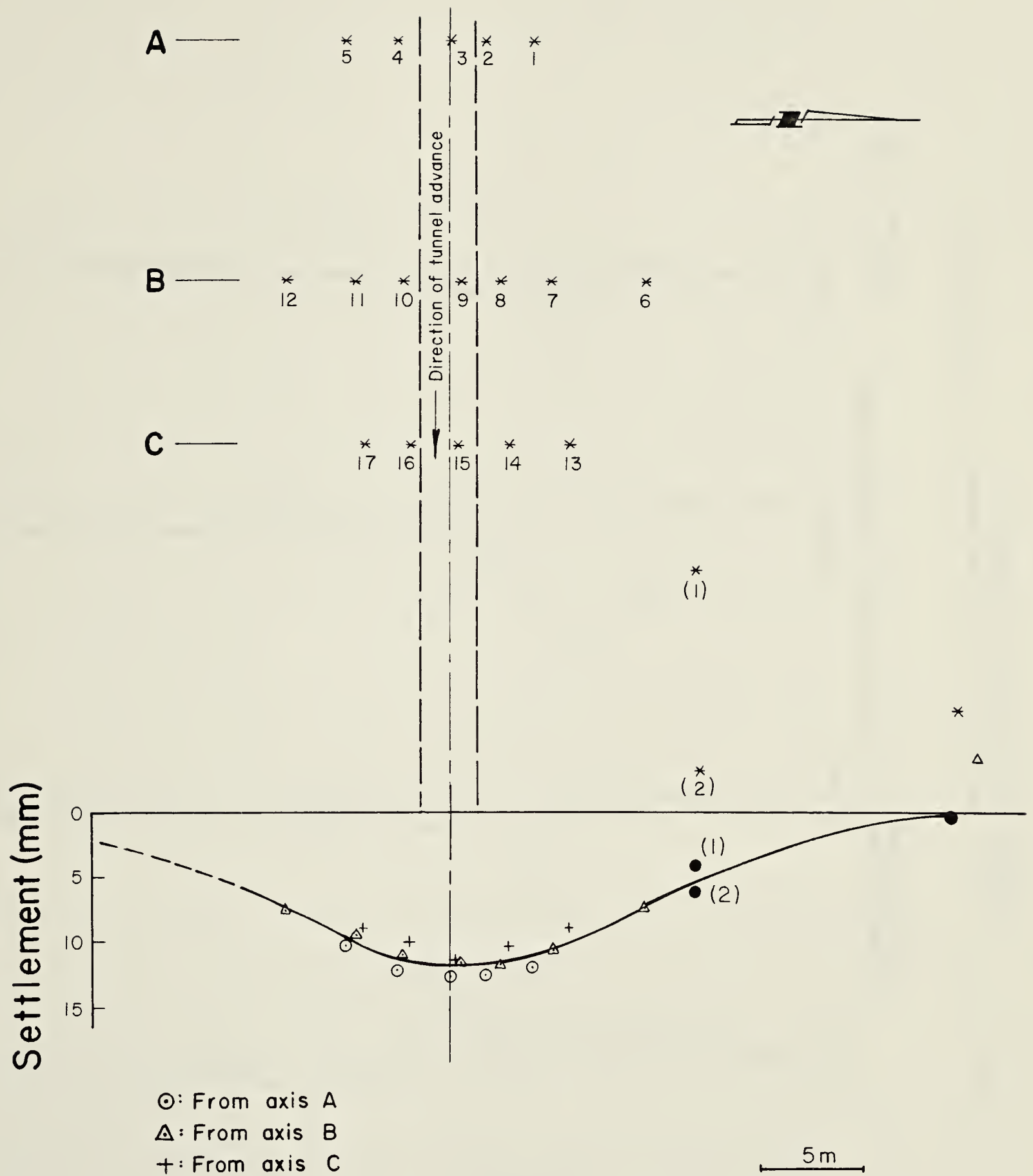


Figure 4.23 Final Settlement trough at Test Section 3

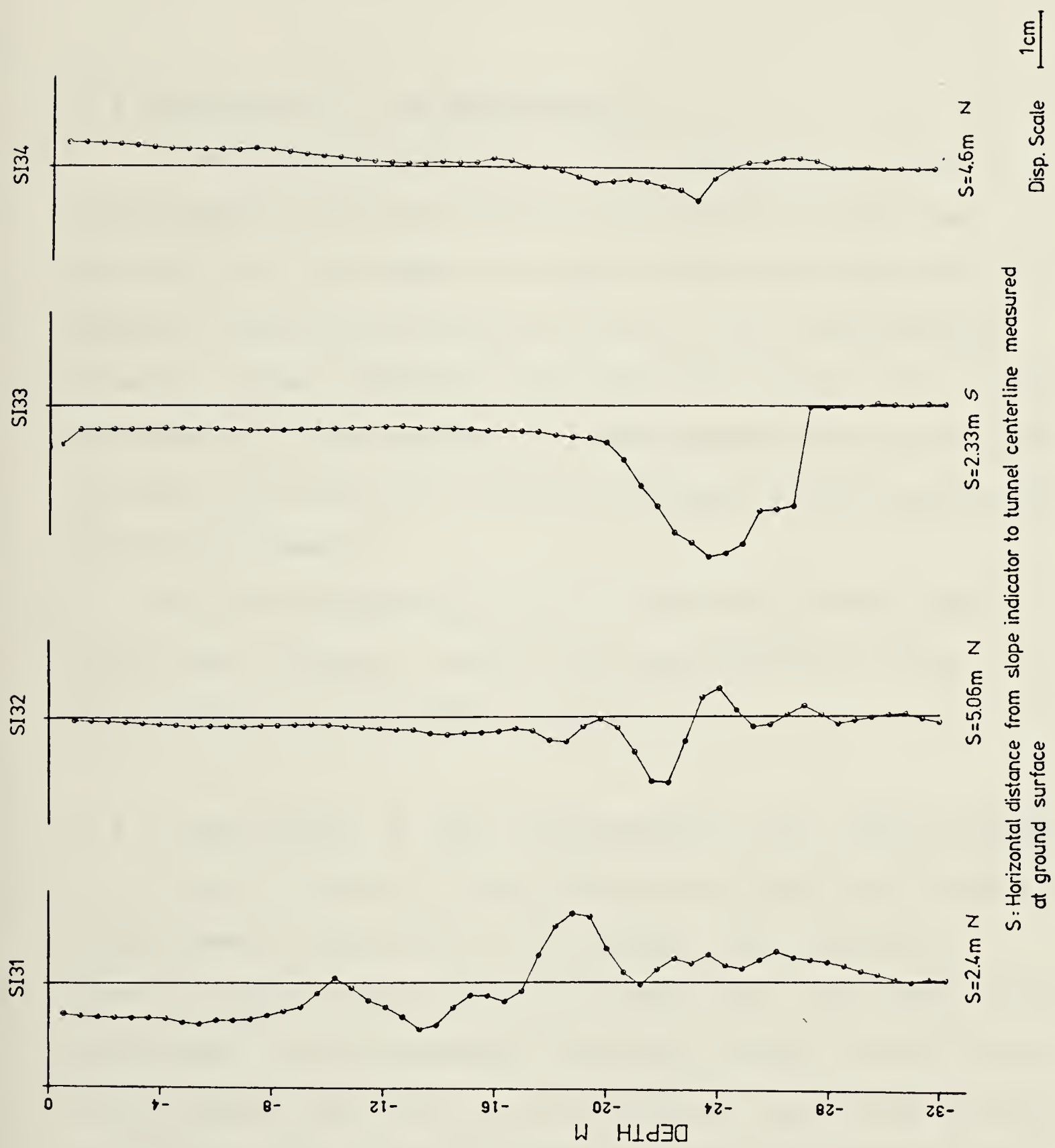


Figure 4.24 Final horizontal displacement in direction A measured at Test Section 3

indicators, while Figure 4.25 shows the final displacement parallel to the tunnel center line. Complete records of slope indicator measurements obtained from this test section are given in Appendix B.

4.4 DISCUSSION OF THE MEASUREMENTS

A detailed examination of the measurements of soil displacement obtained from the experimental tunnel was carried out. The immediate objective was to formulate the general trends and characteristics of soil displacement around a tunnel advancing through stiff glacial till using a shielded drilling machine. The measurements were also used to study the effect of the two different lining systems on soil displacements.

The following discussion is limited to these two objectives; however, a more detailed analysis of the measurements is included in Chapter 6.

4.4.1 Development of Soil Displacements with Tunnel Advance

A small portion of the ultimate vertical and horizontal displacement occurs before the tunnel face reaches a specific point (see Figures 4.14 and 4.26). The rate of the development of the movement increases sharply as the tunnel face reaches that point, and then drops significantly when the tunnel face has been advanced about seven metres (2.7 diameters) beyond the point. Soil near the ground surface could experience some heave while the tunnel is approaching

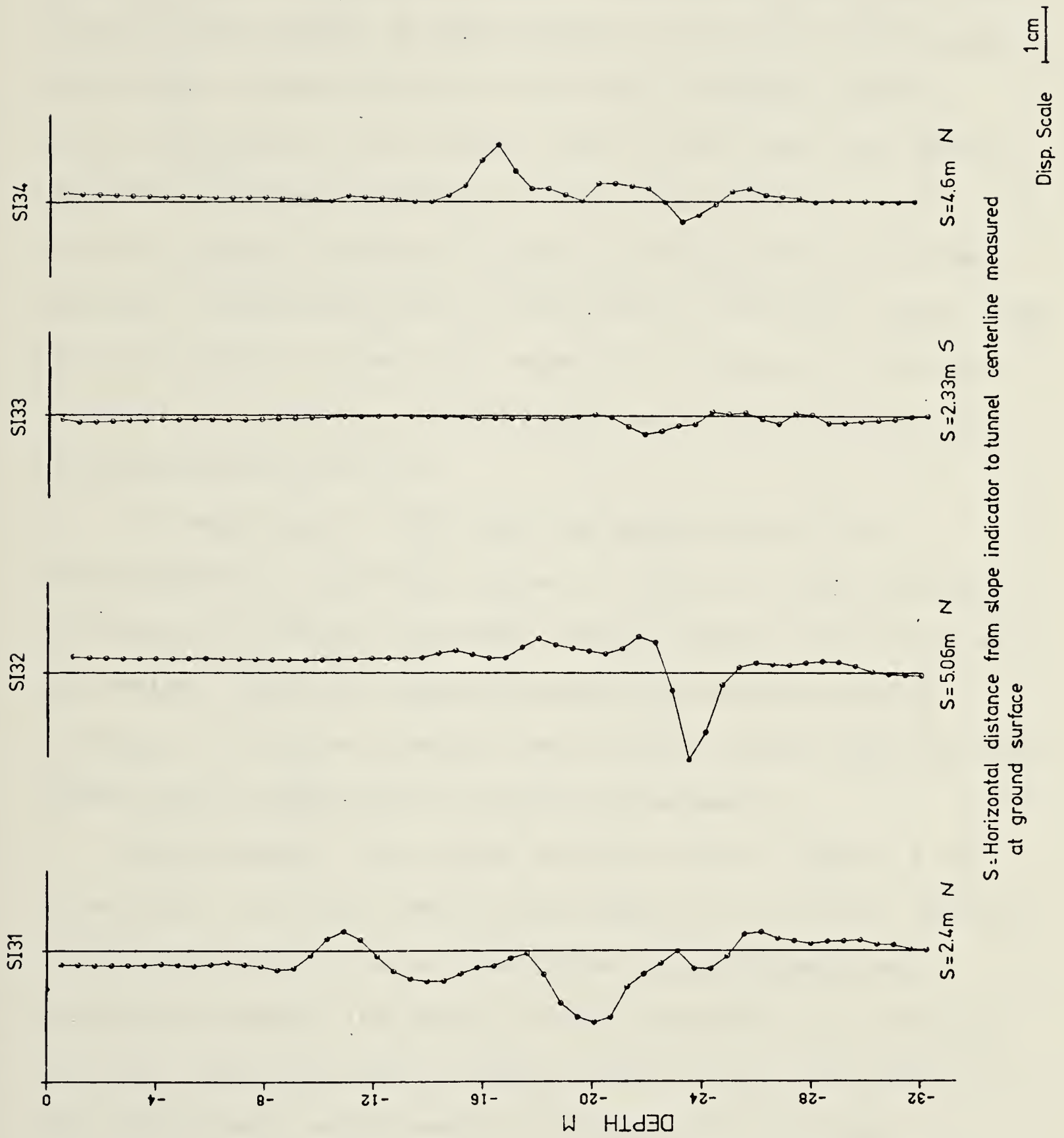


Figure 4.25 Final horizontal displacement in direction B measured at Test Section 3

as shown in Figures 4.10 and 4.11.

The dashed curve in Figure 4.26, which was drawn by connecting the measured points, illustrates that there are two distinct stages of development of the soil displacement around the tunnel which are different from the portion occurring ahead of the tunnel face. First, the soil moved rapidly to close the annular space resulting from soil overcut around the mole. As soon as this space was filled, the soil displacement was stabilized by the mole itself. The soil was able to move again when the tailpiece of the mole cleared the section. This movement soon stabilized as the lining became effective.

A comparison of the relative magnitude of soil displacements at various stages of tunnel boring indicates that most of the soil movement occurs before the lining was activated. Hence the size of tunneling overcut and the timing of lining activation are the most significant factors affecting the magnitude of such displacement.

Measurements from slope indicator SI21 (Figure 4.19) show that, with the tunnel face close by ($L=1.5$ m), the soil along the center line of the tunnel experiences a net outward movement. The sense of this movement is a function of both tunneling machine design and the soil stiffness. On the other hand, measurements from most of the slope indicators placed beside the tunnel indicate a significant longitudinal displacement opposite to the direction of tunnel advance (Figure 4.13 and 4.25).

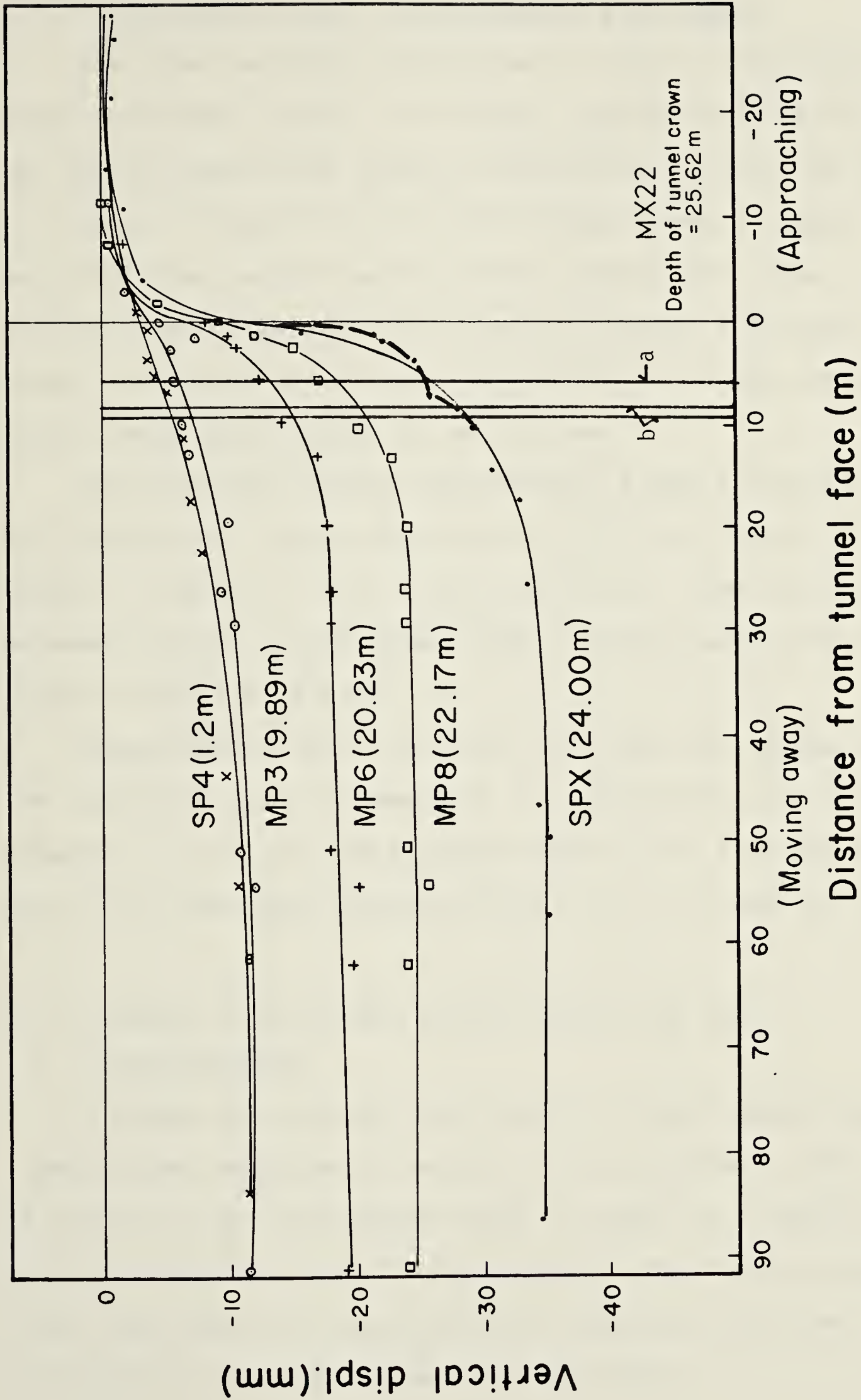


Figure 4.26 Vertical displacement vs. tunnel advance

4.4.2 Variation of Soil Displacements with Depth

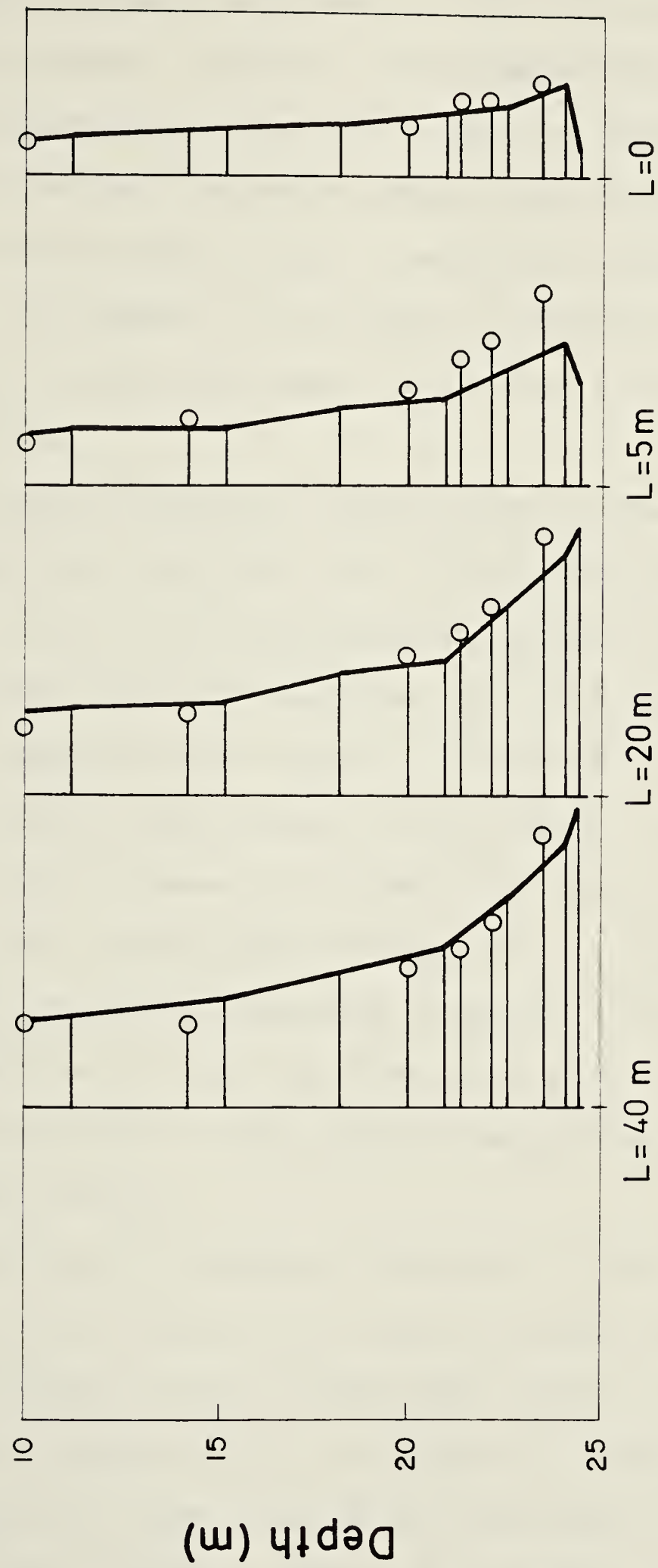
The final vertical displacement along a line directly above the tunnel center line decays rapidly from 30-40 mm at the tunnel crown to 8-12 mm at the ground surface, as shown in Figure 4.10 and 4.16. Vertical displacements along vertical lines away from the tunnel center line show different profiles as illustrated in Figures 4.20 and 4.21. These two figures also show that points below the tunnel invert experience heaves of up to 6 mm.

The final horizontal displacement along a vertical line just beside the tunnel occurs mainly in the vicinity of the tunnel, (Figures 4.13-SI11 and 4.24-SI33). Some horizontal movements occur at shallower depths further away from the tunnel (Figure 4.24-SI32).

Measurements from the three test sections showed that the horizontal soil movement at the springline and vertical movement at the crown are almost equal. This indicates that K_0 in this overconsolidated glacial till is close to 1.0.

4.4.3 Effect of Different Lining Systems on Soil Displacements

A comparison between the vertical displacement near the tunnel crown measured at Section 1 by extensometer MX11 and at Section 2 by extensometer MX22 is shown in Figure 4.27. Both extensometers were installed above the tunnel center line. The tunnel is lined with rib-lagging at Section 1 and with precast concrete segments at Section 2.



L: Distance from tunnel face to instrument (m)

10mm Displ.

— Section 1 (MXII) RIB and LAGGING

o Section 2 (MX22) PRECAST SEGMENTS

Figure 4.27 Soil displacement around different lining systems

When the tunnel face had advanced to a point exactly under each of these instruments, both experienced the same vertical movement. However, extensometer MX22 showed a greater displacement than MX11 when the tunnel face had advanced another five metres beyond the instruments. At that time the shield had not yet cleared the location of either of these instruments. This seems to indicate a larger size of overcut around the tunnel at Section 2 compared to that at Section 1.

As soon as the mole cleared each of the instruments and the lining was installed, the difference between the movement of the two extensometers reduced significantly, and with further travel of the mole, vertical displacements at Section 1 became almost equal to those of Section 2. Although overcut was greater at Section 2, final soil movement was the same at the two sections. This indicates that the soil around the rib-lagging is allowed to move more than that around the segmented concrete lining because of the difference in their stiffness and more importantly due to the difference in the size of the gap left between the lining and the soil.

Expanding the segmented concrete lining is considered to practically eliminate the annular space around the tunnel, leaving a few isolated small gaps, as will be discussed in more details in Chapter 5. Usually the space left around the steel ribs is on the order of 2-3.5 cm (Thomson and El-Nahhas, 1980). As a result, the soil around

the steel ribs is more free to move.

It should be noted, however, that the effect of different linings on soil displacement is more significant for points closer to the tunnel. The settlement at the ground surface seems to be independent of the lining method at least over the time period of these measurements.

4.5 SUMMARY

This chapter reviewed the different instruments which can be used for measuring soil displacements around a tunnel. The instruments chosen for the experimental tunnel were described in some detail and the principles of operation, as well as installation and measurement procedures were given.

Measurements of soil displacement obtained from three test sections of the experimental tunnel analyzed to establish the general trends and characteristics of soil displacements around a tunnel advancing through stiff glacial till using a shielded drilling machine.

Although more analysis of these measurements is given in Chapter 6, the following immediate conclusions were reached:

1. The final vertical soil settlement at the tunnel crown above the two linings is on the order of 30-40 mm. The final horizontal displacement at the elevation of the springline is on the order of 25-30 mm and directed toward the tunnel. The maximum settlement of the ground

surface above the tunnel center line varies from 8-12 mm.

2. A small portion of the ultimate vertical and horizontal soil displacement of a specific point occurs before the tunnel face reaches that point. Most of the remaining displacement occurs while the mole is passing the point and before the soil-lining interaction starts.
3. Measurements of horizontal movement at the tunnel face indicate that the soil at that location is actually displaced outwards by the drilling machine rather than being allowed to move towards the tunnel.
4. Vertical soil movement in the region of the crown is a little larger when rib-lagging lining is used rather than segmented concrete lining. The effect of the lining is less pronounced on the soil movement at shallower depths and at the ground surface the vertical movement seems to be independent of lining.
5. The measurements of soil displacement indicates that K_0 in the overconsolidated glacial till of Edmonton area is close to 1.0.

CHAPTER 5

BEHAVIOUR OF TWO SYSTEMS OF TUNNEL LINING

5.1 INTRODUCTION

The last decade represented an active period for a worldwide exchange of tunneling technologies. One of the most significant features of this exchange is the trial of European lining systems in North America, specifically to examine their feasibility in local contracting practice and ground conditions and to assess their cost. Precast segmented lining and shotcrete gradually became competitive with the conventional rib and lagging lining (Mason, 1968; Bartlett et al., 1971; Cording, 1973; Mahar et al., 1975; Tilp and Shoeman, 1977; Morton et al., 1977). During 1978, alternate lining methods for the tunnels in Edmonton area were examined.

More than one hundred kilometers of sewer tunnels have been constructed in the Edmonton area since 1955. All of these tunnels were built with the conventional North American lining, which consists of a two-phase support system, (a temporary rib and lagging system and a permanent cast-in-place concrete lining). These tunnels have been drilled through glacial till and Upper Cretaceous clay-shale, using both shielded and unshielded moles.

Field measurements on the primary lining in these tunnels (Eisenstein and Thomson 1978; Thomson and El-Nahhas,

1980) showed that the equilibrium state of soil-lining interaction is reached within two weeks for glacial till and within three months for the clay-shale. If placement of the secondary concrete lining is delayed until the primary lining has reached this equilibrium state, no stresses will be immediately transmitted from the soil to the final lining. This lining is acted upon only by secondary stresses resulting from shrinkage, temperature change, construction of buildings above the tunnel or drilling of tunnels near-by. The final lining also provides water tightness and smoothness which are important requirements in sewer tunnels. However, if the rib and lagging system deteriorates with time, the soil pressure will be carried gradually by the secondary concrete lining.

From the foregoing discussion, it is concluded that if the primary lining is protected against deterioration, there will be no need for the secondary lining except to withstand secondary effects mentioned and to provide hydraulic characteristics. Furthermore, the two supports can be replaced by a single lining designed to resist both the earth pressure and the secondary effects.

In this chapter, alternates to the conventional lining system are examined. A description of the lining instruments used to monitor the behaviour of the steel ribs and the precast segmented lining in the experimental tunnel is given. The results obtained from each of the three field test sections are presented. The strength and mode of

failure of the longitudinal joints of precast concrete segments were determined in the laboratory and the results of these tests are discussed in this chapter. Finally, the behaviour of the conventional lining and precast segmented lining is discussed, based on the field measurements and laboratory tests.

5.2 ALTERNATES TO THE CONVENTIONAL LINING SYSTEM

The conventional two-phase lining has been used successfully for many years in most tunnels in North America and has developed a long record of short term and long term satisfactory performance in differing ground conditions that range from hard rock to soft soil. However, its use requires that the construction be carried out in two operations, viz. drilling the tunnel and installing the rib-lagging system followed by casting the secondary concrete lining in place. Thus the construction using this support system is relatively slow and consequently the cost of the lining and its installation tends to constitute a large percentage of the total cost of the tunnels.

The conventional lining presently in use in Edmonton, for example, accounts for about 50% of the total cost of a tunnel. Peck et al. (1969) suggested that the cost of linings form 20-42% of the total cost of soft ground tunnels. They showed that this can be reduced to as little as 5-10% if new systems of lining such as shotcrete are used. Bartlett et al. (1971) estimated that the cost of the

cast iron lining in Toronto subway tunnels was 40-50% of the total cost. Savings of 25% of the tunnels cost were achieved by using bolted segmented concrete lining. This indicates the range of savings which may be expected if one of these new linings is used. Such a reduction in tunneling cost would make rapid transit tunnels more competitive with other techniques, such as cut and cover or surface systems.

Shotcrete has been used successfully on many occasions, with or without a system of anchors, as a temporary retaining structure for excavations in glacial till of the Edmonton area. In Edmonton tunnels, shotcrete was used a few years ago in a field trial to replace the steel ribs before the secondary concrete lining was placed (Oster, 1978).

A tunnel in the glacial till is usually excavated using a shielded mole which is advanced by longitudinal jacking against the lining. Shotcrete, as a sole lining, can not provide the required resistance to the mole thrusts. An interesting example of using shotcrete with a drilling machine in a 10.70 metre diameter tunnel is described by Alberts (1973). A precast concrete segment was placed at the tunnel invert and the machine reactions were shared between this segment and hydraulic rams jacked to the tunnel wall. The system used allows spraying of shotcrete while the mole is advancing. The shotcrete ultimately forms a continuous ring with the invert segment. Using a similar lining system in an Edmonton tunnel would require many modifications to the present tunneling machines. However, such a system can

reduce the lining cost and increase the rate of tunnel advance, since the mole would stop only to place one segment at the invert.

Segmented lining is another alternative to the conventional lining of North America. Cast iron segments have been used as a lining system of tunnels in the United Kingdom since the 1860's. Bolted, segmented reinforced concrete lining was introduced in these tunnels due to the shortage of cast iron in the 1930's. The manufacturing cost of this lining was 60 per cent of the cost of the grey iron lining (Craig and Muir Wood, 1978). The success of this trial and the significant savings obtained, enhanced the development of different types of precast concrete linings as illustrated in Figure 5.1.

The introduction of expanded lining (Donovan, 1974) made the construction progress faster since the bolts connecting the segments and the grouting operation were eliminated. In most cases, this lining is provided with only light reinforcement to take handling and installation stresses. The expanded lining, however, can only be used in stiff soil which is self supporting at least for a few hours. During this period the shield is advanced clearing the outside surface of the lining before the lining is expanded.

In Canada, bolted reinforced concrete segments were used in portions of the Toronto subway tunnels (Bartlett et al., 1971). Unreinforced unbolted grouted segmented concrete

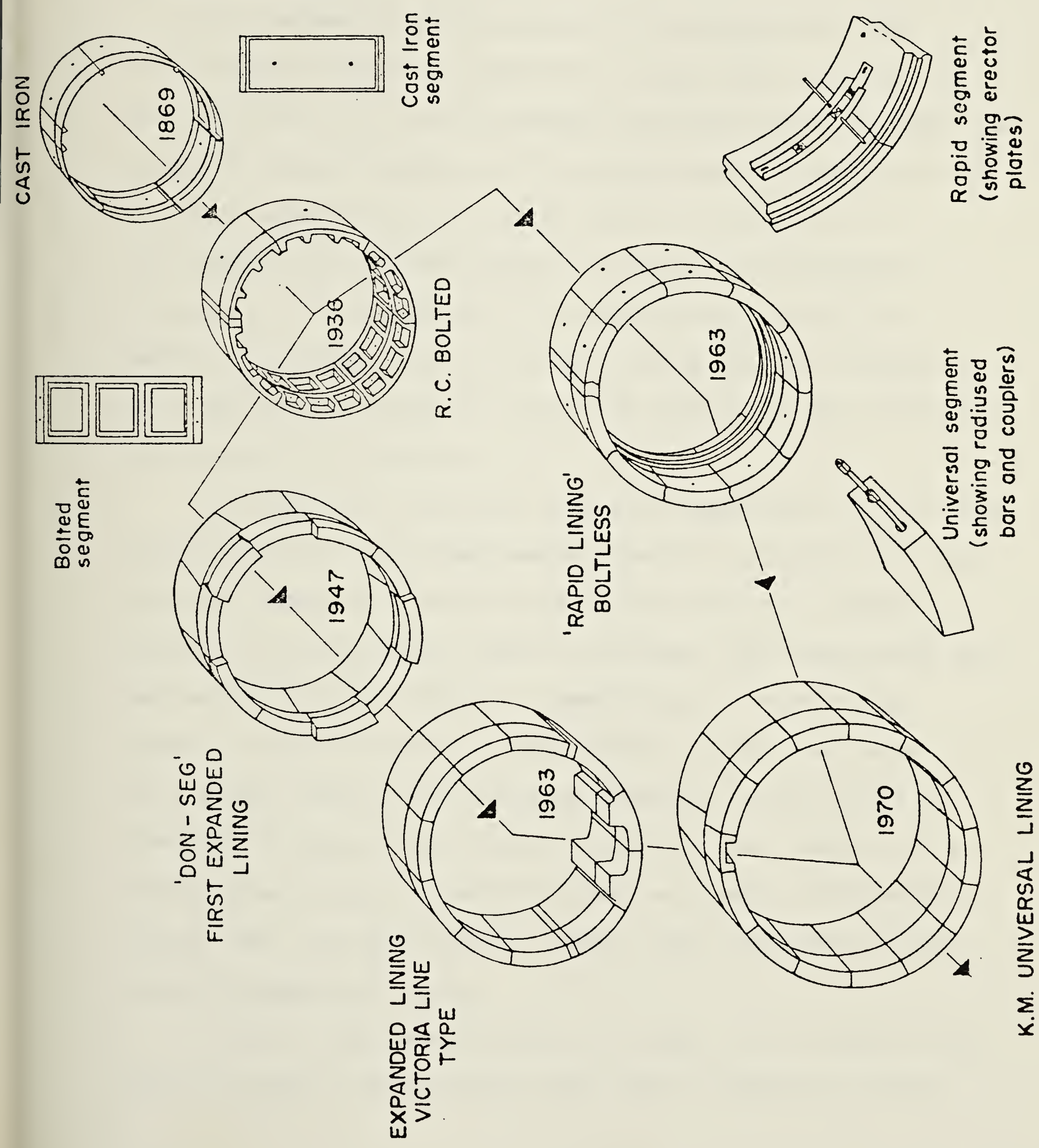


Figure 5.1 Development of segmented lining in the United Kingdom (McBean and Harries, 1970)

lining was used in a soft clay tunnel in Thunder Bay, Ontario (Morton et al., 1977). A similar system was used in a large diameter tunnel in Arizona, U.S.A. (Tilp and Schoeman, 1977).

The segmented lining especially designed for the experimental tunnel in Edmonton is described in detail in section 3.4.2. It is an expanded ungrouted type. In order to compare the performance of the conventional lining with the precast segments and, in particular, to study the performance of the new system, a field instrumentation program was implemented in the experimental tunnel to monitor the behaviour of the two lining systems. Results of this monitoring program is given in detail in the following sections of this chapter.

Through use of precast concrete segmented lining in the construction of the experimental tunnel, valuable data was obtained concerning unit costs (costs per unit length of tunnel) and achievable rates of advance, when employing this method of lining. Table 5.1 summarizes, in a detailed manner, the unit costs of this tunnel as well as those of four other tunnels, of the same diameter, constructed in Edmonton using similar moles. The first four tunnels were constructed using the conventional two phase lining while tunnel #5, the experimental tunnel, was lined mainly with precast segmented lining.

Prior to the construction of tunnel #1, a Lovat M-100 drilling machine have never been used in Edmonton before.

Table 5.1 Cost of tunnels in Edmonton (Data Courtesy of City of Edmonton)

Tunnel No.	Length (m)	Lining	Cost of Labour (1)	Cost of Equipments (2)	Cost of Materials (3)	Cost of Miscellaneous (4)	Cost of tunnel (1+2+3+4)	Total* Cost of tunnel	Notes
1	480	(1)	\$930	\$352	\$342	\$194	\$1818	\$2821	First trial of mole
2	1270	(1)	\$393	\$124	\$351	\$51	\$919	\$976	No shafts
3	1340	(1)	\$394	\$182	\$290	\$52	\$918	\$1345	
4	1830	(1)	\$388	\$208	\$297	\$56	\$949	\$1489	
5	1310	(2)	\$229	\$228	\$284	\$79	\$820	\$1056	Experimental Tunnel

Notes: * Including cost of shafts and undercuts
 - All costs are per linear metre of tunnel length
 - All tunnels have excavated diameter = 2.5 metres
 - Lining (1): Conventional, and Lining (2): Precast Concrete Segments

This accounts for the relatively high cost of this tunnel. However, with continued use, in constructing tunnels #2, #3, and #4 costs were reduced significantly.

The effect of utilizing precast segmented lining in such tunneling operations can be ascertained by comparing the unit costs of tunnel #5 with those of the previous ones. Such a comparison leads to the following conclusions:

- a) the unit cost of labour dropped by about 40%. It is believed that constructing the tunnel in one phase contributed significantly to that reduction.
- b) the unit cost of equipment (charged to different tunnel projects on a rental basis) was slightly higher for Tunnel #5. Several special machines were used in that tunnel to handle the segments.
- c) saving of about \$100 per metre of tunnel was realized. This represents about 12% of the unit cost of tunnels in Edmonton and was achieved even though the segmented lining was still being used on a trial basis.

While advance of the drilling machine was relatively slow during the early stages of construction of the experimental tunnel, about 3 metres per 8 hour shift, as soon as the tunneling crews became familiar with the new equipment and procedures, the rate of advance doubled. This rate is approximately the same as that achieved when advancing a tunnel using rib and lagging lining. However, it

should be noted that, in the latter case, the time required to finish the tunnel is almost double due to the casting in place of the secondary lining.

5.3 LINING INSTRUMENTATION

A complete instrumentation program to examine the performance of a tunnel lining should include monitoring of both the stress in and the deformation of the lining. Stresses in the lining can be measured directly or indirectly using pressure cells, strain gauges or load cells. Tape or rod extensometers and optical surveying are usually used to monitor the deformation of the lining.

5.3.1 Pressure Cells

Difficulties encountered with pressure cells used to measure the earth pressure on tunnel linings have been reported by Tattersall et al. (1955), Burke (1957), Cording et al. (1975), DeLory et al. (1979), and Thomson and El-Nahhas (1980). Cording et al. (op. cit.) concluded that:

" . . . A realistic evaluation, however, of the various instrumentation attempts over nearly 40 years shows pressure cells to be too small and too sensitive to installation details to measure a representative load on the lining. . . ."

5.3.2 Strain Gauges

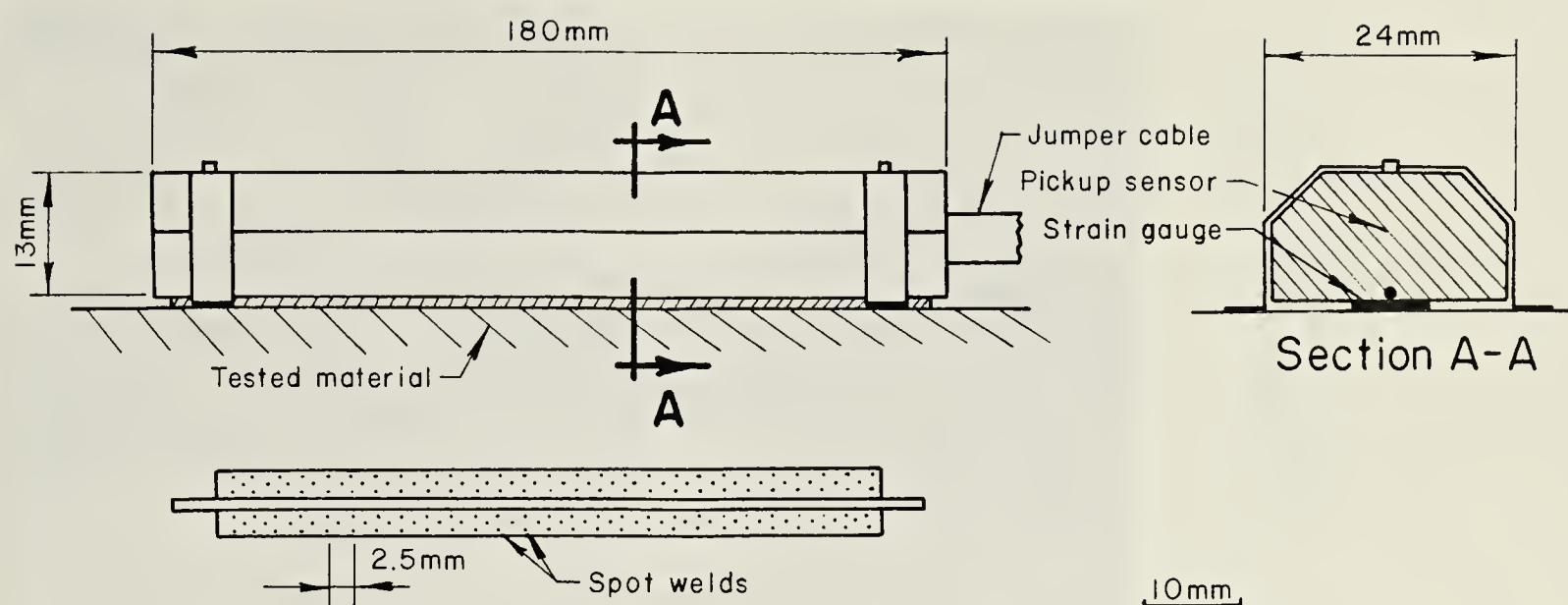
Different types of strain gauges can be used to measure strains across the lining thickness. These measurements are used to determine both normal forces and bending moments in

the lining. Experiences with the use of strain gauges in tunnel lining are reported by Skempton (1943), Cooling and Ward (1953), Burke (1957), Ward and Thomas (1965), and Curtis et al. (1976).

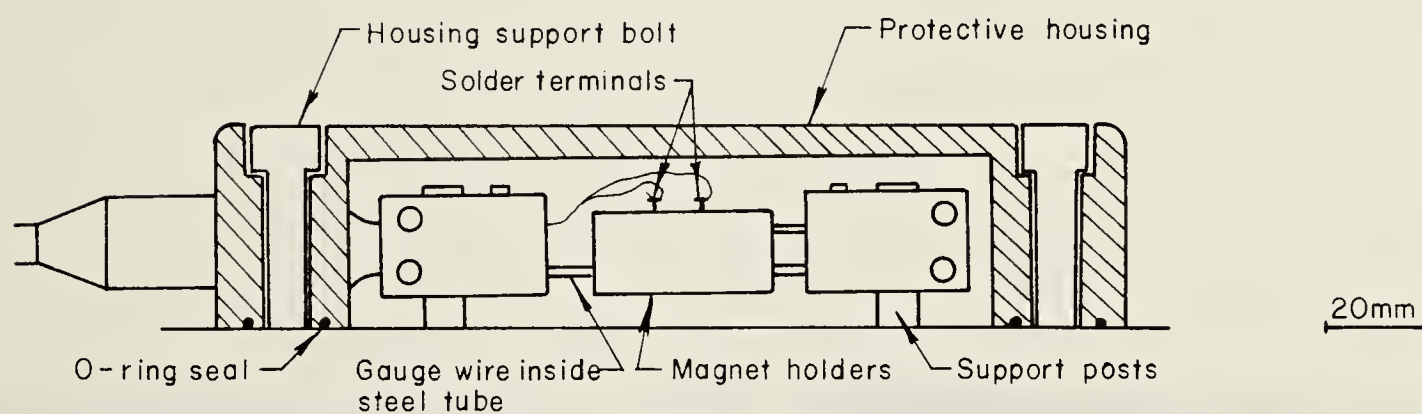
Figure 5.2 shows the three vibrating wire strain gauges used in the experimental tunnel. Plates 5.1, 5.2 and 5.3 show these gauges during or after the installation on the lining. The principle employed in the vibrating wire strain gauges is explained in detail by the Norwegian Geotechnical Institute (1962) and by Thomas (1965). It is based on the fact that the natural frequency of a vibrating wire, restrained at both ends, varies with the square root of the tension in the wire. Any change of strain in the lining to which the gauge is attached is indicated by a change in the frequency of the vibrating wire.

This type of strain gauge is most suitable for use in tunnels because of its resistance to the dusty, humid environment. It has the added advantages of long-term stability and independence of length of leads. The recent development of a digital, portable readout unit, (which displays strains directly), has made the reading of these gauges easier and faster.

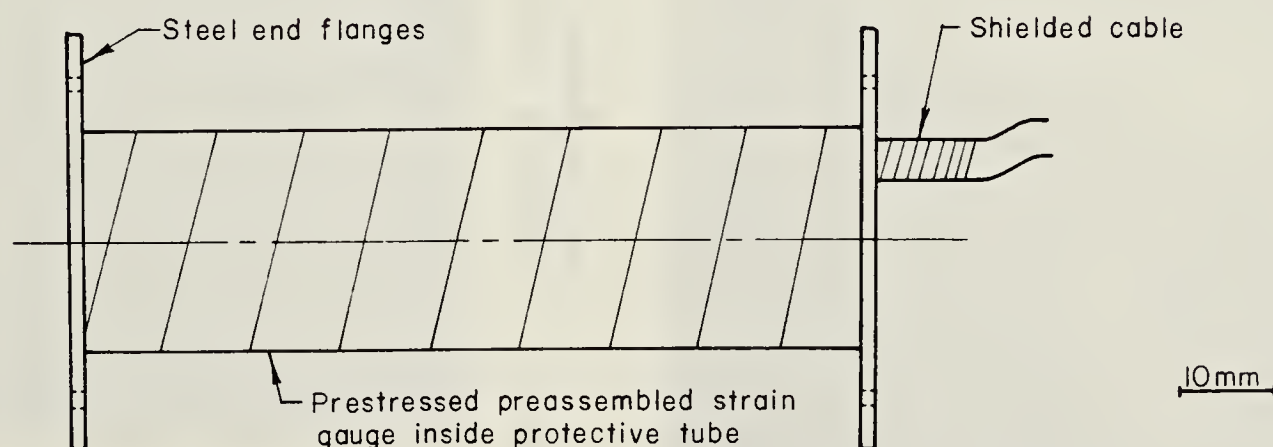
The strains in a steel rib at Test Section 1 were monitored using four weldable vibrating wire strain gauges. A pickup sensor (SINCO Model 52622) was mounted on each gauge and the readings of strain and temperature were obtained using a Model 52601 strain indicator. This gauge



(SINCO 52621)
**Weldable vibrating wire
 strain gauge**



(GEONOR P200-220)
**Surface vibrating wire
 strain gauge**



(GEONOR P250)
**Embedded vibrating wire
 strain gauge**

Figure 5.2 Strain gauges used in the experimental tunnel

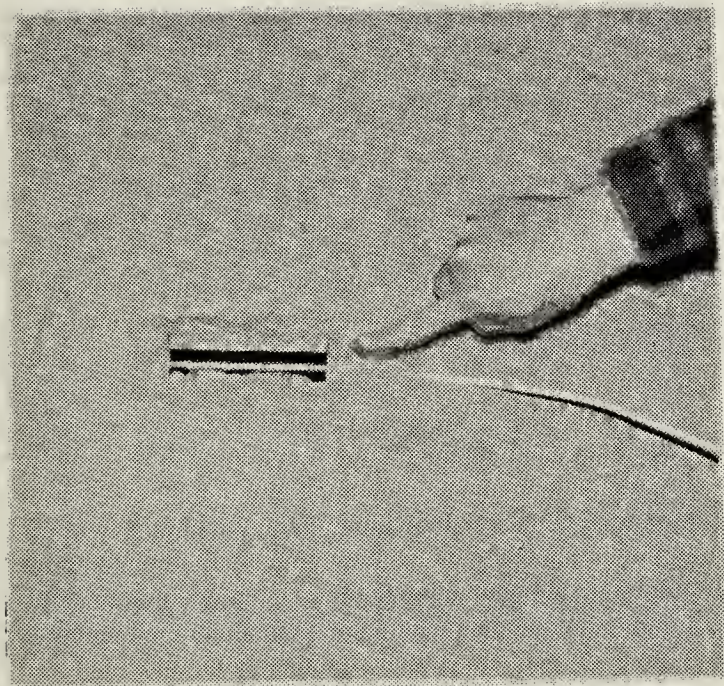


Plate 5.1 Embedded vibrating wire strain gauge during casting

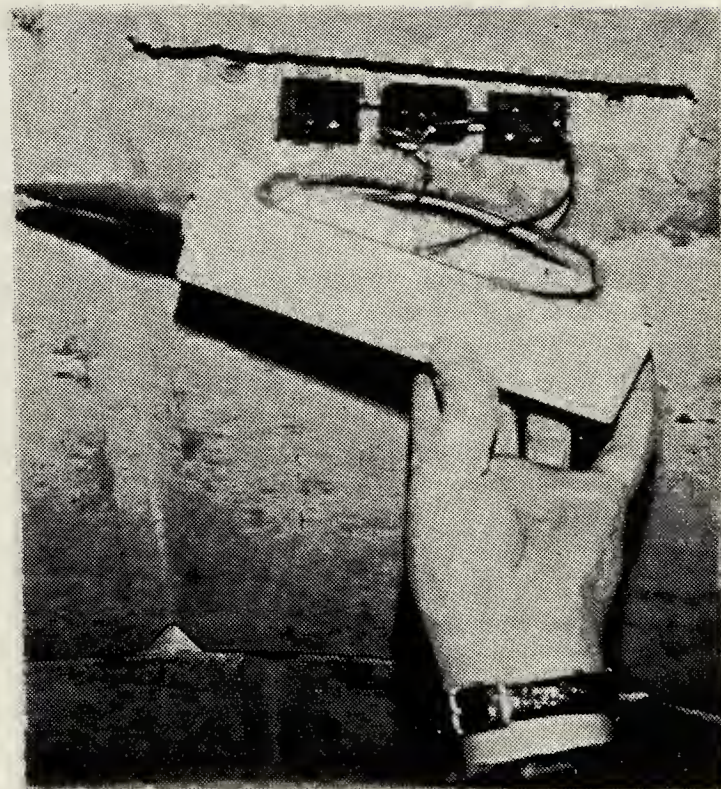


Plate 5.2 Surface vibrating wire strain gauge

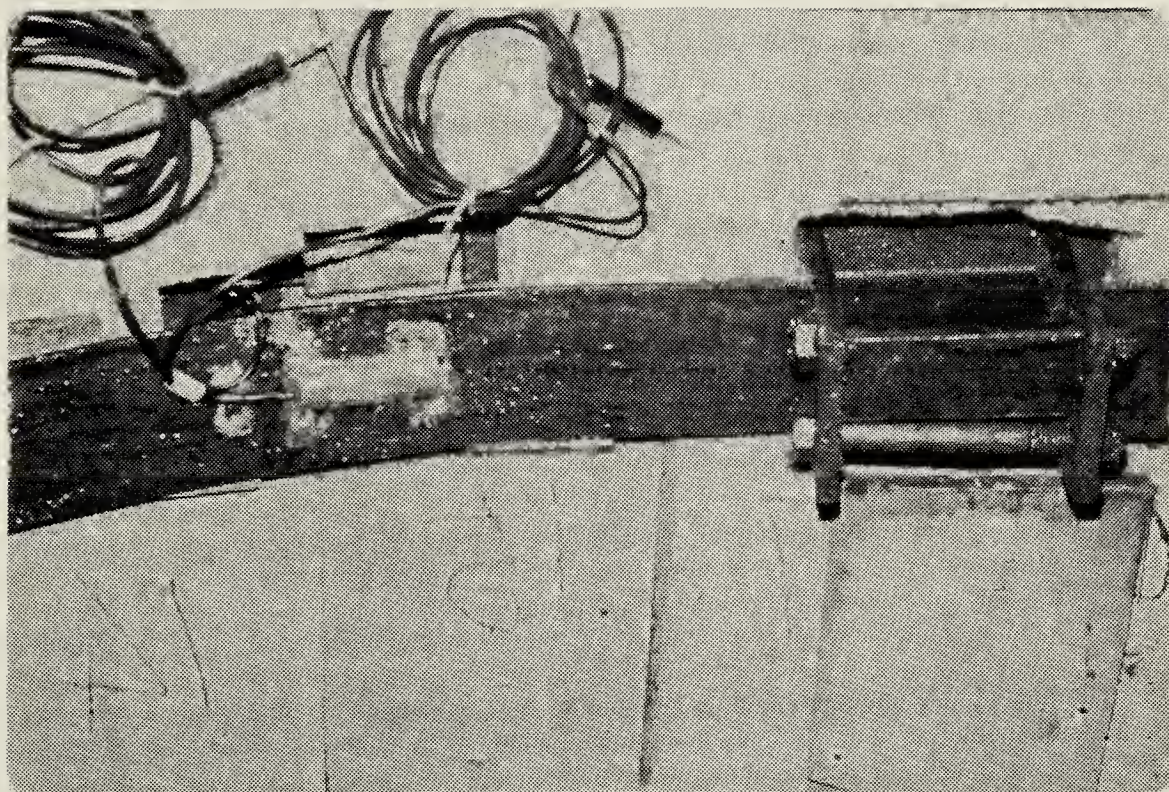


Plate 5.3 Weldable vibrating wire strain gauge

was also used as a sensing element in the load cells. It is supplied as a pre-tensioned unit, hence no field adjustment of wire tension is necessary.

Strains in the concrete segments at Test Section 2 were measured using four Geonor vibrating wire strain gauges; two being of the embedded type, Model P250, and the others being surface gauges, Model P200-220. Some details of these strain gauges are given in Figure 5.2. The use of surface gauges to measure strut loads in a retaining structure is discussed by the Norwegian Geotechnical Institute (1962). The performance of this gauge was compared with two other models of vibrating wire strain gauges by O'Rourke and Cording (1974). Sensitivity and precision of ± 1.5 microstrain with little or no zero drift were reported.

Geonor P250 strain gauges were embedded in the concrete near the outside surface of the segments during casting (see Plate 5.1). The wires were routed through the concrete to the inside surface of the segment as shown in Figure 5.3.a. Geonor strain gauges (Model P200-220) were installed on the inside surface of the segments just after their expansion. This required the embedment of anchors with internal threads into the concrete, to enable the attachment of the gauge posts and the housing bolts. Provision was also made for a recess in the concrete surface around the anchors of about 1 cm. This ensured that the gauge wire was level with the inside surface of the segment. Figure 5.3.b illustrates the procedure followed to embed these anchors and create the

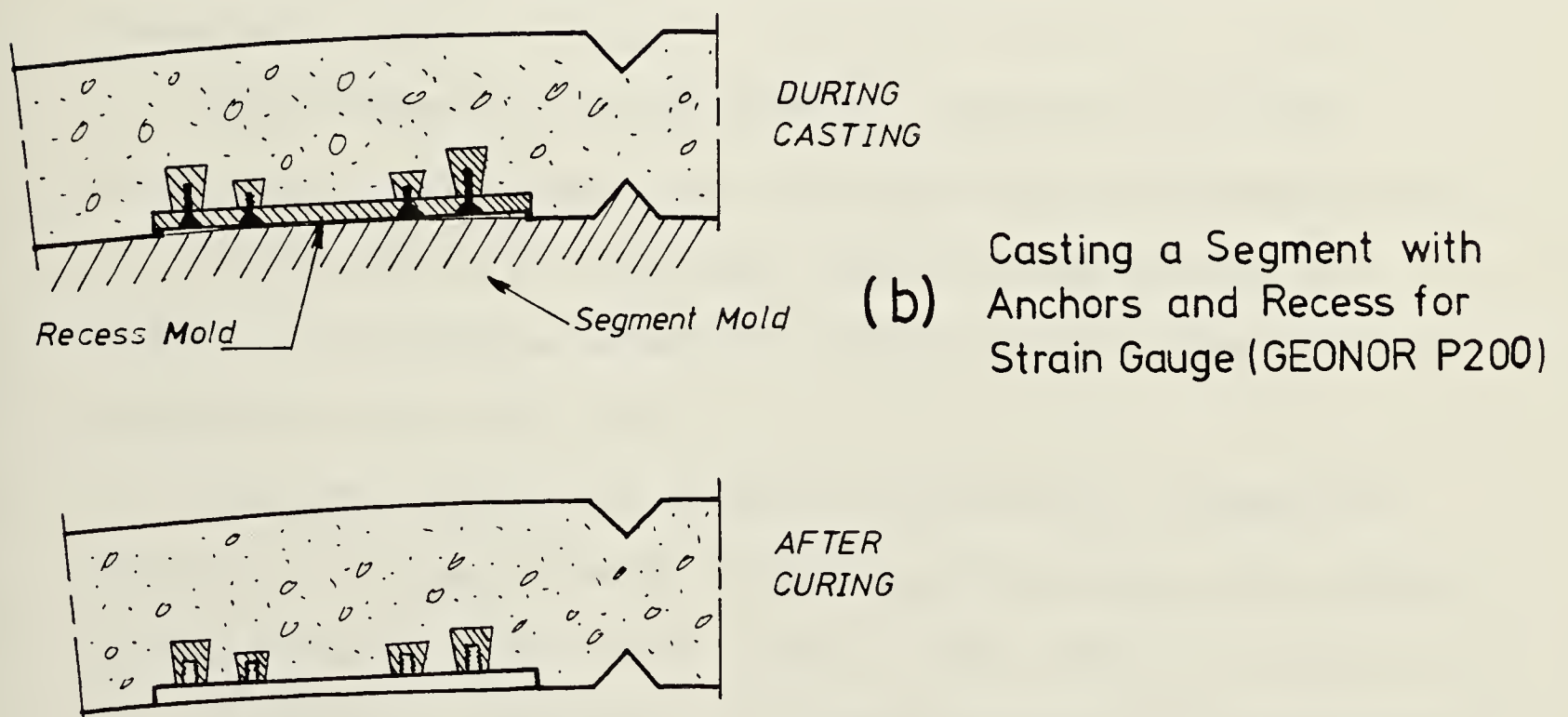
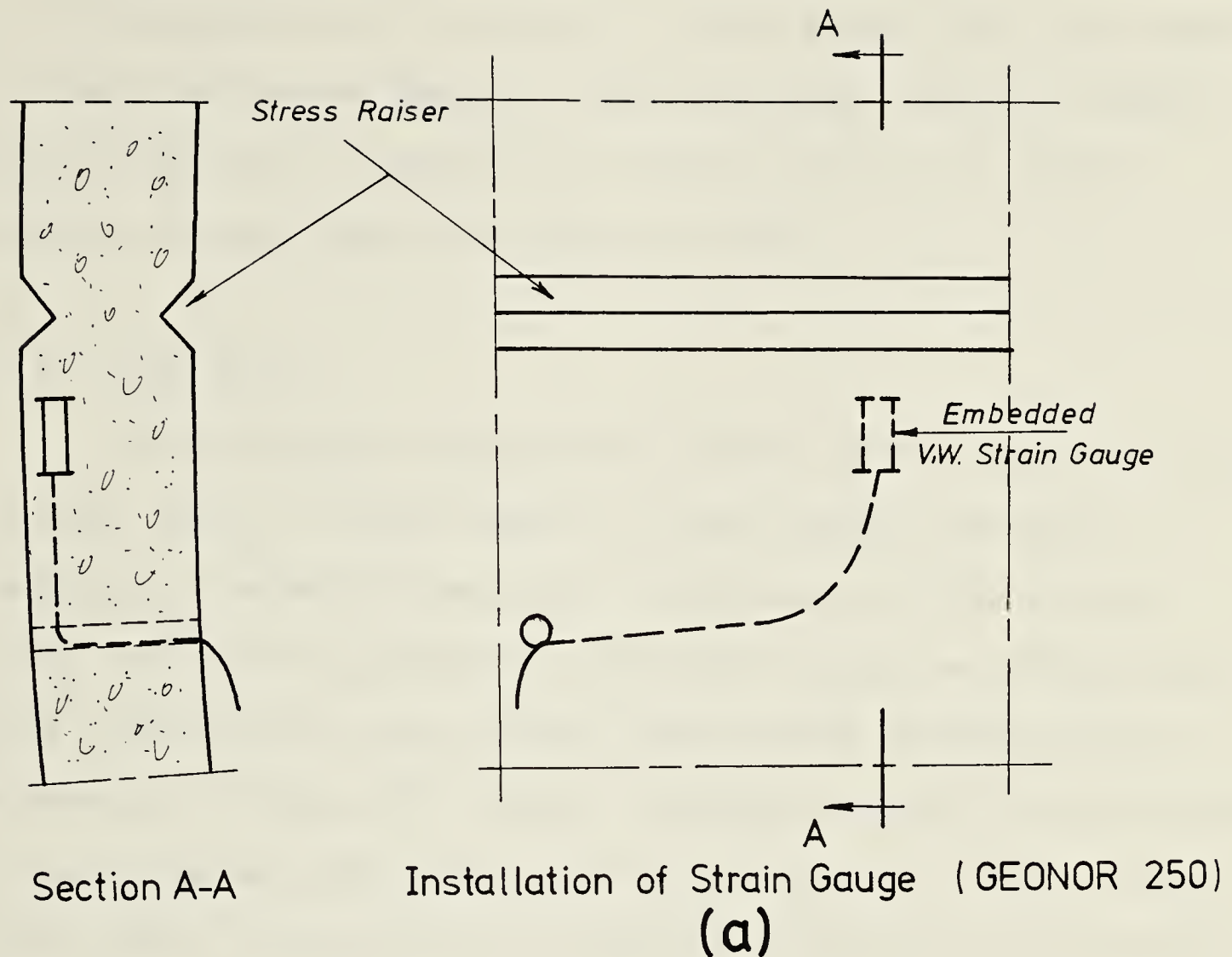


Figure 5.3 Installation of concrete strain gauges

recess.

The same strain indicator (SINCO Model 52601) was used to read the Geonor gauges. These readings, however, had to be multiplied by a factor of 0.68 to obtain the actual strains (Slope Indicator Company, 1978).

5.3.3 Load Cells

A strain gauge measures the strain at one point in the lining, hence a large number of these gauges would be required to examine the overall behaviour of the lining. Since each strain gauge is relatively expensive (P250 costs \$270 and P200-220 costs \$220), this would usually be too expensive. On the other hand, a single load cell provides an overall average measurement of normal forces in the lining. Since fewer cells would be required to monitor a particular section of the lining, this could proceed for a more reasonable cost.

Measurements of liner thrust, (resultant of hoop stresses), using load cells are reported by Tattersell et al. (1955), Barratt and Tyler (1976) and Curtis et al. (1976). An extensive study of vibrating wire load cells is reported by the NGI (1965).

The development of thrust in the precast segmented lining in the experimental tunnel was measured using twelve vibrating wire load cells, (two in Test Section 2 and ten in Test Section 3). The load cells were designed, machined and calibrated at the University of Alberta especially for the

experimental tunnel. Figure 5.4 shows the design of these load cells.

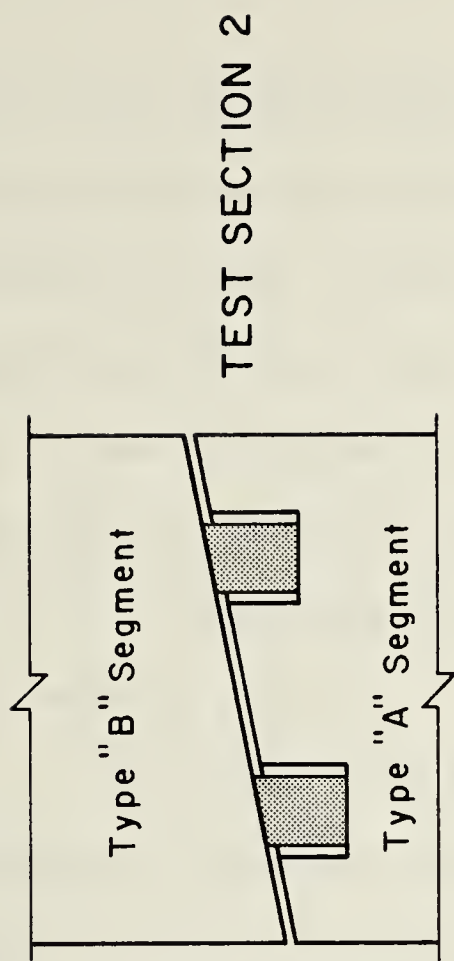
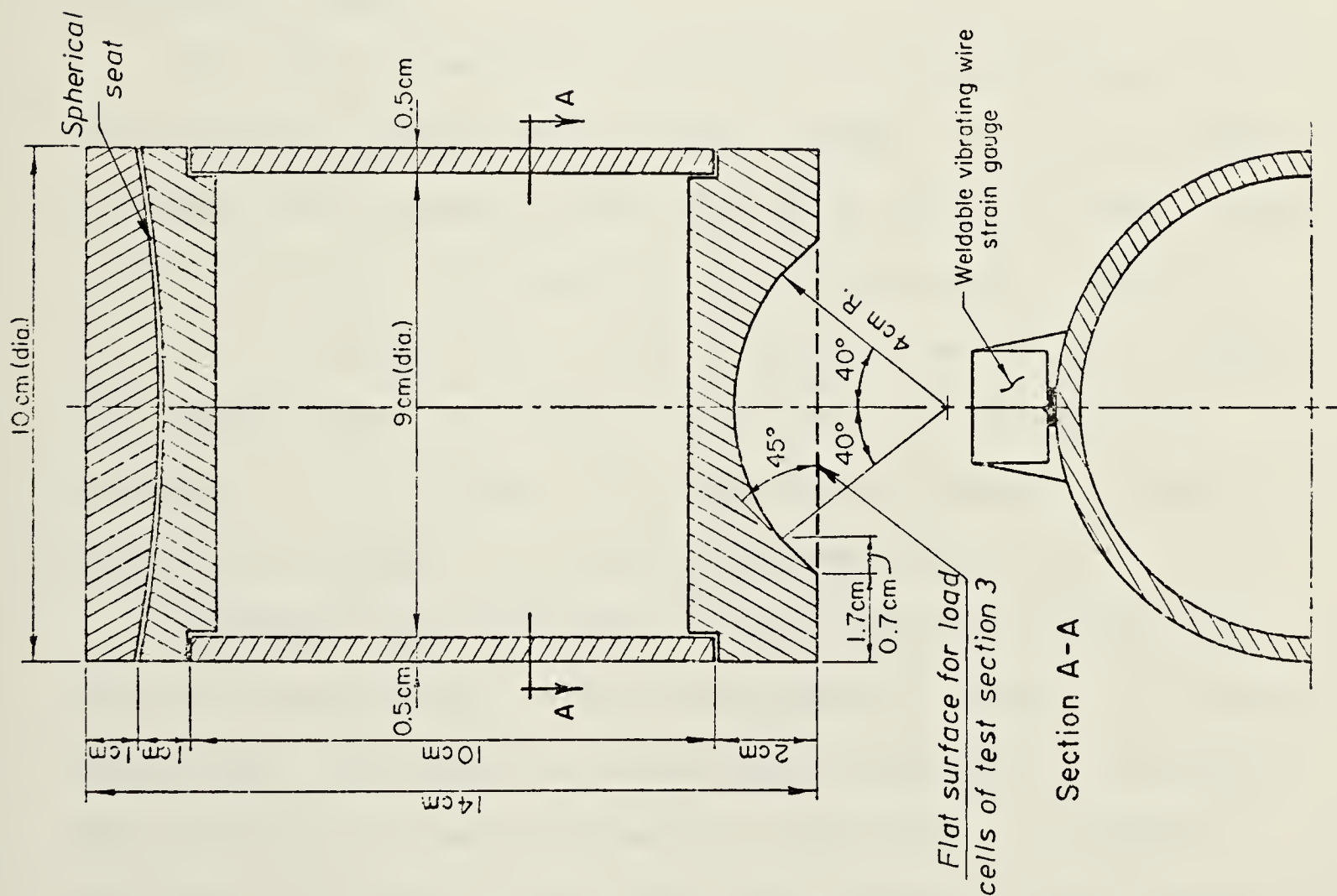
Each load cell is provided with a spherical seat to take up residual non-alignment due to machining and to reduce eccentricity on the load cells. Two vibrating wire strain gauges were welded to the outside surface of the cell wall.

The design of the load cells used in Test Sections 2 and 3 differ only in the geometry of the lower cap. Those used in Section 2 have a curved surface which fits on longitudinal joints of type B segments. Thus, recesses in type A segments only were required for their installation, as shown in Figure 5.4. Some difficulties were experienced during machining, calibrating and installing the cells in the tunnel. Consequently, the design of the load cell was modified, with those of Section 3 having a flat ended lower cap. Installation of these load cells required recesses in both type A and type B segments as shown in Figure 5.4.

Working capacity of each of these load cells is 220 KN, which is about half their ultimate capacity. Their sensitivity is about 2 KN. The maximum load actually measured by any of these load cells was 125 KN. Calibration was performed by loading and unloading several times to ensure the repeatability of the results.

5.3.4 Tape Extensometer

Measurement of lining distortion is an essential part



INSTALLATION OF LOAD CELL IN LONGITUDINAL JOINT

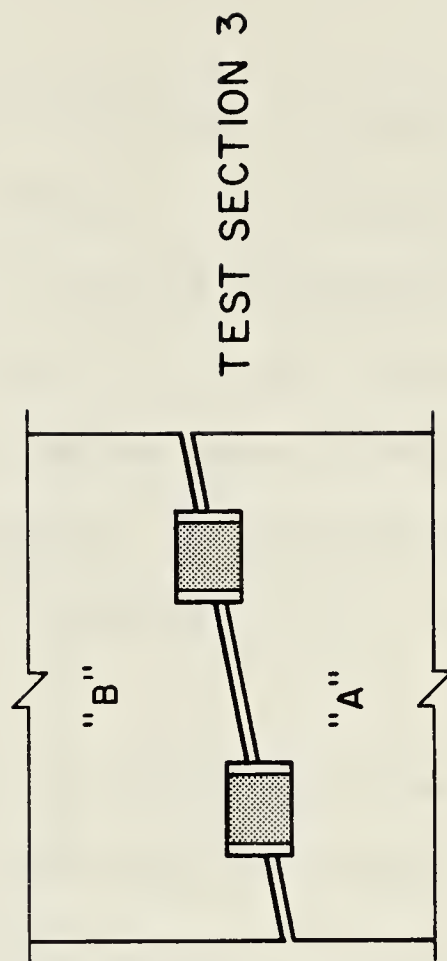


Figure 5.4 Design and installation of load cells

of field monitoring of tunnel performance. It can be accomplished by measuring the change in the diameters and chords of the lining using rod or tape extensometers and monitoring the level change of a point at the tunnel invert or crown using optical surveying techniques. Different designs of rod and tape extensometers are described by Burke (1953), Obert and Duvall (1967), Cording et al. (1975), and El-Nahhas (1977).

The tape extensometer shown in Figure 5.5 was used to measure diameter change in the experimental tunnel. It has a sensitivity of ± 0.03 mm and an accuracy of ± 0.3 mm. A similar type of instrument was used to measure the deformed shape of steel ribs in two tunnels in Edmonton (Thomson and El-Nahhas, 1980).

The tape extensometer consists of a steel tape in series with a spring and two dial gauges. The steel tape is provided with a hook on one end and a series of small holes on the other end. The spring is used to apply a tensile force in the tape. This force is controlled using the small dial gauge shown in Figure 5.5 so that for successive readings it is constant. The second dial gauge is used to measure the change in distance between two points.

Eye-bolts were anchored in the concrete segments at Test Sections 2 and 3 of the experimental tunnel. To take a measurement, the tape is hooked to an eye-bolt at one end and attached to the instrument at the other. A constant tension is applied to the tape. The change in the reading of

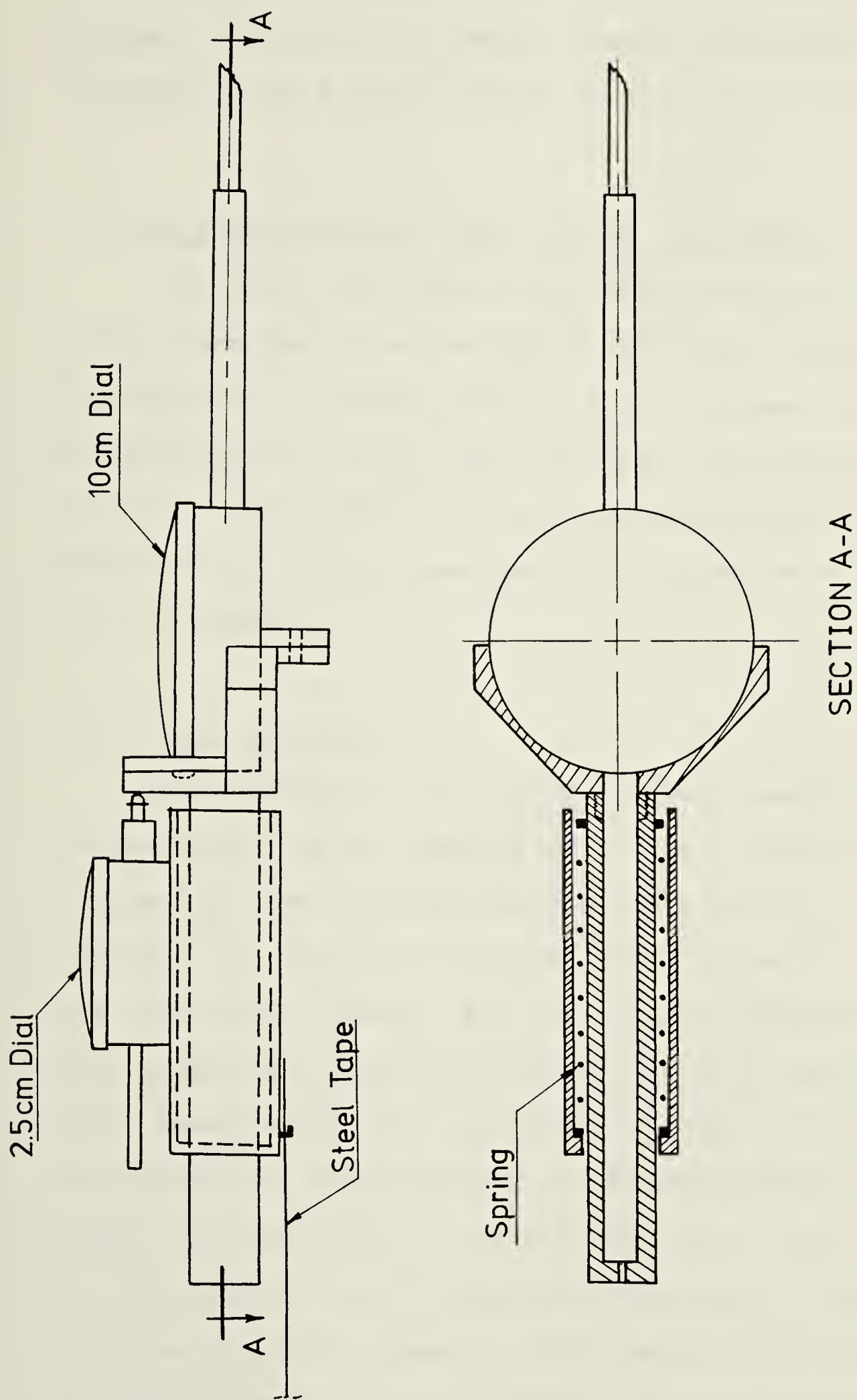


Figure 5.5 Details of tape extensometer

the larger dial gauge, from an initial reading taken just after the lining was expanded, indicates the diameter change. Every set of diameter change measurements was accompanied by a level survey on one point on the lining.

5.4 FIELD MEASUREMENTS FROM LINING INSTRUMENTS

The lining instrumentation was concentrated at three sites, referred to as Section 1, Section 2 and Section 3. The location of these test sections is shown on Figure 3.8. The field measurements obtained from the lining instruments at each of the test sections are presented here. A discussion of these measurements is given in a later section of this chapter.

5.4.1 Test Section 1

Four weldable vibrating wire strain gauges were installed on the top segment of a steel rib as shown in Figure 5.6. The instrumented rib was placed in the tunnel on February 19, 1979 at a location 23 metres west of the end of the curve (see Figure 3.9). The strains measured during the four gauges are plotted in Figure 5.7 as a function of time. These measurements are replotted in Figure 5.8 to show the development of normal forces and bending moments assuming a linear distribution of strain across the lining thickness.

The distortion of the steel ribs was not measured in this test section. However, the change in horizontal and vertical diameter and the invert level change of three steel

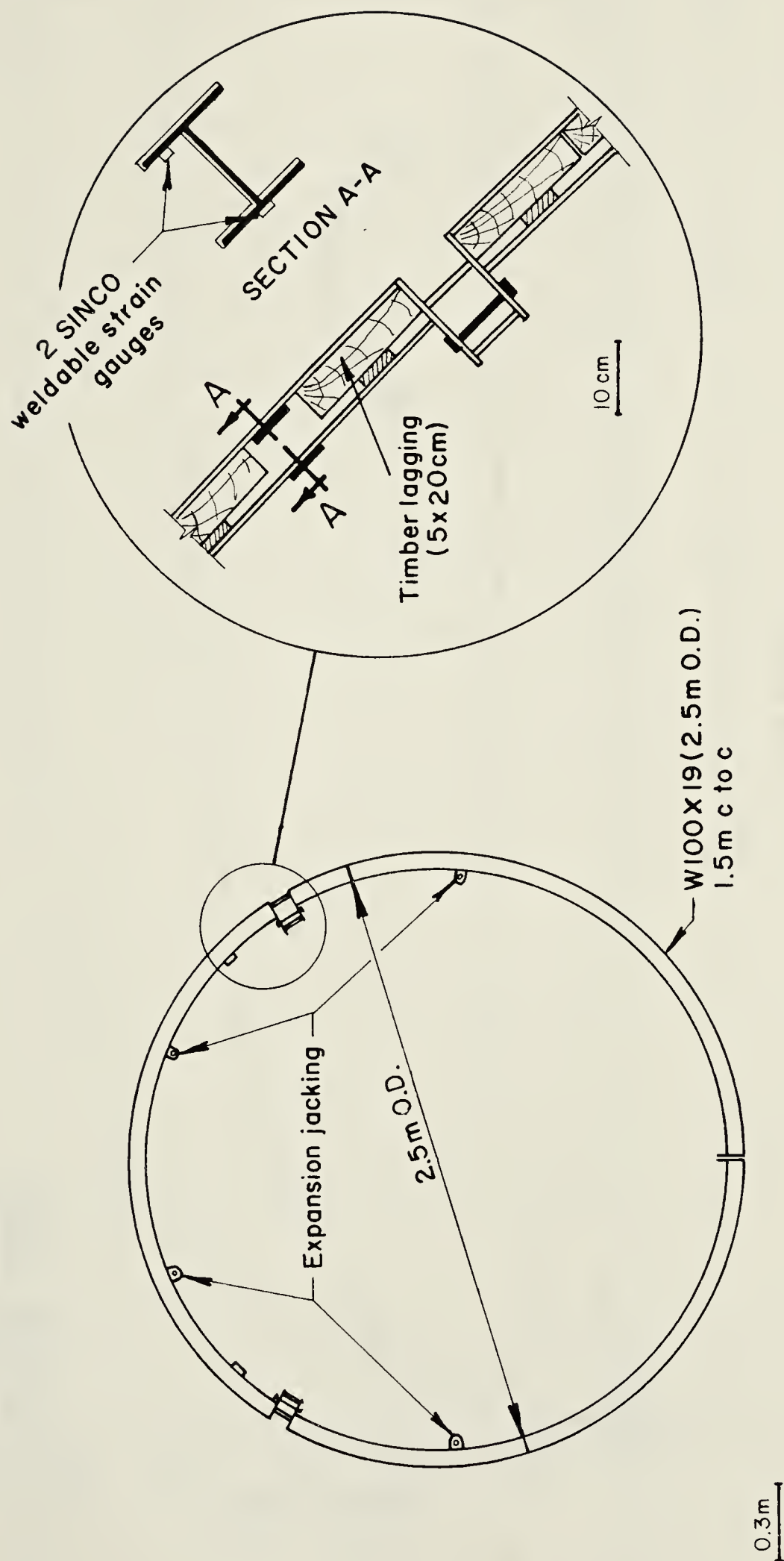


Figure 5.6 Instrumented steel rib of Test Section 1

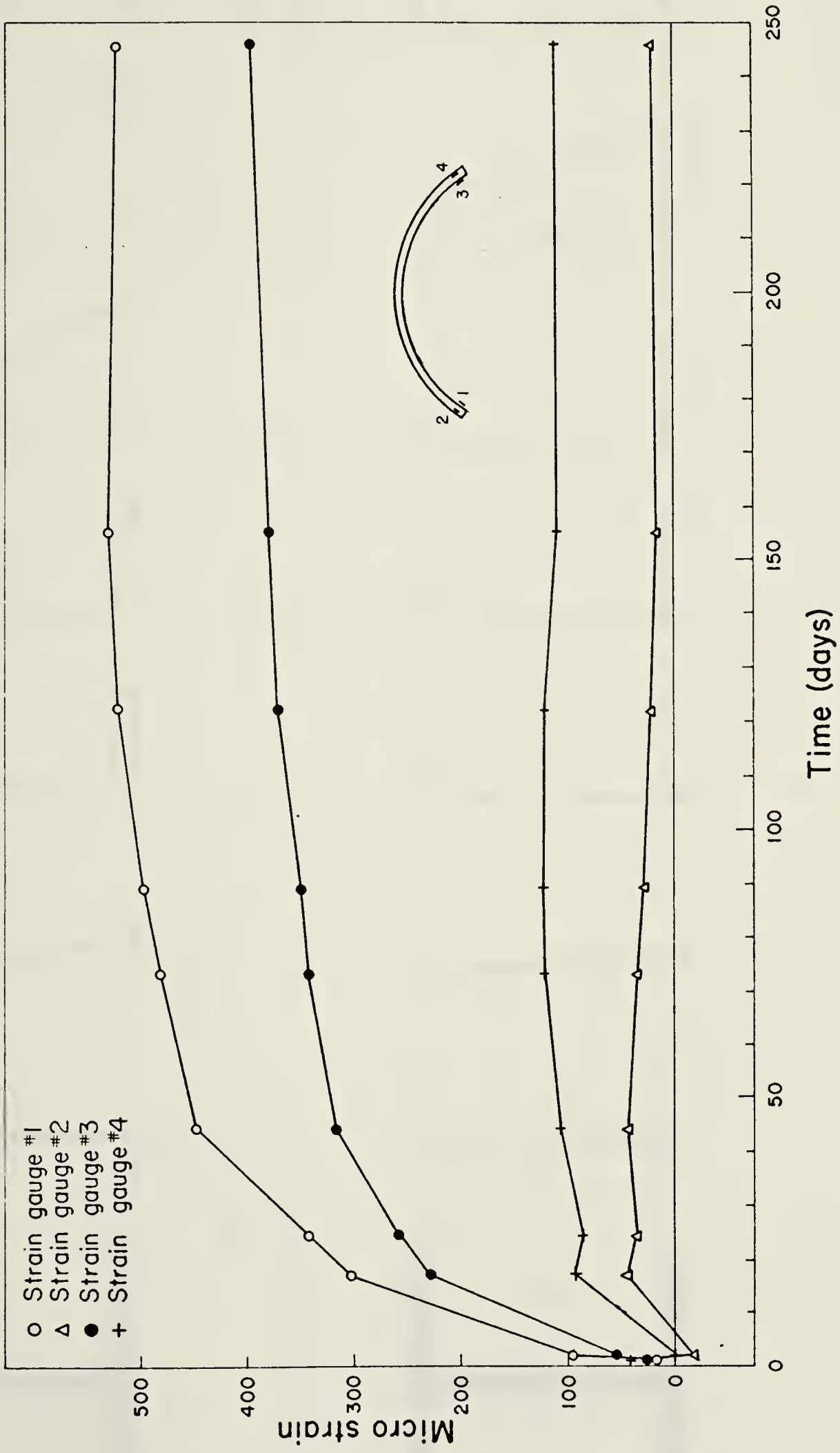


Figure 5.7 Strains in the steel rib vs. time (Test Section 1)

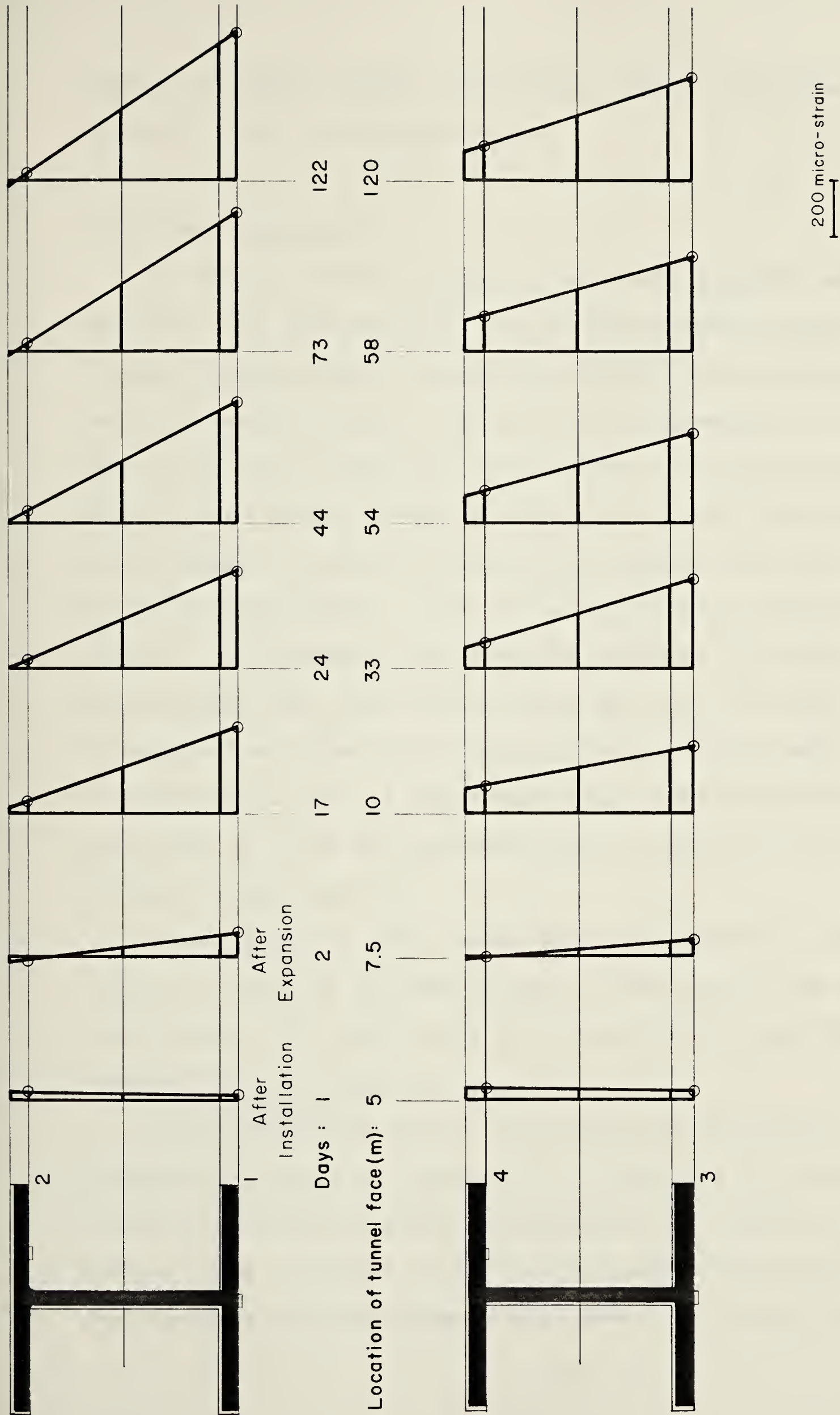


Figure 5.8 Strain distribution in steel sections

ribs in a similar tunnel, (El-Nahhas, 1977), are shown in Figure 5.9 and 5.10 respectively.

5.4.2 Test Section 2

On June 7, 1979, two special concrete segments were cast for this test section. One of these segments was of the A type, having convex longitudinal joints. Provision was made for space at one of the joints to accommodate the load cells, and for a recess and some anchors near the stress raiser to allow the installation of a surface vibrating wire strain gauge. A similar recess, with anchors, was provided on the second segment, (type B, having concave longitudinal joints). Both segments contained an embedded vibrating wire strain gauge near the stress raiser and four circular holes to enable the inspection of any gap occurring between the lining and the soil. A Demec mechanical strain gauge was also used to allow the determination of strains on the surface of the concrete.

These segments were installed in the tunnel on July 18, 1979 at a location 300 metres east of the end of the curve (see Figure 3.8). Details of this test section are shown in Figure 5.11 and Plate 5.4.

The strains measured at the crown and springline sections are given in Figure 5.12. To be able to calculate the corresponding stresses, compression tests were carried out on three cylinders cast from the same batch from which the concrete for the segments was taken. An average value of

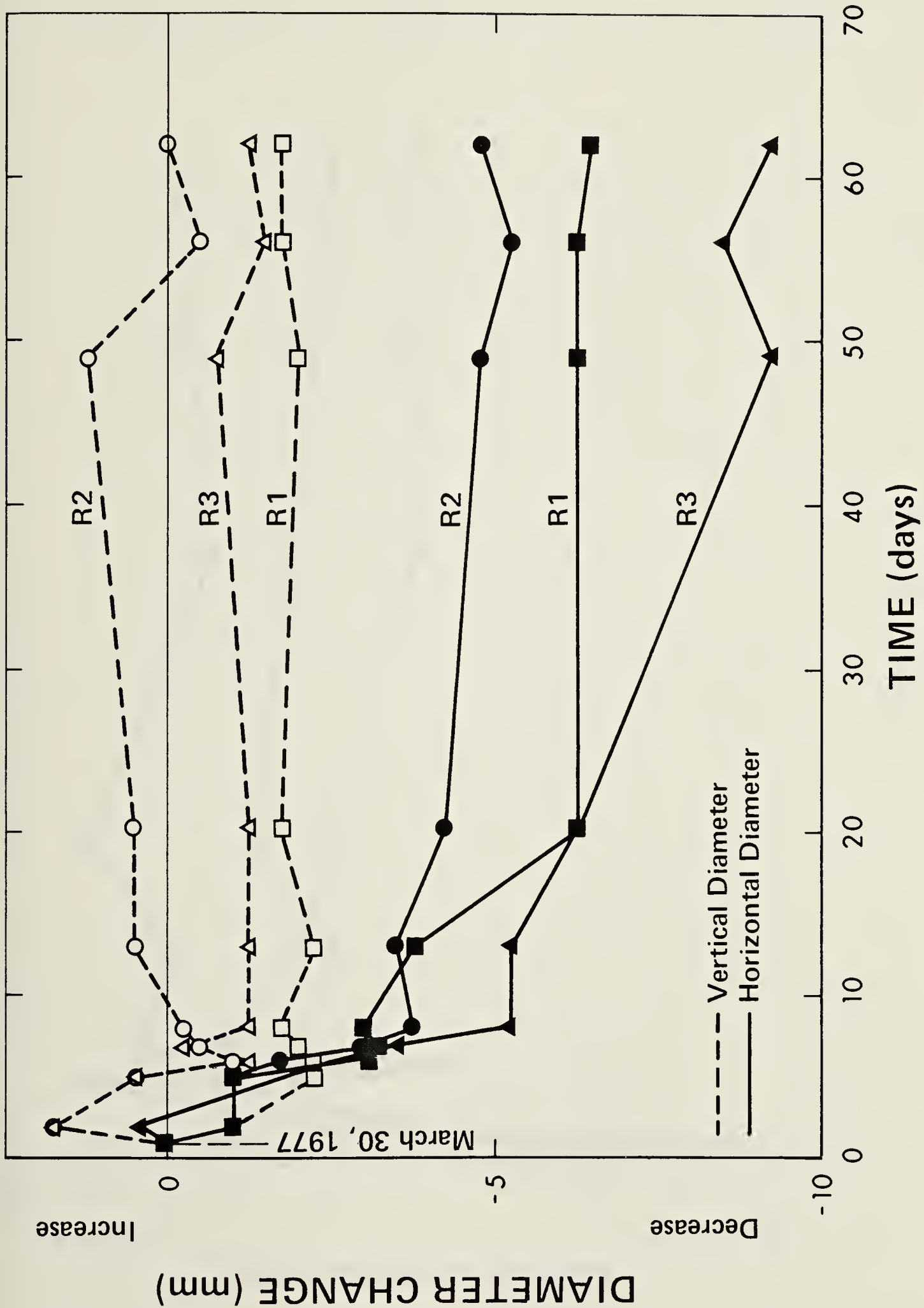


Figure 5.9 Change in horizontal and vertical diameters, 170 Street tunnel (after El-Nahas, 1977)

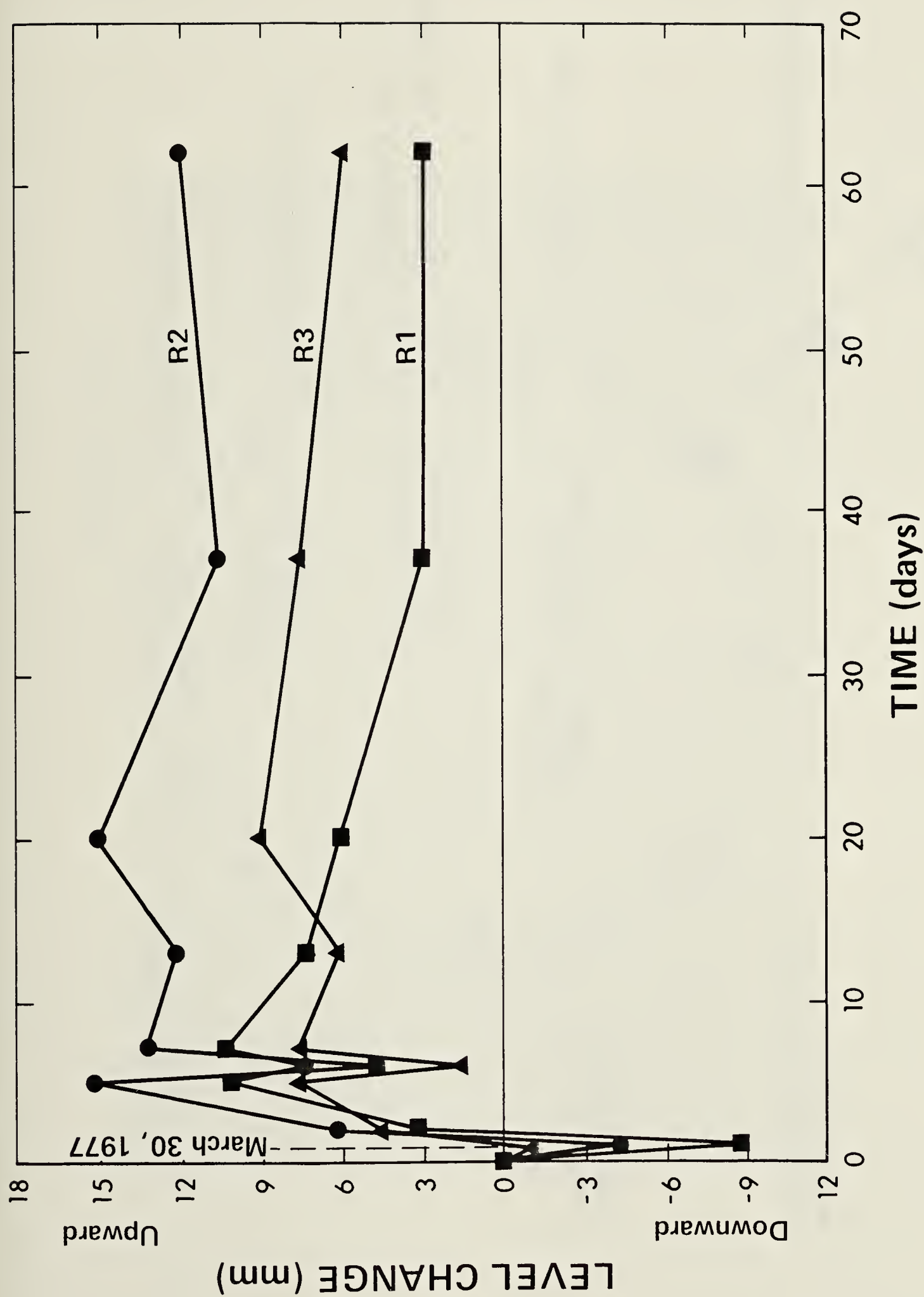


Figure 5.10 Level change of tunnel invert, 170 Street tunnel (after El-Nahhas, 1977)

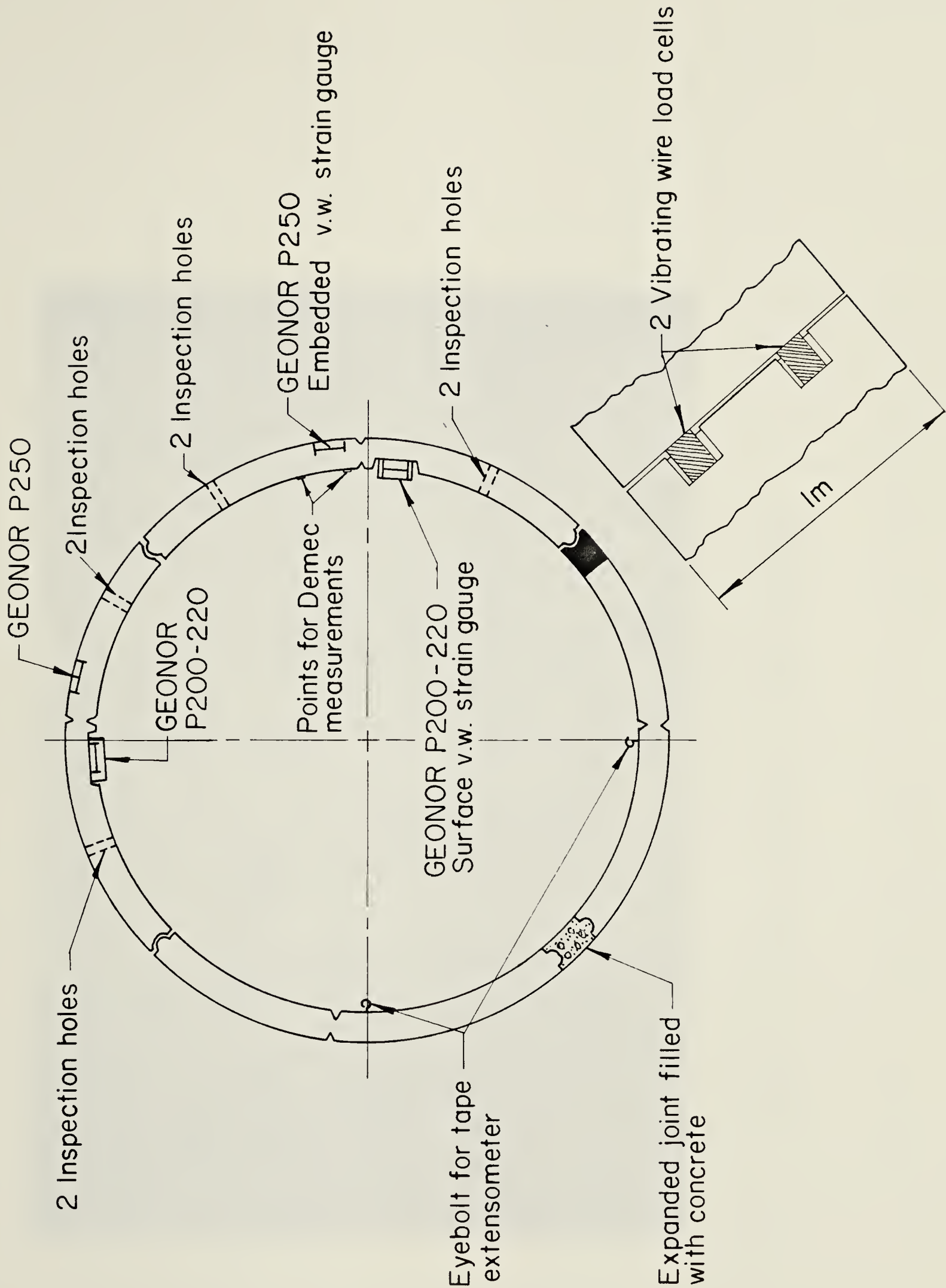


Figure 5.11 Details of Test Section 2 (lining instruments)

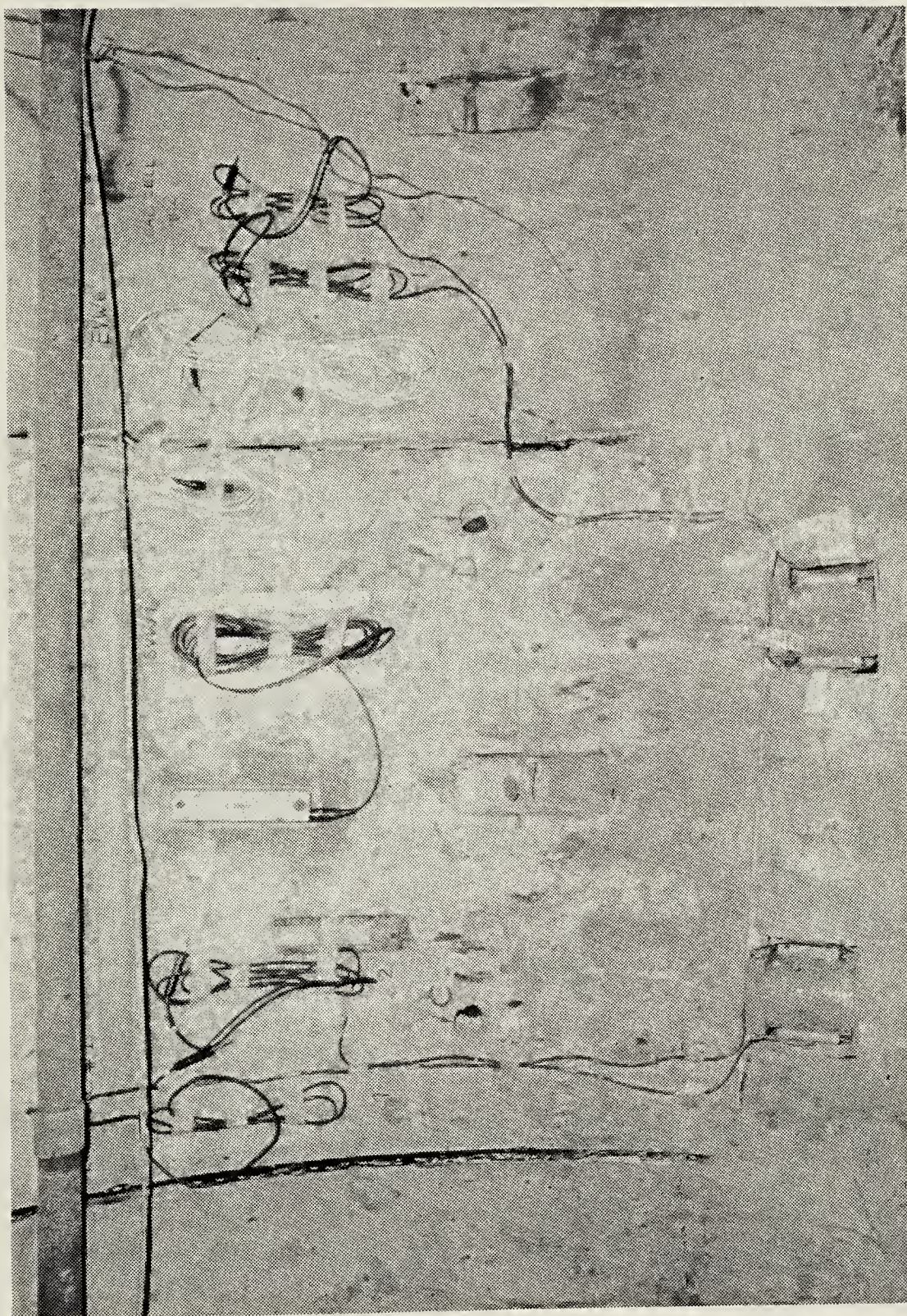


Plate 5.4 Lining instruments at Test Section 2

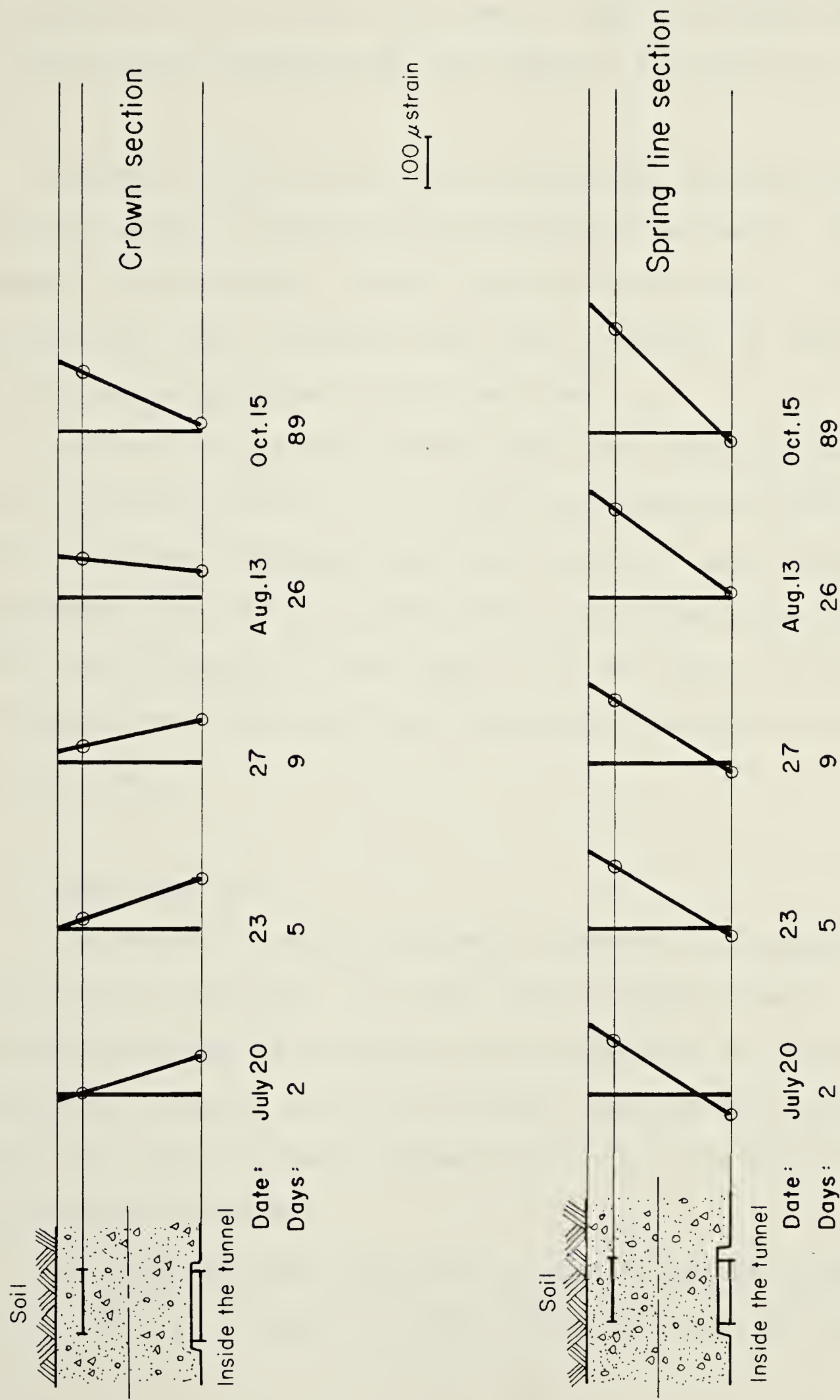


Figure 5.12 Measured strains in the concrete at the crown and springline of the tunnel (Test Section 2)

Young's modulus of 25,100 MPa was obtained. The results obtained using the Demec mechanical strain gauge were within the repeatability of the instrument. Load cell measurements of the reaction between the two segments are given in Figure 5.13.

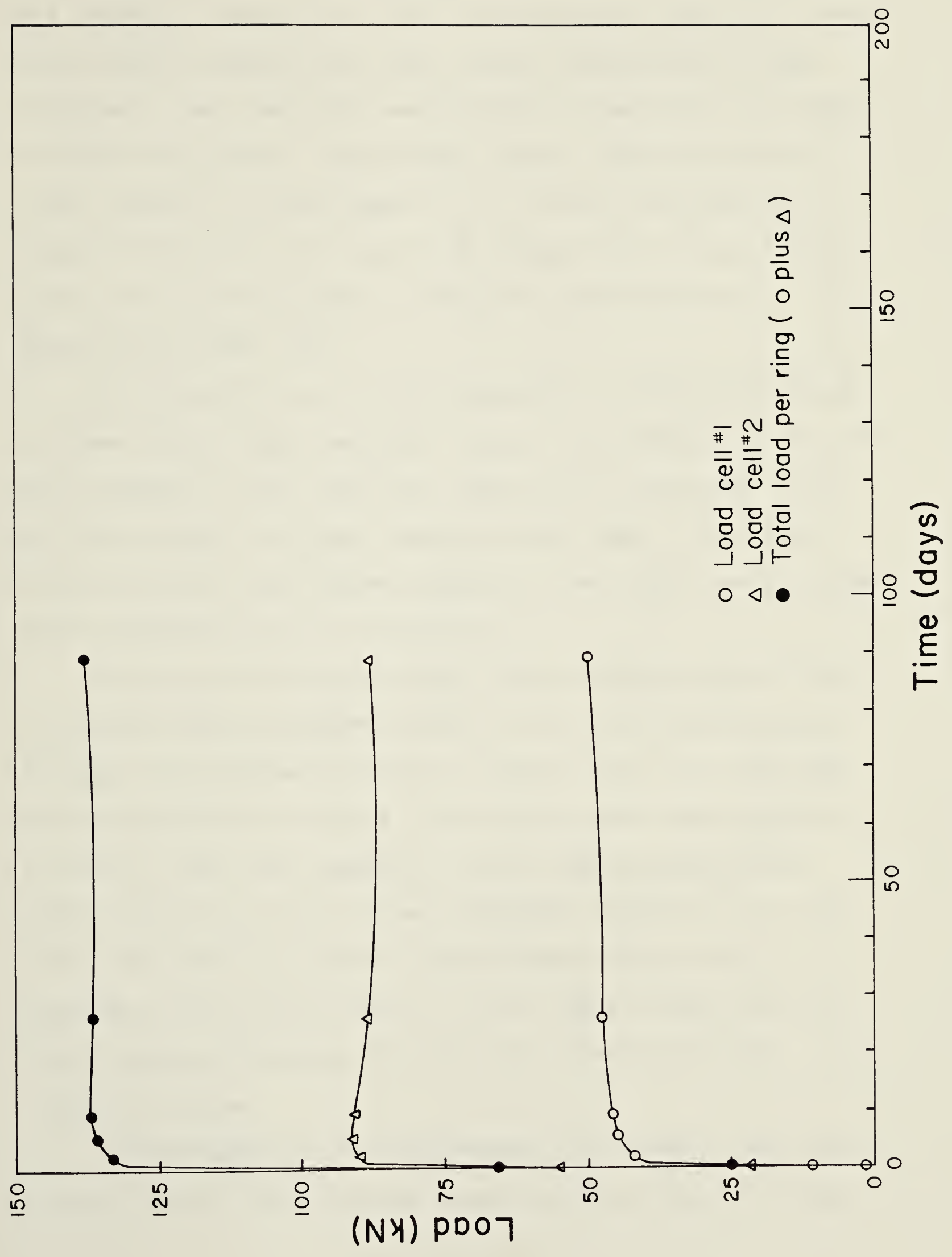
Changes in the vertical and horizontal diameters were measured using a constant tension tape extensometer. The movement of the tunnel invert was monitored using a level survey. Very small diameter and level changes, on the order of 2 mm, were measured at this section.

Just after expansion, small gaps were observed between the lining and the soil. Utilizing the inspection holes, their width was measured and found to be 2-3 mm. It was recognized that if valid detailed conclusions concerning the nature and closure of these gaps is to be drawn, the number of observation holes must be increased to perhaps 12 holes in each ring.

5.4.3 Test Section 3

Five sets of special concrete segments (20 segments) were cast on September 13, 1979. These segments were provided with special recesses to accommodate two load cells to be positioned at one of the lower longitudinal joints of each ring. Each of these segments was also provided with four inspection holes.

The segments were installed in the tunnel on October 16 and 18, 1979 at a location about 625 metres east of the end



of the curve (see Figure 3.8). Details of this test section are shown in Figure 5.14. Ten vibrating wire load cells were installed to measure the liner thrust (resultant of hoop stresses). Two load cells were placed in each of five rings, in one of the lower longitudinal joints. Measurements of liner thrust in rings number 1, 2, 3 and 5 are given in Figure 5.15, 5.16, 5.17 and 5.18 respectively. One of the load cells in ring number 4 malfunctioned before the expansion of that ring.

The installation of the load cells in ring #2 differed to some extent from the other rings. The recesses in ring #2 were somewhat larger than the load cells. Therefore, a 0.5 cm thick rough plate was inserted under each of the load cells of this ring. Rubber cushions, 3 mm thick, were placed above and below all the load cells.

The size of the gap between the outside surface of the lining and the excavated surface of the soil was measured through sixty inspection holes. Each of the five rings was provided with four holes at the tunnel crown and four holes in each of the side segments. Initial measurements were taken as soon as the ring was expanded. Figures 5.19, 5.20, 5.21, 5.22 and 5.23 contain measurements of gap size measured at the five rings vs. time. Negative gap size in these figures indicates that the soil moved into the inspection holes.

The averages of the measurements of diameter and level change taken at Test Section 3 were on the order of 2-4 mm.

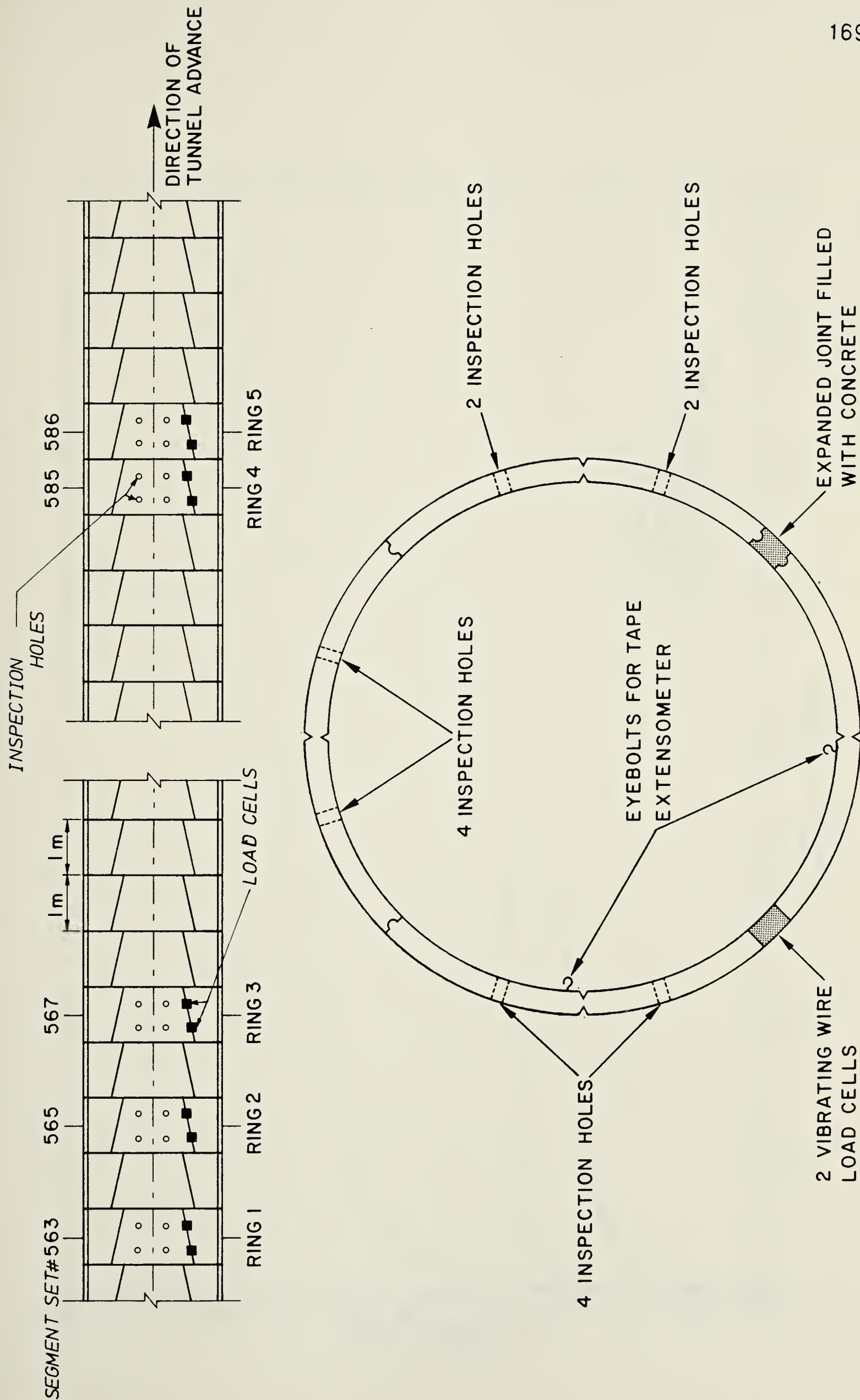


Figure 5.14 Details of Test Section 3 (lining instruments)

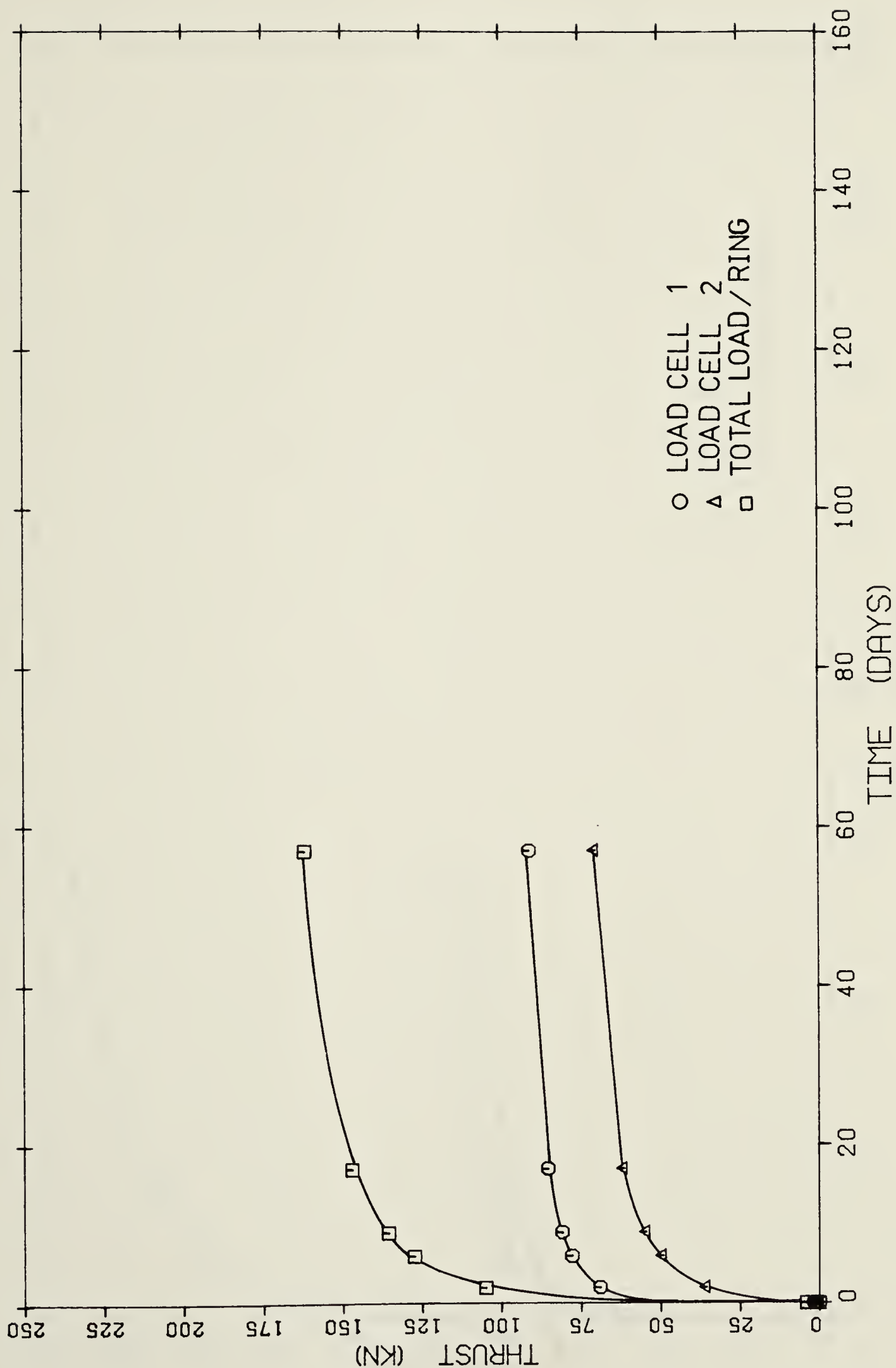


Figure 5.15 Measurements of liner thrust (Section 3 - Ring 1)

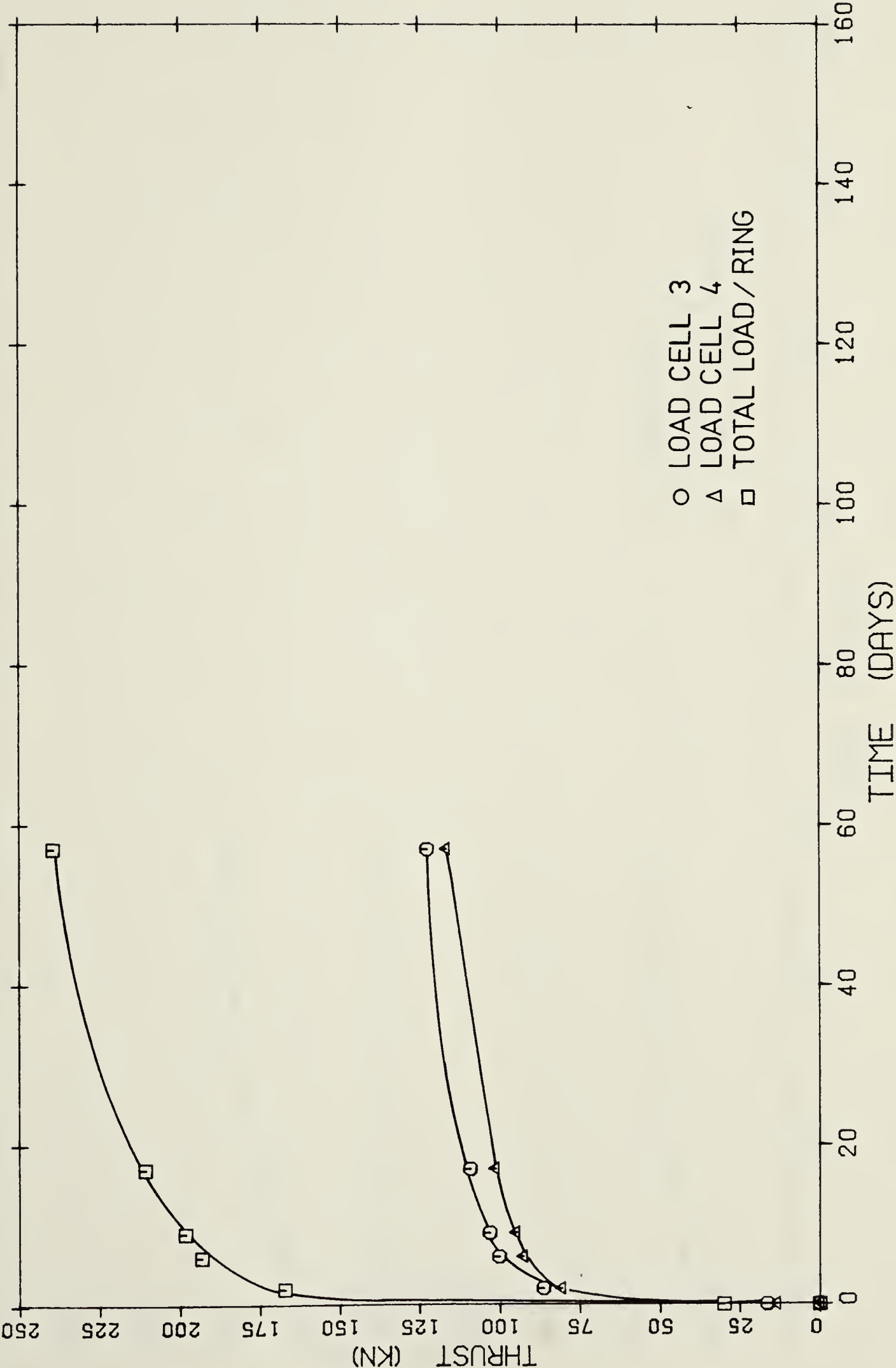


Figure 5.16 Measurements of liner thrust (Section 3 - Ring 2)

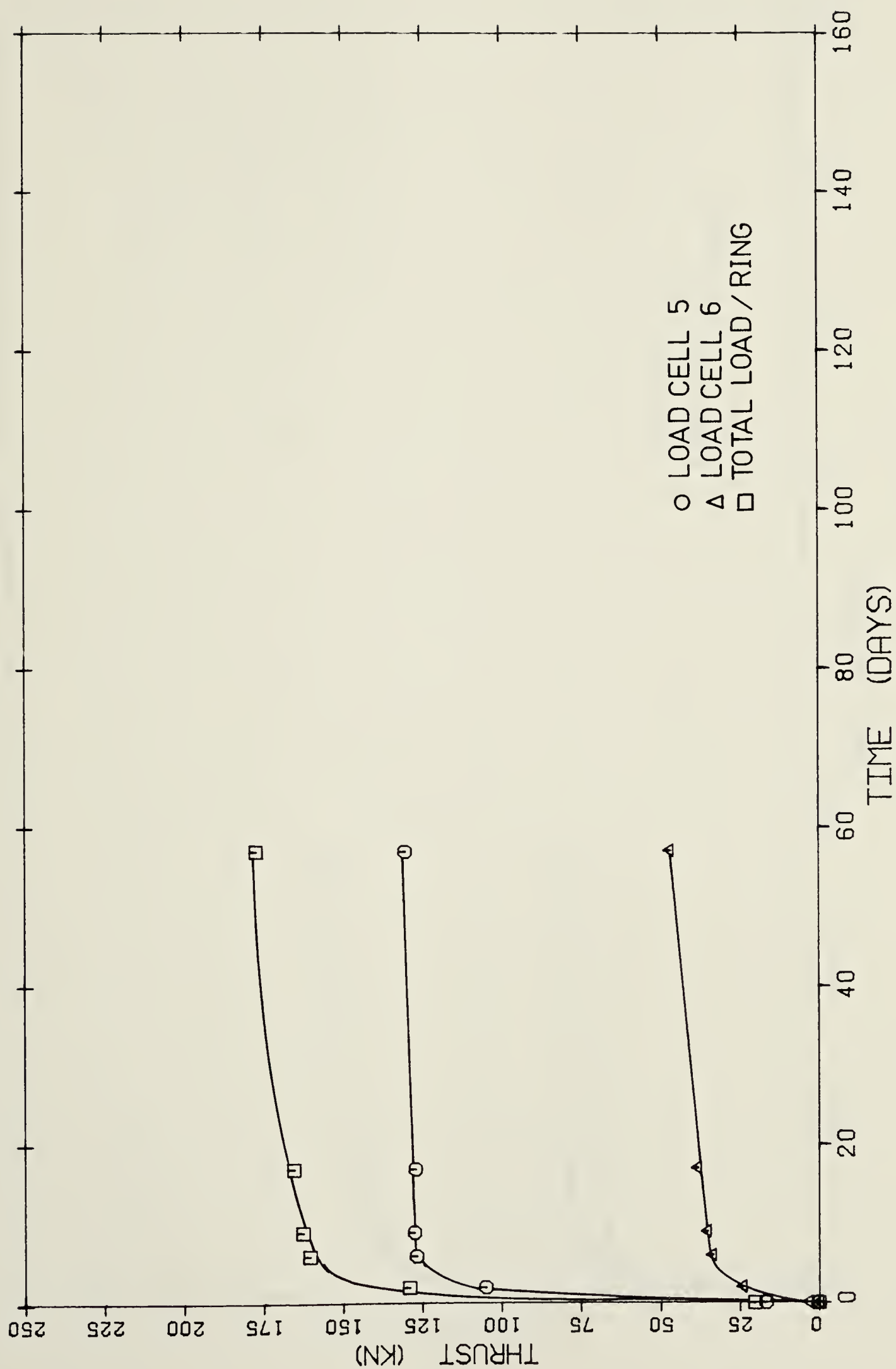


Figure 5.17 Measurements of liner thrust (Section 3 - Ring 3)

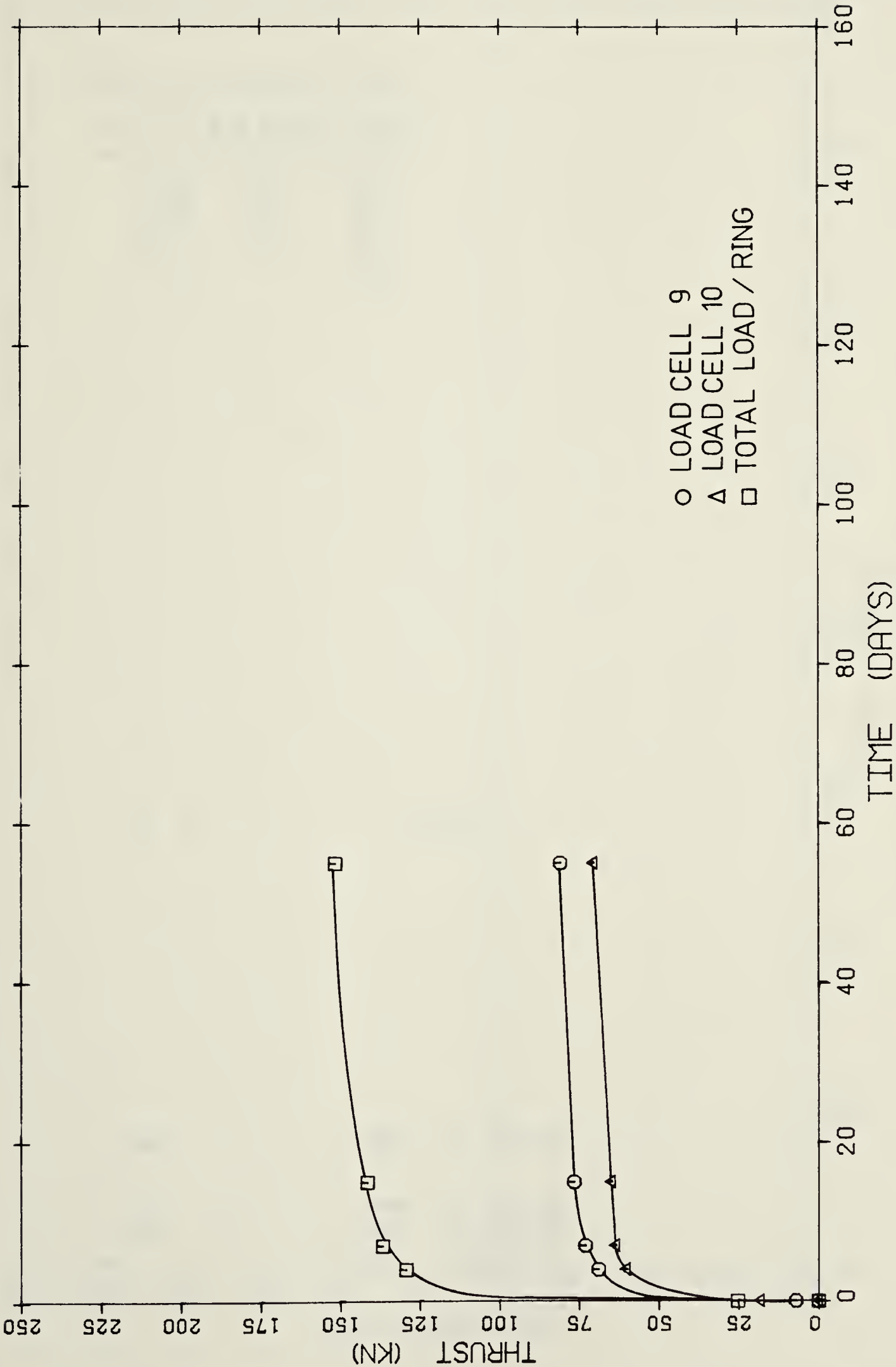


Figure 5.18 Measurements of liner thrust (Section 3 - Ring 5)

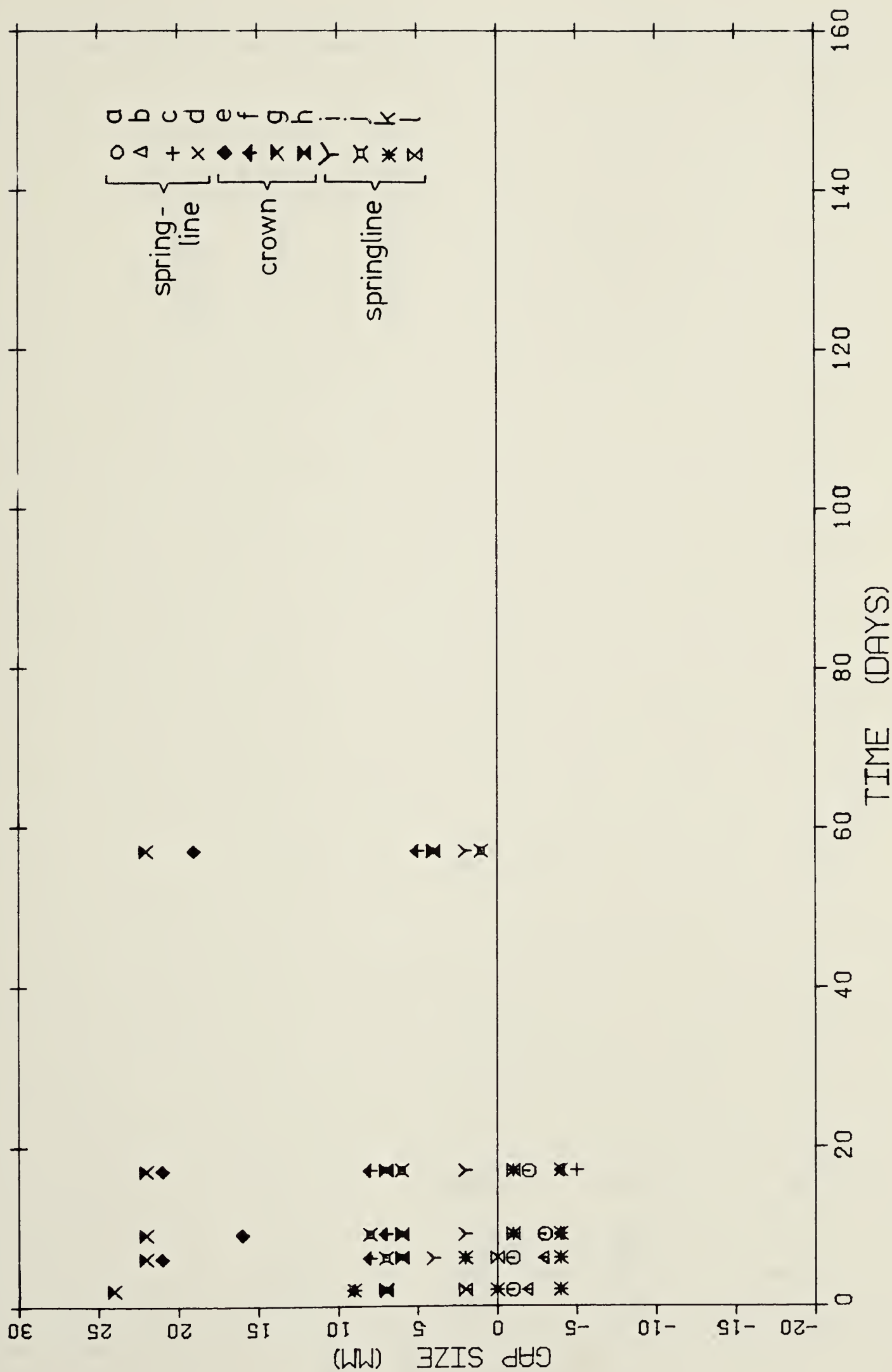
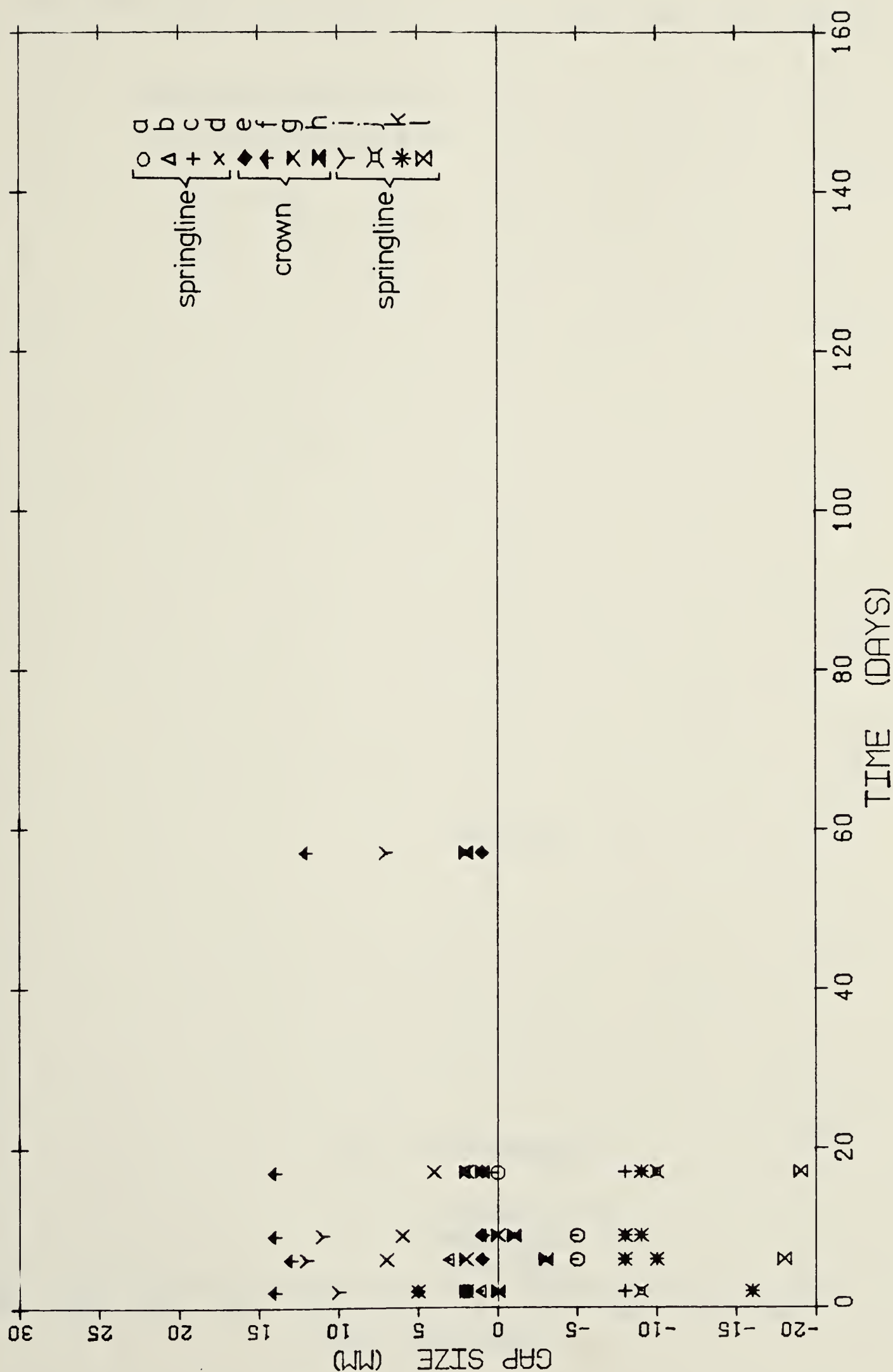
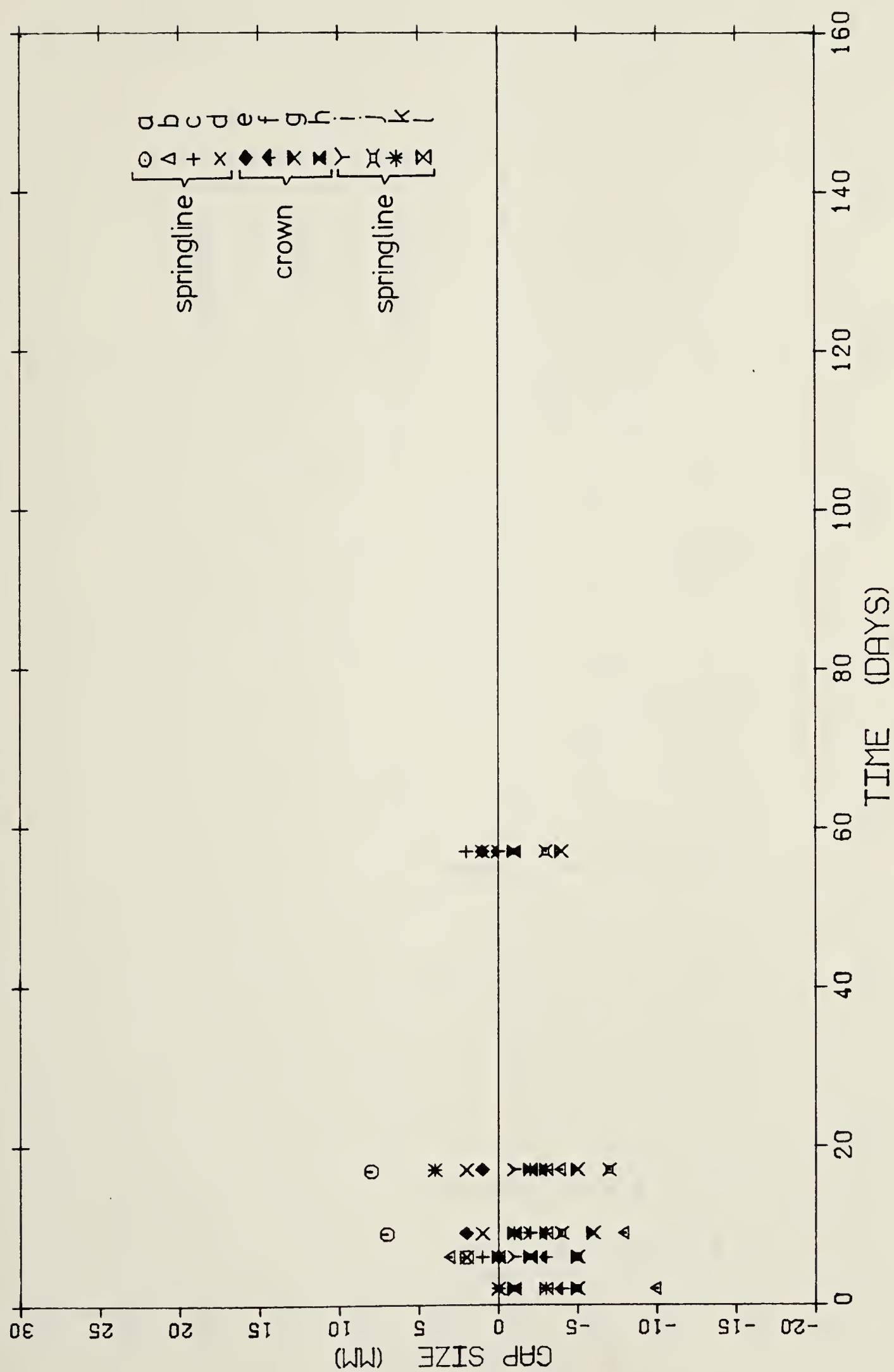


Figure 5.19 Size of gap between lining and soil (Ring 1)



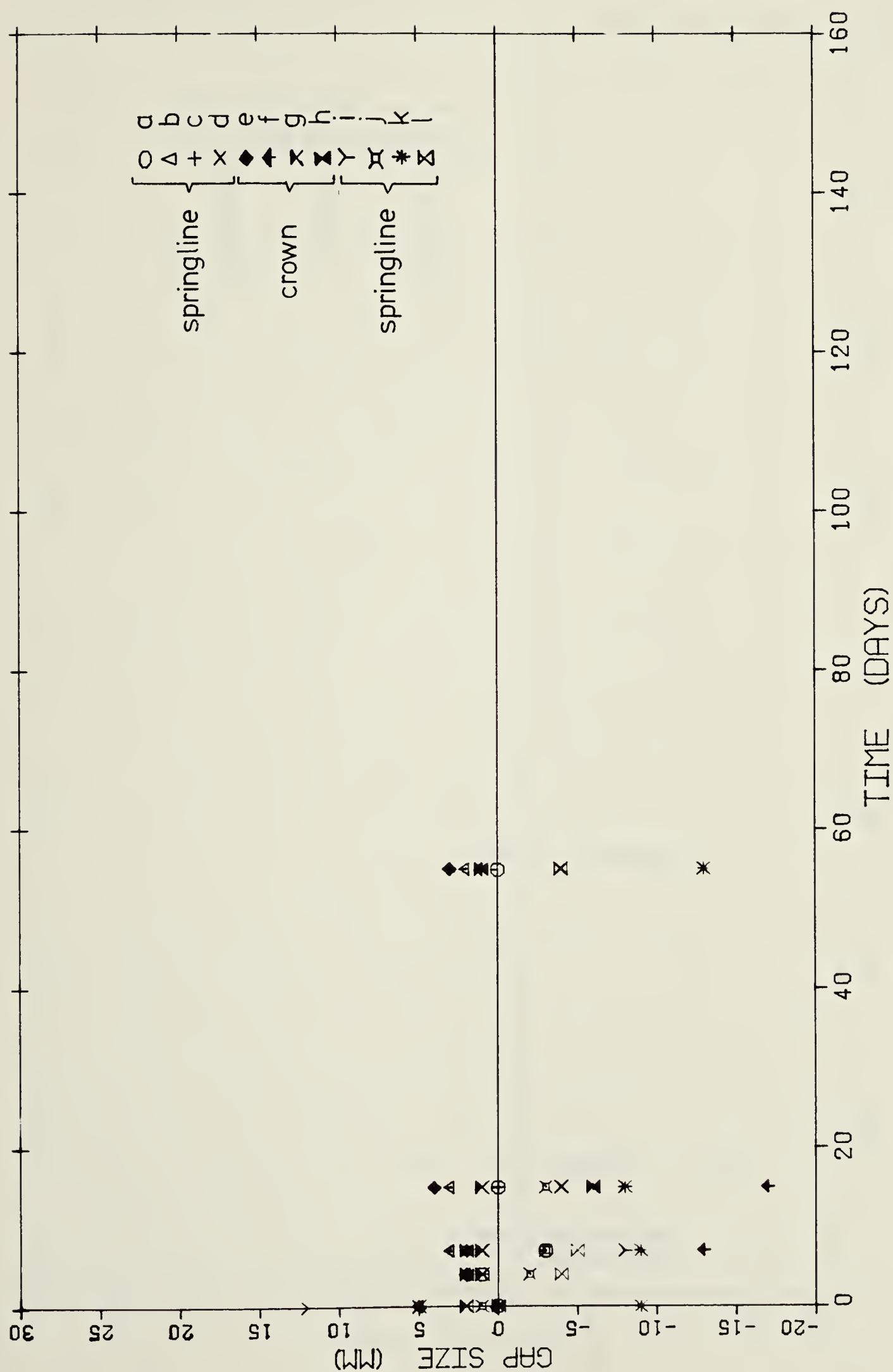
RING#2 - TEST SECTION 3

Figure 5.20 Size of gap between lining and soil (Ring 2)



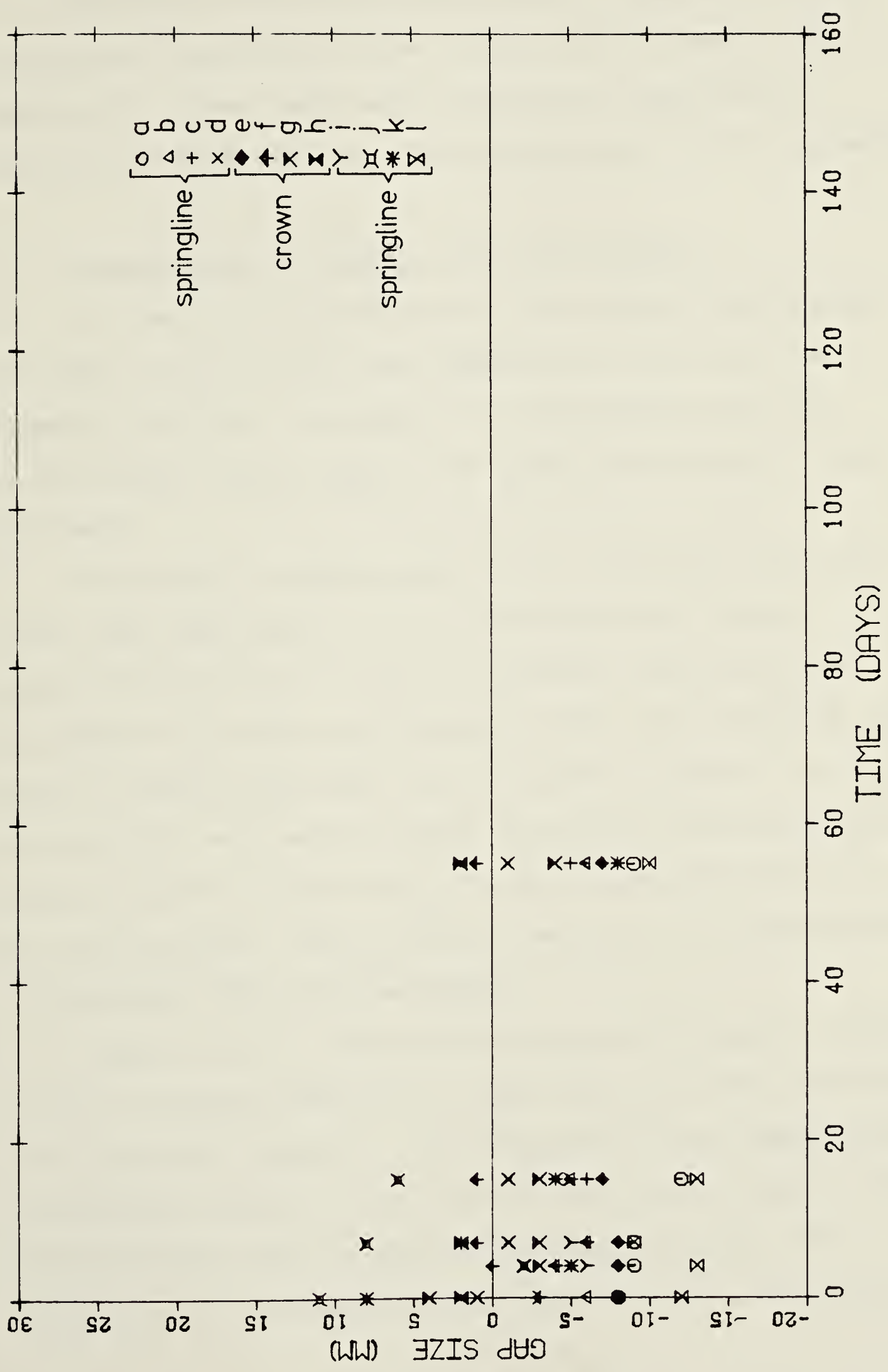
RING#3 - TEST SECTION 3

Figure 5.21 Size of gap between lining and soil (Ring 3)



RING#4 - TEST SECTION 3

Figure 5.22 Size of gap between lining and soil (Ring 4)



RING#5 - TEST SECTION 3

Figure 5.23 Size of gap between lining and soil (Ring 5)

5.5 STRENGTH OF LONGITUDINAL JOINTS OF SEGMENTS

An extensive testing program was carried out in the structural laboratory at the University of Alberta. The samples for these tests were prepared and supplied by Supercrete (Alberta) Ltd., the manufacturer of the segments.

5.5.1 Description of Samples and Test Results

The tests were performed to investigate the strength and mode of failure of the longitudinal joints of the segments and their dependence on the concrete mix and reinforcement used. Figure 5.24 shows the details of typical specimens.

Five sets of samples were tested. Each of the first three sets consisted of three reinforced and three unreinforced pairs of joints. Different concrete mixes, designed to give 28 day strengths of 25, 30 and 35 MPa, were used in these three sets. Two different batches of 40 MPa concrete mix were used in sets #4 and #5. Only unreinforced concrete joints, three pairs in set #4 and four pairs in set #5, were tested. Three cylinders were cast from each batch to determine the actual strength.

Sample sets #1, #2 and #3 were cast in special molds giving the same dimensions of the joints as those obtained for production segments. The curvature of the segments was eliminated though, to simplify the testing procedure. Sets #4 and #5 were cast in one of the molds used for the production of the segments. The outer curved surface was

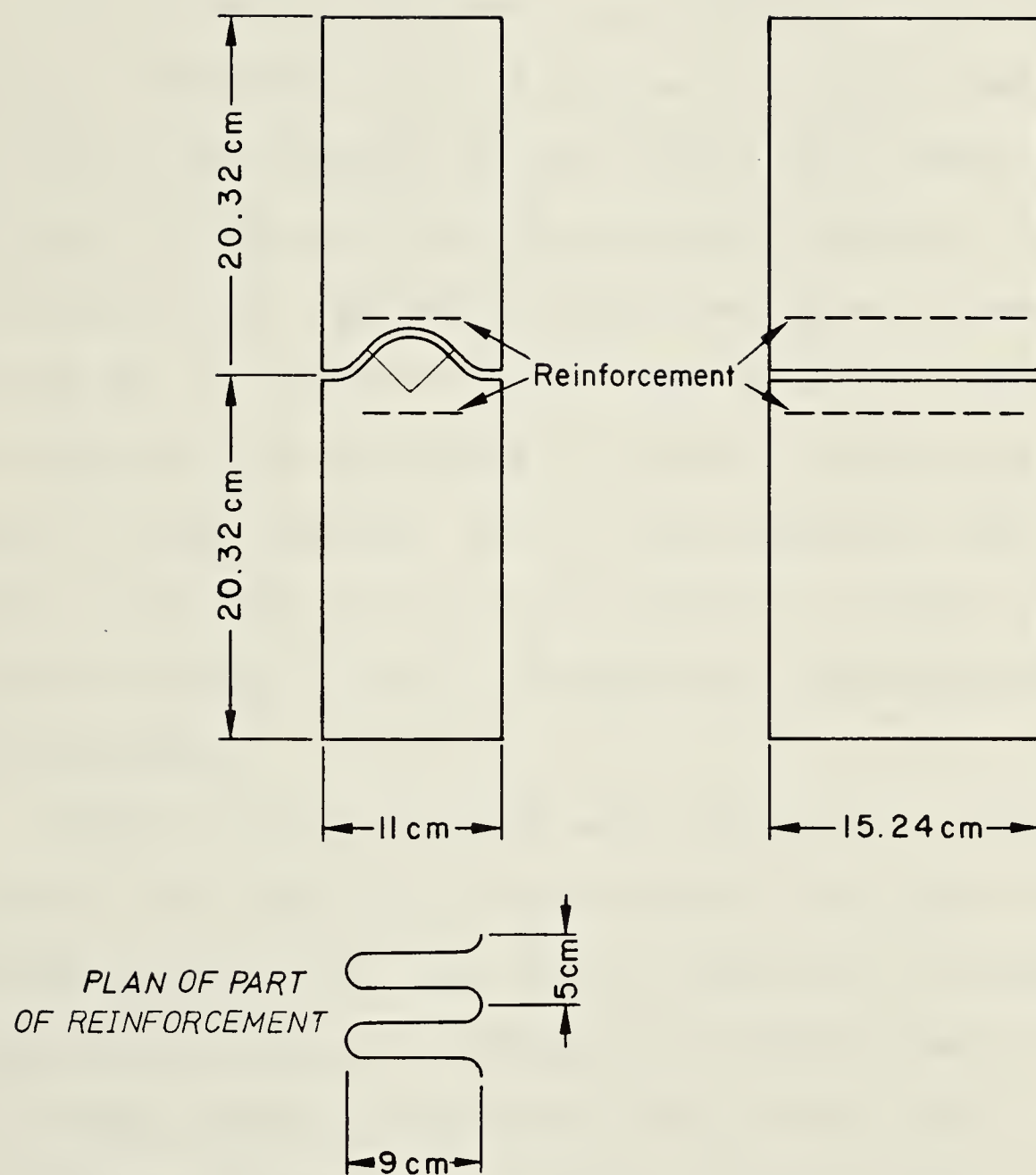


Figure 5.24 Details of longitudinal joint samples

replaced by a flat one to avoid eccentricity of load during testing.

All tests were performed one week after casting. The results are summarized in Table 5.2.

5.5.2 Discussion of Test Results

Test results obtained from the first three sets of samples indicated that the concrete strength does not appear to affect the strength of the joints. Any effect of the strength of the concrete was probably masked by the noticeably poor casting procedure employed in preparing sets #2 and #3. An eccentricity of load of up to 5 mm, between the upper and lower pieces of joints tested, was measured on some of these samples. Also, it was apparent that the gravel used in the concrete mix was relatively coarse (19 mm). A slight increase in joint strength was recorded with reinforcement.

Higher joint strengths were measured in sets #4 and #5. This was the result of using concrete of higher strength, smaller gravel size, and a better method of casting. One of these samples gave a strength even higher than all of the reinforced samples. Excluding this unique sample, the strengths of longitudinal joints, from sets #4 and #5, ranged between 36-42% of the strength of the concrete cylinder.

The effect of reinforcement on the mode of failure was significant as shown in Plates 5.5 and 5.6. The unreinforced

Table 5.2 Strength of longitudinal joints

Set# Concrete Mix (MPa)		Failure Stress (MPa)								
		Unreinforced			Reinforced			Cylinders		
		1	2	3	1	2	3	1	2	3
1	25	10.22	10.48	11.68	11.94	13.27	13.27	20.58	21.49	21.51
2	30	8.86	9.98	10.48	13.27	15.95	14.22	30.70	31.39	31.34
3	35	10.77	9.87	9.87	14.60	15.10	11.49	32.12	32.44	32.54
4	40	14.07	12.18	13.92	-	-	-	31.73	34.73	34.00
5	40	13.53	17.52	12.74	14.07	-	-	32.07	34.03	35.73

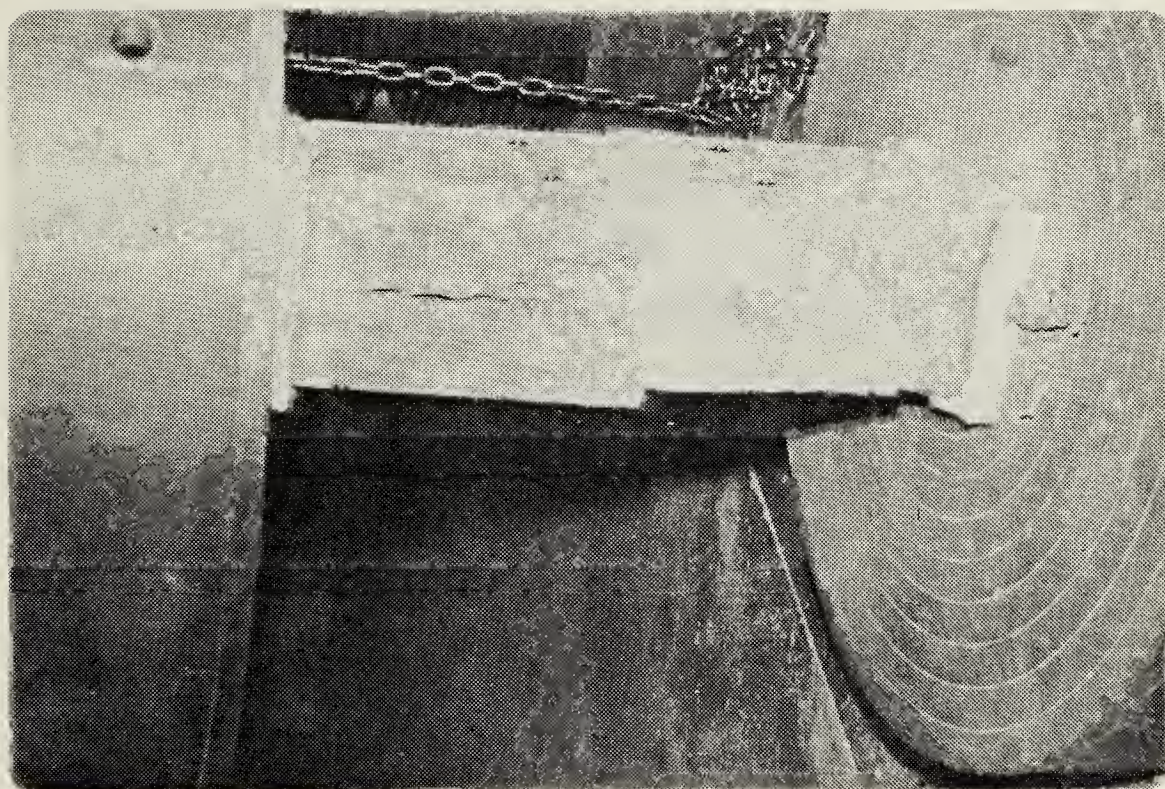


Plate 5.5 Failure of unreinforced longitudinal joint

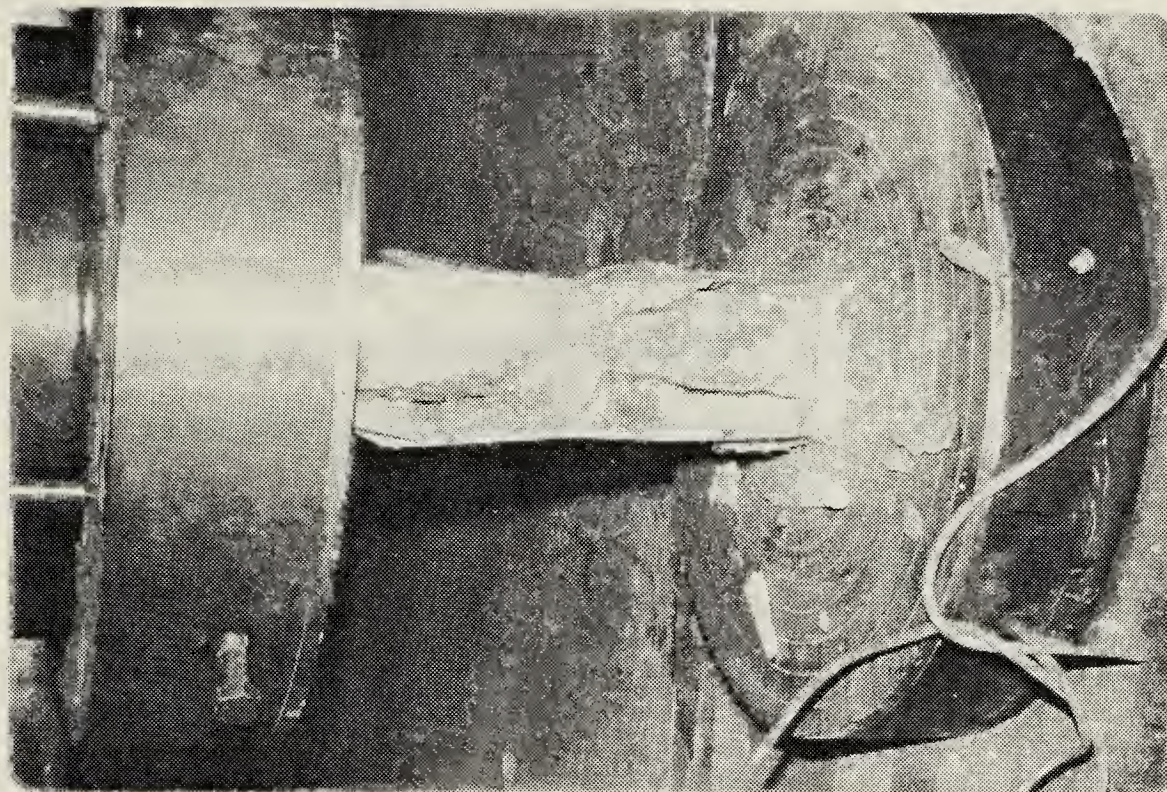


Plate 5.6 Failure of reinforced longitudinal joint

joints failed by sudden vertical splitting through the center line of the segment. This is shown in Figure 5.25. The reinforced joints failed slowly after vertical cracks had developed on all of the vertical surfaces of the samples, as shown in Figure 5.25. These cracks were first observed at loads of 40-60 KN lower than failure loads. This improvement in the mode of failure was offset by the difficulties encountered during casting with this special reinforcement in the molds. Because of these difficulties the use of such reinforcement was eliminated.

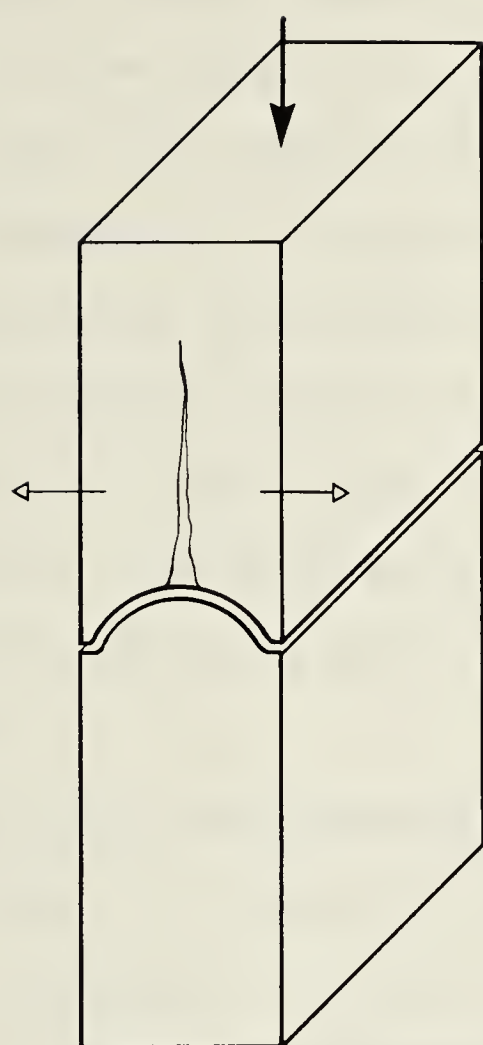
5.6 DISCUSSION ON LINING BEHAVIOUR

The measurements obtained from the lining instruments of the three test sections and the results of the laboratory tests were analyzed to investigate the behaviour of the two lining systems employed in the experimental tunnel.

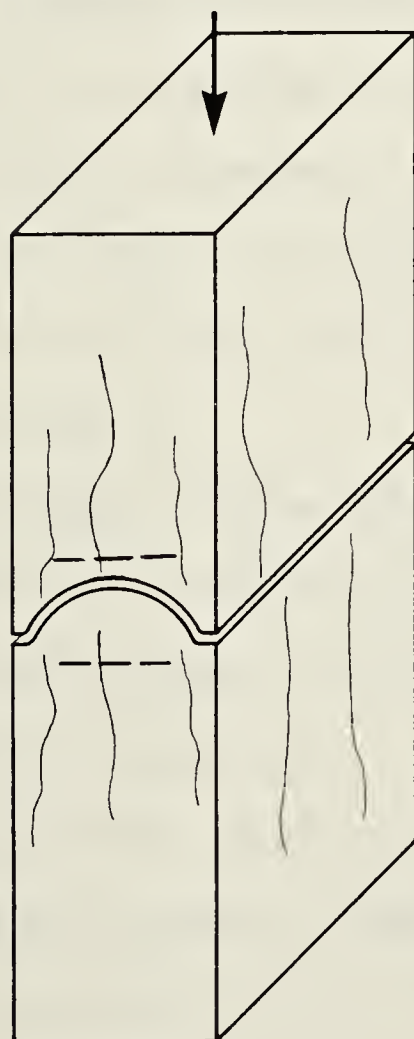
5.6.1 Rib-Lagging System

The measurements of strains in the steel rib, shown in Figure 5.8, indicate the development of both normal forces and bending moments. The maximum normal force corresponds to an average soil pressure on the lining of 63 KPa. This is equivalent to 12% of the overburden pressure.

The bending moments in the steel rib can be related mainly to the eccentric wedging of the upper joints which is shown in Figure 5.6. The bending moment measured by strain gauges 1 and 2 was larger than that measured by strain



UNREINFORCED JOINT



REINFORCED JOINT

Figure 5.25 Modes of failure of reinforced and unreinforced joints

gauges 3 and 4. This is a result of different eccentricities at the upper joints. However, the normal forces at the two sections of the steel rib, represented by the strains at the neutral axes, are almost the same, as shown in Figure 5.26. The measurements also suggest that bending stresses constitute up to 50 percent of normal stresses due to normal forces and bending moments combined. The strain measurements also indicate, (see Figure 5.7), that the equilibrium state of the steel ribs develops within a short period after installation and well before the secondary concrete lining is placed.

Distortion measurements of three ribs in a similar tunnel, shown in Figure 5.9, indicate that the vertical diameter undergoes a change of 2 mm or less while the horizontal diameter decreases by 5 to 9 mm. Level changes of invert elevation measured in that tunnel are given in Figure 5.10. The initial decrease in this elevation, due to settling in of the lining system, is followed by an upward movement which reflects the load release and swelling of the till at the invert.

A continuous annular space between the soil and the lining, from the crown to the springline, was observed. It varies in size between 2-4 cm and closes within two days to one week after expansion.

Previous field studies on the behaviour of rib and lagging lining system in Edmonton tunnels are given in detail by Eisenstein et al. (1977) and El-Nahhas (1977).

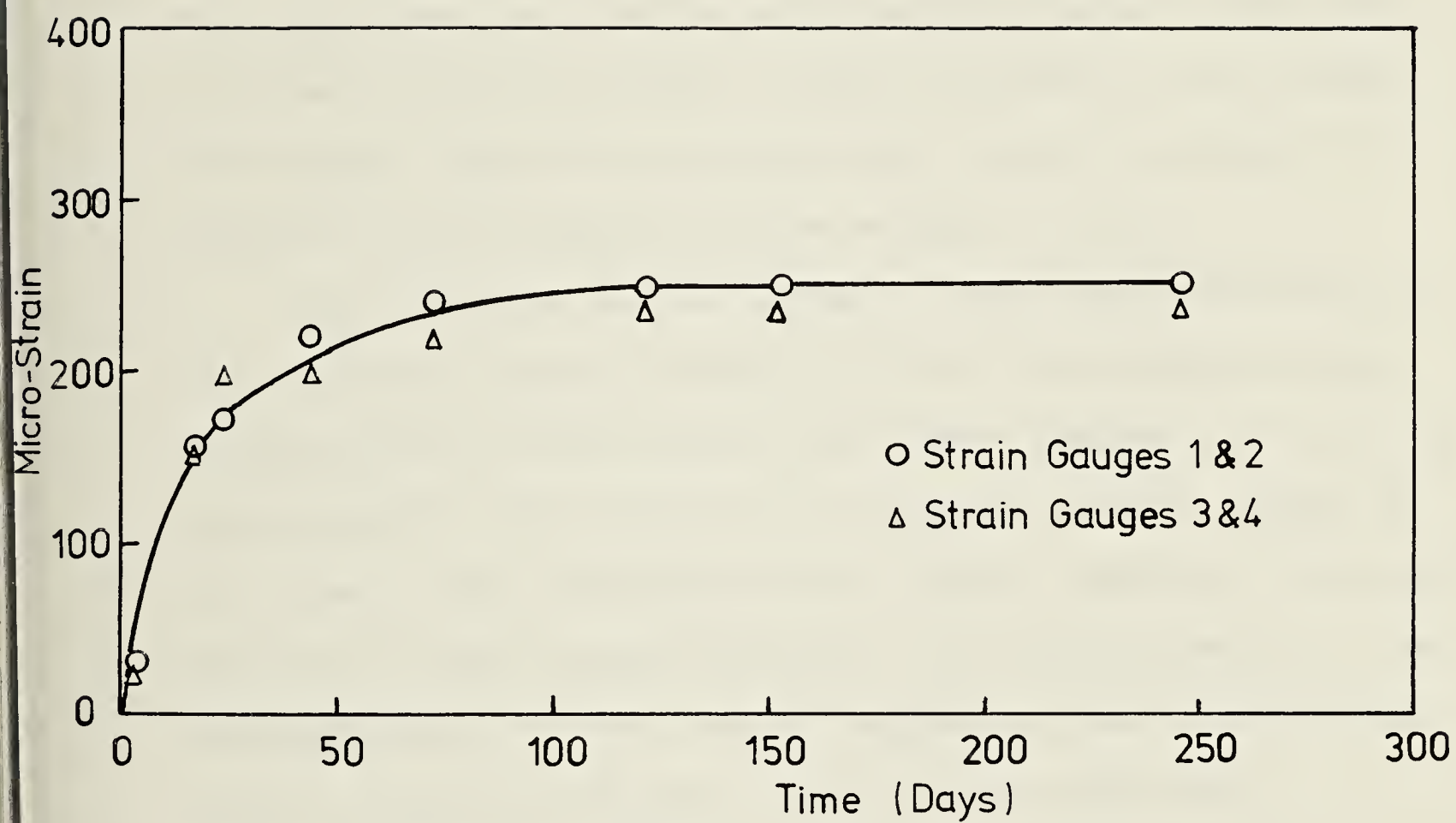


Figure 5.26 Strains at neutral axes in the steel rib of Section 1

Their results are summarized and discussed in the papers by Eisenstein and Thomson (1978) and Thomson and El-Nahhas (1980). These studies established the fact that the equilibrium state of the soil-lining interaction was reached within two weeks for glacial till and within three months for the Upper Cretaceous clay-shale. This concept was confirmed again for the till by the measurements obtained from Test Section 1 of the experimental tunnel. Since the secondary concrete lining is usually placed in the tunnel after much longer than this period, the soil pressure is actually carried solely by the primary lining.

Soil pressure on the primary lining was determined in the previous studies either by direct measurements using pressure cells installed on the timber lagging, or indirect measurements using electrical resistance strain gauges on the steel ribs or deformation of timber laggings, or by back analysis of the lining using the field measurements of the deformed shape of the ribs as imposed boundary conditions. Table 5.3 gives a summary of the results and some information on each tunnel. The results obtained from Test Section 1 of the experimental tunnel are also included in this table. Many factors contribute to the difference between the pressure acting on the lining of these tunnels such as: soil type, construction procedure, depth/diameter ratio . . . etc.

The Whitemud Creek tunnel, for example, was excavated through clay-shale using unshielded drilling machines

Table 5.3 Soil pressure on the primary lining in Edmonton tunnels

	Depth (Z) Diameter (D)		Z/D	$\overline{P_V}$ (kPa)	$\overline{P_L}$ (kPa)	$\overline{P_L}/\overline{P_V} \times 100$	\overline{h} metre	$n=h/D$	References
Rapid Transit Tunnel	10.2	6	1.7	125	100	80	4.71	0.8	Eisenstein et al. (1977) Eisenstein and Thomson (1978)
Whitemud Creek Tunnel	47.2	6.05	7.8	575	114.7	20	5.41	0.9	El-Nahhas (1977) Thomson and El-Nahhas (1980)
170th Street Tunnel	20	2.56	7.81	380	6.1-12.6 (a) 112-240 (b)	1.6-3.3 (a) 29.5-63 (b)	0.29-0.59 (a) 5.28-11.31 (b)	- -	El-Nahhas (1977) Thomson and El-Nahhas (1980)
Experimental Tunnel	27	2.56	10.54	550	63	12	2.79	1.09	(Present study)

Notes: $\overline{P_V}$: Overburden pressure. $\overline{P_L}$: Pressure on lining. \overline{h} : Height of soil carried by lining = $\overline{P_L}$ /soil unit weight

(a) = From pressure cells.

(b) = From lagging deflection.

whereas the other tunnels were drilled through glacial till using shielded moles. Higher strength of the clay-shale allows more arching of soil pressure around the tunnel. The use of unshielded drilling machines allows the installation of the primary lining very close to the face, hence more load tends to be taken by the lining. The Rapid Transit tunnel was relatively shallow (depth to center line = 1.7 diameters) while the depth of the other tunnels is more than seven times the diameter. These differences between the Whitemud Creek tunnel and the Rapid Transit tunnels have contributed significantly to the ratio between the soil stress arched around the tunnel and those attracted by the lining. However, it was interesting to note that the height of overburden carried by the lining of both tunnels were equal.

The 170th street tunnel and the experimental tunnel at Test Section 1 were both drilled through glacial till using the same construction procedure. The soil pressure measured by the pressure cells were very low mainly because of the transfer of soil pressures directly to the steel ribs. The calculated values of soil pressure based on deflection of three pieces of lagging varied over a wide range (29.5-63% of overburden). The calculated pressure based on the measurements of the more reliable vibrating wire strain gauges in the experimental tunnel, seems to indicate more reliably the actual load carried by the steel ribs in these small deep tunnels.

Finally, it is of interest to note that the height of the soil (above the crown) which is carried by this lining varies within the range of 0.8 to 1.09 tunnel diameters.

5.6.2 Precast Segmented Lining

5.6.2.1 Strains and Stresses in the Lining

Stresses at the neutral axis at the springline and crown sections were calculated using the measured strains given in Figure 5.12 and an average value of Young's modulus of 25,100 MPa. The calculated stresses are shown in Figure 5.27. Their ultimate values are 2.9 MPa at the springline and 1.7 MPa at the crown which represents 48 and 28 percent respectively of the stresses that would develop in the lining if a uniform pressure equal to the overburden were applied. If unequal horizontal and vertical pressures are assumed, the calculated stresses could result from the pressure distribution shown in Figure 5.28.

Although the strain gauges were installed or embedded close to a stress raiser, the measurements indicate the occurrence of large bending strains, especially at the springline section. It was also noticeable, that most of the stress raisers at the springline were uncracked. These observations suggest that the stress raisers, particularly those at the springline level, carry some residual bending moments.

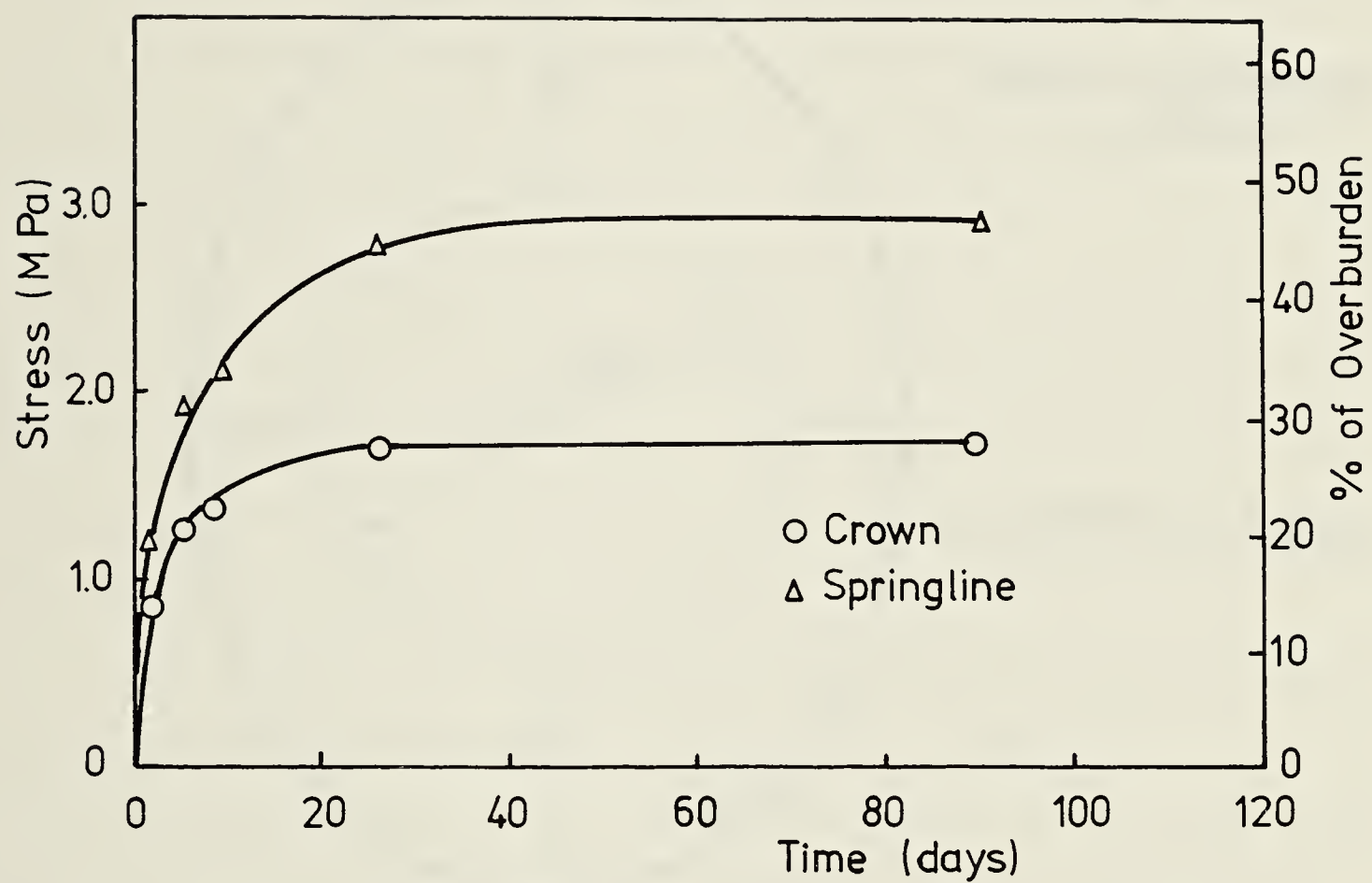


Figure 5.27 Stresses at the neutral axis of segmented lining (Test Section 2)

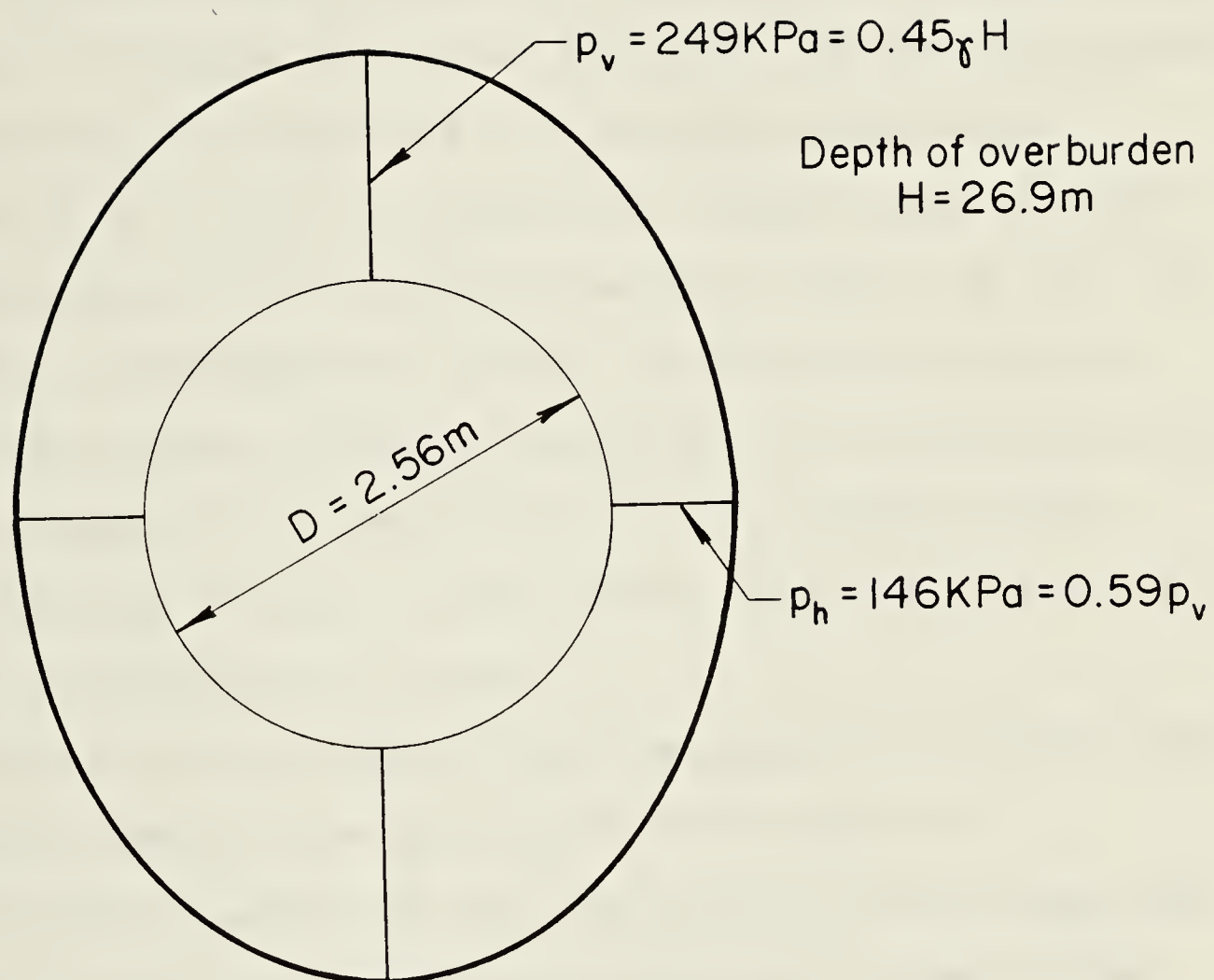


Figure 5.28 Estimated pressure distribution on segmented lining (Test Section 2)

5.6.2.2 Liner Thrust and Soil Pressure

The ultimate liner thrust (resultant of hoop stresses) measured in Section 2 by the load cells was 138 KN/ring, as shown in Figure 5.13. This is equivalent to an average soil pressure on the lining of 22% of the overburden stress. Slightly higher thrust loads were taken by the segments at Section 3. Ultimate thrusts of 170, 250, 180 and 155 KN/ring were measured in ring #1, #2, #3 and #5 respectively (Figures 5.15, 5.16, 5.17 and 5.18). These loads indicate average values of soil pressure on the rings of 27, 40, 29 and 24% of the overburden stress. At both test sections, each of the loads attains at least 85% of its ultimate value within a week of the installation of the lining in the tunnel. During this period the tunnel face had advanced 45 metres (18 diameters) or more.

The relatively higher thrust measured in ring #2 (Test Section 3) seems to be the result of the special installation procedure of the load cells in this ring (see section 5.4.3). The insertion of additional steel plates under the load cells caused a significant prestress in this ring. Excluding the results from ring #2, the ultimate load measured in the segmented rings varies between 138-180 KN, indicating an average uniform soil pressure on the lining of 22-29% of the overburden stress. These values are consistent with measurements of strain at crown (Test Section 3) but are relatively lower than those measured at the springline.

No strain gauges were used in Test Section 3 because of

their high cost. Hence, the ten load cells provided only a range of variation of liner thrust carried by five rings. On the other hand, strain measurements in Test Section 2 gave an indication of the ratio between the vertical and horizontal pressure on one ring only. The liner thrust in this ring was also measured using two load cells. Combining all these measurements, the range of variation of non-uniform pressure on the precast segmented lining was determined. As shown in Figure 5.29, the pressure distribution has an elliptical pattern with vertical pressure between 45-59% of the overburden stress and horizontal pressure between 27-36% of overburden stress.

Comparison of the pressure distributions on the two lining systems with the original in-situ stresses ($K_0=0.8$ to 1.0) indicates a significant change in the soil stresses in the vicinity of the tunnel. This decrease in stress occurred mainly while the soil was moving radially to fill the annular space around the drilling machine as suggested by the soil deformation measurements shown in Figure 4.26.

5.6.2.3 Distortion of Lining

Each ring of the precast segmented lining is provided with four stress raisers and four joints as shown in Figure 5.14. These joints and stress raisers act as sections of low moment resistance. They were included in the design with the intention of increasing the flexibility of the lining and reducing the bending moments in the segments.

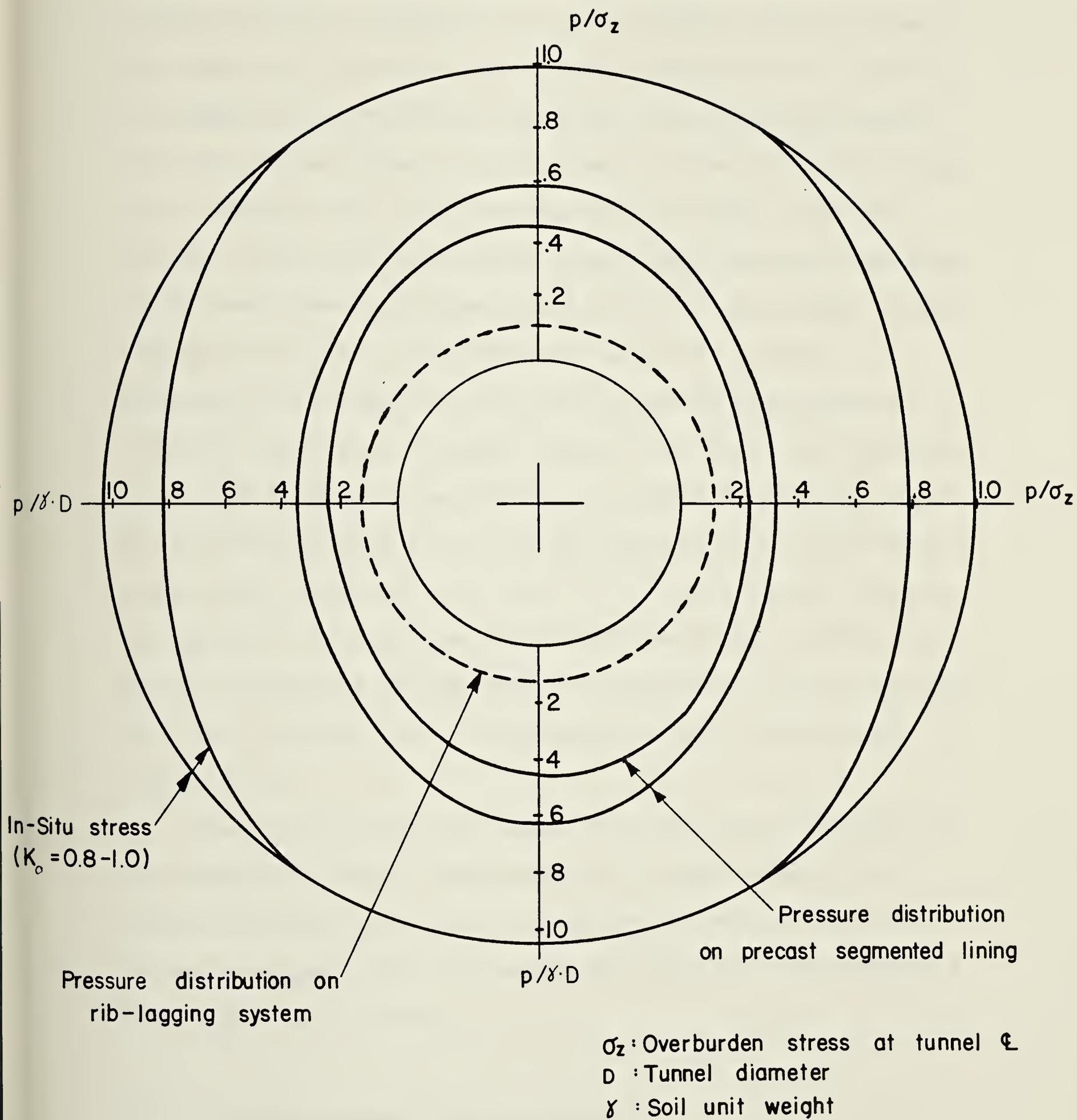


Figure 5.29 Variation of soil pressure on the lining systems

Measurements of lining distortion in Test Sections 2 and 3 showed very small diameter changes, on the order of 2-4 mm. Similar movements were measured for level changes of the crown and invert of the tunnel. Inspection of cracking of segmented lining after the tunnel was completed showed that the stress raiser at the crown of almost all the rings were cracked. Most of these cracks were about 1 mm wide. Only at a few locations wider cracks were observed and some cracks were developed even outside the stress raiser. These unusual cracks are the combined result of residual deformations during handling and expanding the segments. Possible correlation between these wide cracks and location of boulders encountered during the tunnel excavation could only be established at one or two locations. Only hairline cracks were observed in a few of the stress raisers at the springline. It should be noted that the higher tendency of cracks to develop at the crown is consistent with the higher vertical component of soil pressure on the lining shown in Figure 5.28.

Despite the measures taken to reduce the stiffness of the segmented lining, measurements of small distortions, large bending strains and indications of non-uniform soil pressure suggest that the segmented rings are behaving as a relatively stiff lining.

5.6.2.4 Gaps Between Lining and Soil

The measurements of the size of the gap between the

lining and the soil are given in Figure 5.19 to 5.23.

Negative gap size in these figures indicates that the soil moved into the inspection hole. From these figures the following observations are offered:

1. Most of the measurements indicate a gap size less than 5 mm, with only a few gaps ranging in size from 10 to 20 mm. These gaps do not appear to form a continuous annular space, but rather seem to be isolated. Further, there appears to be an equal probability that the gaps might form either above the crown or around springline. These gaps could be resulting from unsmooth areas on the excavated surface of soil.
2. A significant number of the measurements indicate movement of the soil into the inspection holes. This is represented in Figures 5.19 to 5.23 as a negative gap size. Again, this was observed through holes at both the crown and springline. Low rates of water flow into the tunnel through some of the inspection holes were observed at the springline. This made measurement of the gap size impractical 57 days after installing the lining.

Although the gap size measurements might not portray with great accuracy the dependence of gap closure on time or tunnel advance, they do show a clear trend toward a reduction of size with time. Some of the gaps have never closed but they are isolated and do not form a continuous

space. On the other hand, if the segments were not expanded a continuous annular space with average size on the order of 20-25 mm would exist.

From these above observations, it is concluded that radial expansion of the segments essentially, eliminates the annular space between the lining and the soil. This indicates clearly that grouting is not needed if this type of tunnel construction, which utilizes expanded segmented lining, is used in stiff overconsolidated clay similar to the Edmonton glacial till.

5.6.2.5 Strength of Longitudinal Joints

Results of laboratory tests on the longitudinal joints of the concrete segments are presented and discussed in section 5.5. They show that the strength of these joints ranges between 36-42% of the concrete strength as indicated by test cylinders. Failure of the joints occurs by sudden vertical splitting through the center line of the segment. This failure is due to the concentration of bearing stresses along the contact area of the concave-convex surfaces, which cause tensile stresses perpendicular to the segment center line.

5.7 PRESSURE-DEFORMATION RELATIONS OF THE TWO LINING SYSTEMS

Soil deformation measurements, presented in the preceding chapter, were combined with the data obtained for the pressure and deformations of the two lining systems to

construct the reaction curves of the soil and the two systems of lining as shown in Figure 5.30. As discussed in section 2.2.3, these curves are of great value when used as a tool for qualitative discussions on some of the parameters involved in the design of linings for tunnels in soils.

Since the measurements indicate that the behaviour of the soil at the crown is significantly different from that at the invert, the ground reaction is represented in Figure 5.30 by curves illustrating the behaviour at the crown and invert zones separately. Several distinctive phases are apparent from the crown curves. Initially, there is stress release due to excavation of the face. Mole clearance allows the soil to close on the shield. This soil deformation is also the single most important source of ground movement and stress release. After the mole clears the profile, the soil closes further on the yet unexpanded lining until its expansion. From this point, the segmented liner begins to counteract the soil pressures until an equilibrium is reached. In case of the rib and lagging, the soil continues to deform to close the annular space around steel ribs and only after this stage the lining begins to be activated. Thus, the final equilibrium with the rib and lagging is reached at a higher displacement but lower lining stresses.

It is interesting to note that the soil at the invert responds very similar to the theoretical elasto-plastic behaviour. However, the behaviour of the soil at the crown departs significantly from such ideal elasto-plastic

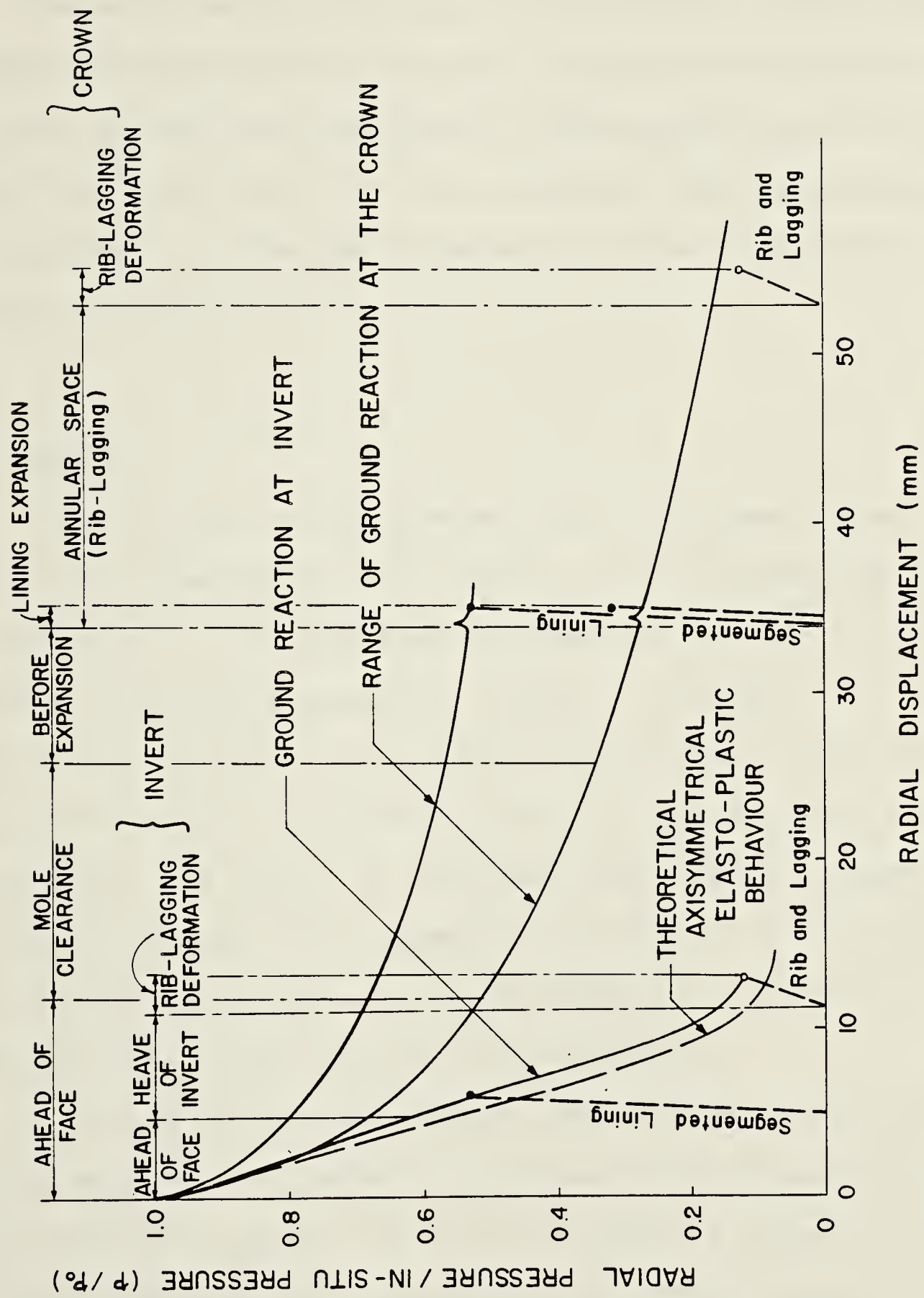


Figure 5.30 Reaction curves for the two lining systems

axisymmetrical condition. As discussed in section 6.5.3, both the mode of shear strength mobilization and partial loosening of soil at the crown contribute to this behaviour.

The relatively low pressures carried by the two linings suggest the possibility of shear strength mobilization for the soil around the tunnel which consequently results in significant arching of in-situ stresses. The development of this process is examined in detail for the experimental tunnel in Chapter 6.

5.8 SUMMARY

An alternate to the conventional two-phase tunnel lining was examined in this chapter. The introduction of shotcrete as a lining system in Edmonton tunnels, as an example, could be successful. However, its use in conjunction with full face tunneling machines would require many modifications to provide proper procedures. On the other hand, the use of an expanded-type precast segmented lining offers possible comparable savings in lining cost, and construction time with fewer changes in the drilling machines and in the construction procedure.

A review of the instruments required to monitor tunnel lining behaviour in general is presented and description of the instruments chosen for the experimental tunnel is given. It was recognized that vibrating wire strain gauges and load cells are the most reliable instruments for measuring loads carried by the lining. Pressure cells were not used to

measure directly the soil-lining contact pressure. This was a deliberate decision based on a generally unsatisfactory performance of this kind of instrumentation.

Based on the field measurements in the test sections, and the results of the laboratory tests, a detailed discussion of the behaviour of both the conventional lining and the precast segmented lining is presented. From these discussions the following conclusions were reached:

1. Steel ribs of the conventional lining carry a low percentage of the overburden pressure (12%). The ultimate load taken by the segmented concrete lining varies between 138-180 kN/ring, indicating an average soil pressure of 22-29% of the overburden stress. More than 85% of the segmented lining thrust develops within one week, while the tunnel face had advanced a distance of about 45 metres (18 diameters). Stresses in the steel ribs develop at a relatively slower rate.
2. Pressure distribution on the segmented lining has an elliptical pattern with the vertical pressure between 45-59% of the overburden and the horizontal pressure between 27 and 36% of overburden stress.
3. Small diameter changes and level changes (in the order of 2-4 mm) are experienced by the segmented concrete lining. The vertical diameter of the steel ribs usually undergoes a change of 2 mm or less, while the horizontal diameter decreases by 5 to 9 mm. The invert of the rib and lagging system also experience an upward movement on

the order of 3-12 mm. The difference in the deformation of the two lining systems is a reflection of their stiffness relative to that of the soil.

4. A continuous annular space, 20-40 mm wide, is usually left ungrouted between the crown and the springline areas of the rib and lagging system after its expansion. A smaller space about 20 to 25 mm could develop if the segmented lining was not expanded. Radial expansion of this lining, however, practically eliminated this space, leaving isolated gaps distributed randomly along the tunnel circumference. This indicates that grouting is not needed if this type of tunnel construction, which utilizes an expanded segmented lining, is used in stiff overconsolidated clay similar to Edmonton glacial till.
5. The strength of the unreinforced longitudinal segment joints varies from 36-42% of the concrete strength. These joints fail by sudden vertical splitting through their center line. On the other hand, reinforced joints fail slowly after vertical cracks have developed in all directions. However, this improvement in the mode of failure is offset by the difficulties encountered during casting with this special reinforcement.

CHAPTER 6

STRAIN FIELDS AROUND A TUNNEL ADVANCING IN A STIFF SOIL

6.1 INTRODUCTION

Drilling a tunnel in a soil mass results in significant changes in the state of stress in the adjacent soil. These changes can be considered as a reduction of the radial component of in-situ soil pressure and an increase in the tangential component. Additional stress redistribution occurs whenever the shear strength of the soil is exceeded or if the soil behaviour exhibits a time-dependent component. Other stress changes, which usually occur around the tunnel face even in an ideal, elastic soil, are associated with the doming of stresses at the face and soil interaction with the drilling machine. Any change in the stress state results in a subsequent strain and hence deformation. Deformation components are easier to measure than stress, especially in soils.

This chapter presents the spatial deformation field based on measurements around an advancing tunnel in a stiff soil. The deformation field is illustrated by sets of contour maps of the coordinate components of the displacement vectors. It must be emphasized that these contour maps were developed using the field measurements of soil displacement around the experimental tunnel. A computer graphical system (SURFACE II) was used to generate these

plots, based on the measurements given in Chapter 4. Hence some relevant details of this computer package are included in this chapter.

Based on the displacement plots, the gradients of displacement were derived and the strain field around the tunnel was obtained. The strain field is presented here as strain rosette plots, contours of normal and shear strains, and contours of major and minor principal strains. Finally, the maximum shear strain field was used to investigate the mode of mobilization of shear strength around the tunnel.

6.2 SURFACE II GRAPHICS SYSTEM

SURFACE II is a computer program for creating displays of spatially distributed data. It has been developed at the Kansas Geological Survey by Sampson (1978). Although the program was originally prepared for the graphical analysis of geological information, it was used in this thesis to generate and plot contour maps of displacements and strains around the tunnel based on in-situ measurements. Some of the features of this program, which are relevant to its use in producing displacement contour maps are described here. The special features employed in developing strain contour maps are discussed in section 6.4.1.

The program divides the area under study using rectangular grid of any size. The irregularly spaced field data, (eg. measured displacements at different points), are used to estimate the displacement values at the grid nodes.

These values are the numerical representation of the in-situ displacement field. Two numerical interpolation techniques, global fit and local fit, are offered by the program for estimating the displacement at the regular mesh of points. The local fit technique, employed in this study, is based on the hypothesis that a near-by measurement is a better estimate of the value of a point on a surface than a more distant one, and that a small number of the nearest control points provides essentially all of the information that is relevant in an estimate.

The program allows the user to choose one of several ways in which the measurements in the vicinity of a grid point can be combined to create an estimate. The method chosen uses the nearest eight data points as control points. The estimation procedure (called slope projection) consists of two phases as shown in Figure 6.1. First, the slope of the displacement surface is estimated at every data point by a weighted least square fit of a trend-plane to the displacement values at the control points. Second, the local trend-planes of the control points around each grid node are extended to give different estimates of displacement at that node. The weighted average of these estimates is considered the most likely value of the displacement at the grid node.

The program, also, offers different choices of the distance-weight function for the calculations required in the two phases (see Figure 6.2). The more complex function is widely used in the commercial contouring systems and was

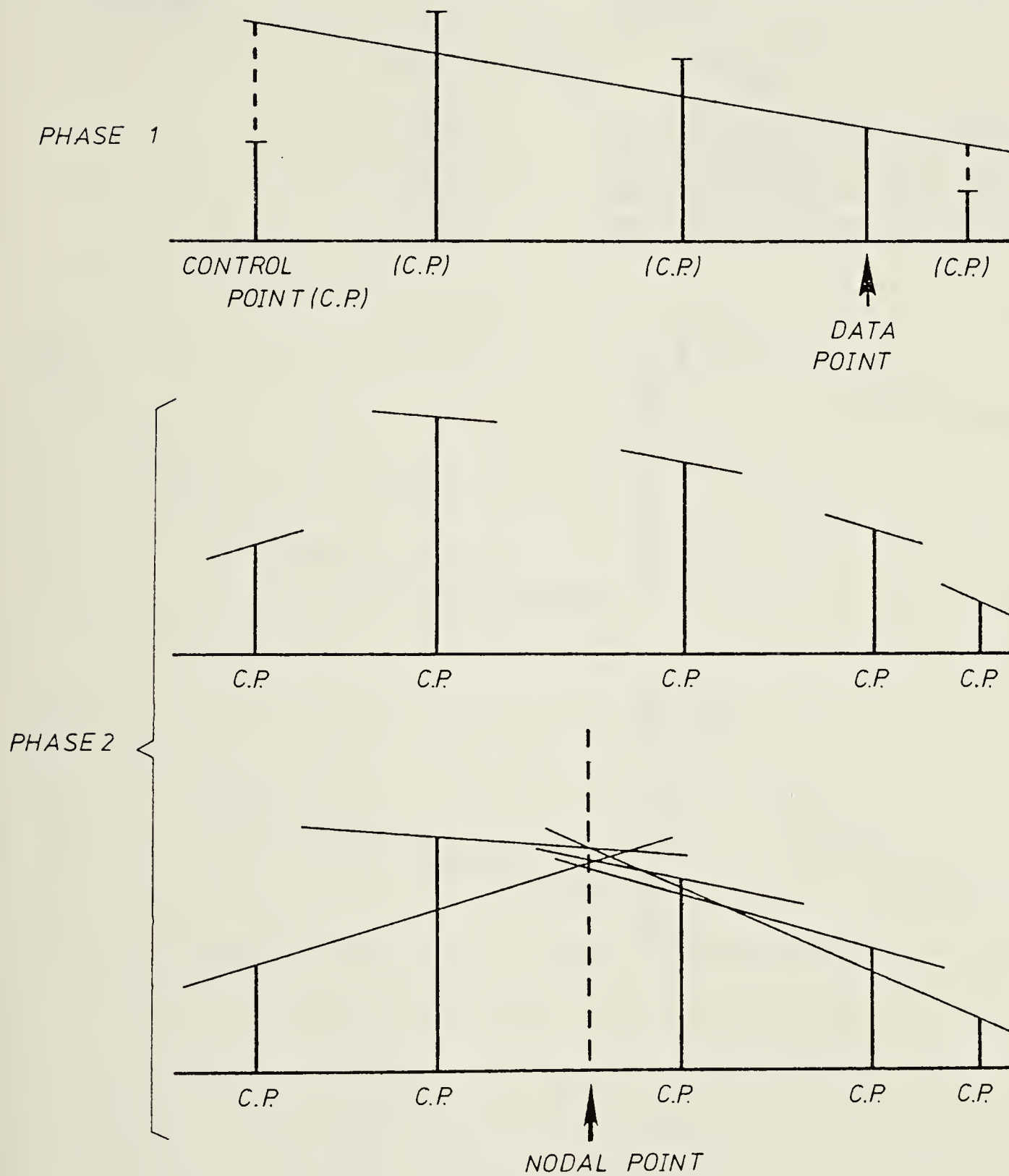


Figure 6.1 Slope projection procedure (after Sampson, 1978)

option	function	
0	$\omega = (1 - \frac{D}{1.1 \times D_{\max}})^2 / (\frac{D}{1.1 \times D_{\max}})^2$	
1	$\omega = 1/D$	ω is the weight attached to a sample data point a distance D from the grid intersection being estimated. D_{\max} is the distance from the grid intersection to the most distant sample point in the set being used in the estimation.
2	$\omega = 1/D^2$	
3	$\omega = 1/D^4$	
4	$\omega = 1/D^6$	

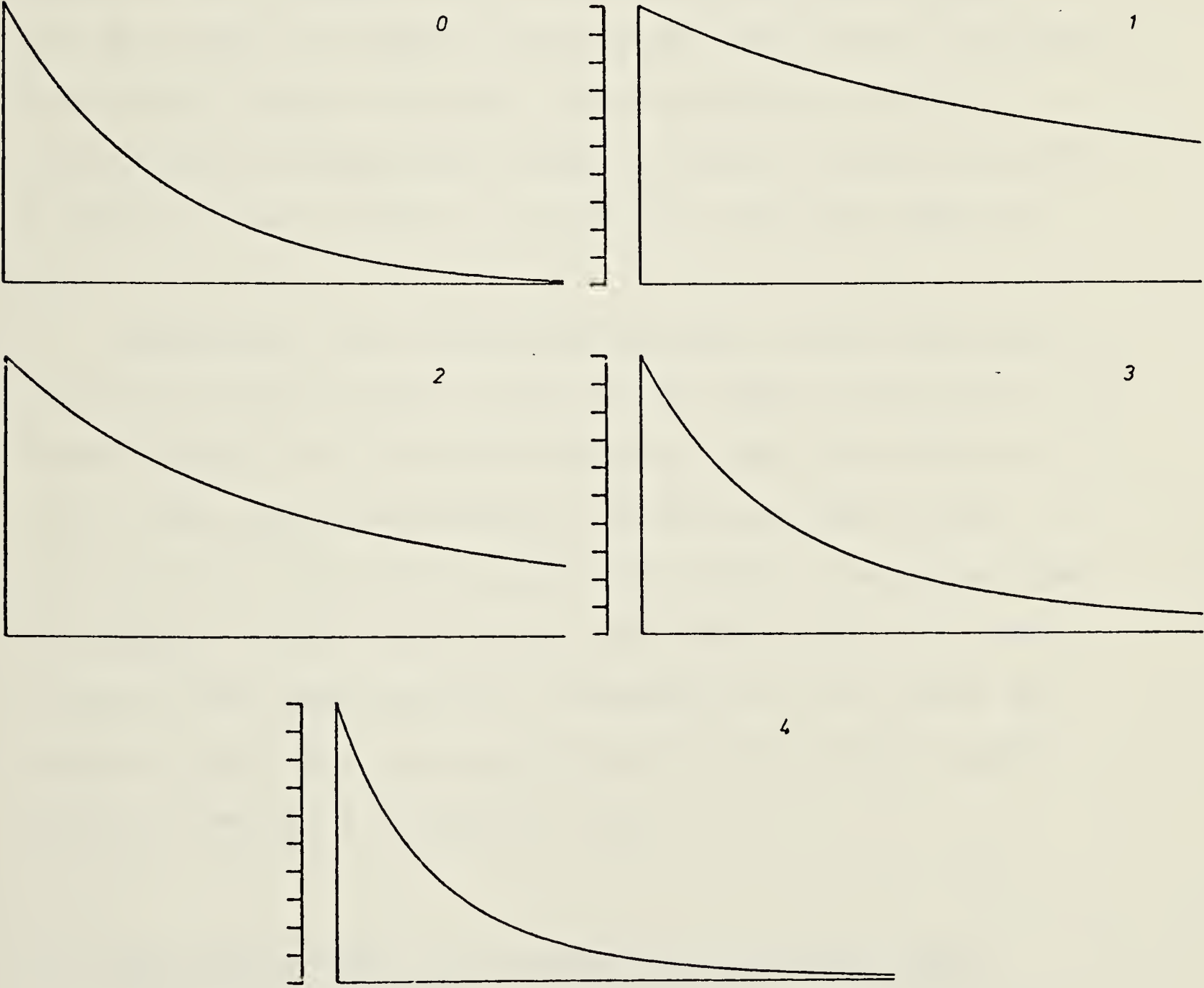


Figure 6.2 Distance weighting functions (after Sampson, 1978)

used in this study.

The procedure described above results in a rectangular mesh covering the area under study with an estimate of displacement at each of the grid nodes. An essential step, (before constructing the contour lines), is to define the area representing the tunnel through which no contour lines should be drawn. A special statement is used for this purpose which assign a very small value to displacement at the grid nodes enclosed in that area. The contour lines are then drawn through the grid. This is done by linearly interpolating between grid nodes to locate the points where a contour line of specific value will cross the edge of a grid.

Admittedly, the estimation procedure described above results in questionable values at the edges of the area under study. This limitation, however, was controlled in this investigation by placing the critical area of the contour map (tunnel face and tunnel center line) away from the edges. Grids of different sizes were tried at an early stage of the investigation. The spacing of grid nodes was chosen to suit the spacing of data points, giving smooth contour lines at a reasonable cost.

6.3 THE DISPLACEMENT FIELD AROUND AN ADVANCING TUNNEL

Although the displacements around an advancing tunnel develop in a three-dimensional mode, most tunneling studies simplify this as a two dimensional problem. This inevitably

masks some of the factors influencing the actual behavior of the soil. For example, the history of soil unloading and the mode of stress concentration around the tunnel differ considerably for two and three dimensional cases. In the two-dimensional model the unloading is carried out in one step in a plane perpendicular to the tunnel. The release of radial pressure is accompanied by a concurrent arching of tangential stresses. In a real tunnel, however, the unloading due to tunneling occurs gradually as a function of the tunnel advance and the soil pressure domes around the tunnel face first, then ultimately arches along the tunnel sides.

One way of illustrating the spatial characteristics of a tunneling problem is contour maps of in-situ displacements and strains. It should be realized, however, that these maps can show the variation of a function over a two-dimensional area only. Since the field of each of the displacement and strain components varies in three-dimensional space, several cross sections through each of these fields are required to investigate their spatial characteristics.

Three sections (A, B and C) were chosen for the present study as shown in Figure 6.3. Section A is a vertical section, perpendicular to the direction of tunnel advance taken at a distance of about 50 metres (20 diameters) behind the tunnel face. At that location all the soil movements due to tunneling were stabilized and had reached their ultimate value. Section B is a vertical longitudinal section through

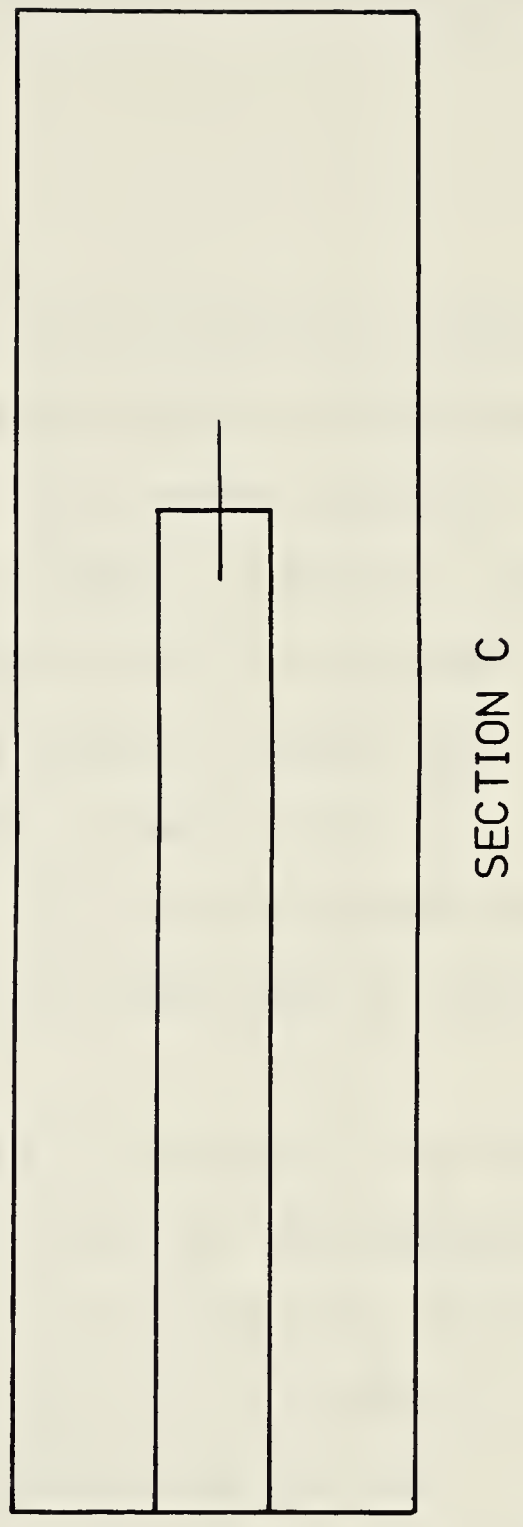
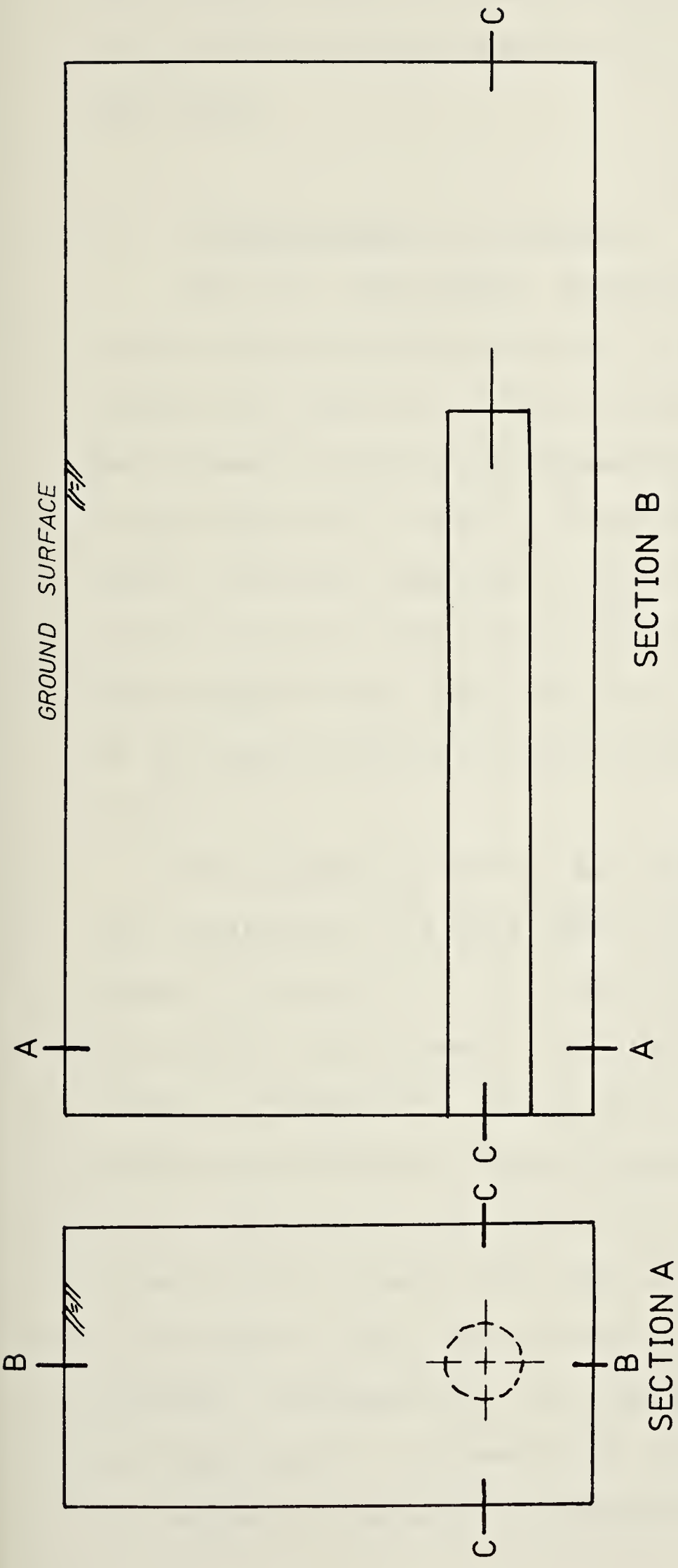


Figure 6.3 Sections chosen for the contour maps

the tunnel center line while Section C is a horizontal longitudinal section taken at the level of the springline of the tunnel.

6.3.1 Displacements at Section A

The soil instruments located at Test Section 3 provided extensive data of the vertical and horizontal displacements around the tunnel as a function of the tunnel advance. Measurements from ten extensometers (MX31 to MX310), three slope indicators (SI32 to SI34) and a set of settlement points from this test section were used to create the contour maps of final displacements at Section A. Measurements from slope indicator SI31 were excluded because of the unsatisfactory installation as described in section 4.2.4.

The boundaries of the map area of Section A, as well as the location of 172 data points of vertical displacement are shown in Figure 6.4. The location of the 342 data points of horizontal displacement over the map area of Section A are shown in Figure 6.5. Due to the limitations of the contouring method at the map edges, (mentioned in section 6.2), the area in the vicinity of the tunnel was intentionally placed near the centre of the map. Symmetry of displacement about the vertical axis of the tunnel was assumed. Consequently, the displacement components at every two data points of symmetrical location in Figure 6.4 and 6.5 actually represent a single measurement. Additional data

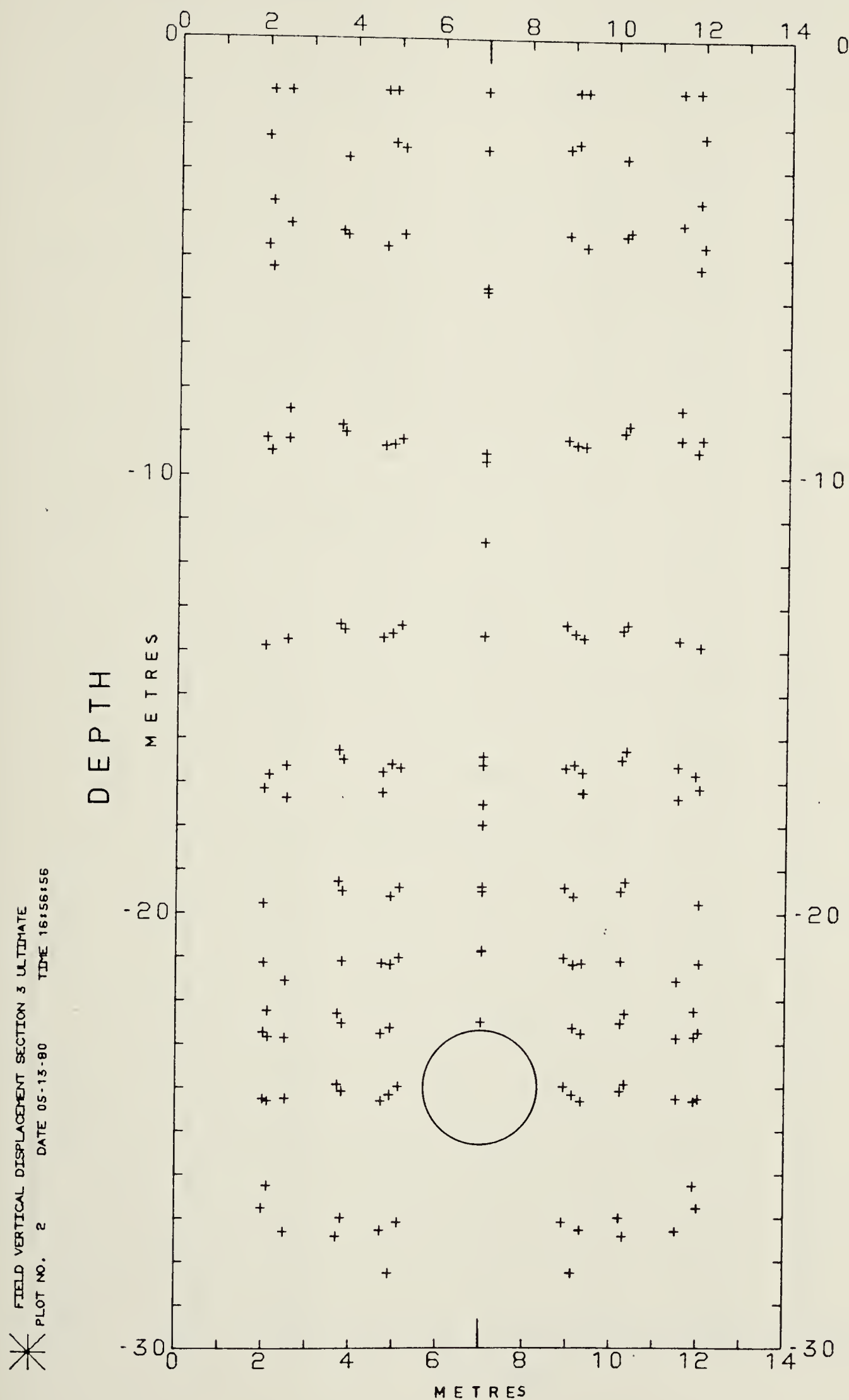


Figure 6.4 Location of data points of vertical displacement in Section A

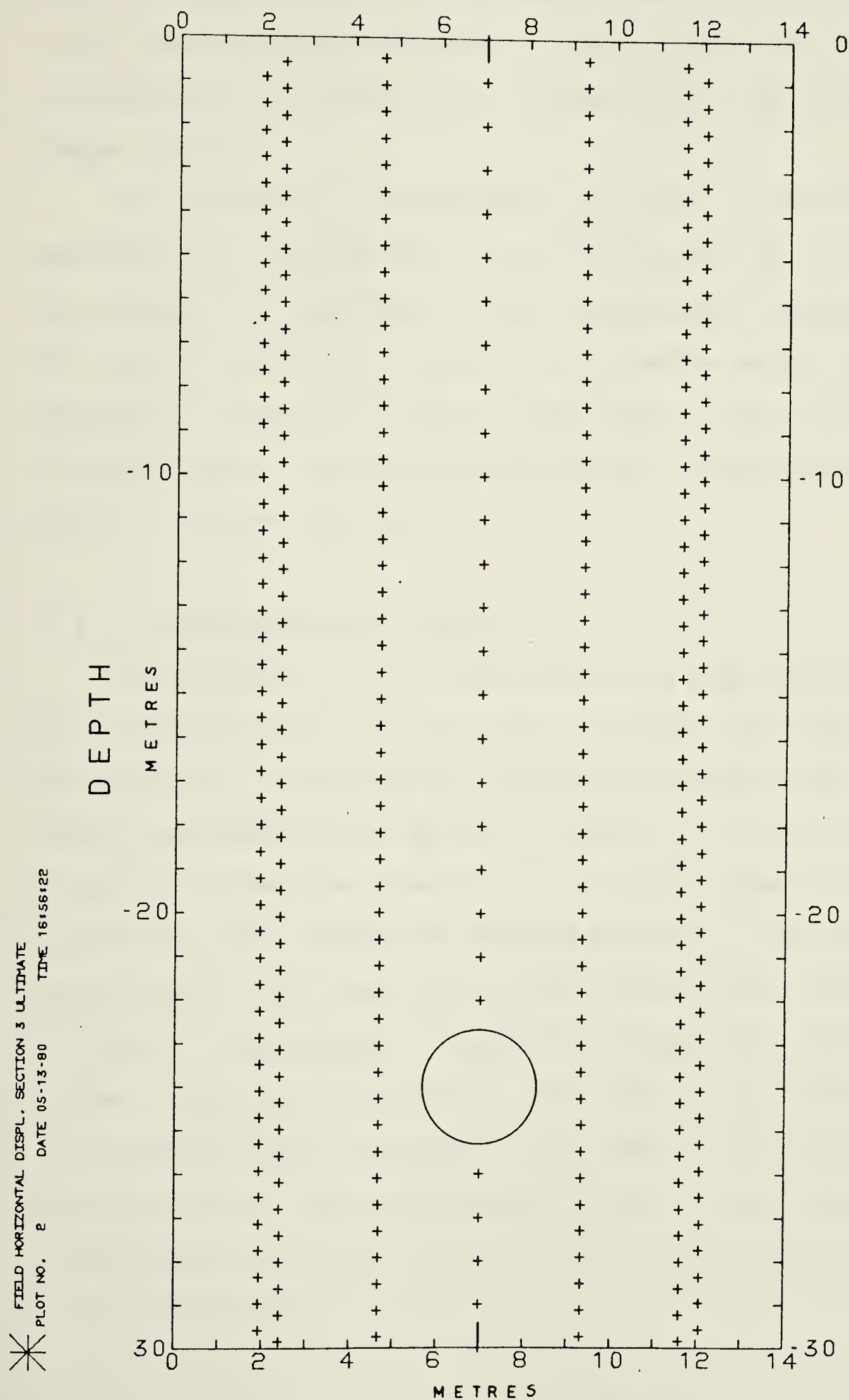


Figure 6.5 Location of data points of horizontal displacement in Section A

points, located directly above and below the tunnel center line, were assigned a horizontal displacement value of zero to implement the assumption of symmetrical displacement at these locations.

For Section A, a rectangular grid with a horizontal spacing of 0.5 metres and a vertical spacing of 0.25 metres was chosen. The magnitude of the displacement components at the nodal points of this grid was estimated using the SURFACE II Graphics System as described in section 6.2. The contour maps of vertical and horizontal displacements are given in Figure 6.6 and 6.7.

6.3.2 Displacements at Section B

Development of soil displacements along Section B can best be described using the data obtained from slope indicator SI21 and the multipoint extensometer MX22. Some of these measurements are given in Figures 4.19 and 4.26. Figure 6.8 shows the dimensions of the map area of Section B as well as the location of 86 data points of vertical displacement. The location of five hundred data points of horizontal displacement is given in Figure 6.9. Based on these irregularly spaced data, the value of the coordinate displacements was estimated at the nodes of a grid 2x2 metres square. The contour maps of vertical and horizontal displacements for this section are given in Figure 6.10 and 6.11 respectively.

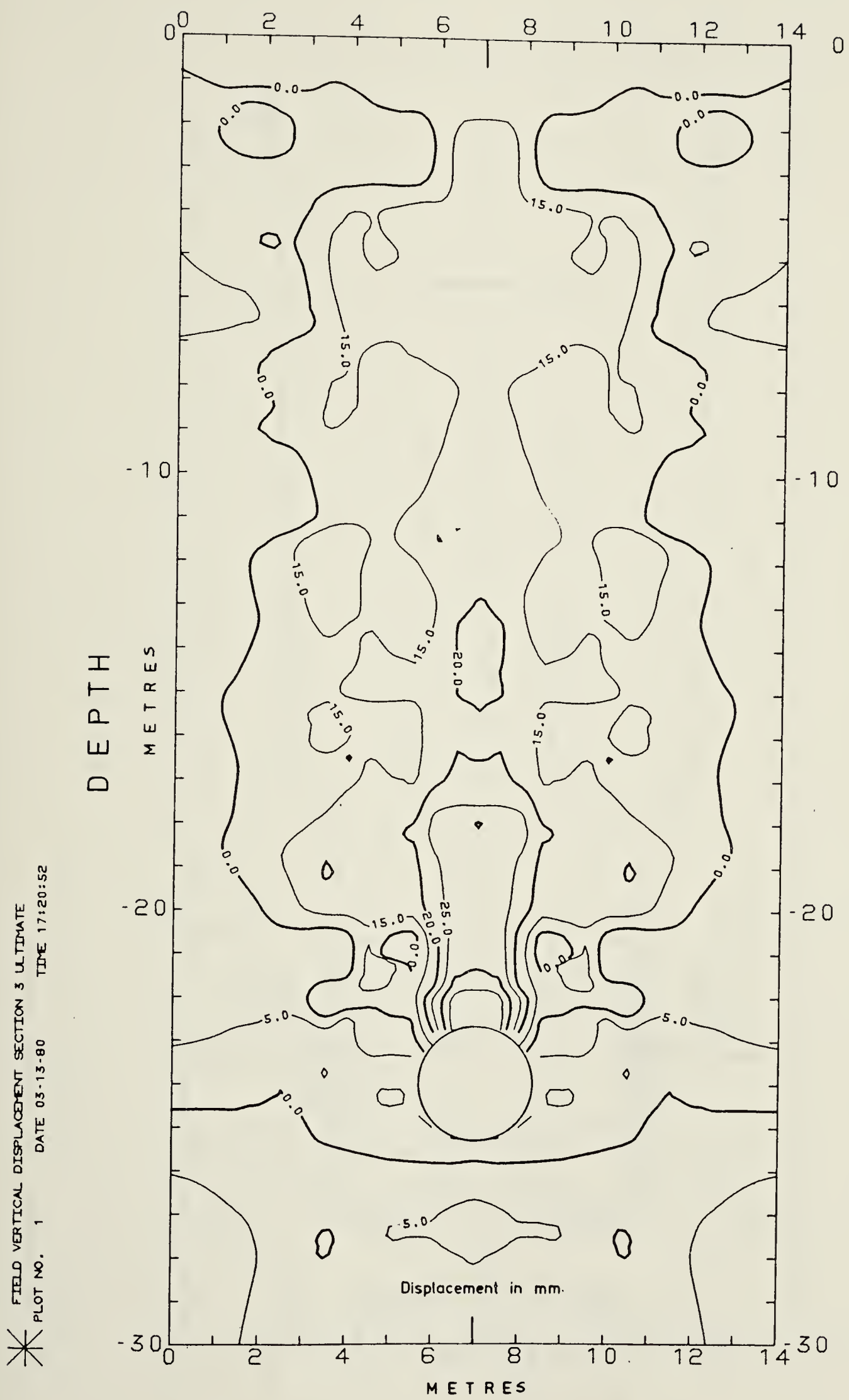


Figure 6.6 Contour map of vertical displacement (Section A)

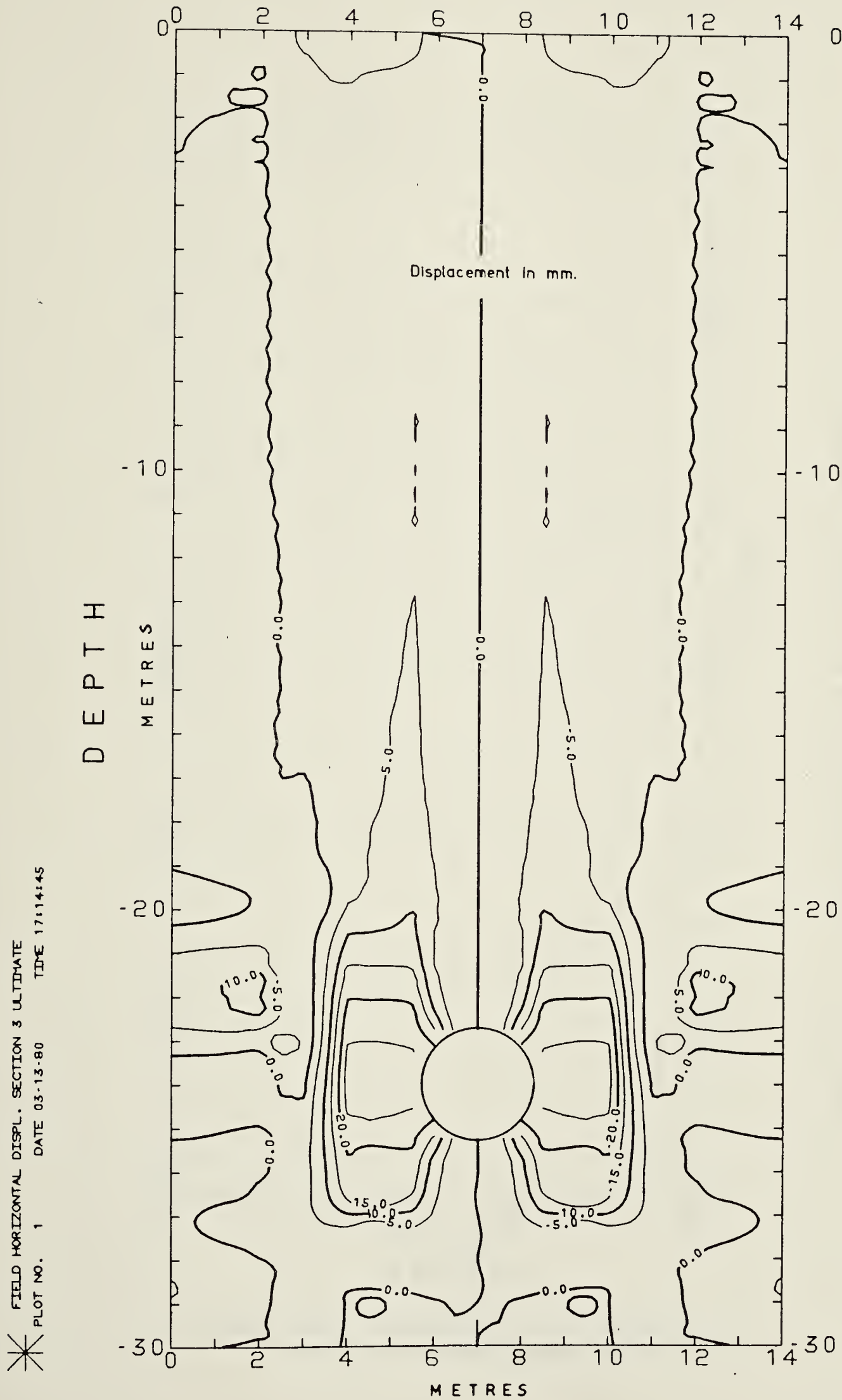


Figure 6.7 Contour map of horizontal displacement (Section A)

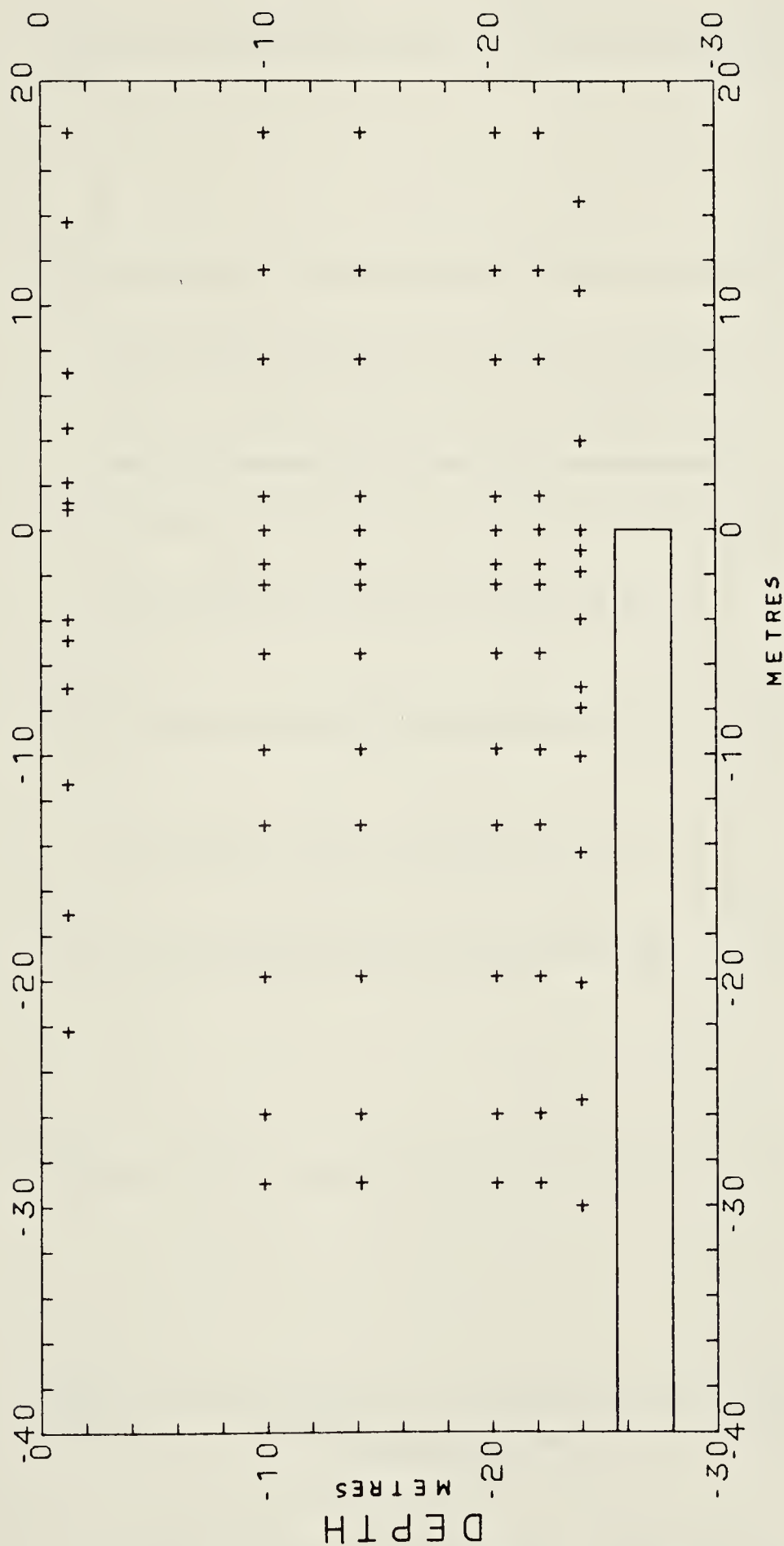


Figure 6.8 Location of data points of vertical displacement in Section B

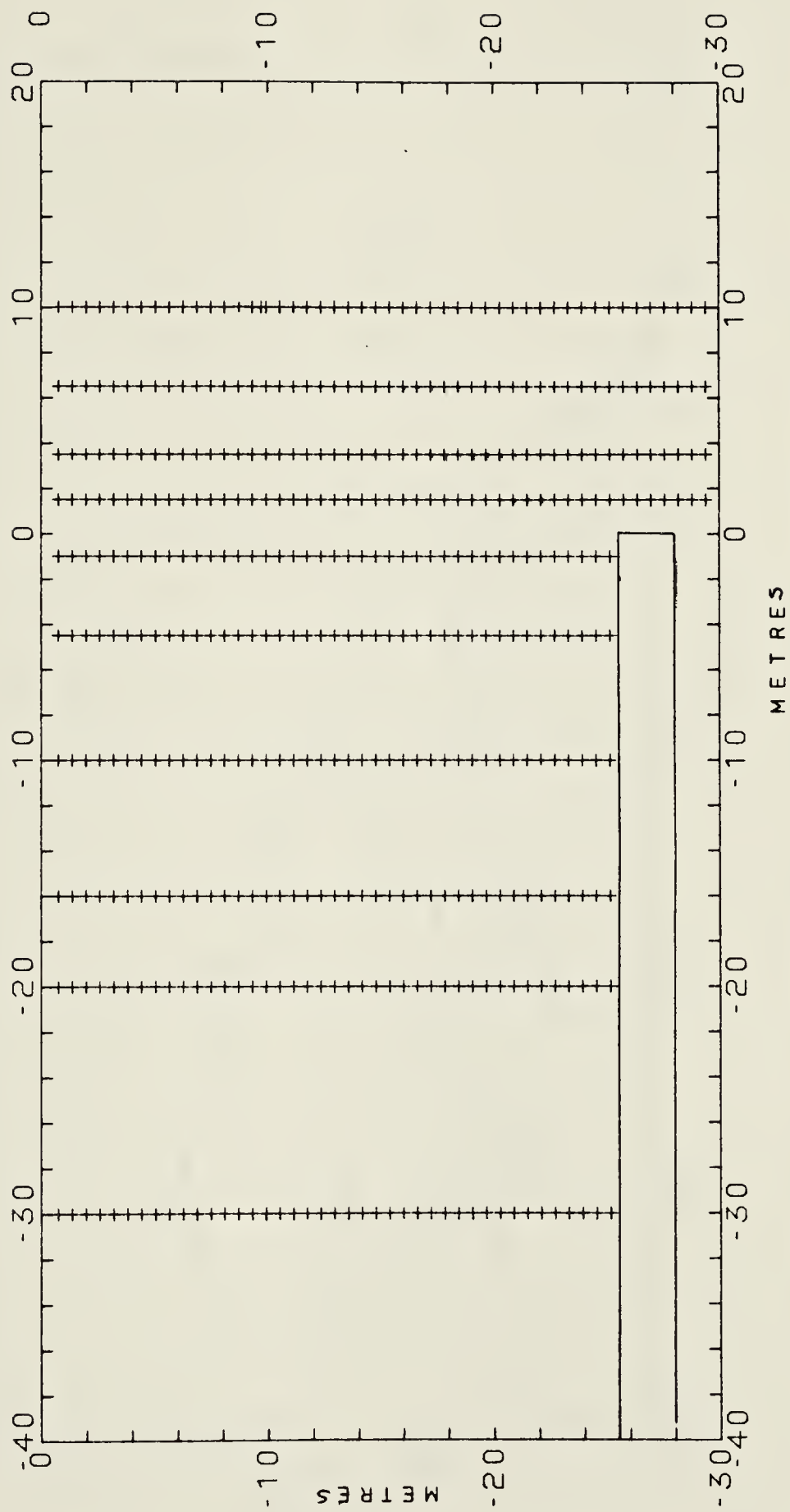


Figure 6.9 Location of data points of horizontal displacement in Section B

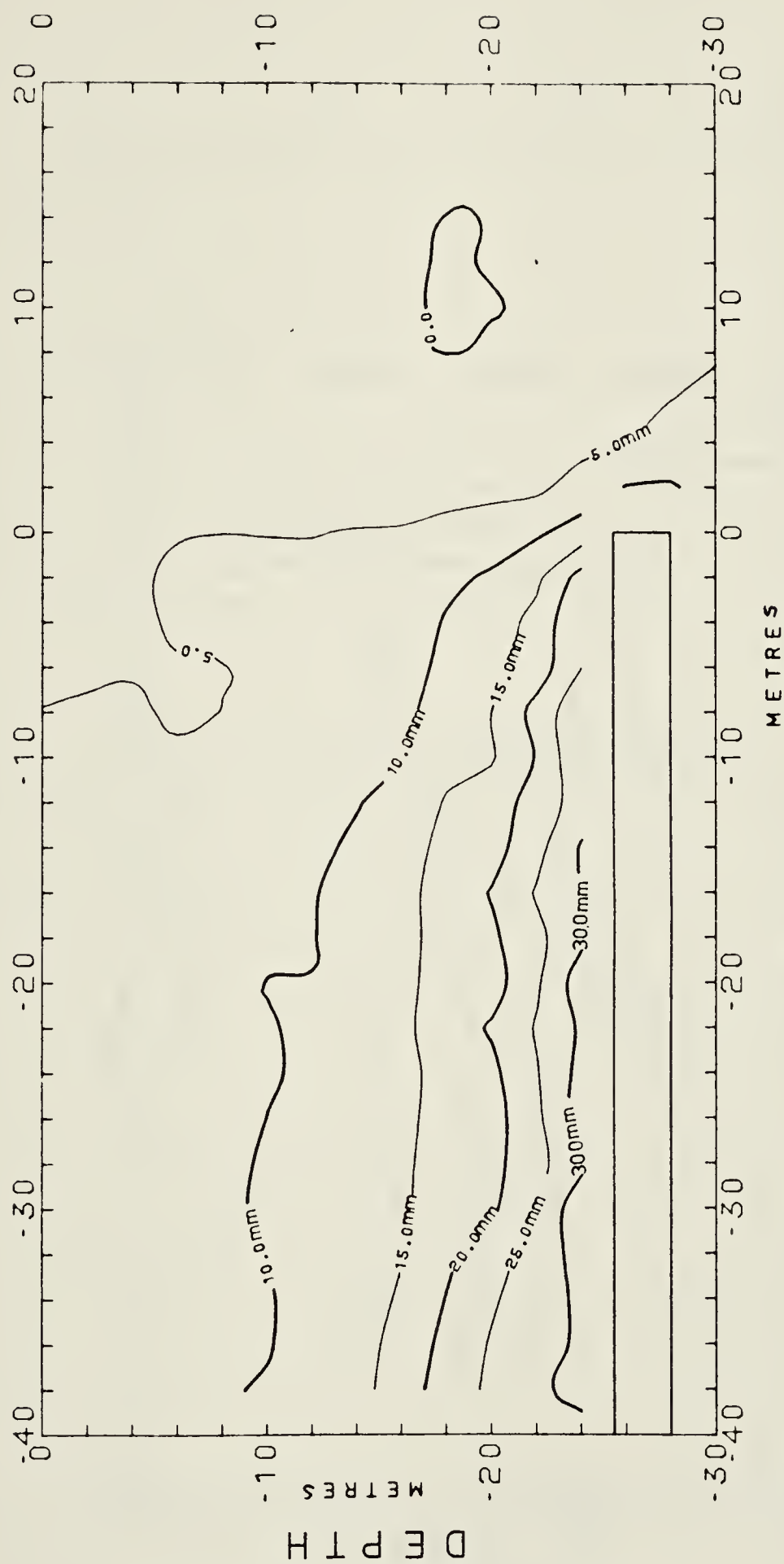
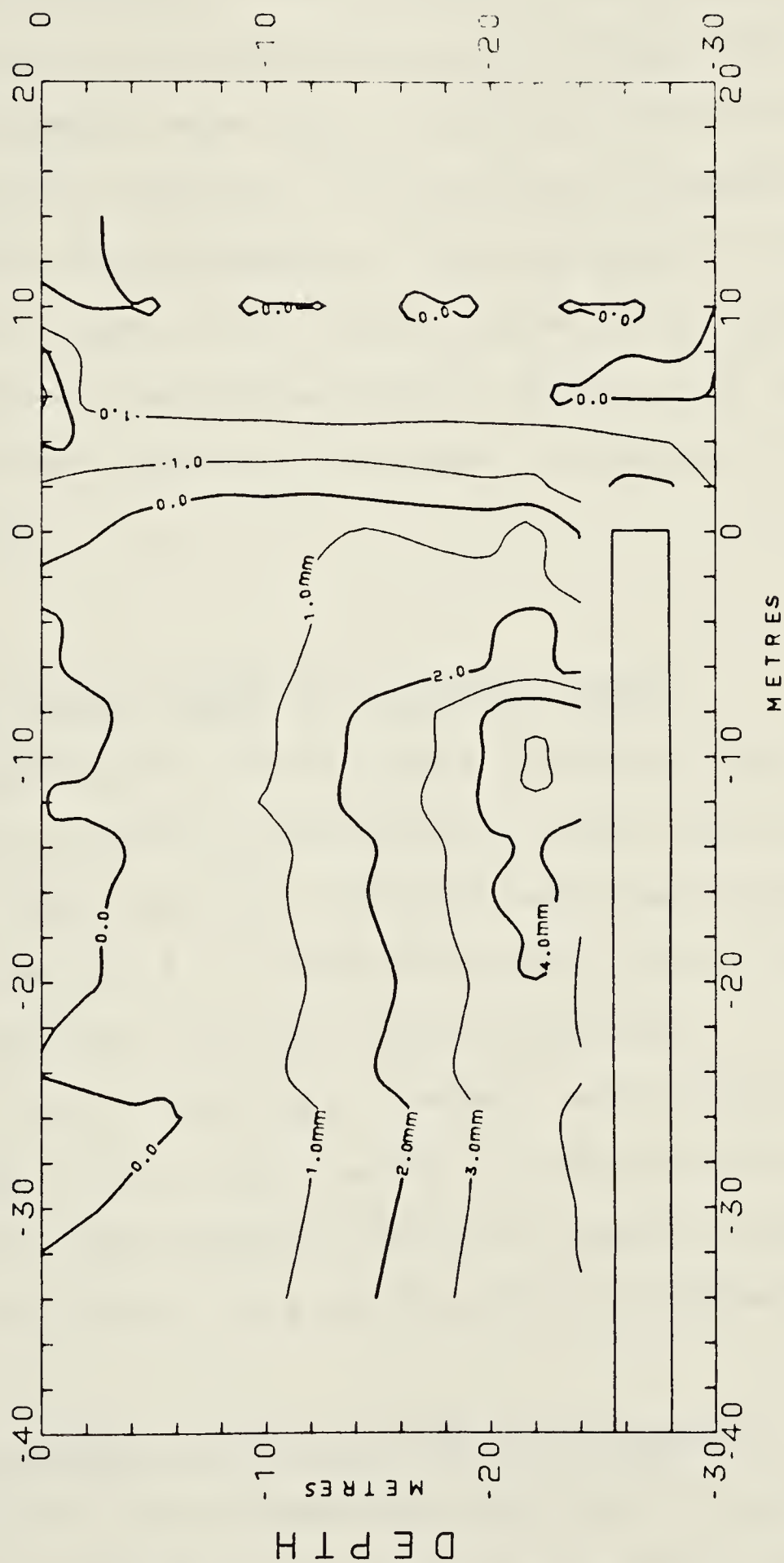


Figure 6.10 Contour map of vertical displacement
(Section B)



IN-SITU HORIZONTAL DISPLACEMENT (SECTION 2)
 PLOT NO. 1
 DATE 05-15-80
 TIME 11:08:53

Figure 6.11 Contour map of horizontal displacement
 (Section B)

6.3.3 Displacements at Section C

Lateral and longitudinal horizontal displacements at the springline level in the vicinity of the tunnel were monitored using slope indicators at the three test sections. These measurements were used to construct the displacement contour maps for Section C. The location of eighty data points within the boundaries of the map area of this section are shown in Figure 6.12. The grid used has a spacing 0.5x0.5 metres. The contour maps of lateral and longitudinal displacement of Section C are shown in Figures 6.13 and 6.14 respectively.

6.4 STRAIN FIELDS AROUND AN ADVANCING TUNNEL

The description of the general trends of soil displacement around the experimental tunnel and the main factors influencing their characteristics were discussed in detail in section 4.4. The contour maps given in the previous section illustrate these trends and characteristics. These maps, however, were specifically produced as a first step towards an investigation of the strain fields and the mobilization of shear strength in the vicinity of a tunnel in a stiff overconsolidated soil.

6.4.1 Calculation of Strains from Displacements

In a full three-dimensional continuum, the displacement and strain fields are fully described by three displacement components and six strain components. These are reduced to

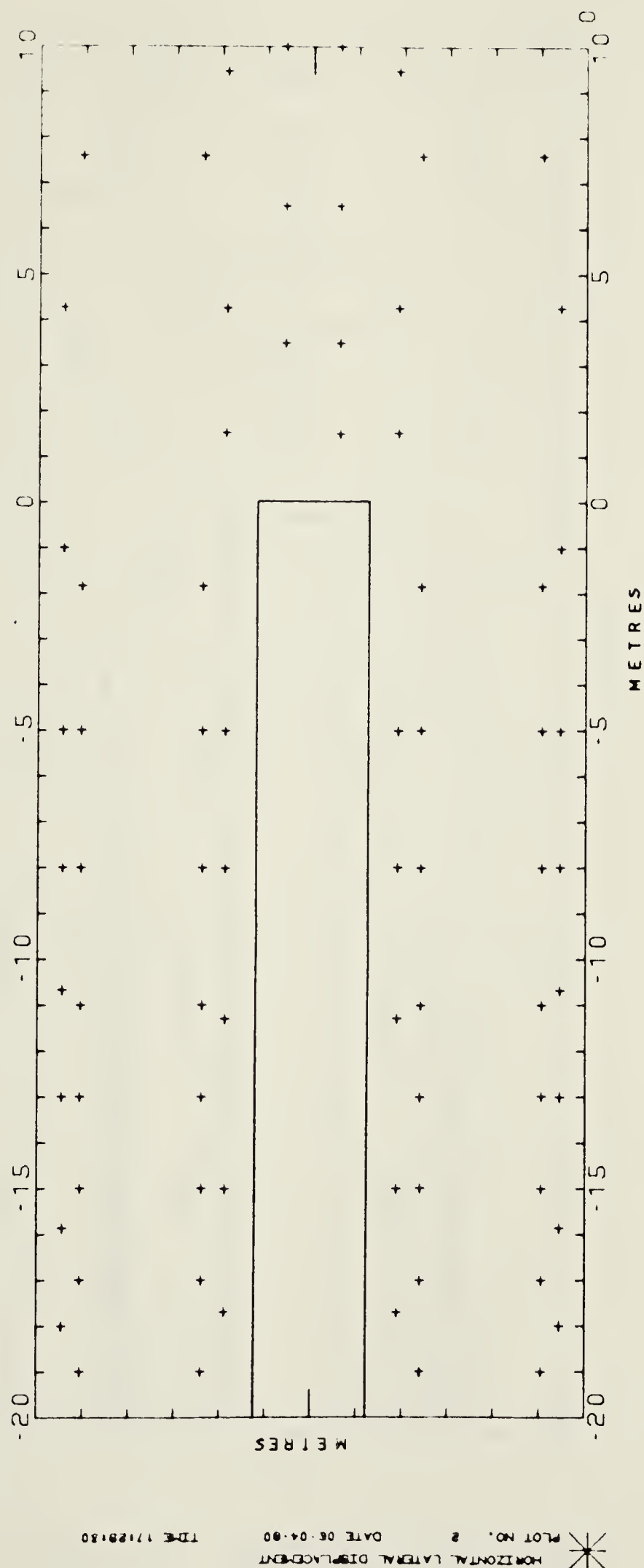


Figure 6.12 Location of data points of lateral and longitudinal displacements in Section C

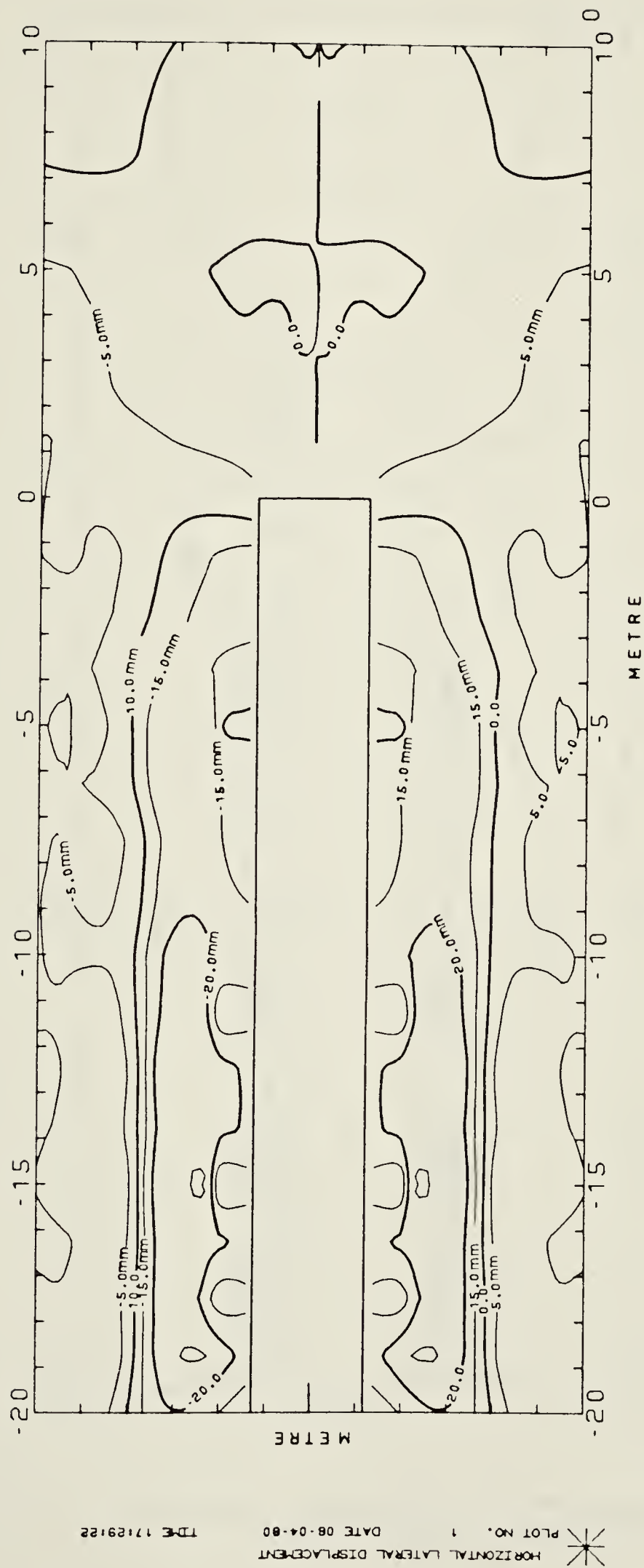


Figure 6.13 Contour map of lateral displacement (Section C)

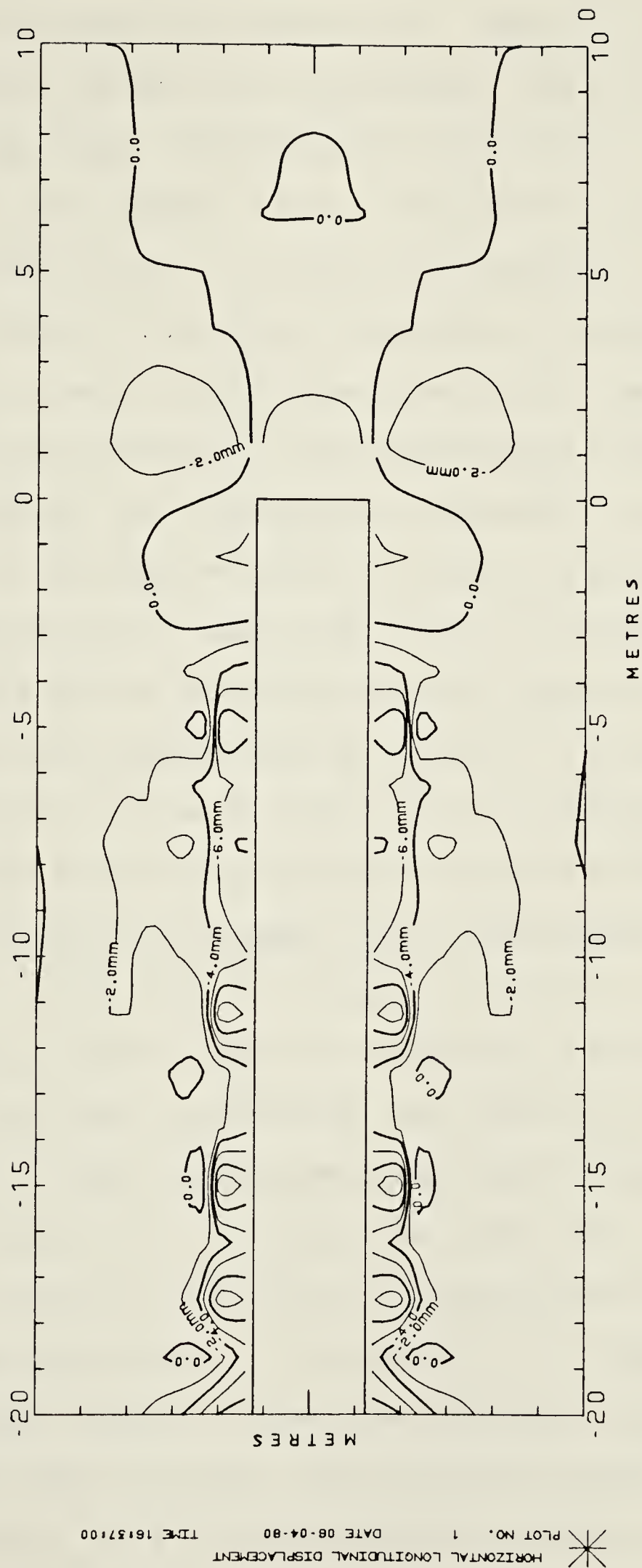


Figure 6.14 Contour map of longitudinal displacement
(Section C)

two components of displacement and three components of strain in the case of plane strain. Table 6.1 contains the relationships between the displacement and strain components in these two cases. To calculate the strains associated with a specific displacement field, the operation of determining the first derivative, or simply the gradient, is required.

The SURFACE II system is capable of simple calculation operations as well as the determination of the gradient of a surface in any direction. The displacement matrix (which contains one of the displacement components at the nodal points of a rectangular grid) is used to calculate a new matrix containing an approximation of the first derivative at the nodal points of the same grid. Figure 6.15 illustrates the method used by SURFACE II to approximate the first derivative at each node. First, two imaginary lines are extended from the grid node in opposite directions. The length of each line is equal to $1/4$ the diagonal length of a grid cell. Values for the surface at points 1 and 2 are estimated by double linear interpolation from the grid values in the cells containing the imaginary lines. The derivative is then calculated according to the equation given in Figure 6.15. It should be noted that this procedure does not allow the calculation of the derivatives for the outer rows and columns of the grid nor for those adjacent to blanked areas. Based on these derivatives, which represent normal and shear strains, the principal strains and their orientation as well as the volumetric strain and maximum

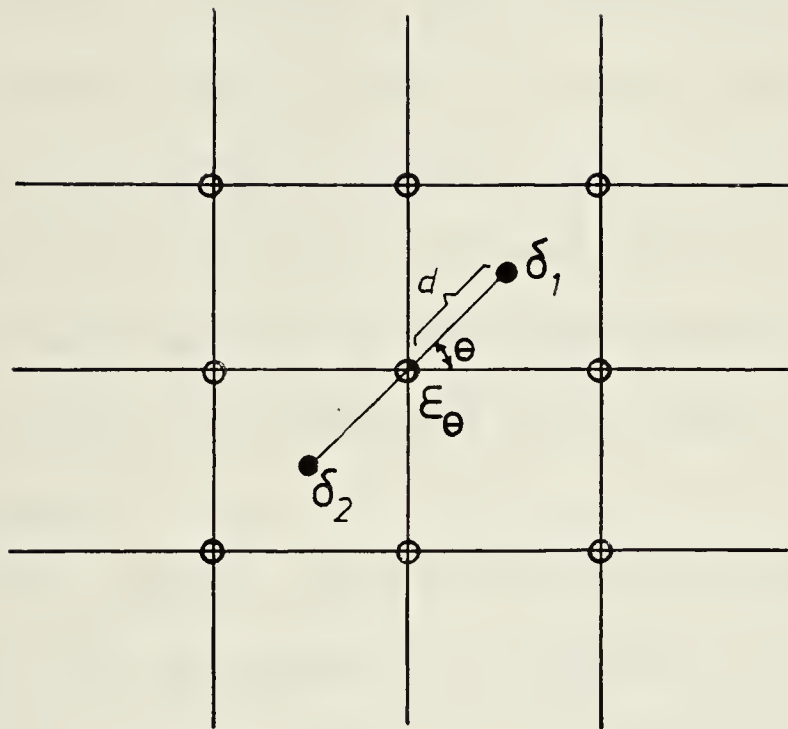
Table 6.1 Strain-Displacement relationship

a) THREE DIMENSIONAL CONTINUUM

$$\left\{ \epsilon \right\} = \left\{ \begin{matrix} \epsilon_x \\ \epsilon_y \\ \epsilon_z \\ \epsilon_{xy} \\ \epsilon_{yz} \\ \epsilon_{zx} \end{matrix} \right\} = \left\{ \begin{matrix} \frac{\partial u}{\partial x} \\ \frac{\partial v}{\partial y} \\ \frac{\partial w}{\partial z} \\ \frac{\partial u}{\partial y} + \frac{\partial v}{\partial x} \\ \frac{\partial v}{\partial z} + \frac{\partial w}{\partial y} \\ \frac{\partial w}{\partial x} + \frac{\partial u}{\partial z} \end{matrix} \right\}$$

b) TWO DIMENSIONAL CONTINUUM

$$\left\{ \epsilon \right\} = \left\{ \begin{matrix} \epsilon_x \\ \epsilon_y \\ \epsilon_{xy} \end{matrix} \right\} = \left\{ \begin{matrix} \frac{\partial u}{\partial x} \\ \frac{\partial v}{\partial y} \\ \frac{\partial u}{\partial y} + \frac{\partial v}{\partial x} \end{matrix} \right\}$$



○ NODAL POINT

● DATA POINT

$$\epsilon_\theta = (\delta_1 - \delta_2) / 2d$$

Figure 6.15 First derivative at a nodal point using SURFACE II

shear strain are calculated. Figure 6.16 summarizes the procedure for a plane strain condition.

6.4.2 Strains at Section A

As defined previously, Section A is a vertical lateral section at a distance about 50 metres (20 diameters) behind the tunnel face. At that location, the in-situ soil displacements have reached their final values. Thus, the longitudinal strains (perpendicular to this section) were almost zero which is the condition of plane strain. Accordingly, the procedure outlined in Figure 6.16 was followed.

The contour maps of the major and minor principal strains are presented in Figures 6.17 and 6.18 and the strain rosette plot is given in Figure 6.19. These figures show that most of the strains actually occurred within 1 diameter (2.5 meters) of the tunnel wall. There was a significant rotation of principal strains from the directions of the original in-situ stresses, particularly at points located around radial lines inclined at 45 degrees above and below the horizontal. The major principal strains vary between -0.69 and 2.99%, and the minor principal strains, between -2.46 and 1.85%.

The contour map of volumetric strains, shown in Figure 6.20, indicates that a column of soil extending above and below the tunnel has experienced a decrease in volume, whereas the soil elsewhere showed an increase in volume.

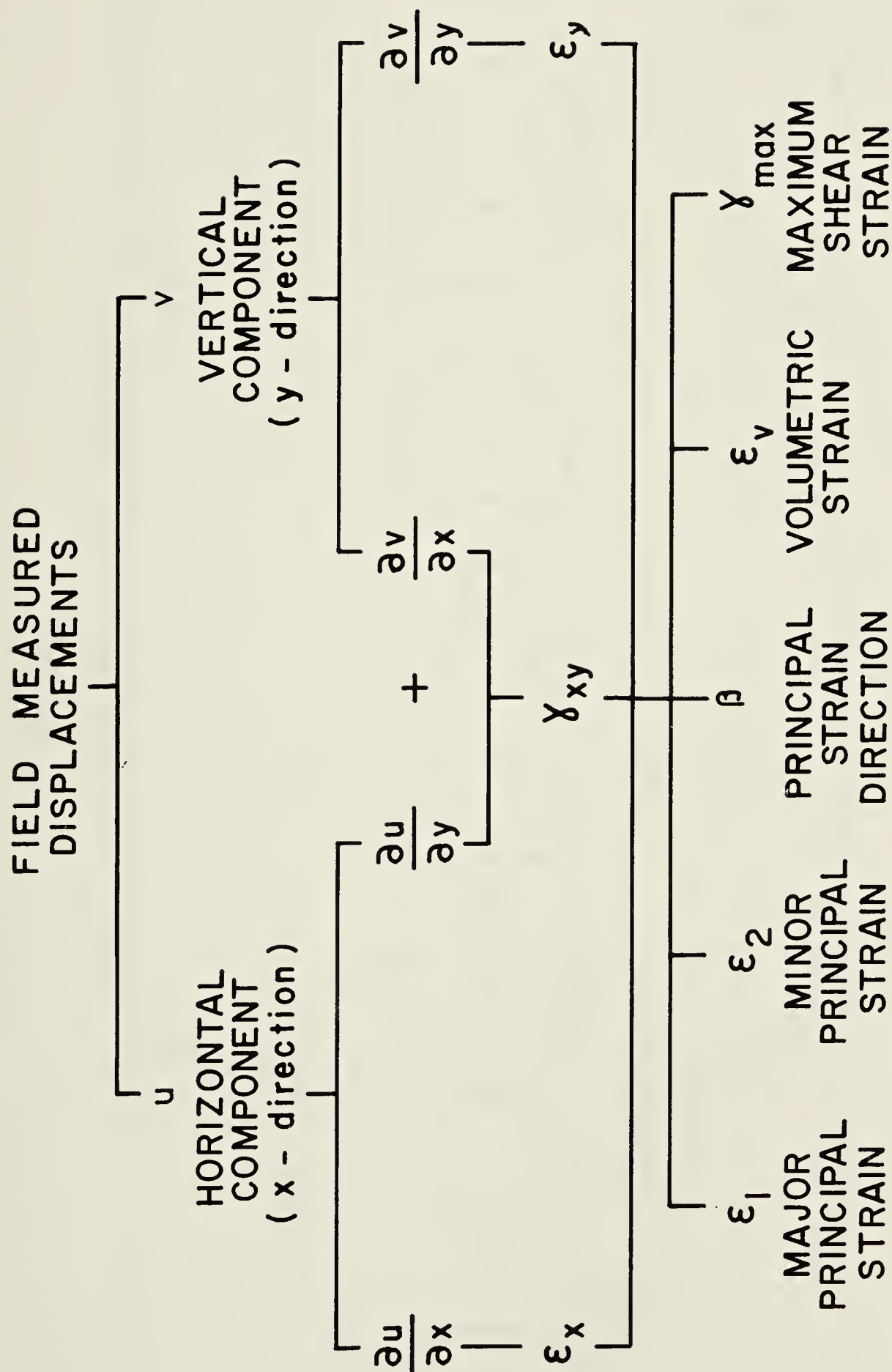


Figure 6.16 Flow chart of calculation of strains from displacements

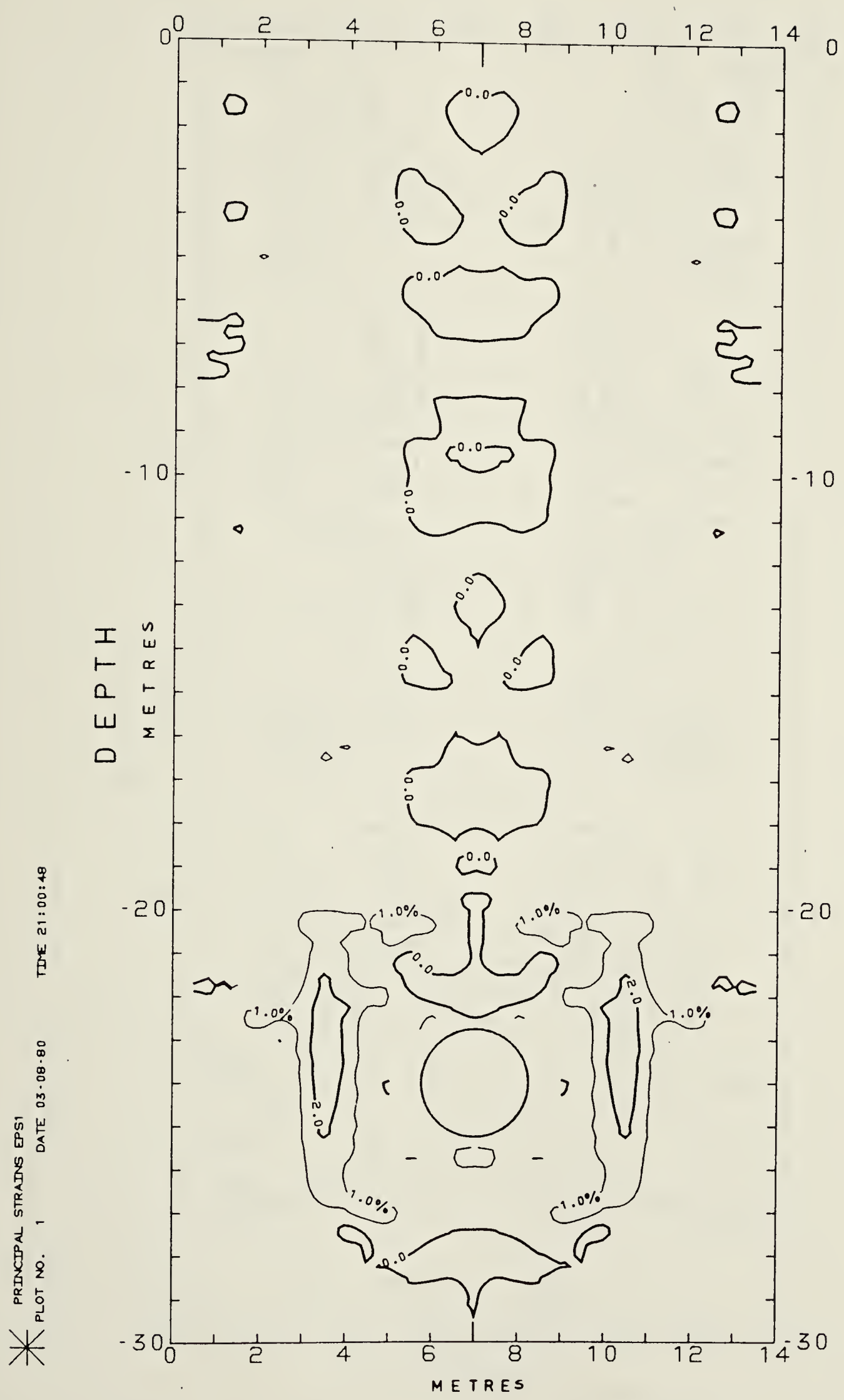


Figure 6.17 Contour map of major principal strains (Section A)

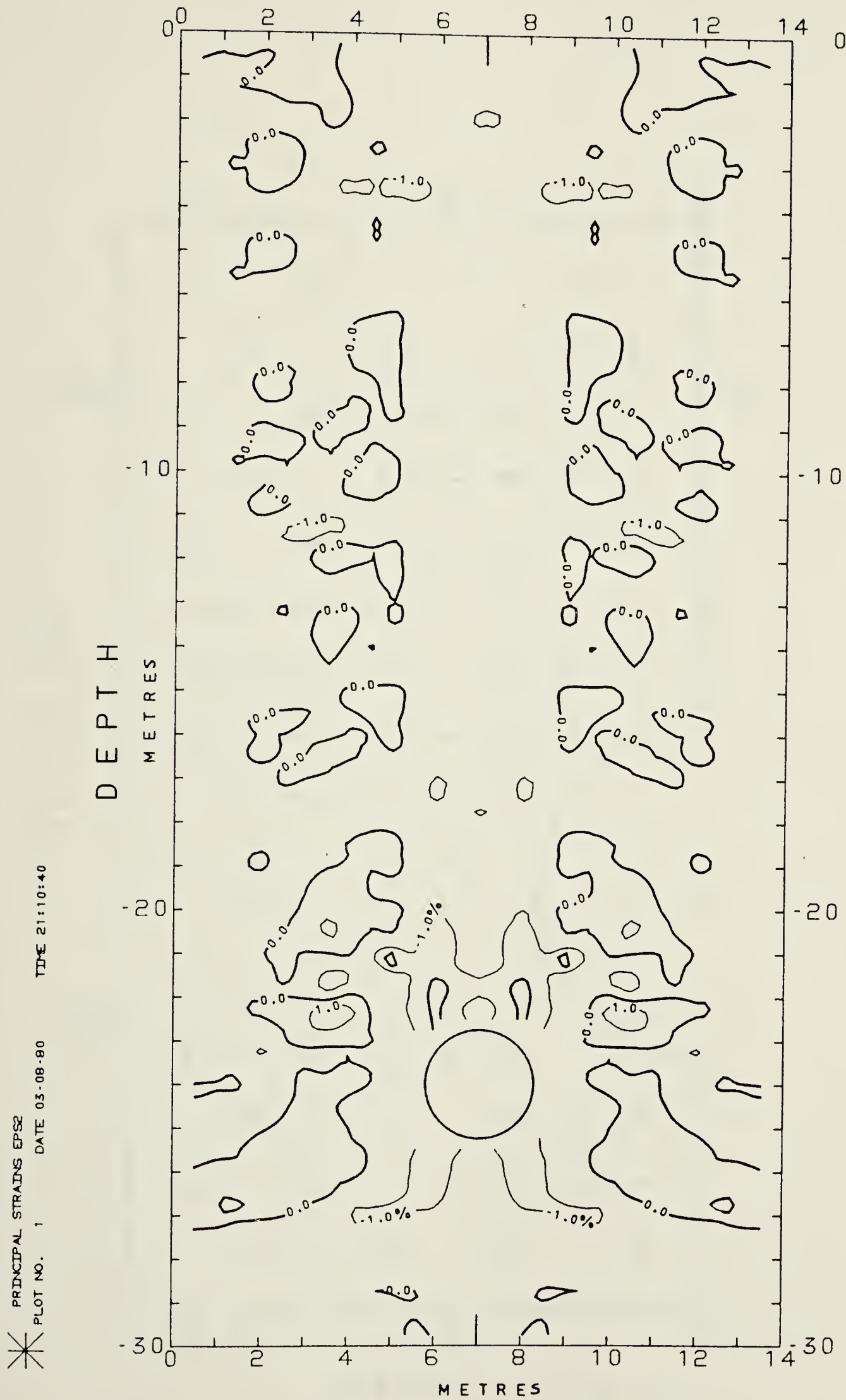


Figure 6.18 Contour map of minor principal strains

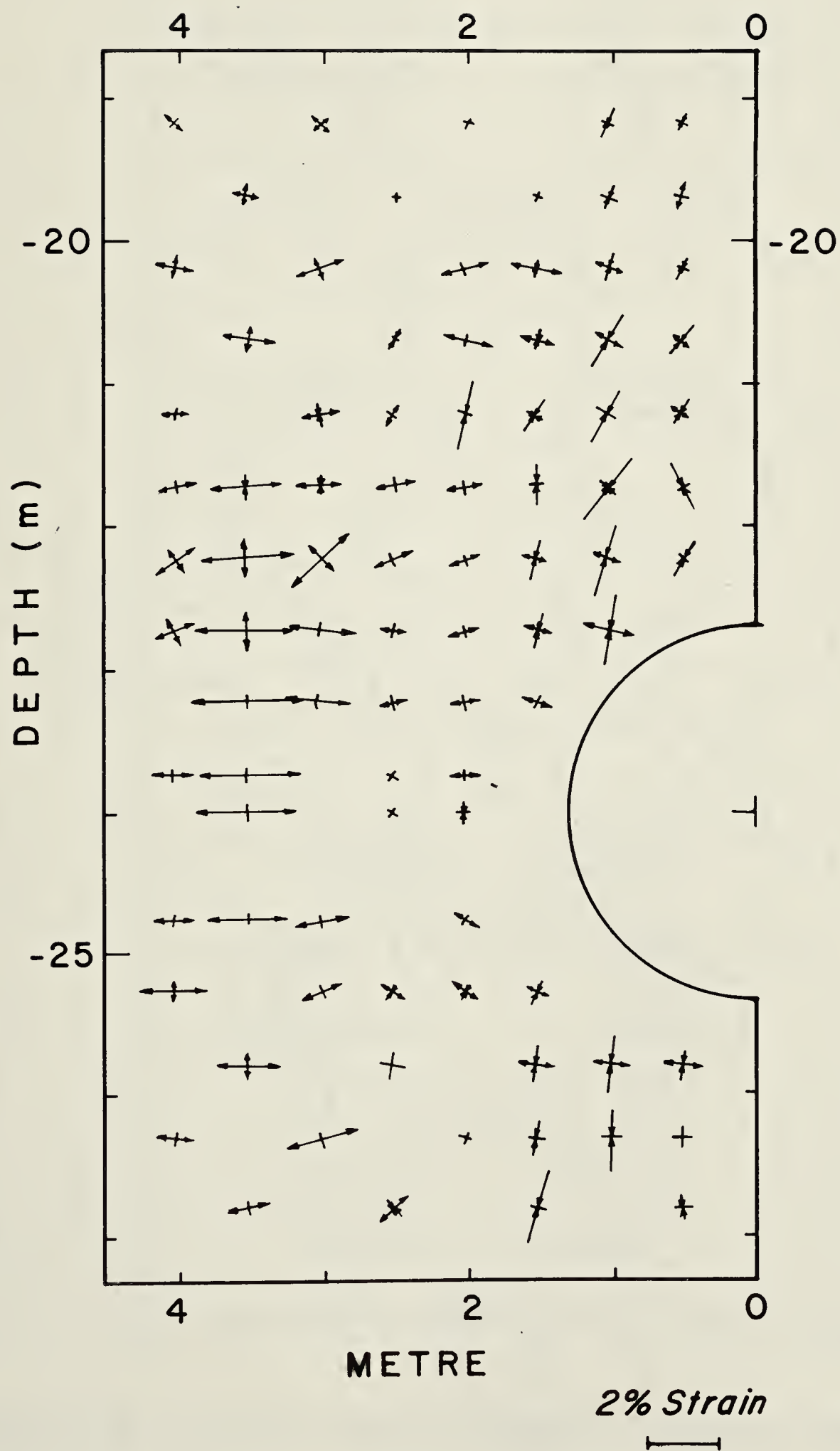


Figure 6.19 Strain rosette plot (Section A)

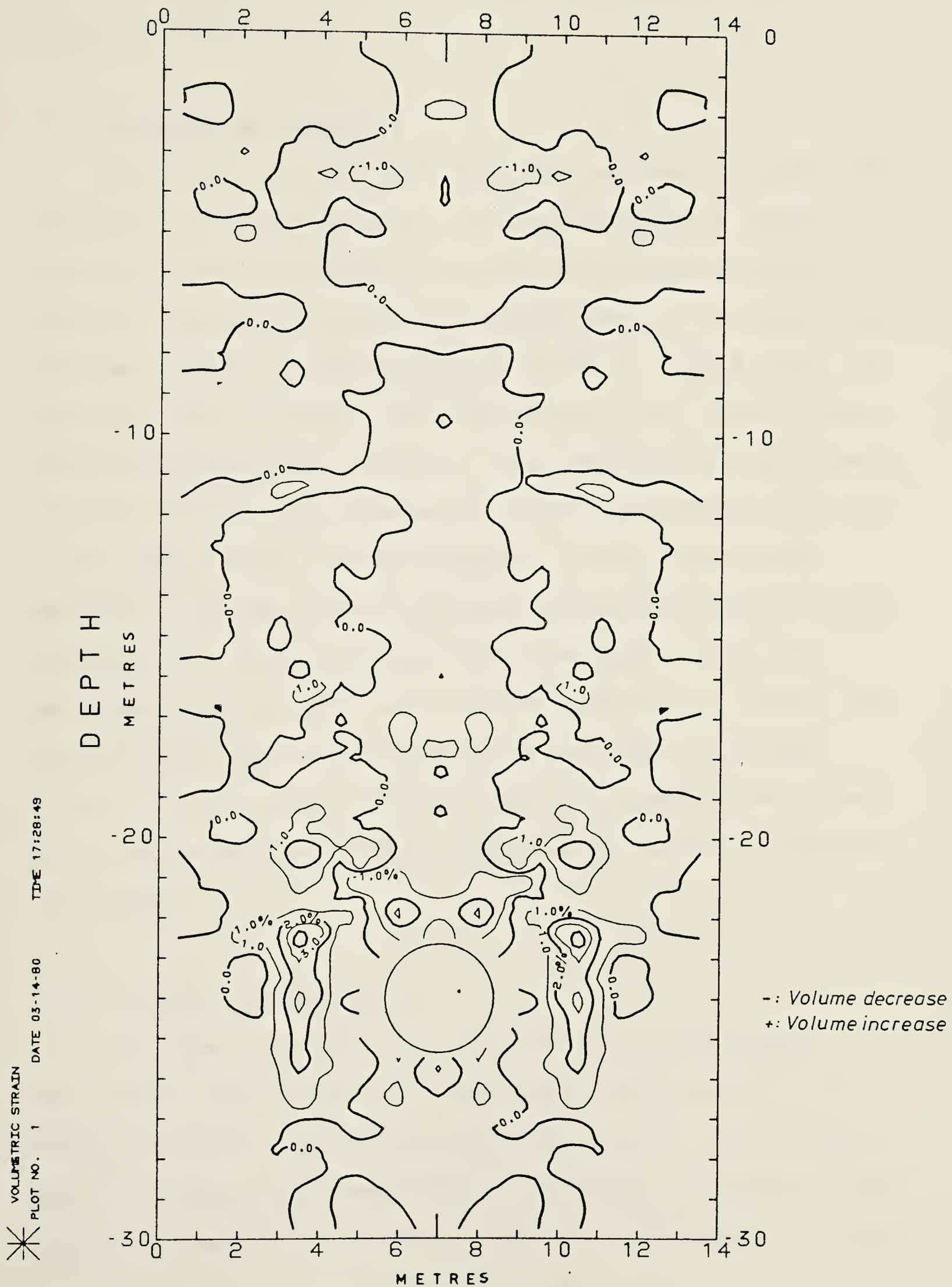


Figure 6.20 Contour map of volumetric strains (Section A)

This volume increase was noticeably large at the areas adjacent to the tunnel.

6.4.3 Strains at Section B

Section B is a vertical longitudinal section along the direction of tunnel advance. The contour maps of normal strains in the longitudinal and vertical directions are given in Figures 6.21 and 6.22 respectively. The contour map of shear strains in this plane is given in Figure 6.23. In general, the strains in this section are much smaller than those calculated for Section A. The longitudinal and lateral strains varied within ranges of -0.07 to 0.06% and -0.37 to 0.04% respectively, while the shear strain values were between -0.22 and 0.05%. The longitudinal and shear strains reached their maximum values near the tunnel face, and decreased significantly with further advance of tunnel face. On the other hand, the vertical strains were initiated within 10 to 12 metres (4 to 5 diameters) behind the tunnel face, and were only slightly affected by further advance of the tunnel.

6.4.4 Strains at Section C

As shown in Figure 6.3, Section C is a horizontal section at the springline extending in the direction of tunnel advance. Figures 6.24 and 6.25 contain the contour maps of lateral and longitudinal horizontal strains at this level. The magnitude of the strain varies between -3.4 and

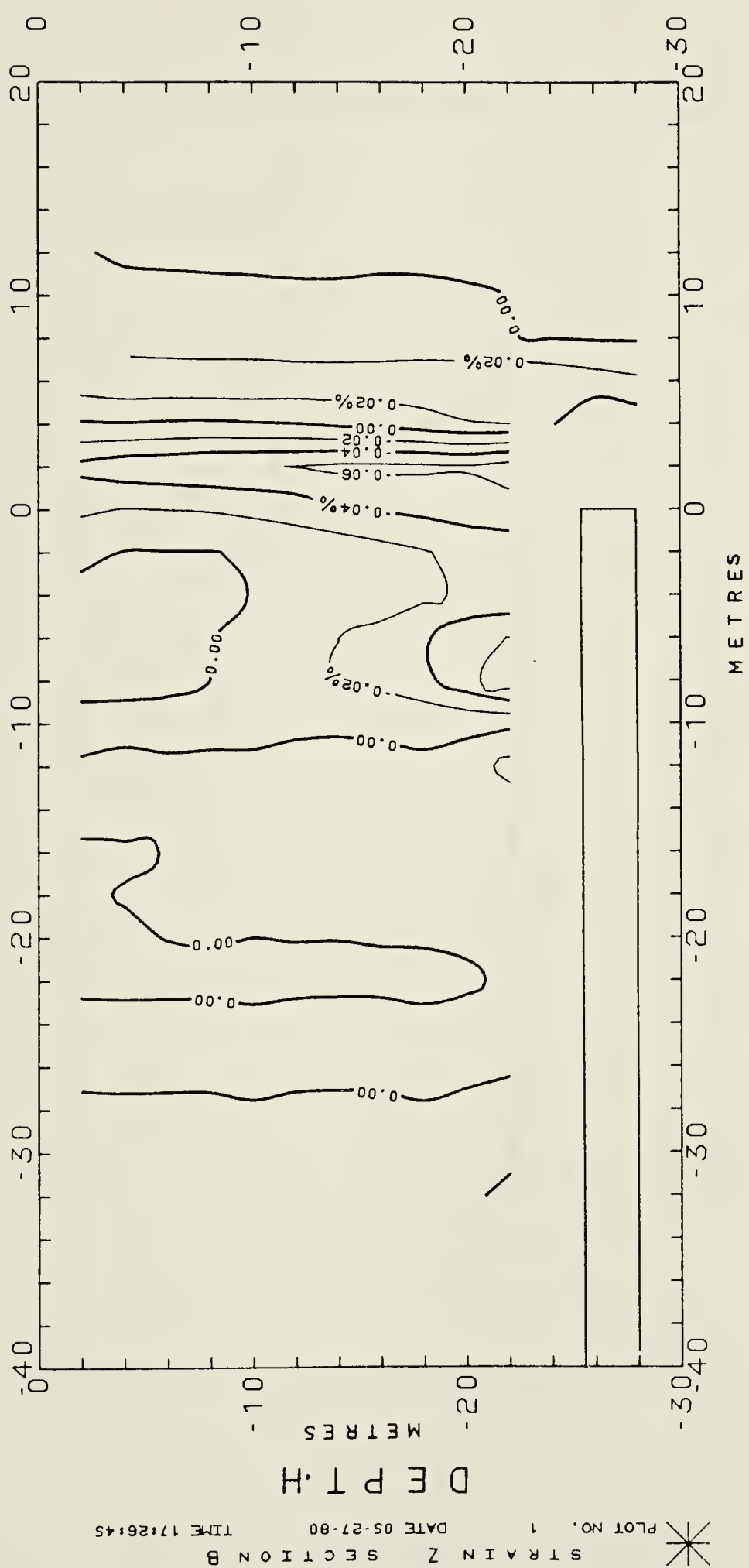


Figure 6.21 Contour map of longitudinal strains (Section B)

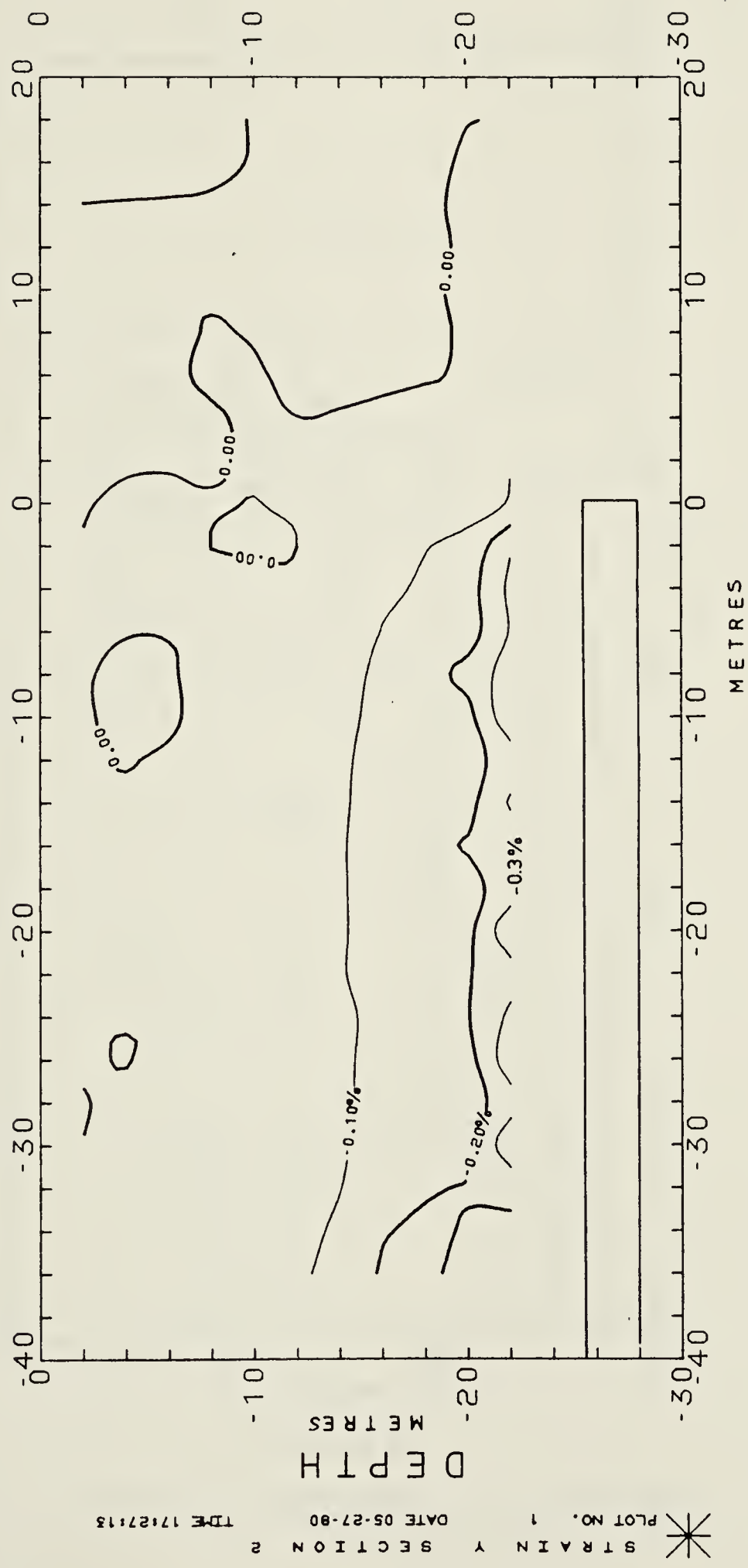


Figure 6.22 Contour map of vertical strains (Section B)



Figure 6.23 Contour map of shear strains (Section B)

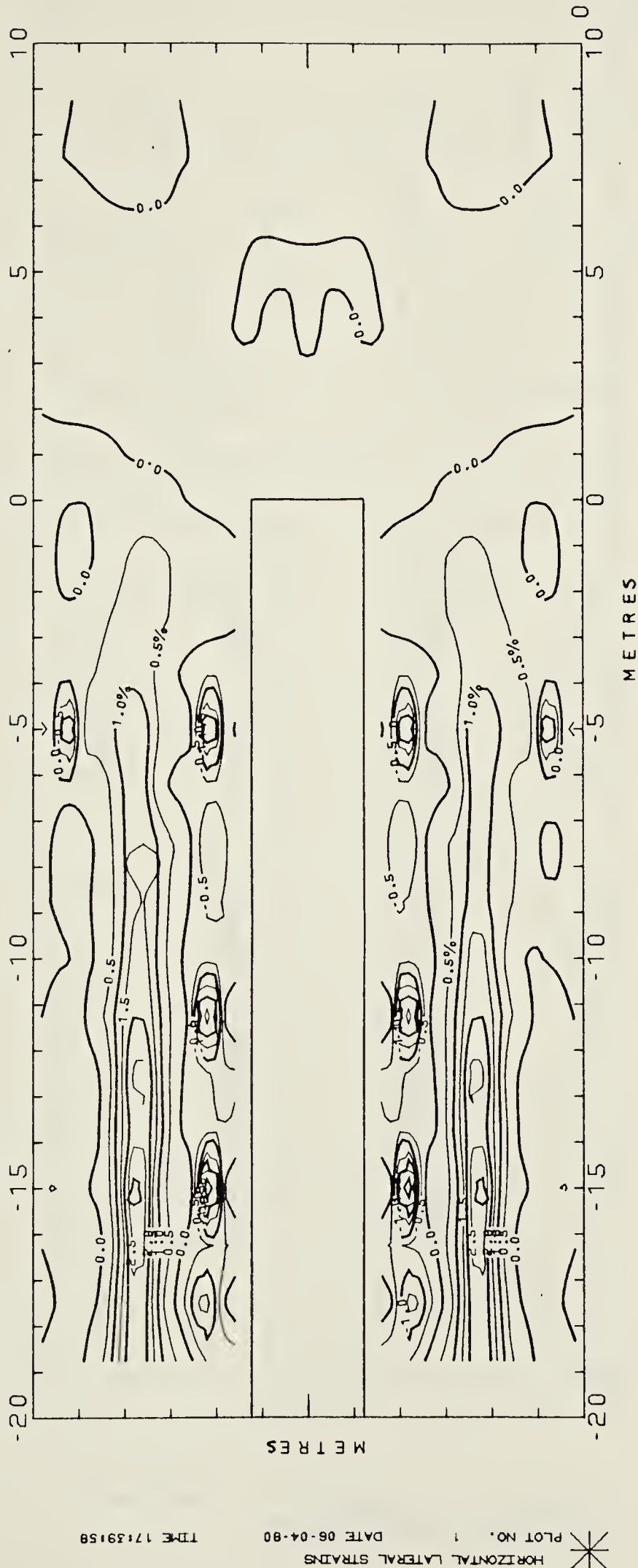


Figure 6.24 Contour map of lateral strains (Section C)

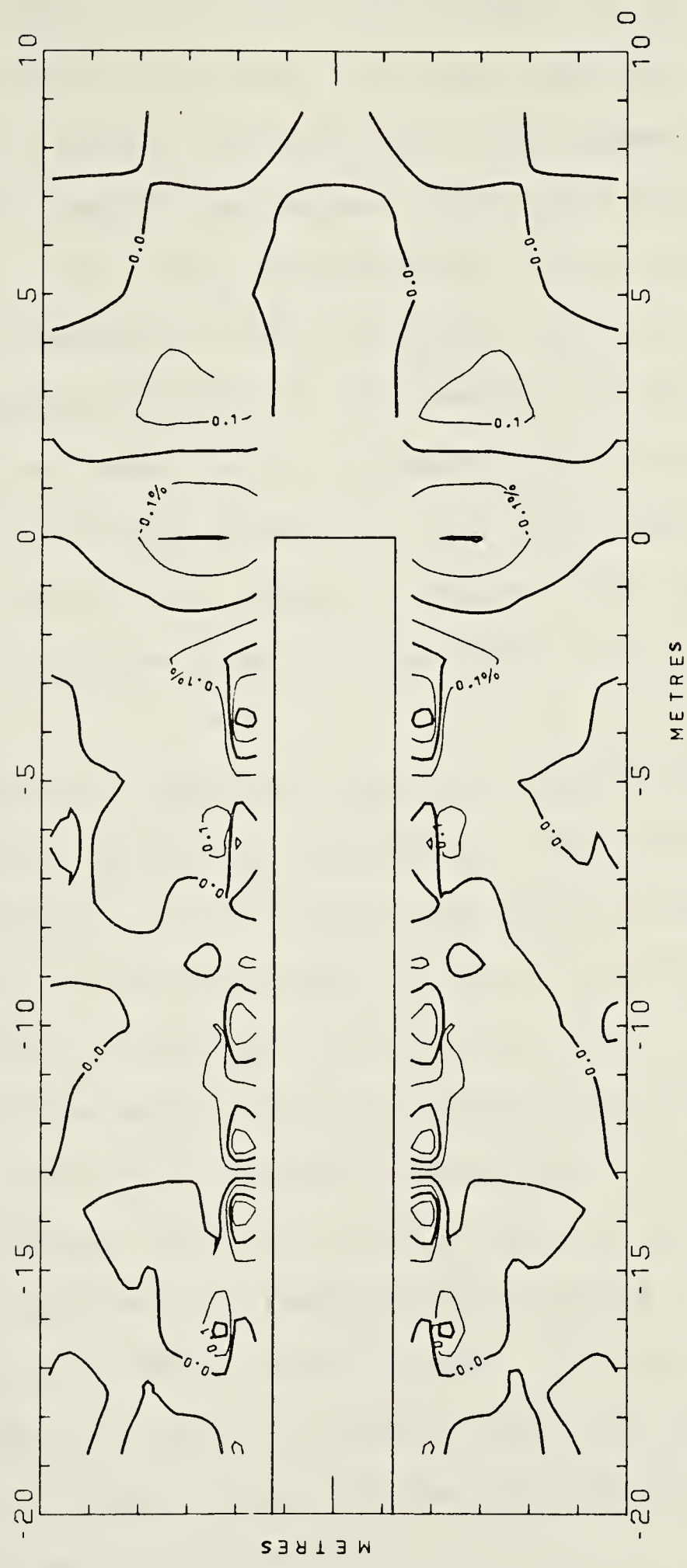


Figure 6.25 Contour map of longitudinal strains (Section C)

HORIZONTAL LONGITUDINAL STRAINS
PLOT NO. 1
DATE 06-04-80
TIME 17:40:29

3.1% in the lateral direction, and between -0.37 and 0.43% in the longitudinal direction. The maps show that the lateral strains were first developed just beyond the tunnel face, and their magnitude became larger with further advance of the tunnel, until they reached their final values about 12 metres (5 diameters) from the tunnel face. On the other hand, the longitudinal strain had reached its maximum value just beyond the tunnel face, the magnitude then dropped significantly with the advance of the face. The shear strains in this section, shown in Figure 6.26, seem to concentrate along the sides of the tunnel. They vary between -3 and +3%.

It should be noted that the strain conditions at Sections B and C are three-dimensional. The calculation of principal strains in such a condition must include all the six components of strains shown in Table 6.1. Producing all these components using the existing facilities of the SURFACE II System would require extensive work which is beyond the scope of the present investigation. It was concluded, however, that the contour maps of strains in the coordinate directions of these sections could illustrate the general trends of these strain fields. This will help in investigating the extent of plastic zones and the mobilization of shear length in the vicinity of the tunnel as discussed in the next section.

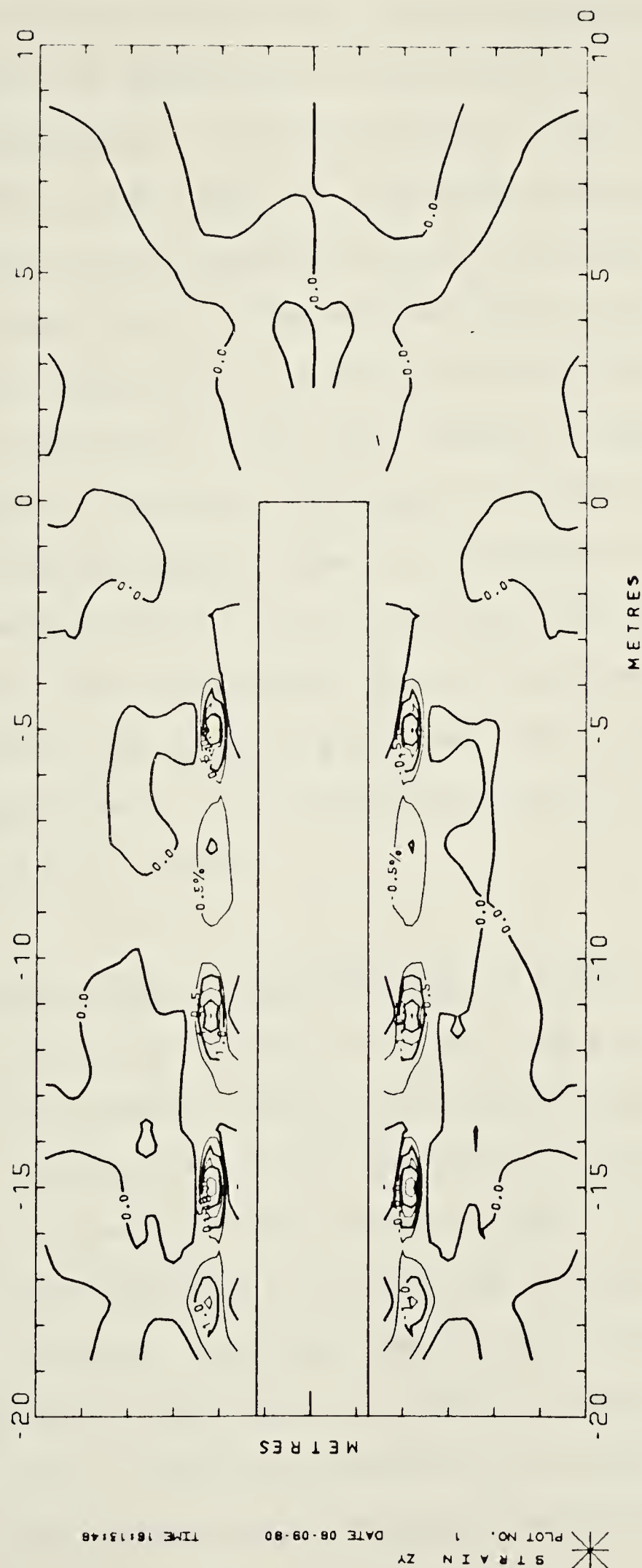


Figure 6.26 Contour map of shear strains (Section C)

6.5 MOBILIZATION OF SHEAR STRENGTH

One of the aims of this research program was to investigate the mechanism of mobilization of shear strength and the development of plastic zones in the vicinity of the tunnel. The contour maps of strains can be used, together with stress-strain characteristics of the soil for this purpose. Specifically, the maximum shear strains occurring in-situ are compared to those associated with the onset of inelastic behaviour of the soil based on laboratory tests on representative samples. The manner in which the soil strength was mobilized leads to conclusions concerning the failure mechanism of the soil and the arching process around the tunnel. This information has a direct bearing on the prediction of the stability of the tunnel walls, in the case of unlined tunnels, or the determination of soil pressure on the lining of a tunnel.

6.5.1 Contour Maps of Maximum Shear Strains

The strain at a point in a soil mass can be fully described in terms of magnitude and orientation of principal strains. On the other hand, the mobilization of the shear strength of the soil and the development of plastic zones can be investigated by utilizing the maximum shear strains. For this purpose, a contour map of these strains was constructed for Section A as shown in Figure 6.27. Those strains vary in magnitude between 0 to 3.67%, and are primarily developed within 4 metres of the tunnel wall. The

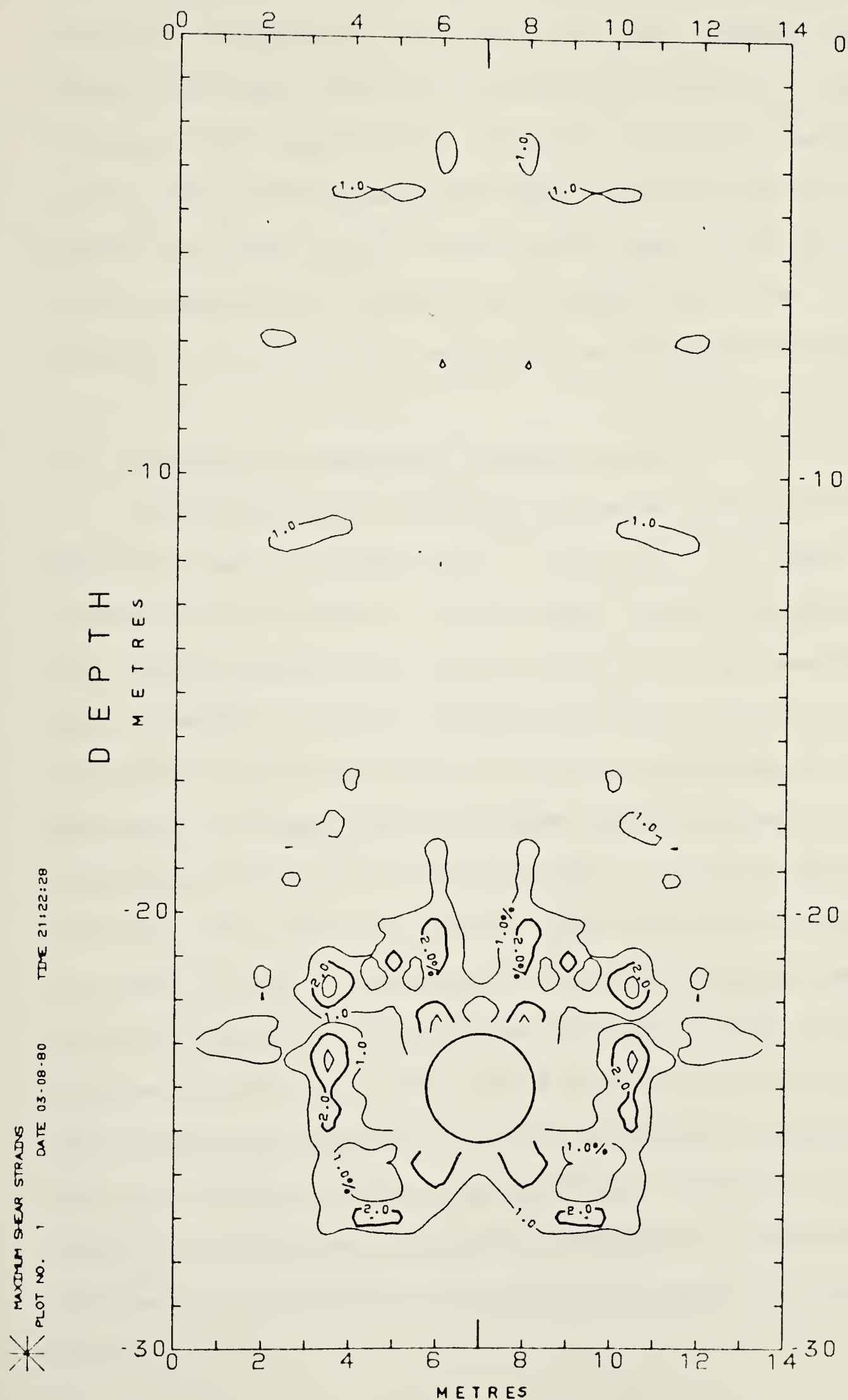


Figure 6.27 Contour map of maximum shear strains
(Section A)

strain components calculated for Section B did not indicate any zones of possible significant maximum shear strain. The lateral and shear strains of Section C, given in Figures 6.24 and 6.25 respectively, show the possible development of another zone of high maximum shear strain which is located beside the tunnel at the springline level. This zone could not be identified from Section A alone since the longitudinal strains at Section A had dropped to zero.

6.5.2 Results of Laboratory Tests on Till

The geotechnical characteristics of glacial till of the Edmonton area are summarized in Table 3.2. Of special interest here, however, is the magnitude of the maximum shear strain associated with failure and the development of shear strength. A direct measure of these strains can be obtained in the laboratory using the simple shear testing apparatus. Alternatively, maximum shear strains can be determined employing the measurements of major and minor principal strains in a triaxial test. Monitoring the major principal strain in this test is a routine measurement. The minor principal strain could be measured either directly using a form of the lateral strain gauge, or indirectly by monitoring the volumetric strain. Attempts to monitor the minor principal strain using different types of lateral strain indicators are presently underway at the University of Alberta in a variety of tests performed on different materials.

Problem involved using the volume change readings as an indirect method of monitoring lateral strain for 38 mm diameter samples, were described by Medeiros (1979). Since the degree of saturation of the till is about 100%, and the till characteristics might change with back saturation, the volume change is usually monitored by observing the volume of fluid moving into or out of the triaxial cell. The volume change of small samples could be in the same order as the volume change of the testing system (cell and lines). Even tests on larger samples (100 mm diameter), performed as a part of the present study, yielded unrealistic estimates of lateral strain.

Another method of determining the maximum shear strain at failure from laboratory results involves the idealization of the stress-strain curves obtained from the triaxial test into a bilinear relationship between axial strain and deviatoric stress, similar to that used by Dunlop and Duncan (1970). As shown in Figure 6.28, the initial part of the curve is idealized by a linear elastic relationship. Therefore, Hooke's law can be used to calculate the minor principal strain which corresponds to any major principal strain on this part of the stress-strain curve. The maximum shear strain can then be calculated. Table 6.2 summarizes the relationships required to calculate the maximum shear strains in conventional triaxial (drained and undrained) and active compression triaxial stress paths.

The results of two conventional triaxial tests (one

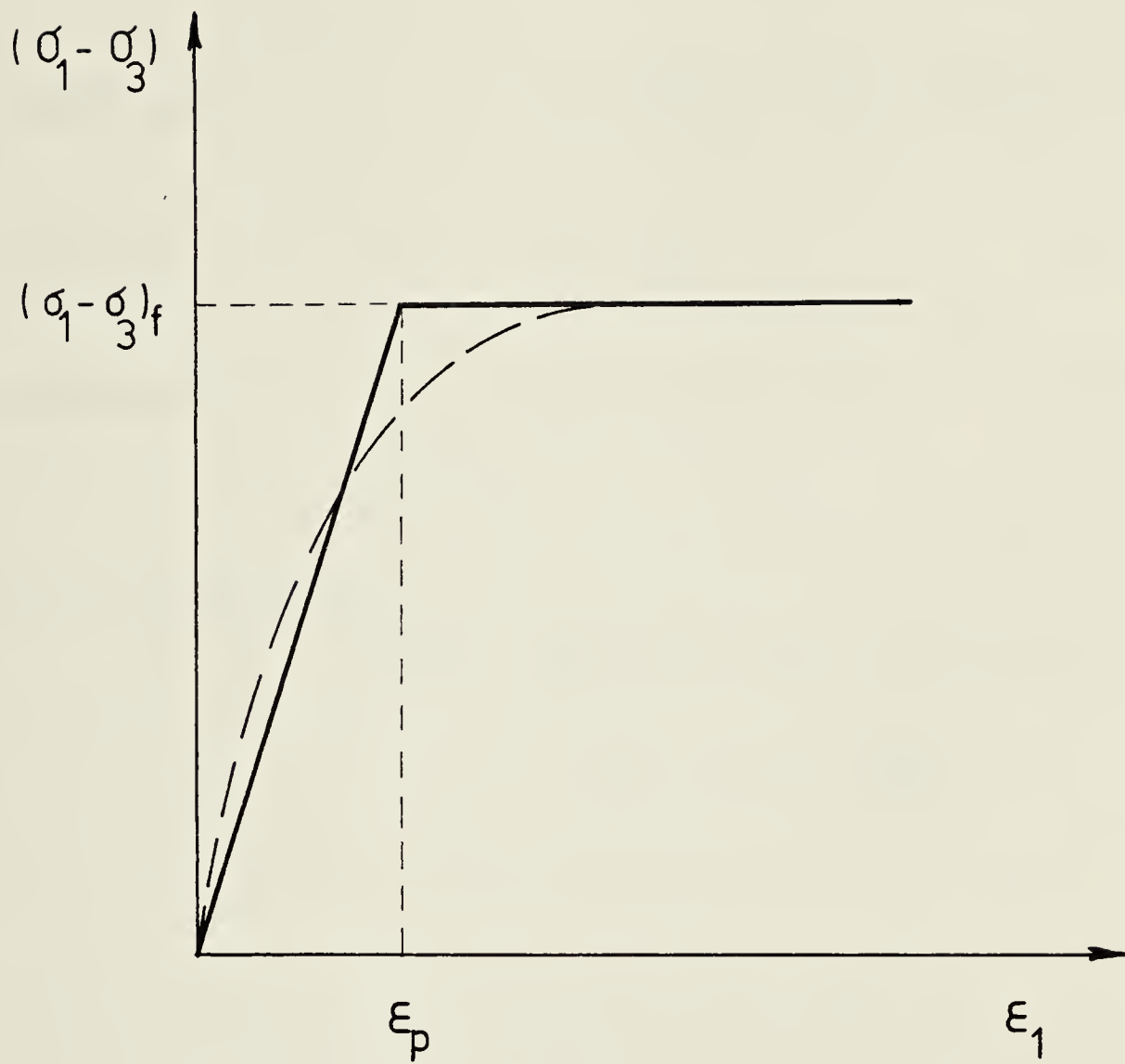


Figure 6.28 Bilinear stress-strain relationship

Table 6.2 Strains in triaxial test samples under different stress paths

General Hooke's Law:

$$\xi_1 = \frac{1}{E} [\Delta\sigma_1 - \nu(\Delta\sigma_2 + \Delta\sigma_3)]$$

Triaxial Drained:

$$\xi_3 = -\nu\xi_1$$

Triaxial Undrained:

$$\xi_2 = \xi_3 = -\nu \frac{\Delta\sigma_1 - \Delta u}{E} + (1-\nu) \left(\frac{-\Delta\xi}{E} \right)$$

Drained Active Compression:

Where $(\Delta\sigma_1 = 0, \Delta\sigma_3 < 0 \text{ and } \Delta u = 0)$

$$\xi_3 = -\xi_1 \left(\frac{1-\nu}{2\nu} \right)$$

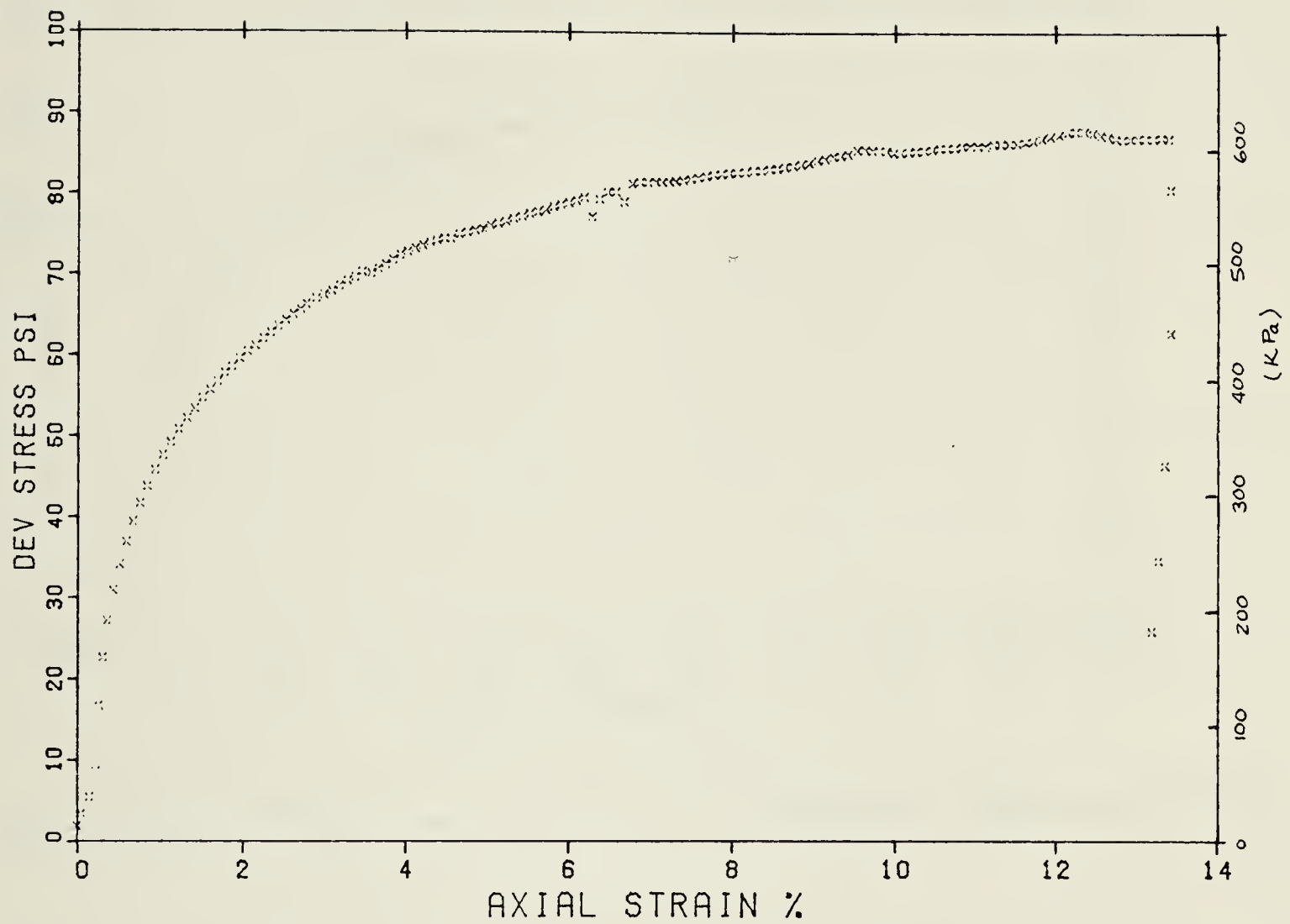
drained and one undrained) performed on 100 mm diameter samples are given in Figures 6.29 and 6.30 respectively. The calculated maximum shear strains based on the results of these two tests as well as the results given by Mederios (1979) are presented in Table 6.3. A Poisson's ratio of 0.4 was used in these calculations. The results suggest that the value of the maximum shear strain is dependent on the stress path. However, the results did not show a clear trend for the dependency of these values on the stress level of pre-shear consolidation.

Based on these observations, it was concluded that the maximum shear strain at failure could range approximately between 1 and 2%. The lower limit would apply to points with stress paths similar to extension or active compression while the upper limit would apply to the stress path of a conventional triaxial test.

6.5.3 Mechanism of Shear Strength Mobilization

Guided by the conclusions reached in the previous section, the contour map of maximum shear strain at Section A (Figure 6.27) was re-examined. The zones where the shear strength of the soil was mobilized were idealized as shown in Figure 6.31(a).

If the shear strength of the till is mobilized at 2% shear strain, four distinct failure zones develop. Two of these zones extend almost vertically for about 2.5 metres, (one diameter), from points on the tunnel wall at 45° above



TRIAXIAL TEST #2

(480.0,0.0 KPA)

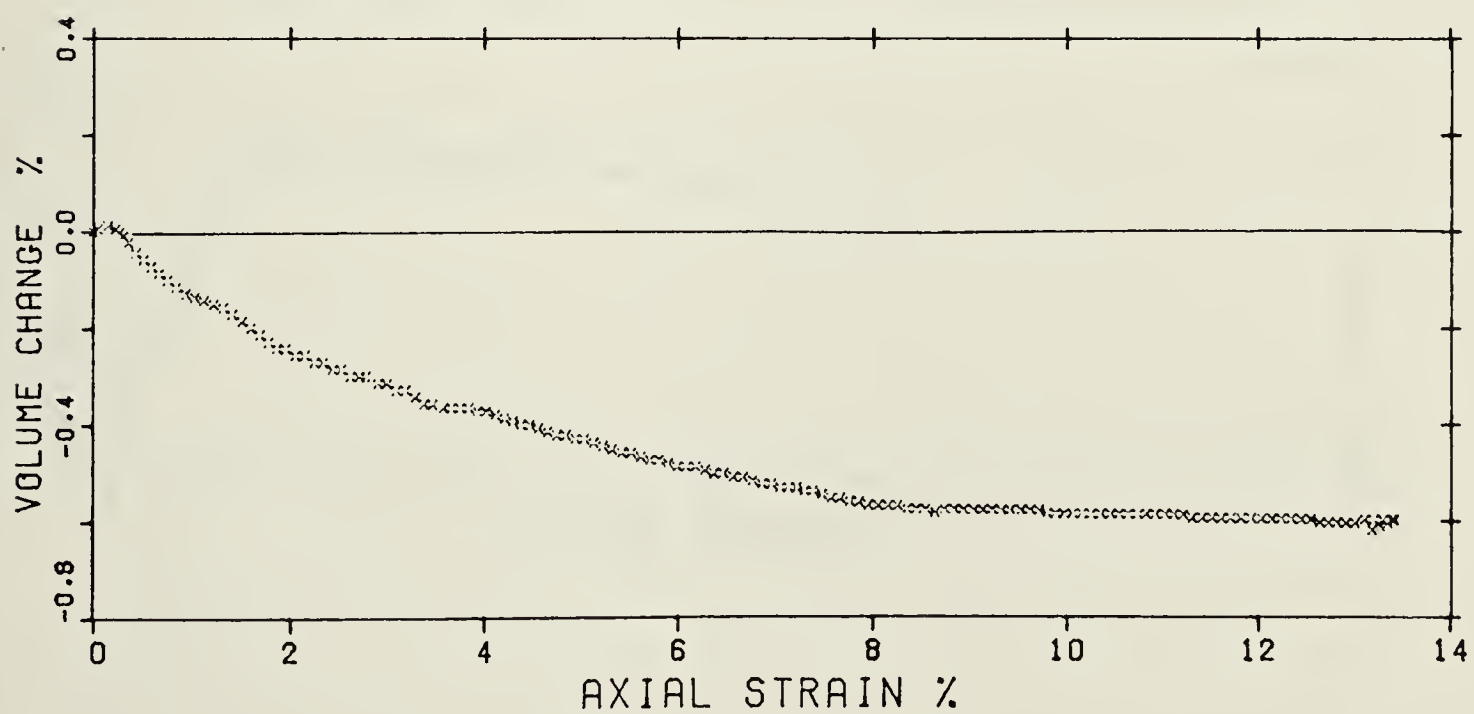
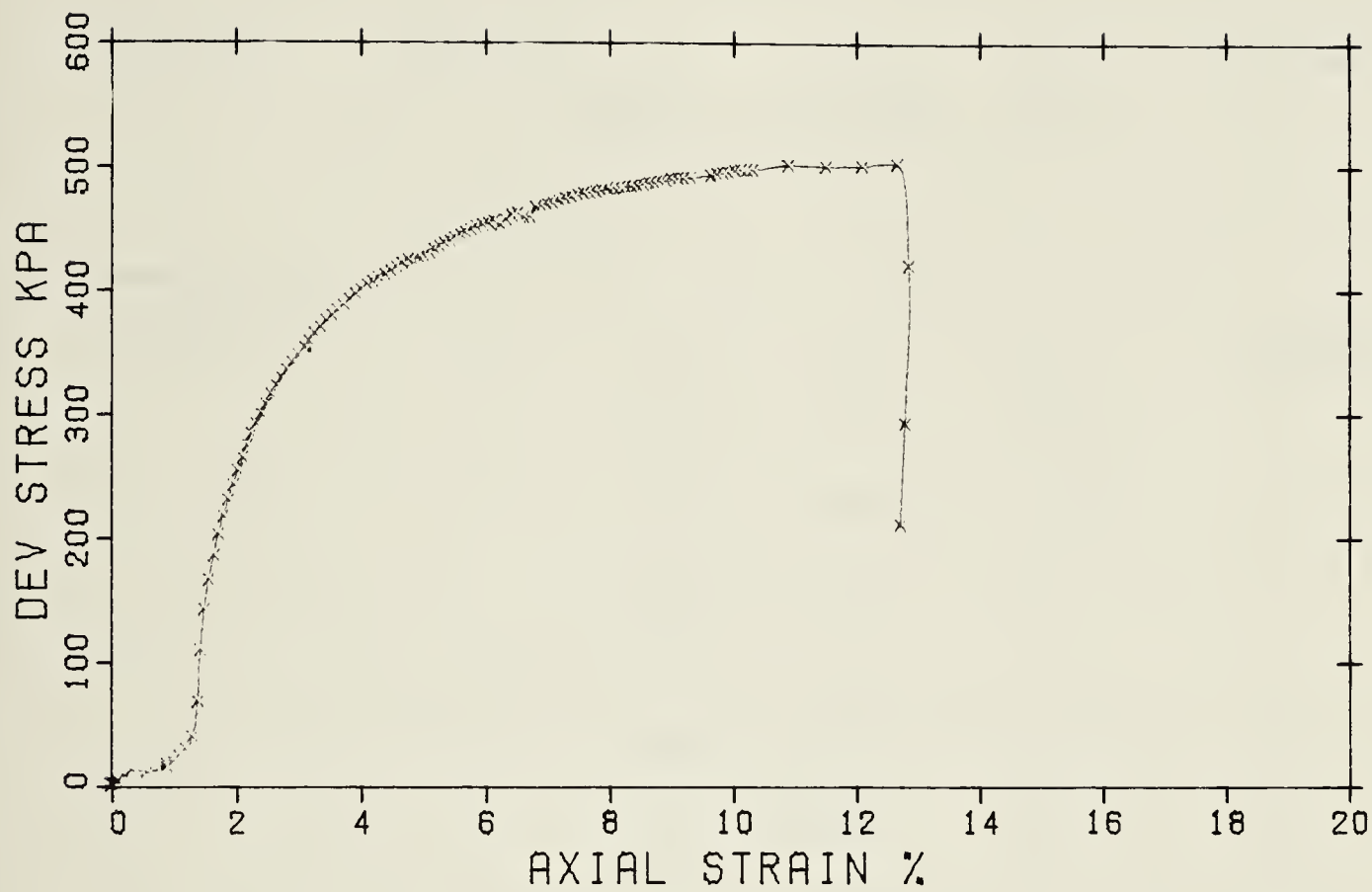


Figure 6.29 Results of triaxial drained test on Edmonton Till



TRIAXIAL TEST #1

(680.0, 200.0 KPA)

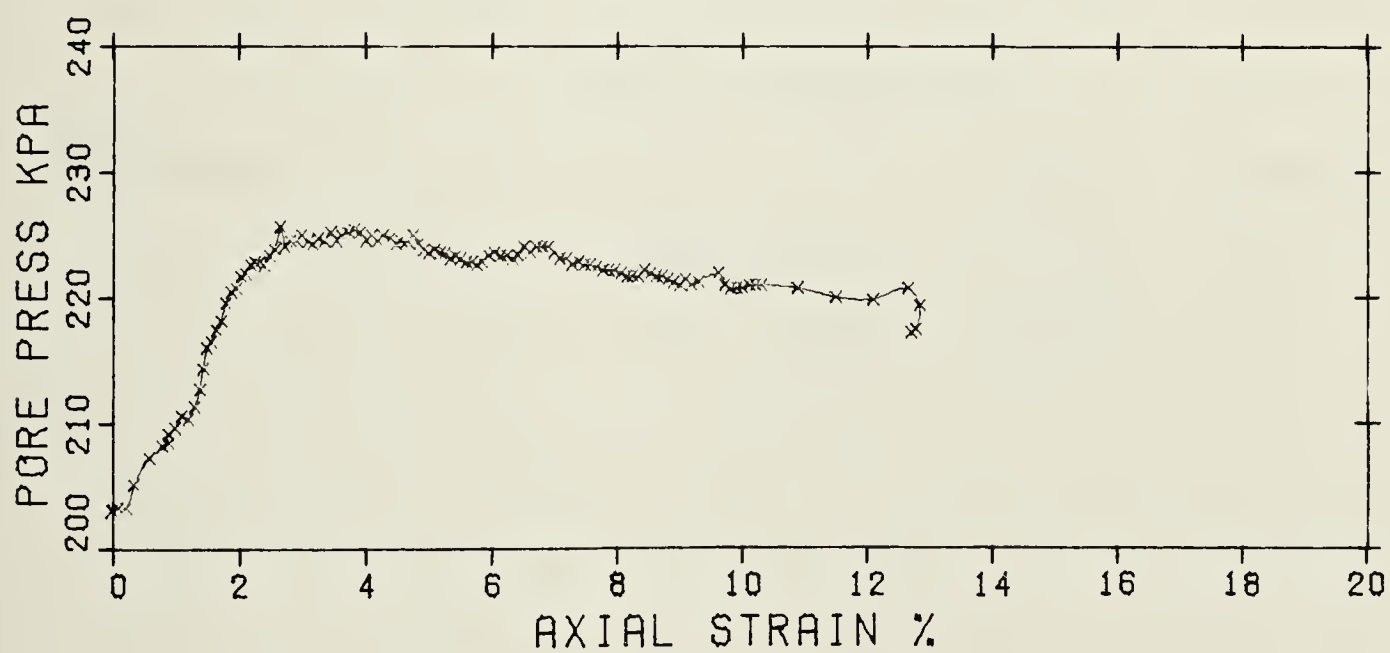


Figure 6.30 Results of triaxial undrained test on Edmonton Till

Table 6.3 Maximum shear strains from laboratory tests

Test Type	Test No.	σ_3 (kg/cm ²)	$\Delta\sigma_1$ (kg/cm ²)	γ % max	Reference
Conventional					
Triaxial	1	1.54	7.5	1.6	Medeiros (1979)
	2	1.89	8.25	2.02	" "
	3	1.82	8.25	2.12	" "
	4	3.05	9.5	2.2	" "
	5	3.36	9.3	1.6	" "
	6	2.59	10.5	1.6	" "
	7	2.24	10.2	1.2	" "
	8	2.07	9.75	1.6	" "
	9	4.89	5.97	2.2	Present Study
	10	4.89	5.10	2.4	Present Study
Active Compression		σ_{30} (kg/cm ²)	$\Delta\sigma_3=(\sigma_1-\sigma_3)_f$		
	1	2.1	-1.7	0.95	Medeiros (1979)
	2	1.925	-1.7	1.01	" "
	3	2.45	-2.0	0.76	" "

the horizontal axis. The other two zones start at points near the invert and extend laterally for two metres then turn upwards terminating about 1 metre above the crown as shown in Figure 6.31(a). On the other hand, assuming shear strength mobilization at 1% shear strain will lead to the formation of two symmetrical rings. Each of these rings surround two of the 2% shear strain zones, with a margin of about 0.5 metre on each side. This indicates that the variation of shear strains within the range 1 to 2% will result only in a slight change in the corresponding zone of shear strength mobilization.

As mentioned previously, the horizontal strains and shear strains measured at Section C show a tendency for the development of a significant difference in principal strains at the sides of the tunnel. This indicates another zone of shear strength mobilization. An approximate configuration of this zone is shown in Figure 6.31(b).

In general, the failure zones do not seem to form a uniform circular ring around the tunnel as commonly assumed for deep tunnels. Their shape, however, has some similarity to those observed in model tests and elasto-plastic finite element analyses, which are shown in Figures 6.32 and 6.33 respectively. The development of plastic zones similar to those shown in Figure 6.31 could be one of the major factors involved in the failure of a tunnel in Edmonton till described by Matheson (1970).

The failure reported by Matheson (1970) occurred in an

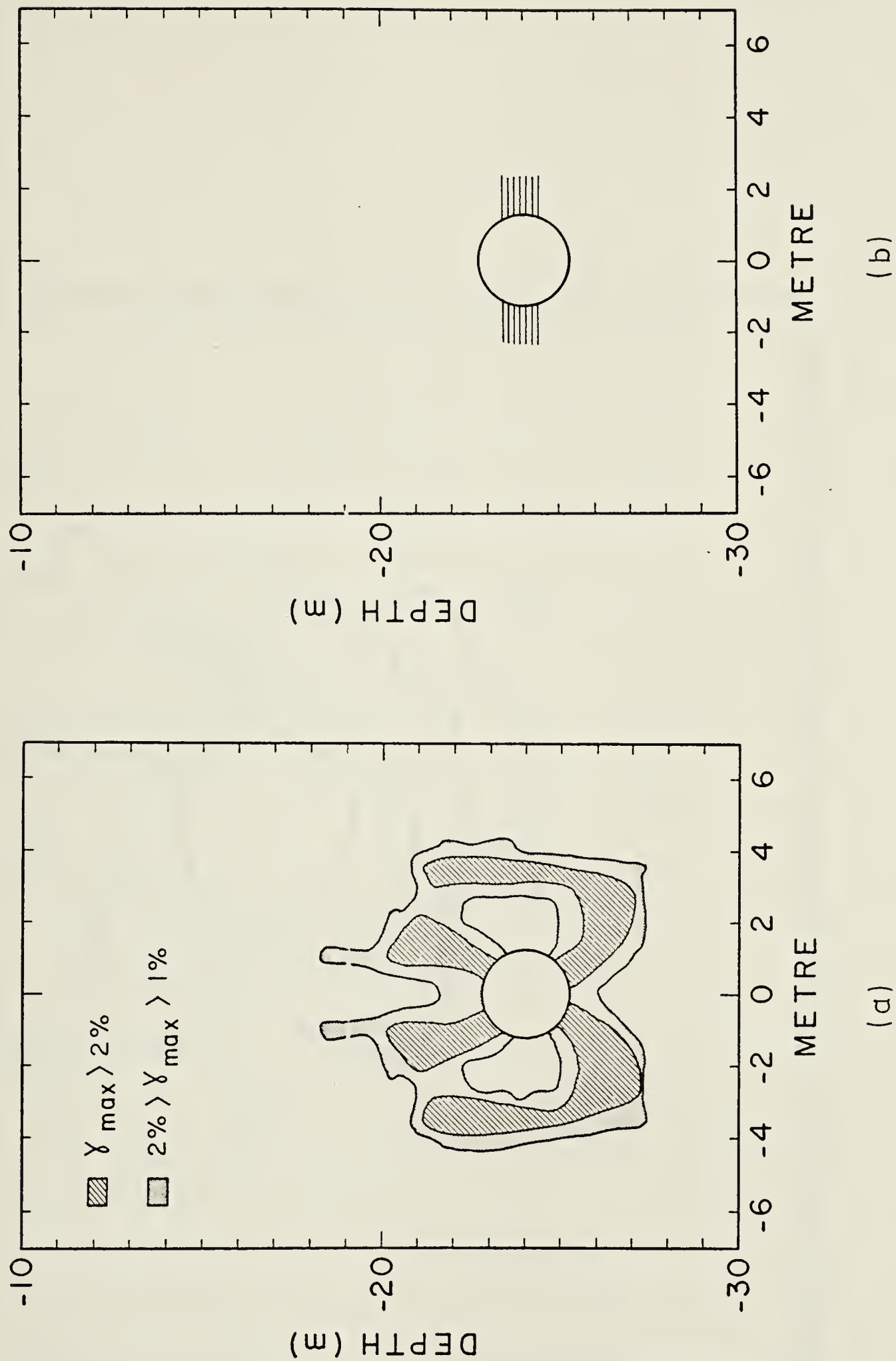


Figure 6.31 Zones of mobilized shear strength

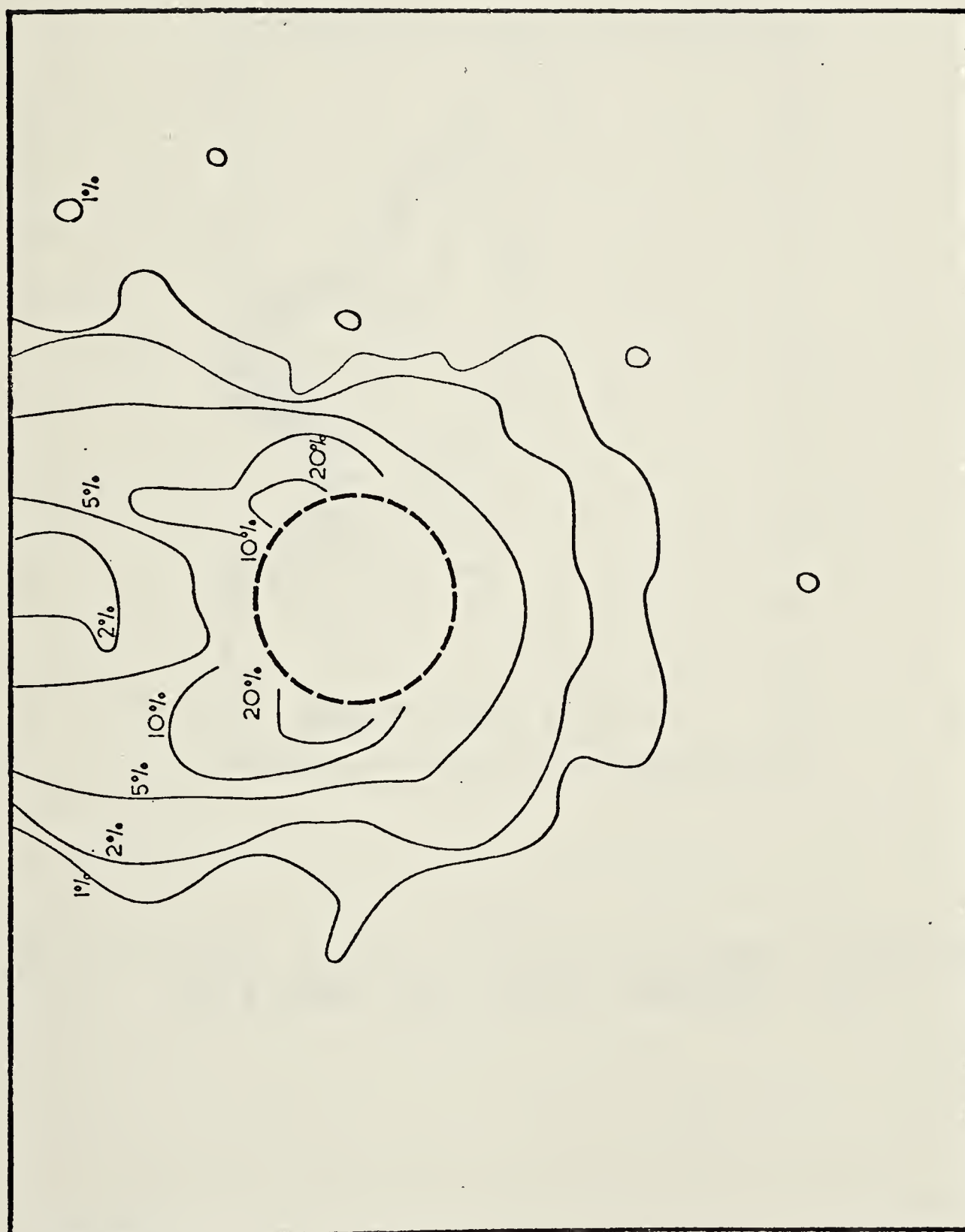


Figure 6.32 Failure zones in model test on overconsolidated Kaolin (after Atkinson and Potts, 1977)

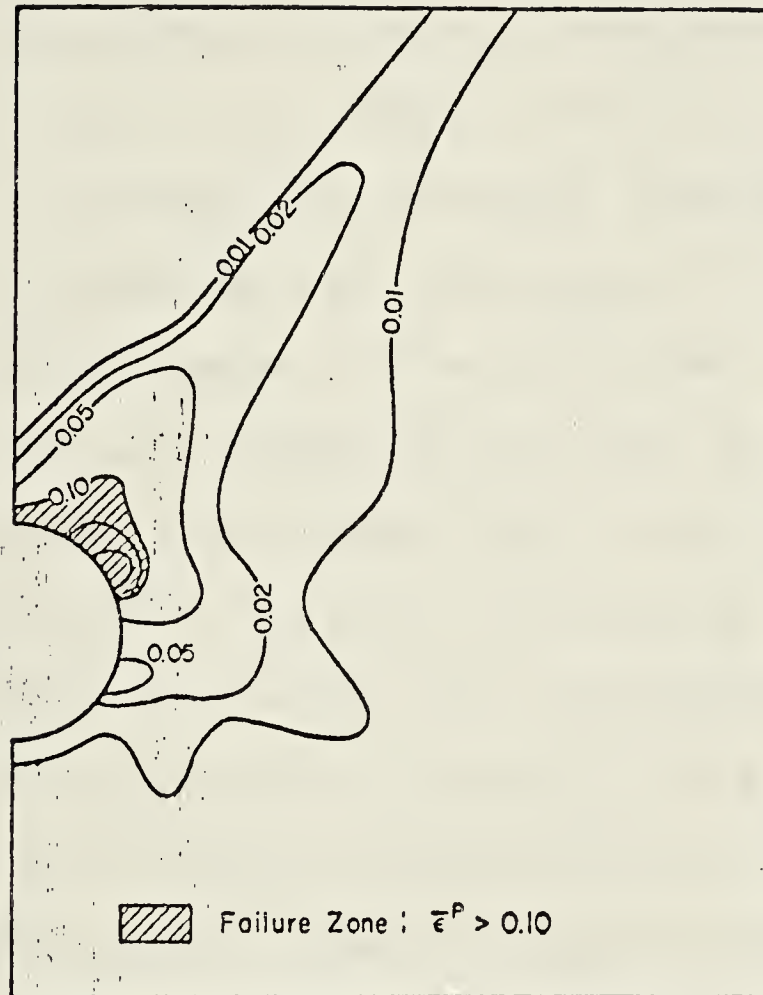


Figure 6.33 Shear strains from finite element simulation of a model test (after Ghaboussi et al., 1978)

unsupported section of a tunnel roof and was preceded by the formation of longitudinal cracks in the tunnel roof as shown in Figure 6.34. The failure consisted of a series of falls of discrete blocks from the crown. Based on the hypothesis that this failure was initiated by the development of tensile stresses at the roof, an unrealistic value of K_0 of 0.33 was calculated. In these calculations, the till was assumed to behave as an ideally elastic material. Matheson (op. cit.) concluded that the sand lenses contributed to the failure and suggested that the apparent low value of K_0 may be due to the presence of the sand lenses.

Both the sand lenses and jointing system in the till have undoubtedly contributed significantly to the development of this failure. For example, the joints, which are parallel to the tunnel wall, were opened as a result of the release of the radial pressure. The presence of small pockets or thin layers of sand enhanced the failure of some of the blocks as that shown in Figure 6.34 near the springline. On the other hand, the mobilization of the shear strength and the accompanying excessive shear strains resulted in a redistribution of the stresses around the tunnel. Reduction of tangential stresses, due to the stress redistribution, consequently opened the longitudinal cracks allowing the blocks to fall under their own weight.

Another important aspect of the mobilization of shear strength is that it explains the significantly low pressure carried by the lining compared to the in-situ stresses in

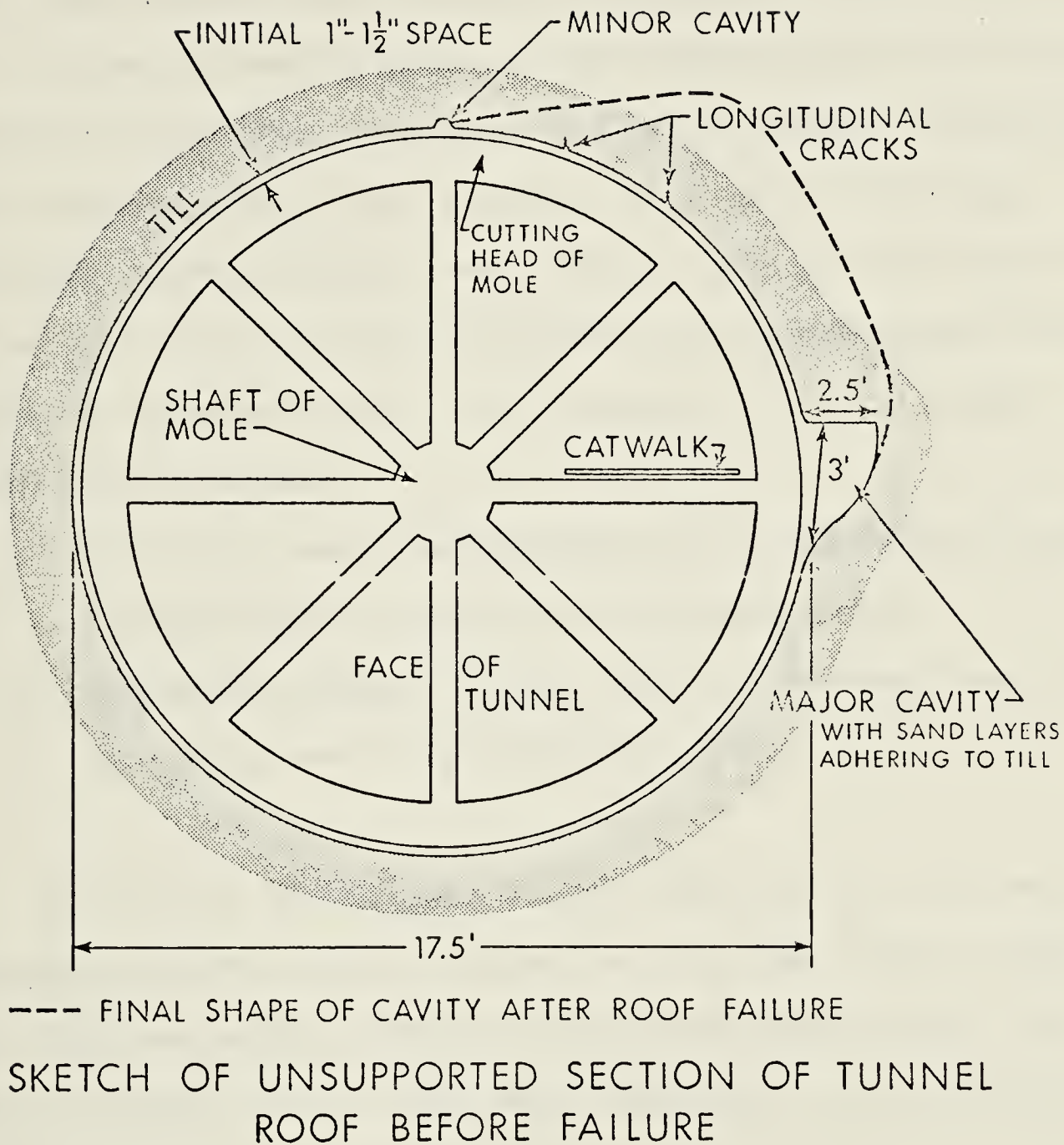


Figure 6.34 Failure zone of unsupported section of tunnel roof (after Matheson, 1970)

the soil. The mobilization of shear strength in the zones shown in Figure 6.31 confirms the presence of arching of the in-situ stresses to the surrounding soil thus leaving only a small portion of these stresses to be carried by the lining.

The measurements given in most published tunneling case histories show that pressures acting on tunnel linings are less than the overburden stress. In a few of the case histories summarized by Peck (1969), pressure acting on the lining was equal (or even exceeded) the overburden stress. In these isolated cases, one or more of the following conditions existed:

- a) Soil was overconsolidated with a horizontal stress exceeding the vertical overburden stress.
- b) expanded wedged lining, such as Don-Seg, was used.
- c) soil had swelling characteristics.

Any one of the above, or any combination can result in pressures on the linings equal or (in some cases) higher than the overburden stress. This could occur even though the shear strength of soil was mobilized and the arching process took place.

It seems more meaningful to use the ratio of the pressure acting on the lining to the average principal in-situ stress as a measure of the degree of arching of in-situ stresses around tunnels. Such a definition is essential when the horizontal and vertical pressures are unequal (case a). Expanding the lining by wedging action

(case b) does not allow any control of the loads applied during expansion and could ultimately prestress the lining to a pressure up to the original in-situ stress. The case of tunnels in swelling soils (case c) is beyond the scope of this thesis but case histories of tunnels in such soils show that the swelling characteristics could result in pressures much higher than those developed due to the in-situ stresses.

Apart from the special cases of swelling soils and expanded wedged lining, excavation of a tunnel results in a mobilization of shear strength to a degree that depends on the soil deformation allowed by the tunneling procedure employed. As a result, the in-situ stresses dome around the tunnel face and ultimately arch on the sides of the tunnel leaving the lining acted upon by only a portion of the in-situ stresses.

6.6 SUMMARY

This chapter has described the strain field around an advancing tunnel in a stiff soil. The in-situ measurement of soil displacement around this experimental tunnel was used to produce contour maps of these displacements. The computer graphical system SURFACE II was used to generate the plots. Three sections were chosen to illustrate the spatial nature of the displacements. Section A is a vertical lateral section about 50 metres from the tunnel face. Section B is a vertical longitudinal section. Section C is a horizontal

section at the level of the tunnel springline. The displacement contour maps showed the same trends and characteristics described and discussed in section 4.4. These maps were specifically produced, however, as a first step towards a study of the strain fields and an investigation of the mode of mobilization of shear strength in the vicinity of the tunnel.

The general trends of the strain fields were identified and all strains were developed mainly within 3 to 4 metres of the tunnel wall. The lateral horizontal strains, perpendicular to the direction of tunnel advance, were first developed just behind the tunnel face, and their magnitude became larger with further advance of the tunnel. They reached their final values when the tunnel face was about 12 metres (5 diameters) beyond their location. A similar history of development was experienced by the vertical strains. On the other hand, the longitudinal strains reached their maximum value just behind the tunnel face. Their magnitudes subsequently dropped to zero with further advance of the tunnel face.

The principal strains and their orientation as well as the volumetric and maximum shear strains were calculated for the final lateral section (Section A). A comparison of the in-situ maximum shear strains to those associated with the inelastic behaviour of the soil based on laboratory testing was carried out. This comparison led to the identification of possible failure zones around the tunnel and showed that

the mobilization of shear strength was limited to a well defined area around the tunnel. This procedure indicated that the plastic zone did not have a uniform circular shape, similar to that which commonly results from two-dimensional closed form analyses of deep tunnels. However, the defined failure zones are similar to the pattern of failure zones observed in model tests and obtained from some elasto-plastic finite element analyses. The shape of these zones also sheds a new light on the failure of a roof observed in an unsupported portion of a tunnel in the same soil ten years ago. The mobilization of shear strength around the tunnel confirmed the existence of an arching process which consequently resulted in a relatively low pressure on the lining.

CHAPTER 7

CONCLUSIONS AND RECOMMENDATIONS FOR FURTHER STUDIES

The characteristic elements of the behaviour of tunnels in stiff soils have been identified, described and discussed in the various chapters of this thesis. These elements are compiled and summarized in this chapter.

Based on the research work given in this thesis, several conclusions have been reached and are presented in this chapter, with recommendations for further studies.

7.1 THE BEHAVIOUR OF TUNNELS IN STIFF SOILS

A review of the literature indicated that analytical methods can be of significant importance for parametric studies of some of the factors influencing tunnel behaviour. However, the inability of these methods to include all the construction details and to represent the soil behaviour around the tunnel realistically, has precluded their use as a design tool. Until the gap between analytical methods and actual behaviour is filled, the role of in-situ monitoring will continue to be important in investigating the performance of tunnels and in studying their actual behaviour.

The present study, therefore, was based on the in-situ measurements of the soil mass response and the records of the lining system performance in an experimental tunnel

advanced in stiff overconsolidated silty clay till using a shielded drilling machine. Conclusions concerning the characteristic elements of the behaviour of tunnels in stiff soils are presented in the following sections.

7.1.1 Soil Response to Tunneling

a) Soil displacement vs. tunnel advance

The soil displacement associated with the advance of a tunnel through a mass of stiff soil can be divided into three distinct stages with respect to the location of the tunnel face. In the first stage, while the drilling machine is advancing, the soil ahead of the tunnel face is pushed in the direction of tunnel advance. The soil in the crown area experiences a slight settlement during this stage while the ground surface heaves slightly then begins a downward settlement. The second stage of soil displacement occurs while the tunnel drilling machine is actually passing through the measurement point. The soil then moves radially to close the annular space resulting from the overcut of the machine. As soon as this space is filled, the soil is temporarily stabilized by the shield. The second stage is also characterized by a longitudinal displacement of points close to the tunnel at the springline in a direction opposite to that of the tunnel advance. In the third stage, the soil again moves when the tail of the shield clears the section. This movement soon stabilizes as the lining is expanded and becomes effective.

In-situ measurements around this experimental tunnel illustrate the relative proportion of soil displacement for each of the three stages in stiff soils. Soil movement near the tunnel crown indicated that the largest portion (47% of the final movement) had developed during the second stage. The first and third stages contributed by 30 and 23% of the final movement, respectively.

The measurements of soil displacements indicated that K_0 in the overconsolidated glacial till of Edmonton area is close to 1.0.

b) Soil displacement vs. depth

The soil settlement decreases rapidly upwards along a vertical line directly above the tunnel center line. Final measurements above the experimental tunnel showed vertical displacements on the order of 30-40 mm at the crown and 8-12 mm at the ground surface which was about 25 m above the crown. Points below the tunnel invert experienced a heave of up to 6 mm which was much less than the settlement at the crown. It is suggested that gravity is the main factor enhancing the downward soil movement at the crown.

It must be noted that whenever the difference in the behaviour of soil at the crown and invert areas is significant, an axisymmetrical idealization of tunnel behaviour cannot be justified.

c) Effect of the lining system on soil displacement

The soil around the conventional lining moves more than that around the segmented concrete lining mainly because of

the difference in the size of the gap between the lining and the soil. The expansion of the segmented concrete lining essentially eliminates the annular space around the tunnel while the continuous space left around the rib and lagging system is usually on the order of 2-3.5 cm. The greater stiffness of the concrete segmented lining also has a secondary effect in reducing soil movements to a greater extent than the conventional lining. The difference between the soil displacements associated with the two lining systems is more significant for points closer to the tunnel.

For deep tunnels, such as the case in the experimental tunnel, the influence of lining systems on the settlement at the ground surface would be within the range of repeatability of the settlement measurements, that is, in this instance the ground surface movements are virtually the same for both types of lining.

7.1.2 Behaviour of Lining Systems

The in-situ behaviour of the two lining systems, (conventional lining and precast concrete segments), was investigated in this thesis. The conclusions of this part of the investigation are summarized in the following sections.

a) Conventional rib and lagging support system

The final average soil pressure on the primary lining installed in the experimental tunnel was equivalent to 12% of the overburden stress. The eccentric wedging of the steel rib joints could develop some bending moments, which could

contribute up to 50% of the normal stresses in the steel ribs.

Previous studies showed that the equilibrium state of the soil-lining interaction was reached within two weeks for a tunnel excavated through the Edmonton till. This concept was confirmed by the strain measurements in this experimental tunnel. Based on these observations it can be concluded that the soil pressure is actually carried solely by the primary lining until the steel ribs and timber lagging start deteriorate.

The primary rib and lagging lining in a tunnel having similar geometry, ground condition and construction procedure to those of the experimental tunnel undergoes a change in the vertical diameter of 2 mm or less while the horizontal diameter decreases by 5-9 mm. The primary lining could also experience a net upward heave reflecting the load release and swelling of the soil at the invert.

b) Precast segmented lining

The distribution of soil pressure acting on the precast segmented lining in the experimental tunnel had an elliptical shape. At the crown the magnitude varied between 45 and 59% of the overburden stress while the springline values ranged between 27-36%. The cracking pattern along the stress raisers of the segments was consistent with this distribution. It should be noted, however, that the development of these cracks was not enough to eliminate the bending moments at the stress raisers. Significant residual

bending strains were measured near the stress raisers, especially those near the springline area. The segmented lining experienced small changes in diameter and at the invert level, on the order of 2 to 4 mm.

If the precast segmented lining was not expanded, a continuous annular space (20 to 25 mm wide) could develop. Radial expansion of the lining, however, practically eliminated this space which indicates clearly that grouting is not needed if an expanded segmented lining is used in similar stiff soils.

The joints of the unreinforced longitudinal segments fail by sudden splitting through their center line. On the other hand, reinforced joints fail slowly after vertical cracks have developed in all directions. However, this improvement in the mode of failure is offset by difficulties encountered during casting when special reinforcement is incorporated into the segment.

7.1.3 Strain Fields around Tunnels

The results of this study indicate that soil strains associated with the excavation of deep tunnels in stiff soils are confined to the area in the vicinity of the tunnel. The vertical strains and the horizontal lateral strains, (perpendicular to the direction of tunnel advance), are initiated just beyond the tunnel face. The magnitudes of both vertical and horizontal lateral strains are enhanced with further advance of the tunnel and reach their final

values when the tunnel face is about 5 diameters beyond the section under study. On the other hand, the longitudinal strains reach their maximum values just beyond the tunnel face. Their magnitudes subsequently decrease with further advancement of the tunnel face.

The orientation of the final principal strains deviates from the direction of in-situ principal stresses. The principal strains tend to have an orientation similar to that of the flow of arching stresses around the opening.

7.1.4 Mobilization of Shear Strength around Tunnels

Failure zones around the experimental tunnel were identified using the maximum shear strain failure criterion by comparing the in-situ maximum shear strains developed in the soil with those associated with the onset of inelastic soil behaviour as determined from the results of triaxial tests on representative samples. The failure zones indicate that the mobilization of shear strength is limited to a well defined area in the vicinity of the tunnel. These zones do not form the uniform circular ring which is commonly obtained using two-dimensional closed form analyses of deep tunnels. However, the defined failure zones are similar to the pattern of the failure zones observed in model tests and to those obtained from elasto-plastic finite element analyses.

The development of failure zones and the mobilization of shear strength, as described here, agree with the mode of

failure of a tunnel roof observed ten years ago in an unsupported portion of a tunnel in the same soil. The mobilization process has also confirmed the occurrence of the arching of soil stresses around the tunnel which consequently results in the relatively low pressures transmitted to the linings.

7.2 GENERAL CONCLUSIONS

Based on the research work described in this thesis as well as that of others, discussed in the various chapters, the following general conclusions were reached:

1. Although the displacement field around an advancing tunnel is three-dimensional in nature, most tunneling studies assume it to be two-dimensional. Inevitably, then, some of the factors influencing the actual soil behavior are masked, since the stress history of the soil mass and pattern of stress concentrations are different for the two cases. Data from the extensively instrumented test sections in the experimental tunnel described in this thesis illustrate the spatial variation of the deformation field around advancing tunnels.
2. Detailed planning of a tunneling monitoring program can contribute significantly to its success. The choosing of appropriate instruments to measure the expected movements and loads as well as the early processing of field data, using computer programs for their reduction

and plotting, make the execution of the monitoring program smoother especially if a large number of instruments are employed. If a large program of instrumentation is planned, one or more small test sections, containing a limited number of instruments, should be used at an early stage of construction to identify the general trends of the tunnel behaviour. Such small test sections help in developing confidence in the instruments, show the need for any modification in their design and permit the usefulness of subsequent larger test sections to be enhanced.

3. Most of the movements due to tunneling in stiff soils occur around the drilling machine and up to 2.5 to 3 diameters behind the face. These displacements can be minimized by reducing the size of the overcut of the drilling machine and activation of the lining, directly behind the tail of the mole as soon as possible. In this regard, the expanded precast concrete segmented lining was found preferable.
4. Points below tunnel invert, in soils and even in rocks, usually experience a heave, due to tunnel excavation, of a much smaller magnitude than the settlement at the crown. It is suggested that gravity is the main factor responsible for the soil movements at the crown being larger. The idealization of tunnel behaviour as axisymmetric cannot be justified under such conditions, even for deep tunnels.

5. The manner in which the strength of the soil around a tunnel is mobilized forms an important part of any description of the failure mechanism of the soil and further clarifies the accompanying process of arching. This information has a direct bearing on the prediction of the stability of the tunnel wall in unlined tunnels and the determination of soil pressure on lined tunnels.
6. Failure zones around deep tunnels in stiff clays, as illustrated in this thesis, indicate that the mobilization of shear strength is limited to a well defined area in the immediate vicinity of the tunnel. They do not form the uniform circular ring, commonly predicted by two-dimensional closed form analyses. However, there are some similarities among the defined failure zones and those observed in model tests and obtained from elasto-plastic finite element analyses.
7. Defining the degree of arching around lined tunnels as the ratio of the average pressure carried by the lining to the overburden pressure can be misleading; especially where the horizontal in-situ stress is the major principal stress. Hence, it is suggested that for K_0 not equal to 1.0, the degree of arching should be taken as the ratio of the pressure carried by the lining to the average in-situ principal stress.
8. It is noticeable that most of the available case histories concerning tunnels in soil give detailed descriptions of either the soil displacement field or

lining performance. Rarely is a balance in depth maintained. It was realized during the undertaking of this research that separation of the soil and lining into two independent elements could simplify the design of tunnels in soil. However, in the study of the behaviour of such tunnels, a similar separation must be avoided. This approach was found to be essential in interpreting the measurements and identifying the most important characteristics of the tunnel's behaviour.

It is difficult to explain the relatively low loads carried by the lining without considering the mode of shear strength mobilization in the surrounding soil. Similarly, it is unrealistic to ignore the presence of the lining and its stiffness when examining the deformation of the soil around the tunnel. The structural element (lining) and the soil interact. Neither may be considered independent of the other if meaningful, realistic interpretations of tunnel behavior are to be made.

7.3 RECOMMENDATIONS FOR FURTHER STUDIES

The relatively high degree of success of the instrumentation program described in this thesis should be enhanced by the full utilization of its results. It is suggested that further studies be conducted in the area of finite element modelling, and specifically that the results of this investigation be used to guide the development of a special three-dimensional finite element program for

tunneling in stiff soils. Such a program should include provisions to allow modelling of the construction procedure, including the tunnel face advance, the soil-mole interaction, and the lining activation. It should also contain a reasonable idealization of the inelastic behaviour of the soil to allow realistic mobilization of shear strength and the proper development of failure zones. As discussed in section 2.2.5, the efficiency of computers has improved in the last few years, which makes the cost of a three dimensional analysis more economical. The mounting need for such analytical tool, on the other hand, may justify the development and use of such a program.

The performance of the precast concrete segments as a support system for the experimental tunnel was satisfactory for the short term. Long-term studies are required to document the behaviour of segmented lining over the life span of the tunnel.

The present study investigated the behaviour of reinforced and unreinforced longitudinal joints of the segments in the laboratory. Further laboratory studies on a full segment and a complete ring of segments may yield more insight into the structural behaviour of this type of lining.

The study included in this thesis was mainly concerned with the case of relatively deep tunnels in stiff soils. Studies on the behaviour of shallower tunnels in the same soils would be valuable. Specifically, such studies could

show the different trend of the development of failure zones and mobilization of shear strength around shallow tunnels.

REFERENCES

- Alberts, C. 1973. Use of remote controlled spraying nozzle. Use of shotcrete for underground structural support, ASCE and ACI SP.45, pp. 65-78.
- Atkinson, J.H., and Potts, D.M. 1977. Subsidence above shallow tunnels in soft ground. Journal of Geotechnical Engineering Division, ASCE, Vol. 103, pp. 307-325.
- Atkinson, J.H. 1973. Design of tunnel linings in soft ground. Report prepared for TRRL, Department of Engineering, University of Cambridge.
- Attewell, P.B., and Farmer, I.W. 1974a. Ground deformation resulting from shield tunnelling in London clay. Canadian Geotechnical Journal, Vol. 11, pp. 380-395.
- Attewell, P.B., and Farmer, I.W. 1974b. Ground disturbance caused by shield tunnelling in stiff overconsolidated clay. Engineering Geology, Vol. 8, pp. 361-381.
- Attewell, P.B., and Farmer, I.W. 1975. Ground settlement above shield driven tunnels in clay. Tunnels and Tunnelling, Vol. 7, No. 1, pp. 58-62.
- Barratt, D.A., and Tyler, R.G. 1976. Measurements of ground movement and lining behaviour on the London underground at Regents Park, TRRL Laboratory Report 684, Crowthorne, Berkshire, U.K.
- Bartlett, J.V., Noskiewicz, T.M., and Ramsay, J.A. 1971. Precast concrete tunnel linings for Toronto Subway. Journal of Construction Division, Paper 8498, ASCE.
- Beaulieu, A.C. 1972. Tunneling experiences, City of Edmonton, Alberta, Canada. Proc. 1st North American Rapid Excavation and Tunneling Conf., American Inst. of Mining Engrs., Vol. 2, pp. 933-964.
- Belshaw, D.J., and Palmer, J.H.L. 1978. Results of a program of instrumentation involving a precast segmented concrete-lined tunnel in clay. Canadian Geotechnical Journal, Vol. 15, pp. 573-583.
- Bjerrum, L. 1963. Allowable settlements of structures. Proceedings of the European Conference on Soil Mechanics and Foundation Engineering, Vol. 2, pp. 135-137.
- Bull, A. 1944. Stresses in the linings of shield-driven tunnels. Journal of Soil Mechanics and Foundations Engineering, ASCE, pp. 1363-1394.

- Burke, H. 1957. Garrison Dam tunnel test section investigation. Journal of Soil Mechanics and Foundations Division, ASCE, Vol. 83, paper no. 1438.
- Burland, J.B., Moore, J.F.A., and Smith, P.D.K. 1972. A simple and precise borehole extensometer. Geotechnique, Vol. 22, pp. 174-177.
- Burland, J.B., and Moore, J.F.A. 1973. The measurement of ground displacement around deep excavations. Field Instrumentation in Geotechnical Engineering, Butterworth and Co., London, pp. 70-84.
- Burns, J.Q., and Richard, R.M. 1964. Attenuation of stresses for buried cylinders. Proceedings on Symposium on Soil-Structure Interaction, Tucson, pp. 378-392.
- Canadian Foundation Engineering Manual, 1978, prepared by the Foundations Committee of the Canadian Geotechnical Society.
- Carlson, V.A. 1967. Bedrock topography and surficial aquifers of the Edmonton district, Alberta. Alberta Research Council, Report 66-3, 21 p.
- Chatterji, P.K., Smith, L.B., Insley, A.E., and Sharma, L. 1979. Construction of Saline Creek Tunnel in Athabasca Oil Sand. Canadian Geotechnical Journal, Vol. 16, pp. 90-107.
- Cheney, J. 1973. Techniques and equipment. Using the surveyors level for accurate measurement of building movement. Field Instrumentation in Geotechnical Engineering, Butterworth and Co., London, pp. 85-99.
- Cooling, L.F., and Ward, W.H. 1953. Measurements of loads and strains in earth supporting structures. Third Int. Conf. on Soil Mechanics and Foundation Engineering, Vol. 2, pp. 162-166.
- Cording, E.J. 1973. Geologic consideration in shotcrete design. Use of Shotcrete for Underground structural support, ASCE and ACI SP-45, pp. 175-199.
- Cording, E.J., and Hansmire, W.H. 1975. Displacement around soft ground tunnels. General report. Proc. of the 5th Panamerican Conference on Soil Mechanics and Foundation Engineering, Buenos Aires, Argentina, Vol. 4, pp. 571-633.
- Cording, E.J., Hendron, A.J., MacPherson, H.H., Hansmire, W.H., Jones, R.A., Mahar, J.W., and O'Rourke, T.D. 1975. Methods for geotechnical observations and instrumentation in tunneling. Report prepared for U.S.

National Science Foundation, Washington, D.C. NTIS No. PB252585-PB252586.

- Craig, R.N., and Muir Wood, A.M. 1978. A review of tunnel lining practice in the United Kingdom. TRRL Supplementary Report 335, Crowthorne, Berkshire, U.K.
- Curtis, D.J. 1976. The circular tunnel in elastic ground. Discussion, Geotechnique, Vol. 26, pp. 231-237.
- Curtis, D.J., Lake, L.M., Lawton, W.T., and Crook, D.E. 1976. In-situ ground and lining studies for the Channel tunnel project. Tunneling '76, pp. 231-242.
- Deere, D.U., Peck, R.B., Monsees, J.E., and Schmidt, B. 1969. Design of tunnel liners and support systems. Report prepared for U.S. Department of Transportation, NTIS No. PB 183 799.
- DeLory, F.A., Crawford, A.M., and Gibson, M.E.M. 1979. Measurements on a tunnel lining in very dense till. Canadian Geotechnical Journal, Vol. 16, pp. 190-199.
- Donovan, H.J. 1974. Expanded tunnel linings. Tunnels and Tunneling, Vol. 6, No. 2, pp. 46-53.
- Dunlop, P., and Duncan, J.M. 1970. Development of failure around excavated slopes. Journal of Geotechnical Engineering Division, ASCE, Vol. 96, pp. 471-493.
- Dunnicliff, C.J. 1971. Equipment for field deformation measurements. 4th Panamerican Conf. on Soil Mechanics and Foundation Engineering, San Juan, Vol. 2, pp. 319-332.
- Ebaid, G.S., and Hammad, M.E. 1978. Aspects of circular tunnel design. Tunnels and Tunneling, Vol. 10, No. 6, pp. 59-63.
- Eisenstein, Z., Kulak, G.L., MacGregor, J.G., and Thomson, S. 1977. Report on geotechnical and construction performance of the twin tunnel. Unpublished report prepared for the City of Edmonton Engineering Dept., Edmonton, Alta., 77 pp.
- Eisenstein, Z., and Thomson, S. 1978. Geotechnical performance of a tunnel in till. Can. Geotech. J., Vol. 15, pp. 332-345.
- El-Nahas, F. 1977. Field measurements in two tunnels in the City of Edmonton. M.Sc. Thesis, Department of Civil Engineering, University of Alberta, Edmonton, Alberta, 85 p.

- Ghaboussi, J., and Gioda, G. 1977. On the time-dependent effects in advancing tunnels. *International Journal for Numerical and Analytical Methods in Geomechanics*, Vol. 1, pp. 249-269.
- Ghaboussi, J., Ranken, R.E., and Karshenas, M. 1978. Analysis of subsidence over soft-ground tunnels. *International Conference on Evaluation and Prediction of Subsidence*, ASCE, Florida, pp. 182-196.
- Green, G.R. 1973. Principles and performance of two inclinometers for measuring horizontal ground movements. *Symposium on Field Instrumentation in Geotechnical Engineering*, Butterworth and Co., London, pp.
- Hanafy, E.A. 1976. Finite element simulation for tunnel excavation in creeping rock. M.Eng. Thesis, Department of Civil Engineering, McMaster University.
- Hanafy, E.A., and Emery, J.J. 1979. Advancing face simulation of tunnel excavations and lining placement. *Research Seminar on Tunnelling and Underground Construction*, Montreal, Quebec.
- Hanna, T.H. 1973. *Foundation Instrumentation*. Trans. Tech. Publications, Cleveland.
- Hansmire, W. 1975. Field measurements of ground displacements about a tunnel in soil. Ph.D. Thesis, University of Illinois at Urbana-Champaign.
- Hedley, D.G.F. 1969. Design criteria for multi-wire borehole extensometer systems. *First Canadian Symposium on Mining Surveying and Rock Deformation Measurements*.
- Hewett, B.H.M., and Johannesson, S. 1922. *Shield and compressed air tunneling*. McGraw Hill Book Company, New York.
- Hoeg, K. 1968. Stresses against underground structural cylinders. *Journal of Soil Mechanics and Foundation Division*, ASCE, Vol. 94, pp. 833-858.
- Hoyaux, B., and Ladanyi, B. 1970. Gravitational stress field around a tunnel in soft ground. *Canadian Geotechnical Journal*, Vol. 6, pp. 54-61.
- Hudson, J.A., Attewell, P.B., Atkinson, J.H., and O'Reilly, M.P. 1976. Understanding ground movements caused by tunnelling. *Ground Engineering*, Vol. 9, No. 3, pp. 47-50.
- Hughes, G.M. 1958. A study of Pleistocene Lake Edmonton and associated deposits. M.Sc. Thesis, Department of

Geology, University of Alberta, 58 p.

- Irish, E.J.W. 1970. The Edmonton Group of south central Alberta. *Bulletin of Canadian Petroleum Geology*, Vol. 18, pp. 125-155.
- Judd, W.R., and Perloff, W.H. 1971. Predicted and measured displacements for tunnels. *Symposium on Underground Rock Chambers*, ASCE, pp. 487-514.
- Kathol, C.P., and McPherson, R.A. 1975. Urban geology of Edmonton. *Alberta Research Council, Bulletin 32*. 61 p.
- Kuesel, T.R. 1972. Soft ground tunnels for BART project. *Proc. of the 1st North American Rapid Excavation and Tunneling Conf.*, Vol. 1, pp. 287-313.
- Kulhawy, F.H. 1974. Finite element modeling criteria for underground openings in rock. *International Journal of Rock Mechanics, Mining Sciences and Geomechanical Abstracts*, Vol. 11, pp. 465-472.
- Kulhawy, F.H. 1975. Stresses and displacements around openings in homogeneous rock. *International Journal of Rock Mechanics, Mining Sciences and Geomechanical Abstracts*, Vol. 12, pp. 43-57.
- Ladanyi, B. 1974. Use of long-term strength concept in the determination of ground pressure on tunnel linings. *Proc. of the 3rd Inter. Cong. on Rock Mechanics*, Vol. 2B, pp. 1150-1156.
- Litviniszyn, J. 1956. Application of the equation of stochastic processes to mechanics of loose bodies. *Arch. Mech. Stosow*, Vol. 8, pp. 393-411.
- Lombardi, G. 1970. The influence of rock characteristics on the stability of rock cavities. *Tunnels and Tunnelling*, Vol. 2, pp. 104-109.
- Lombardi, G. 1973. Dimensioning of tunnel linings with regards to constructional procedure. *Tunnels and Tunneling*, Vol. 5, pp. 340-351.
- Mahar, J.W., Parker, H.W., and Wuellner, W.W. 1975. Shotcrete practice in underground construction. Report to U.S. Department of Transportation, NTIS No. PB 248 765.
- Marsland, A. 1973. Instrumentation of flood defense banks along the River Thames. *Field Instrumentation in Geotechnical Engineering*, Butterworth and Co., London, pp. 287-303.

- Marsland, A., and Quarterman, R. 1974. Further development of multipoint magnetic extensometer for use in highly compressible ground. *Geotechnique*, Vol. 24, pp. 429-433.
- Mason, E.E. 1968. The function of shotcrete in support of lining of the Vancouver railway tunnel. Tunnel and Shaft Conference, University of Minnesota, Minnesota, U.S.A.
- Matheson, D.S. 1970. A tunnel roof failure in till. *Canadian Geotechnical Journal*, Vol. 7, pp. 313-317.
- Mathis, C. 1974. Tunnel design in the City of Edmonton. M.Sc. Thesis, Department of Civil Engineering, University of Alberta.
- May, R.W., and Thomson, S. 1978. The geology and geotechnical properties of till and related deposits in the Edmonton, Alberta, area. *Can. Geotech. J.*, Vol. 15, pp. 362-370.
- McBean, R.J., and Harries, D.A. 1970. The development of high-speed soft ground tunnelling pre-cast concrete segments and tunneling machines. *Proceedings of South African Conference on Tunnelling*, Johannesburg, Africa, pp. 129-134.
- Medeiros, L. 1979. Deep excavations in stiff soils. Ph.D. Thesis, Department of Civil Engineering, University of Alberta.
- Morgan, H.D. 1961. A contribution to the analysis of stress in a circular tunnel. *Geotechnique*, Vol. 11, pp. 37-46.
- Morgenstern, N.R. 1975. Stress-strain relations for soils in practice. General Report. *Proceedings of the 5th Panamerican Conference on Soil Mechanics and Foundation Engineering*, Buenos Aires, Argentina, Vol. iv, pp. 1-41.
- Morton, J.D., Dunbar, D.D., and Palmer, J.H.L. 1977. Use of a precast segmented concrete lining for a tunnel in soft clay. *Proc. of International Symposium on Soft Clay*, Bangkok, Thailand, pp. 587-598.
- Muir Wood, A.M. 1975. The circular tunnel in elastic ground. *Geotechnique*, Vol. 25, pp. 115-127.
- Norwegian Geotechnical Institute 1962. Vibrating-wire measuring devices used at strutted excavations. Technical Report No. 9, 151 p.
- Obert, L., and Duvall, W.I. 1967. *Rock mechanics and the design of structures in rock*. New York, John Wiley and Sons.

- O'Rourke, T.D., and Cording, E.J. 1974. The measurements of strut loads by means of vibrating-wire strain gages. Performance Monitoring for Geotechnical Construction, ASTM Special Technical Publication 584, American Society for Testing and Materials, pp. 58-77.
- Oster, R.T. 1975. Construction of storm tunnel in Edmonton. A summary report. Tunnels and Declines, Report No. DS-75.9, Canada Center of Mineral and Energy Technology, pp. 17-43.
- Oster, R.T. 1978. Personal Communication.
- Pacher, F. 1964. Measurements of deformation in a test gallery as a means of investigating the behaviour of the rock mass and of specifying lining requirements. Rock Mechanics and Engineering Geology, Supplement I, pp. 149-161.
- Peck, R.B. 1969. Deep excavations and tunneling in soft ground. Proc. of the 7th Inter. Conf. on Soil Mechanics and Foundation Engineering, State-of-the-Art Volume, Mexico City, Mexico, pp. 225-290.
- Peck, R.B., Deere, D.U., Monsees, J.E., and Parker, H.W. 1969. Some design considerations in the selection of underground support system. Report for U.S. Department of Transportation NTIS No. PB 190 443.
- Peck, R.B., Hendron, A.J., and Mohraz, B. 1972. State of the art of soft-ground tunneling. Proceedings of the 1st North American Rapid Excavation and Tunneling Conference, Vol. 1, pp. 259-286.
- Rabcewicz, L.V. 1964, 1965. The New Austrian Tunneling Method. Water Power, Vol. 16: pp. 453-457 and pp. 511-515, Vol. 17: pp. 19-24.
- Ranken, R.E., and Ghaboussi, J. 1975. Tunnel design considerations: Analysis of stresses and deformations around advancing tunnels. Report prepared for U.S. Department of Transportation, UILU-ENG75-2016.
- Ryzuk, C.N. 1977. Details of multipoint extensometers used to monitor deformation in a tunnel in oil sands. Memorandum to Dr. N.R. Morgenstern.
- Sakurai, S. 1978. Approximate time-dependent analysis of tunnel support structure considering progress of tunnel face. International Journal for Numerical and Analytical Methods in Geomechanics, Vol. 2, pp. 159-175.
- Sampson, R.J. 1978. Surface II graphics system. Series on Spatial Analysis, Kansas Geological Survey, Second

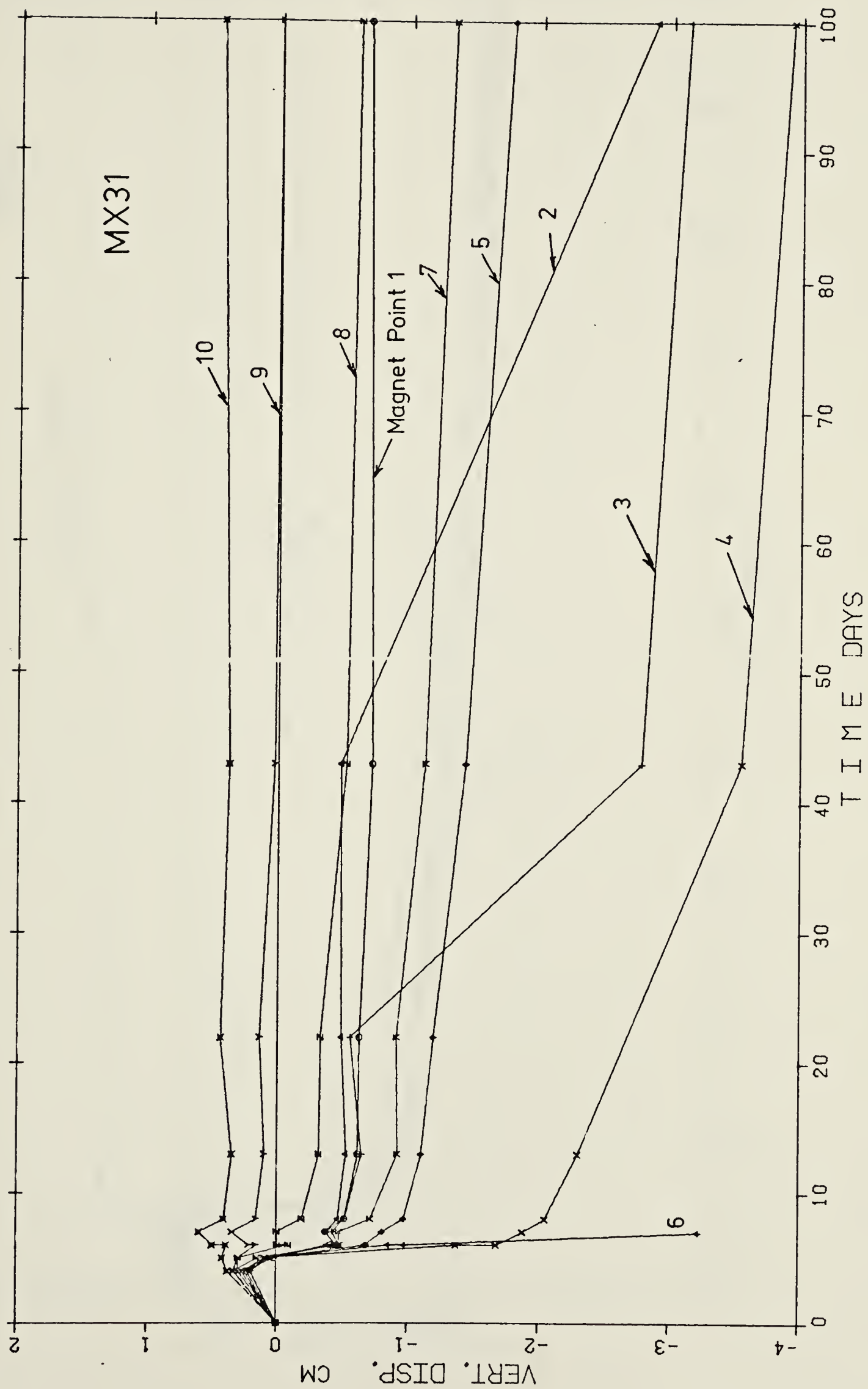
Edition, 240 p.

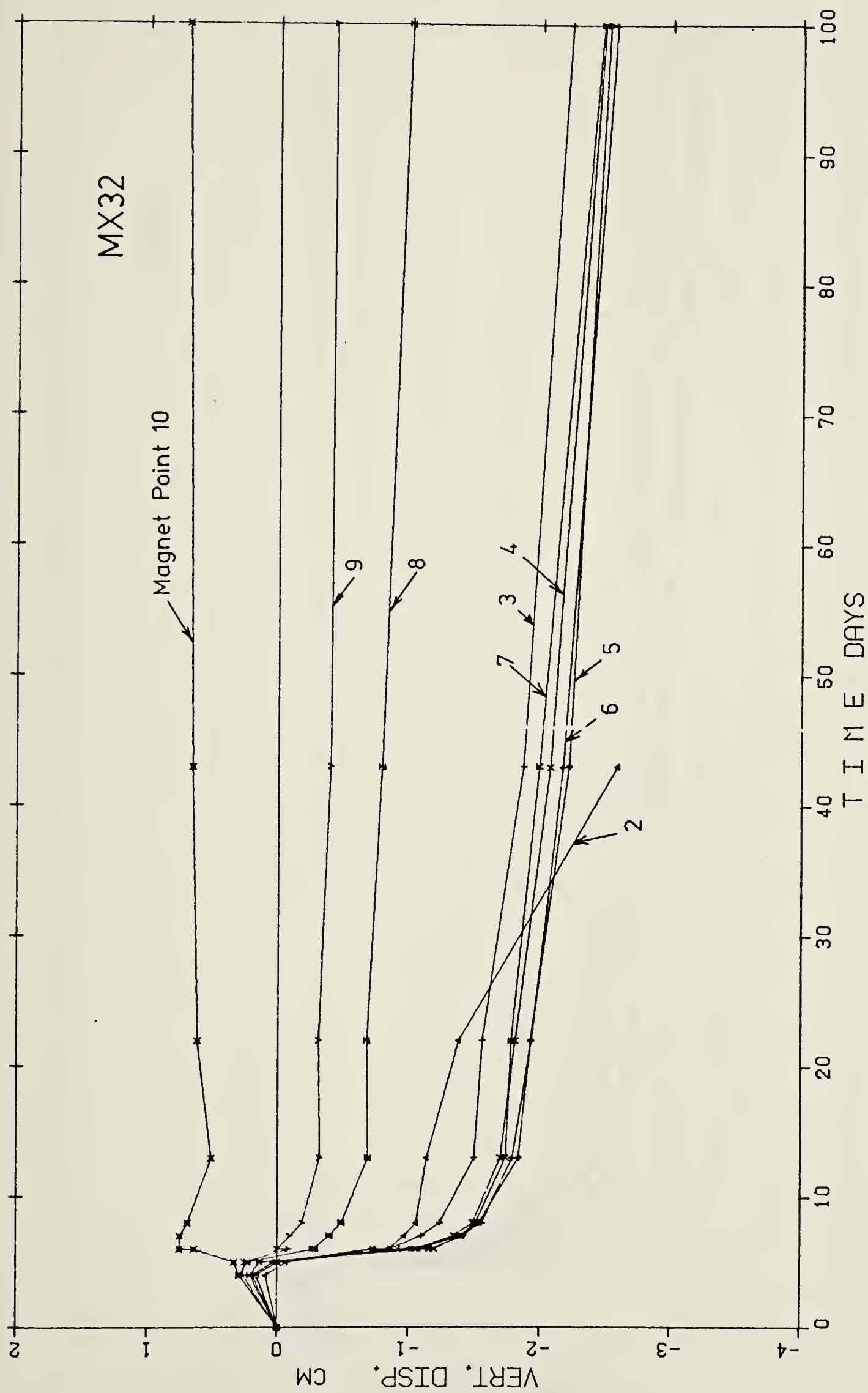
- Savigny, K.W. 1980. In situ analysis of naturally occurring creep in ice-rich permafrost soil. Ph.D. Thesis, Department of Civil Engineering, University of Alberta.
- Schmidt, B. 1969. Settlement and ground movement associated with tunnelling in soil. Ph.D. Thesis, Department of Civil Engineering, University of Illinois, Urbana.
- Schmidt, B., and Dunnicliff, C.J. 1974. Construction monitoring of soft ground rapid transit tunnels. Volume I: A definition of needs and potential developments. Report prepared for Transportation Systems Center, NTIS No. PB 241 536.
- Shannon, W.L., and Strazer, R.J. 1968. Shoring for Seattle first National Bank building, Seattle, Washington, ASCE annual meeting on Structural Engineering, Pittsburgh.
- Skempton, A.W. 1943. Discussion on: Tunnel linings, with special reference to a new form of reinforced concrete lining. Institution of Civil Engineers Proceedings, London, England, Vol. 20, No. 5, pp. 29-64.
- Slope Indicator Company 1978. Personal Communications.
- Smith, P.D.K., and Burland, J.B. 1976. Performance of a high precision multipoint borehole extensometer in soft rock. Canadian Geotechnical Journal, Vol. 13, pp. 172-176.
- Solinst 1975. Instrumentation for Soils and Rocks. Solinst Canada Ltd., Burlington, Ontario.
- Swoboda, G. 1979. Finite element analysis of the new Austrian tunneling method (NATM). Third International Conference on Numerical Methods in Geomechanics, Aachen, Vol. 2, pp. 581-586.
- Szechy, K. 1966. Art of Tunnelling. Translated from Hungarian, Published by Akademiai Kiado Budapest.
- Tattersall, F., Wakeling, T.R., and Ward, W.H. 1955. Investigations into the design of pressure tunnels in London clay. Institution of Civil Engineers Proceedings, London, England, Vol. 4, pp. 400-471.
- Thomas, H.S.H. 1965. The measurement of strains in tunnel linings using the vibrating-wire technique. Conference on Strain Measurement in Difficult Environments.
- Thomson, S., and El-Nahhas, F. 1980. Field measurements in two tunnels in Edmonton, Alberta. Can. Geotech. J., Vol. 17, pp. 20-33.

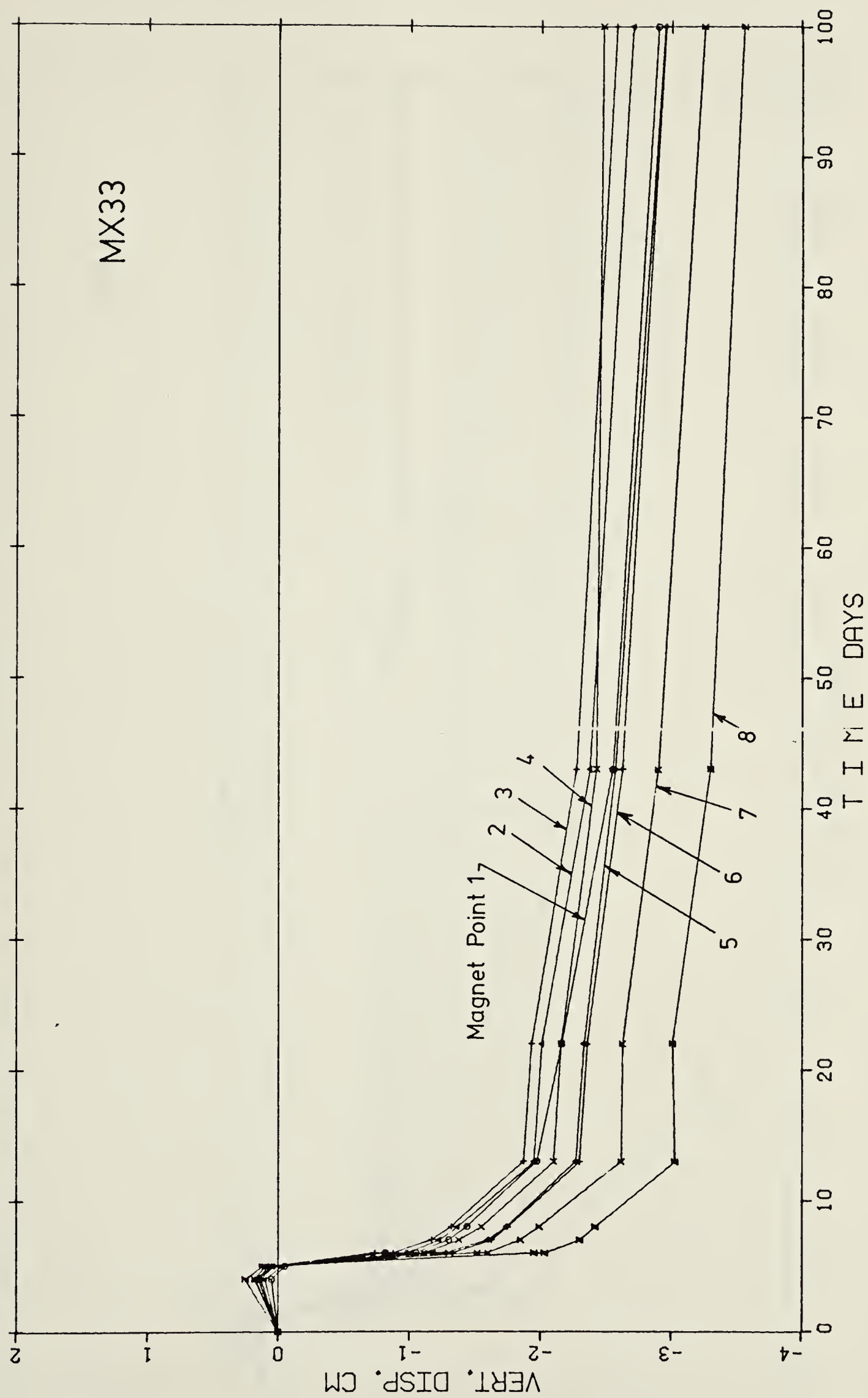
- Terzaghi, K. 1955. Evaluation of coefficients of subgrade reaction, *Geotechnique*, Vol. 3, pp. 57-90.
- Tilp, P.J., and Schoeman, K.D. 1977. Precast concrete liners. *Civil Engineering*, ASCE, November, pp. 54-56.
- Wanninger, R. 1979. New Austrian tunnelling method and finite elements. *Third International Conference on Numerical Methods in Geomechanics*, Aachen, Vol. 2, pp. 587-597.
- Ward, W.H. 1978. Ground supports for tunnels in weak rocks. 18th Rankine lecture, *Geotechnique*, Vol. 28, pp. 133-171.
- Ward, W.H., and Thomas, H.S.H. 1965. The development of earth loading and deformation in tunnel linings in London clay. *6th International Conference on Soil Mechanics and Foundation Engineering*, Vol. 2, pp. 432-436.
- Westgate, J.A. 1969. The Quaternary geology of the Edmonton area, Alberta. In *Pedology and Quaternary research*. Edited by S. Pawluk. University of Alberta Printing Department, Edmonton, Alberta, pp. 129-151.
- Westgate, J.A., and Bayrock, L.A. 1964. Preiglacial structures in the Saskatchewan gravels and sands of central Alberta, Canada. *J. Geol.*, Vol. 72, pp. 641-648.
- Wissmann, W. 1968. Zur statischen berechnung beliebig geformter stollen und tunnelauskleidungen mit hilfe von stabwerkprogrammen. *Der Bauingenieur*, Vol. 43, Heft 1, pp. 1-8.
- Zienkiewicz, O.C. 1971. *The finite element method in Engineering Science*. McGraw-Hill, New York.

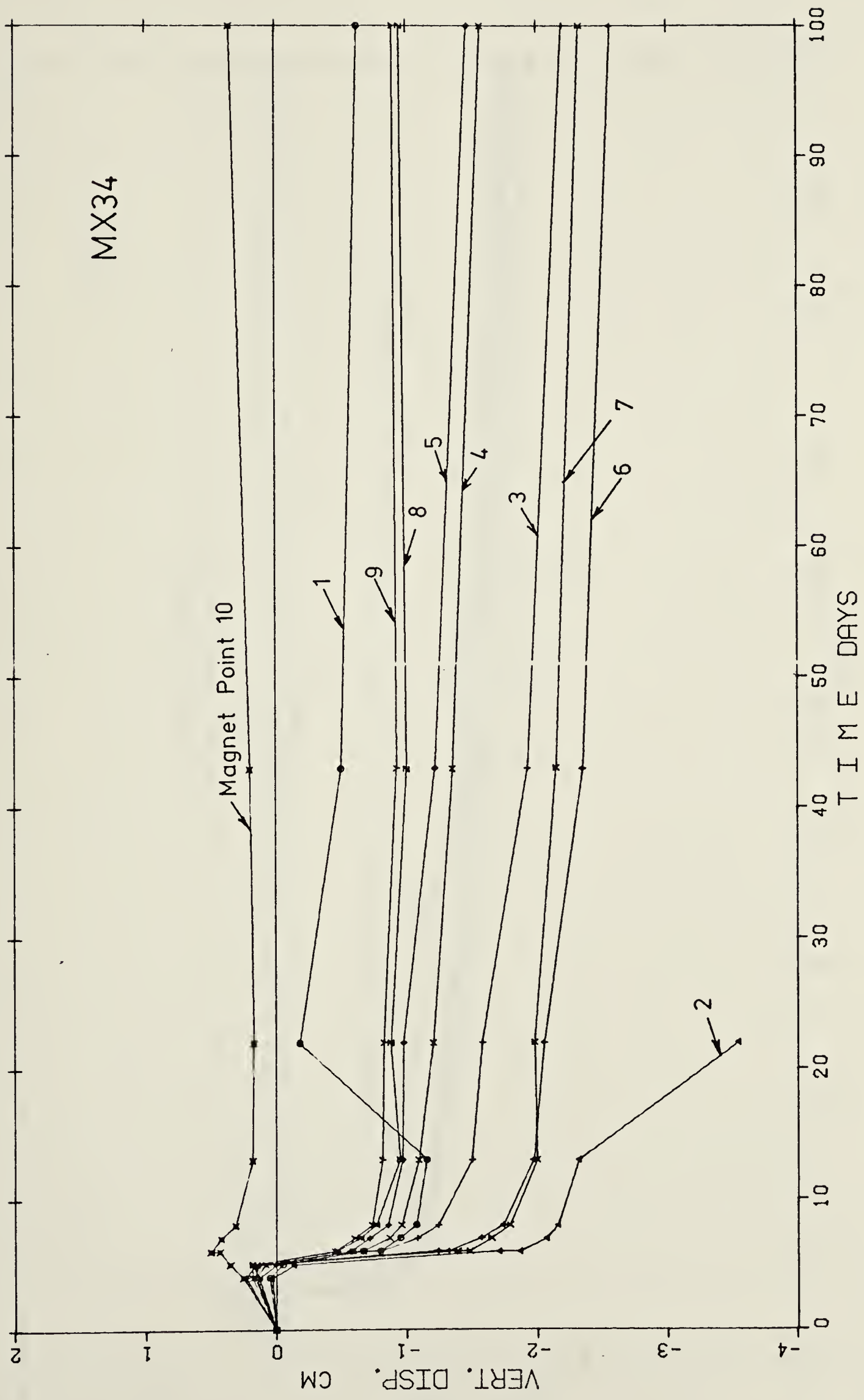
APPENDIX A

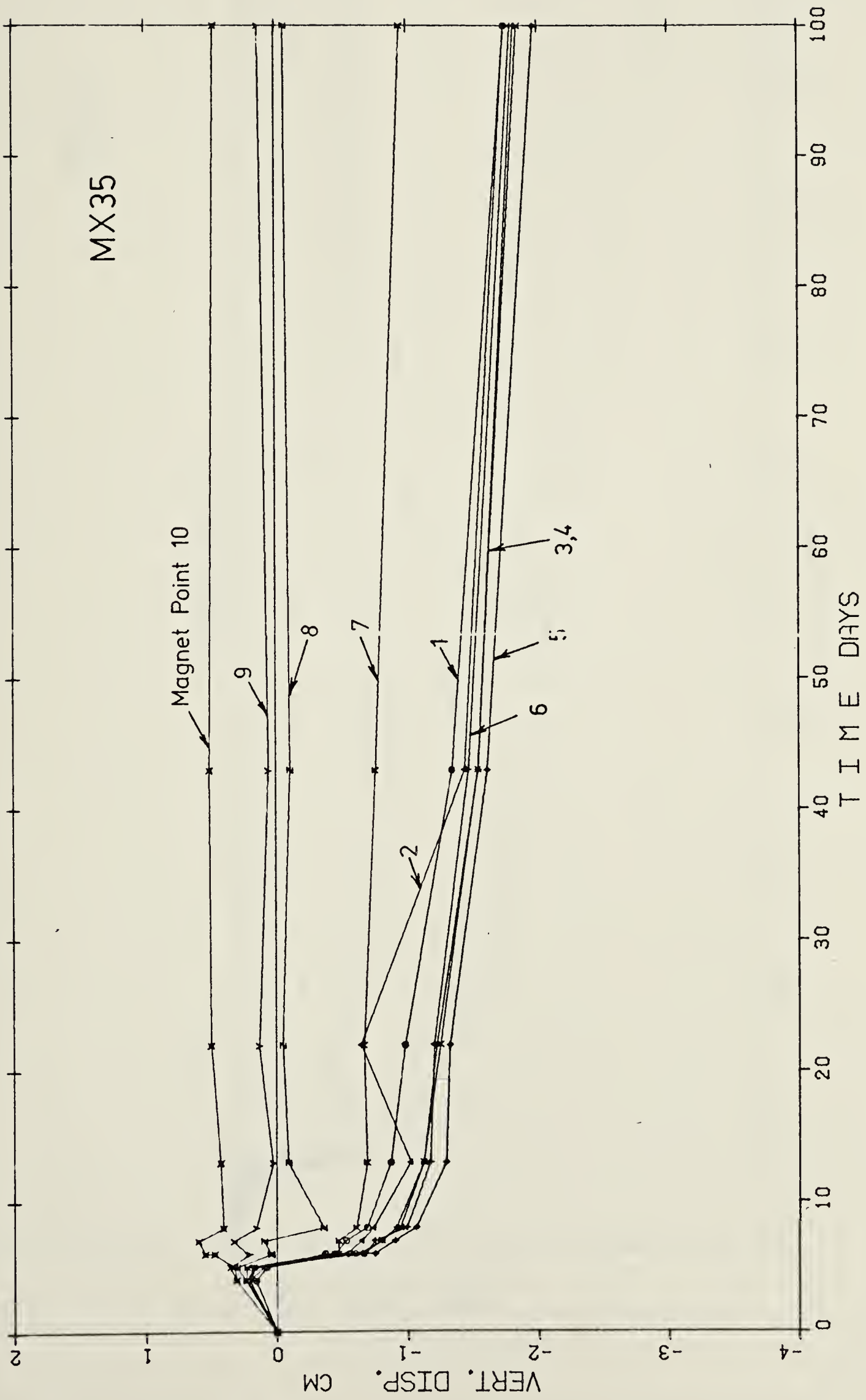
Multipoint Extensometer Measurements of Test Section 3

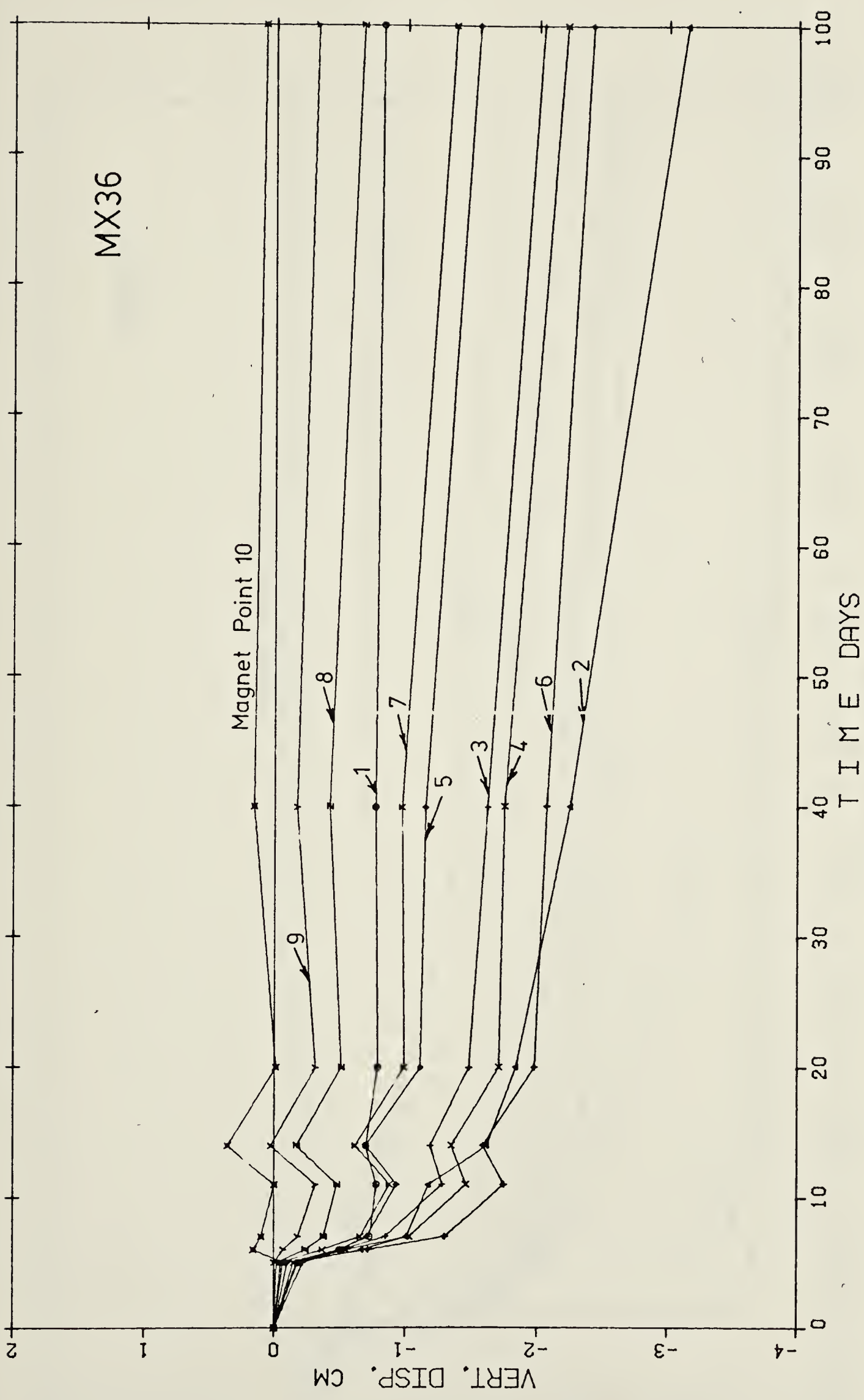


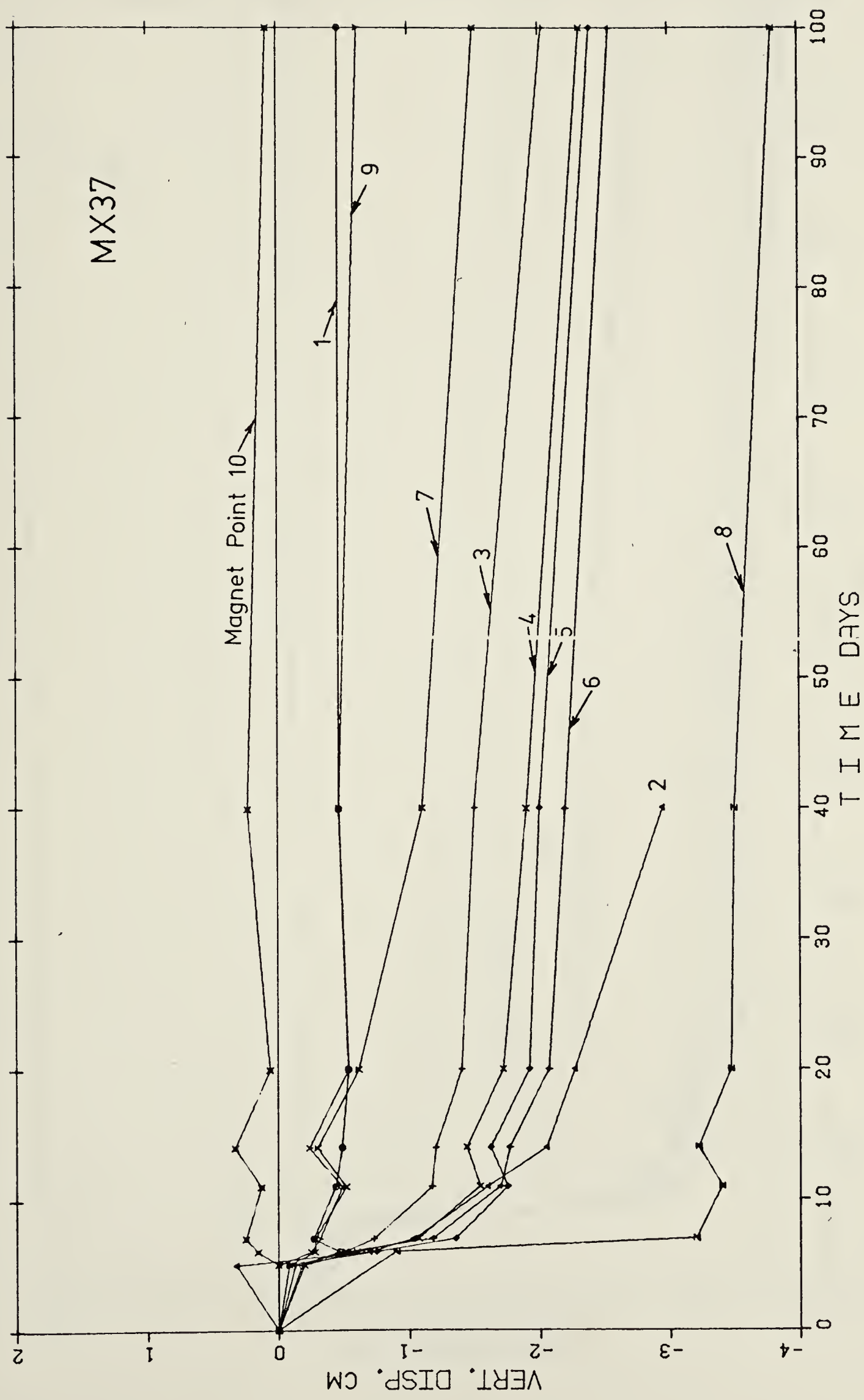


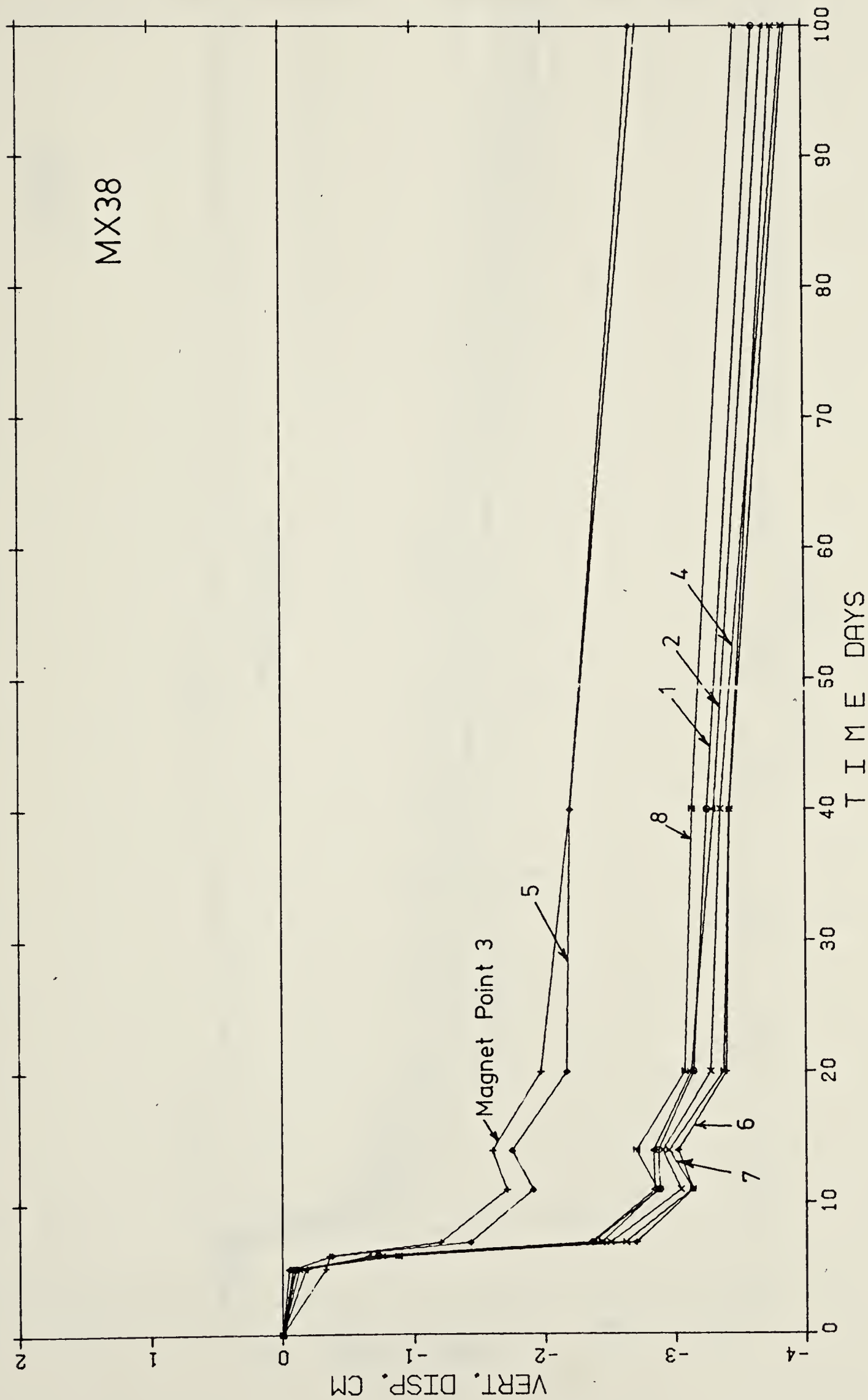


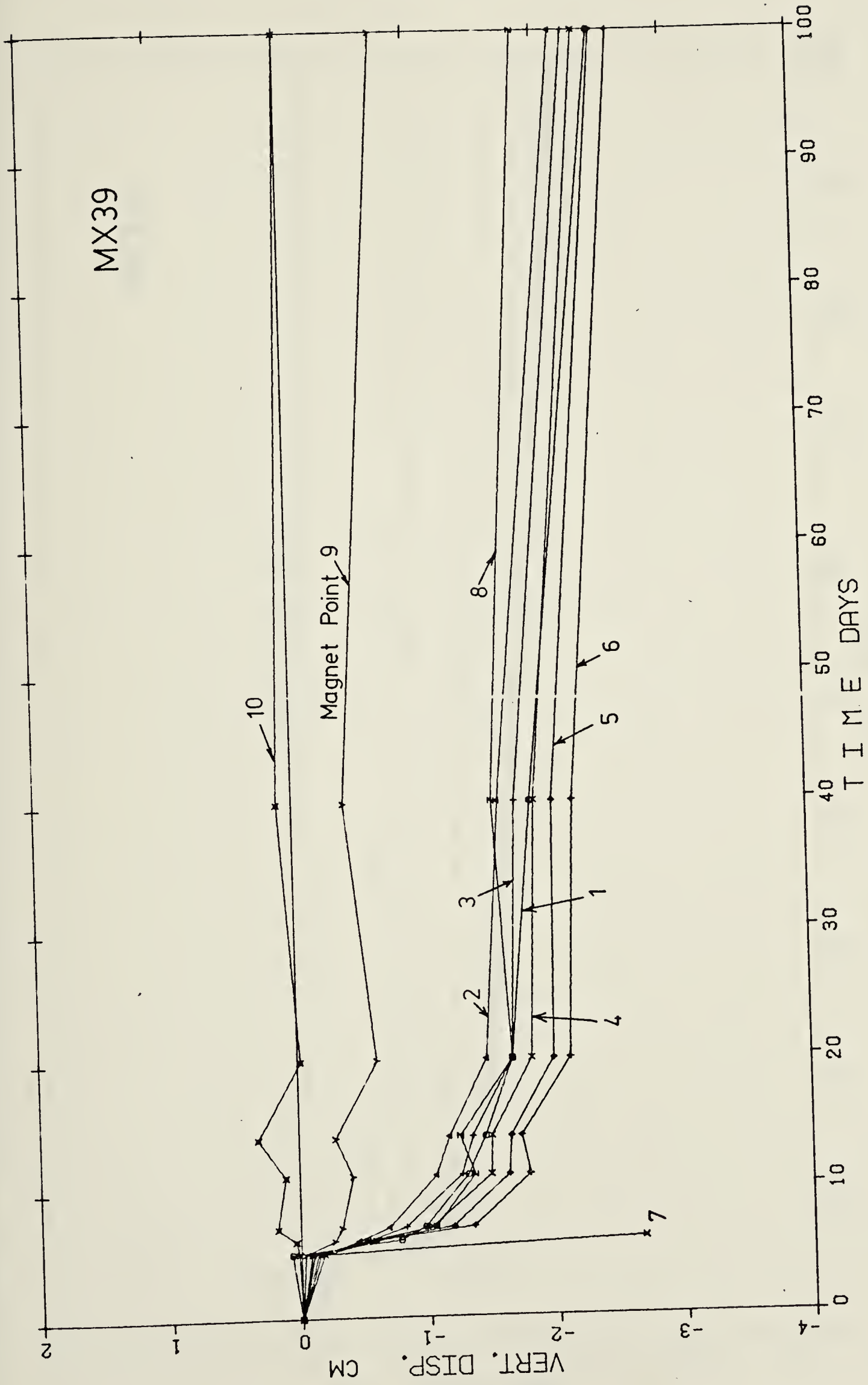


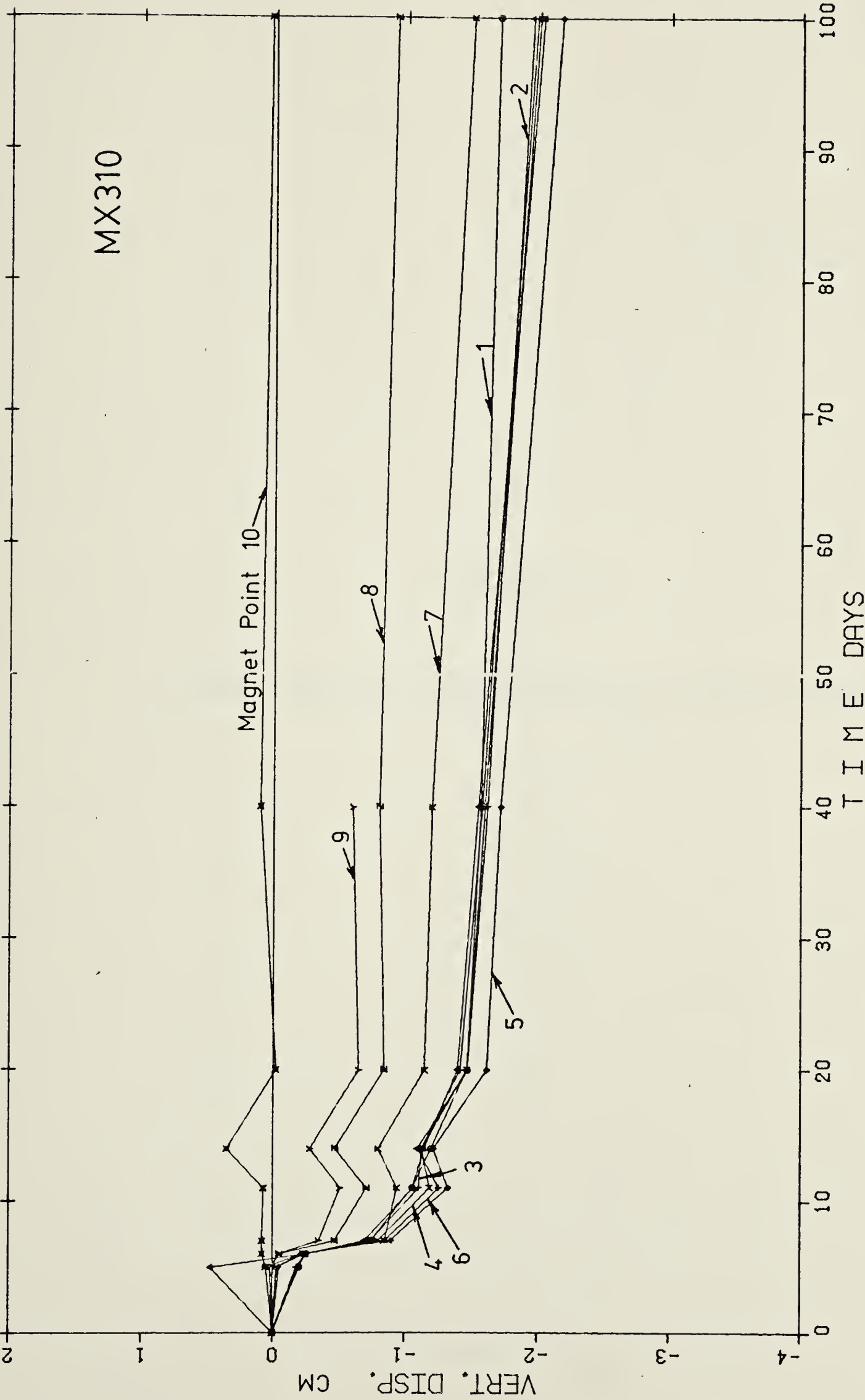






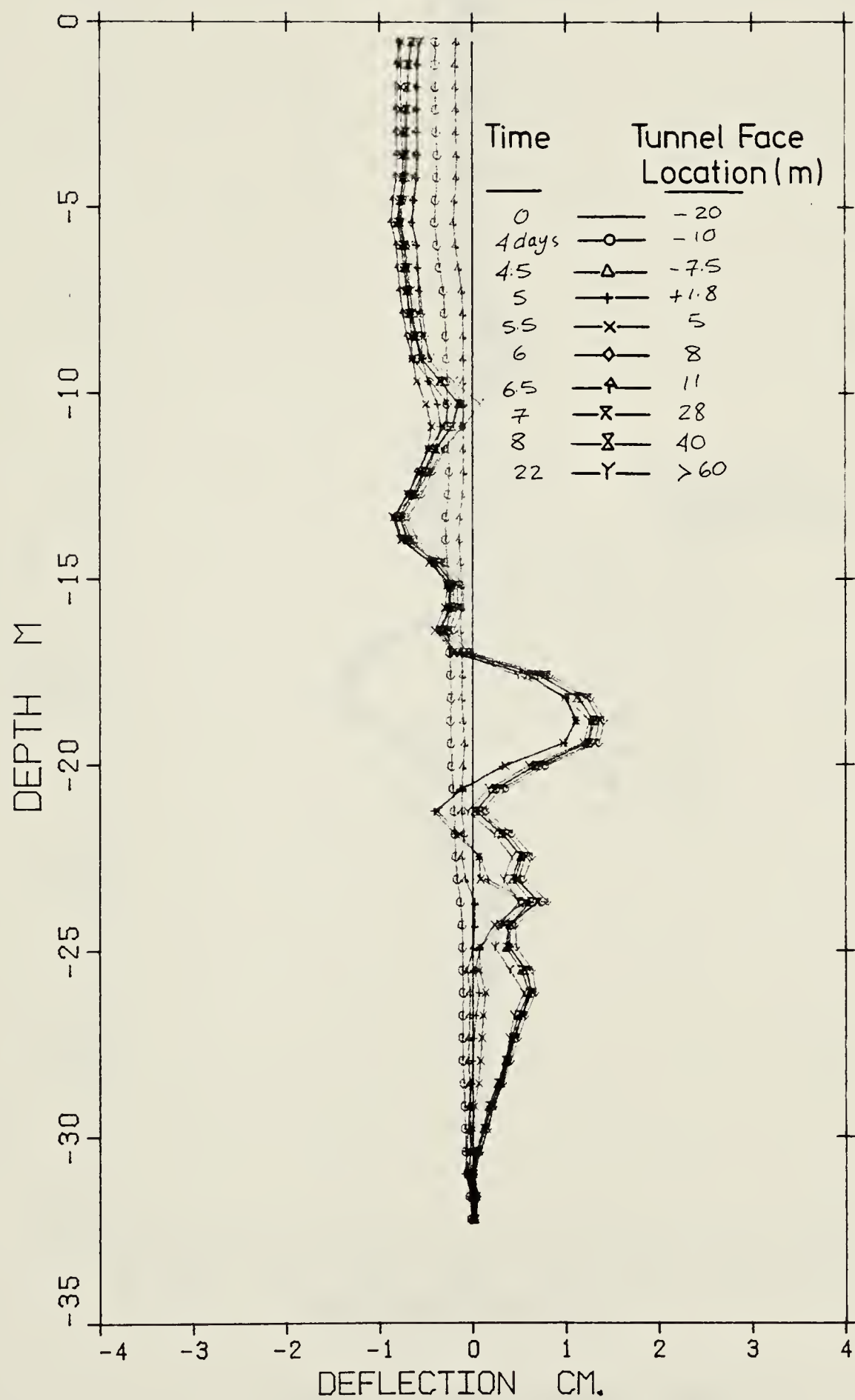


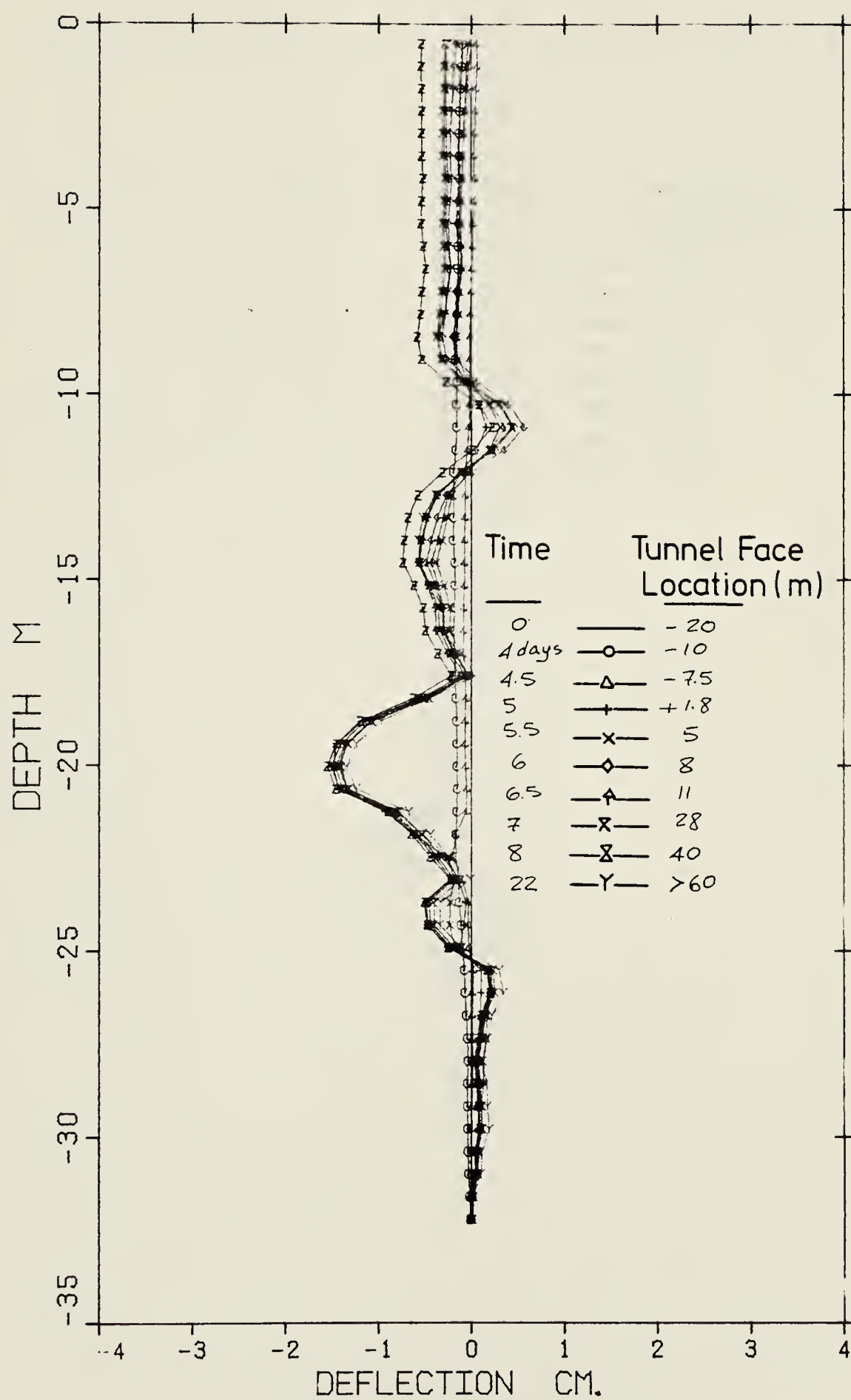




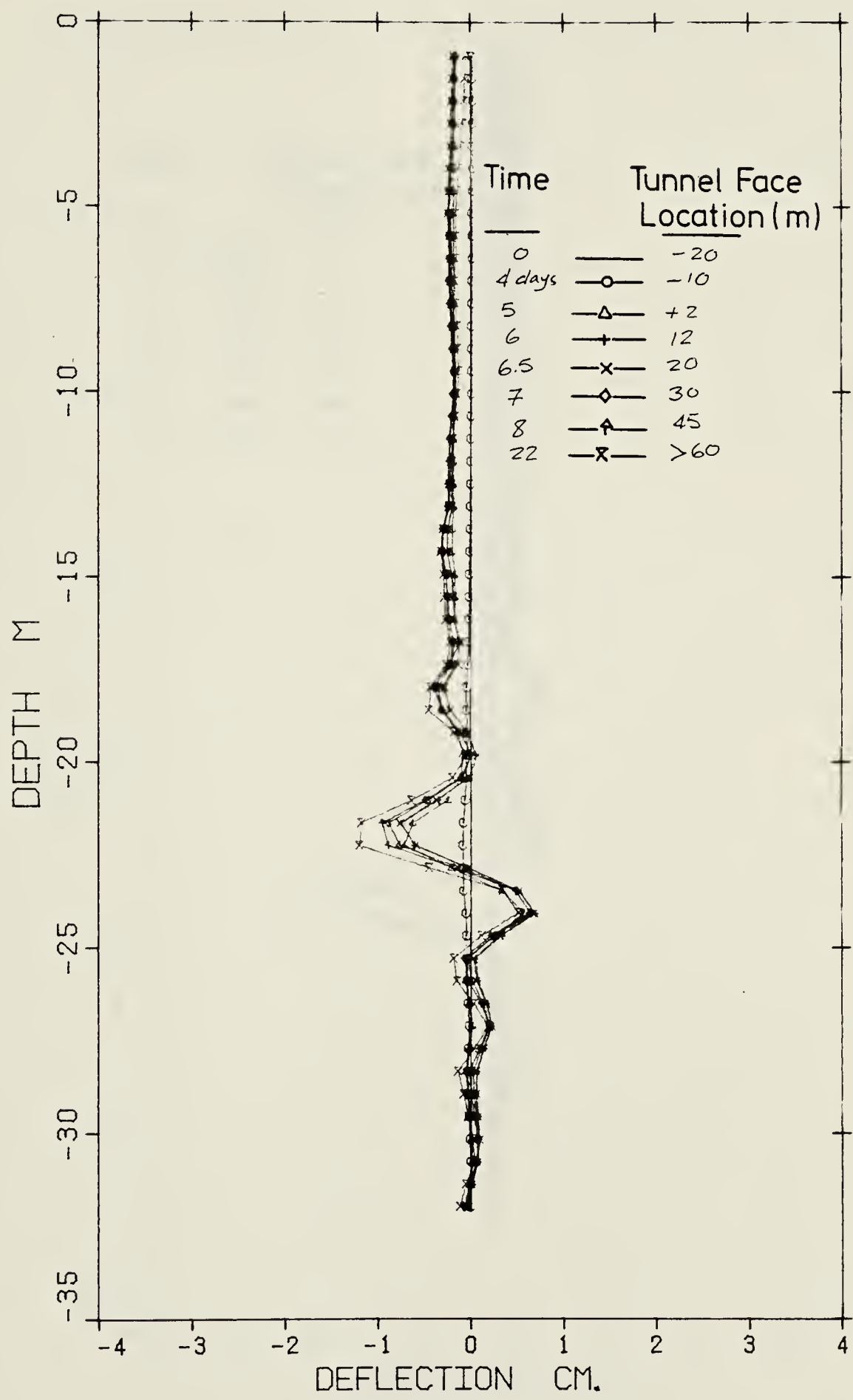
APPENDIX B

Slope Indicator Measurements at Test Section 3

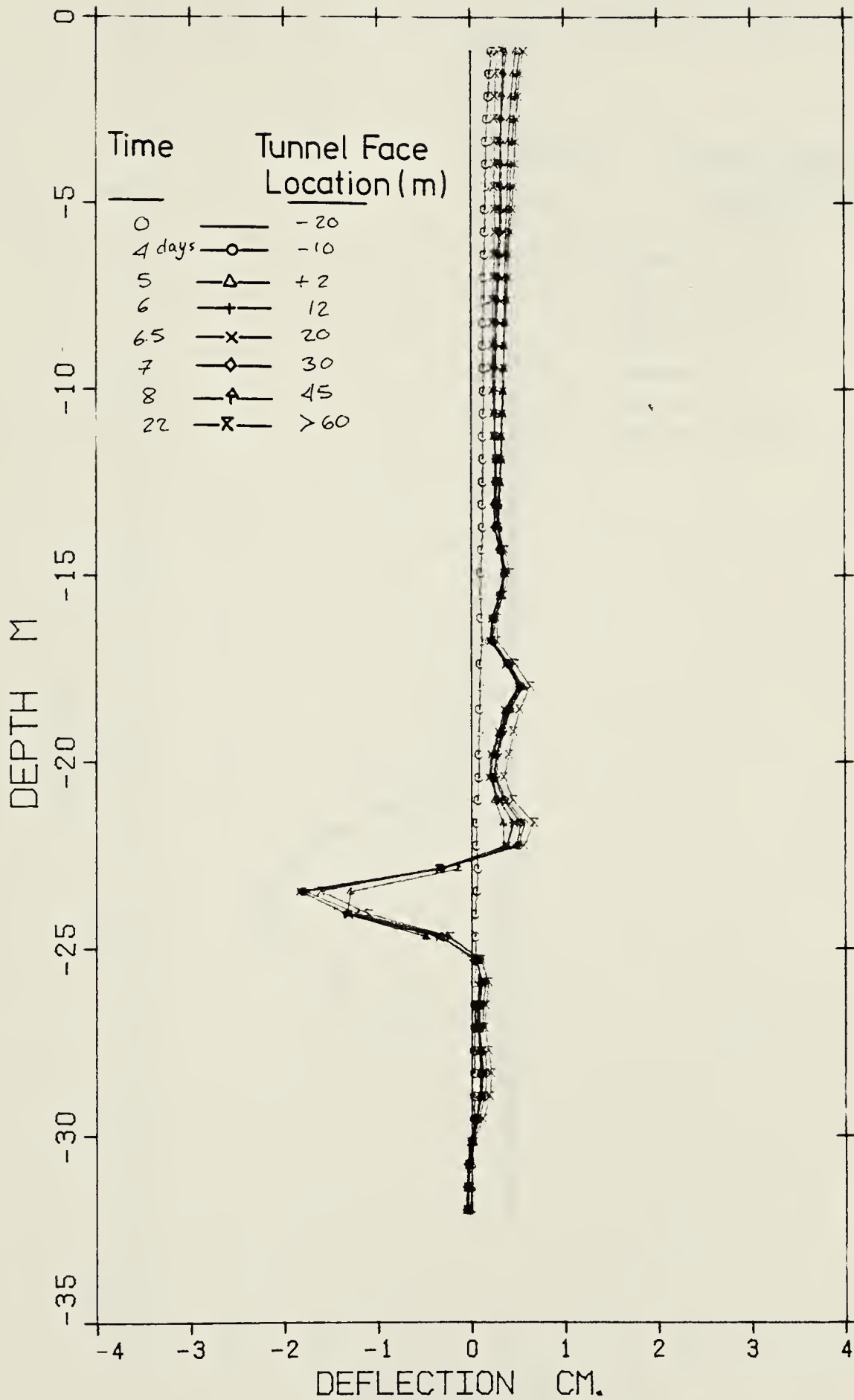




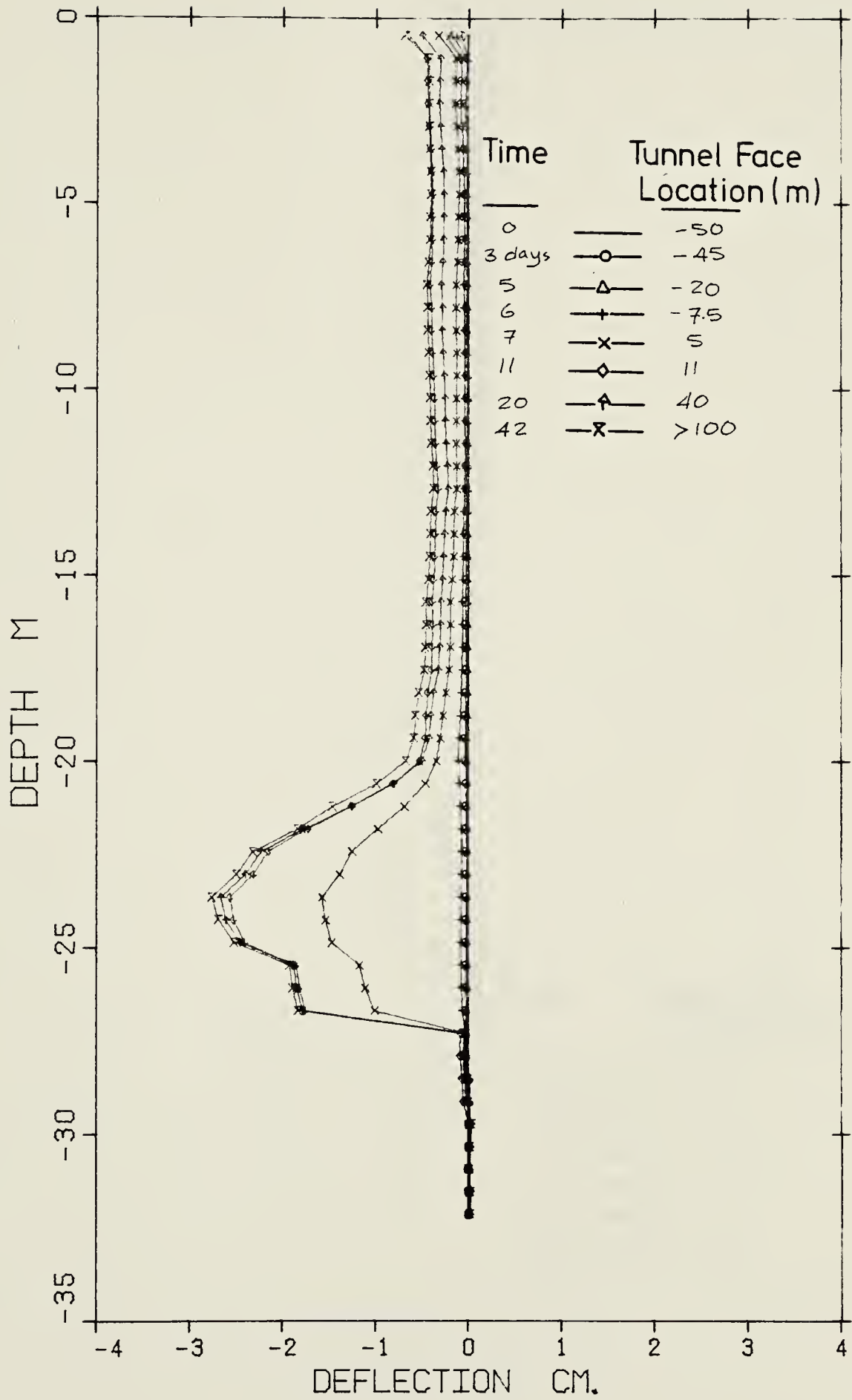
SLOPE INDICATOR #3-1B



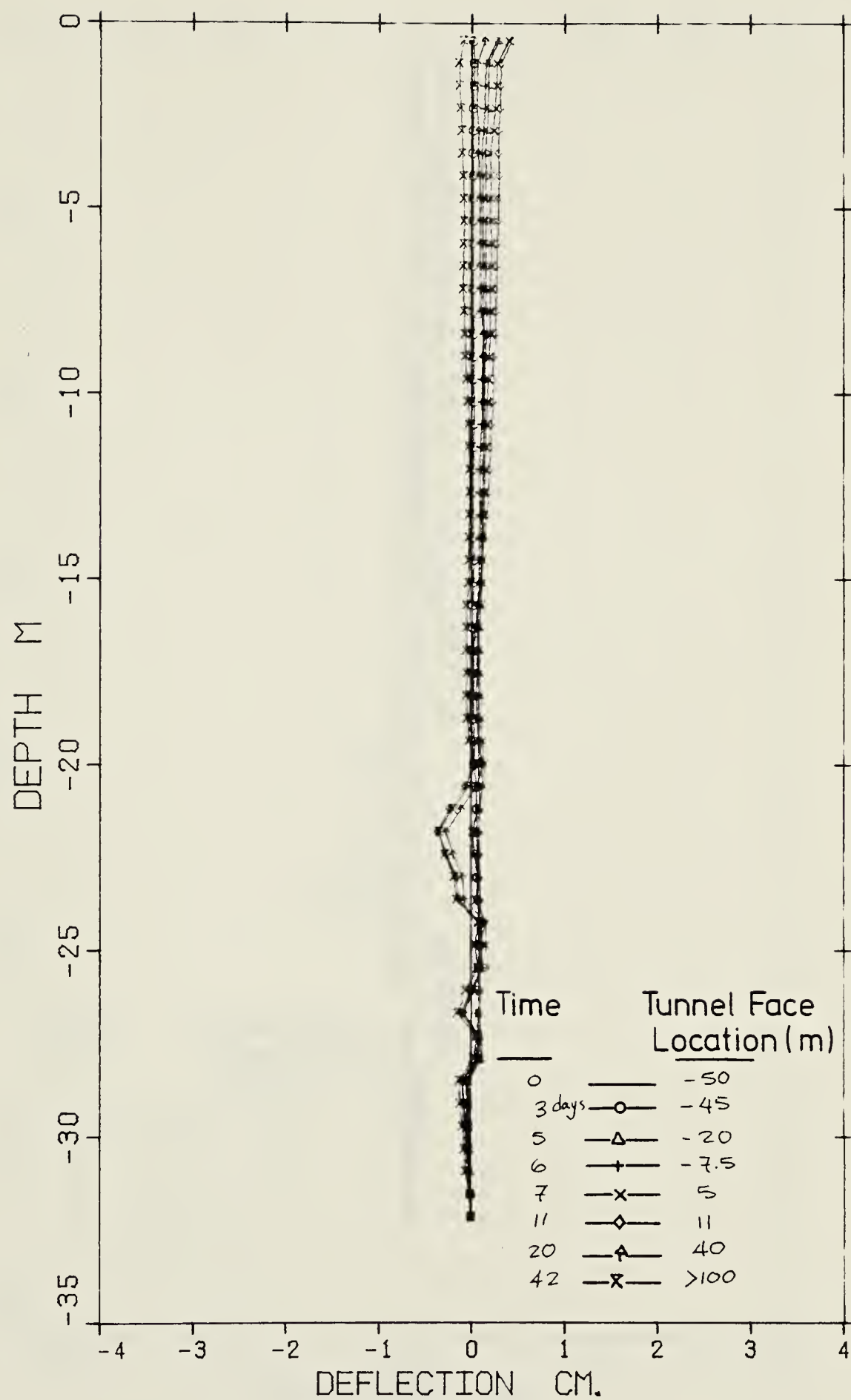
SLOPE INDICATOR #3-2A



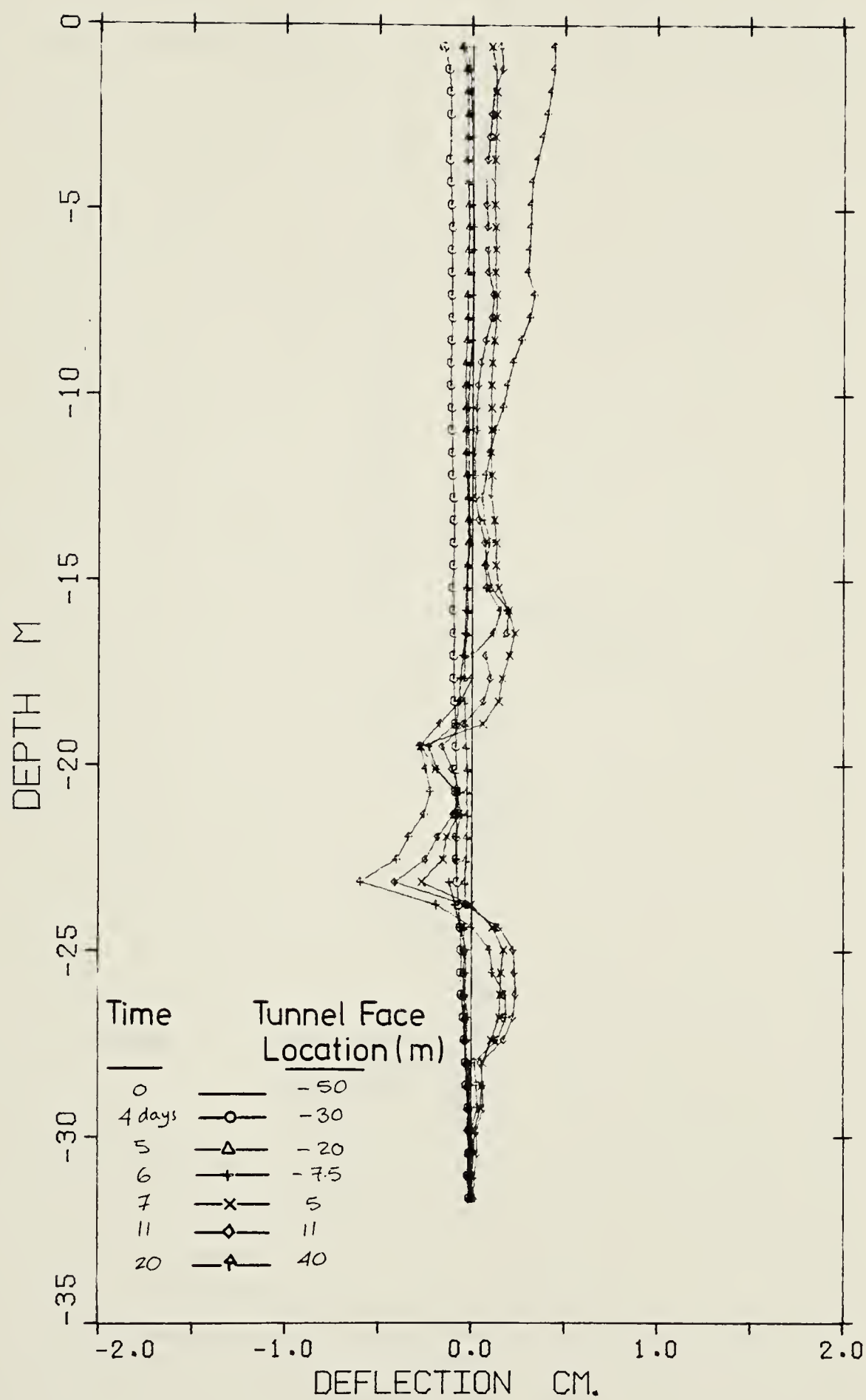
SLOPE INDICATOR #3-2B



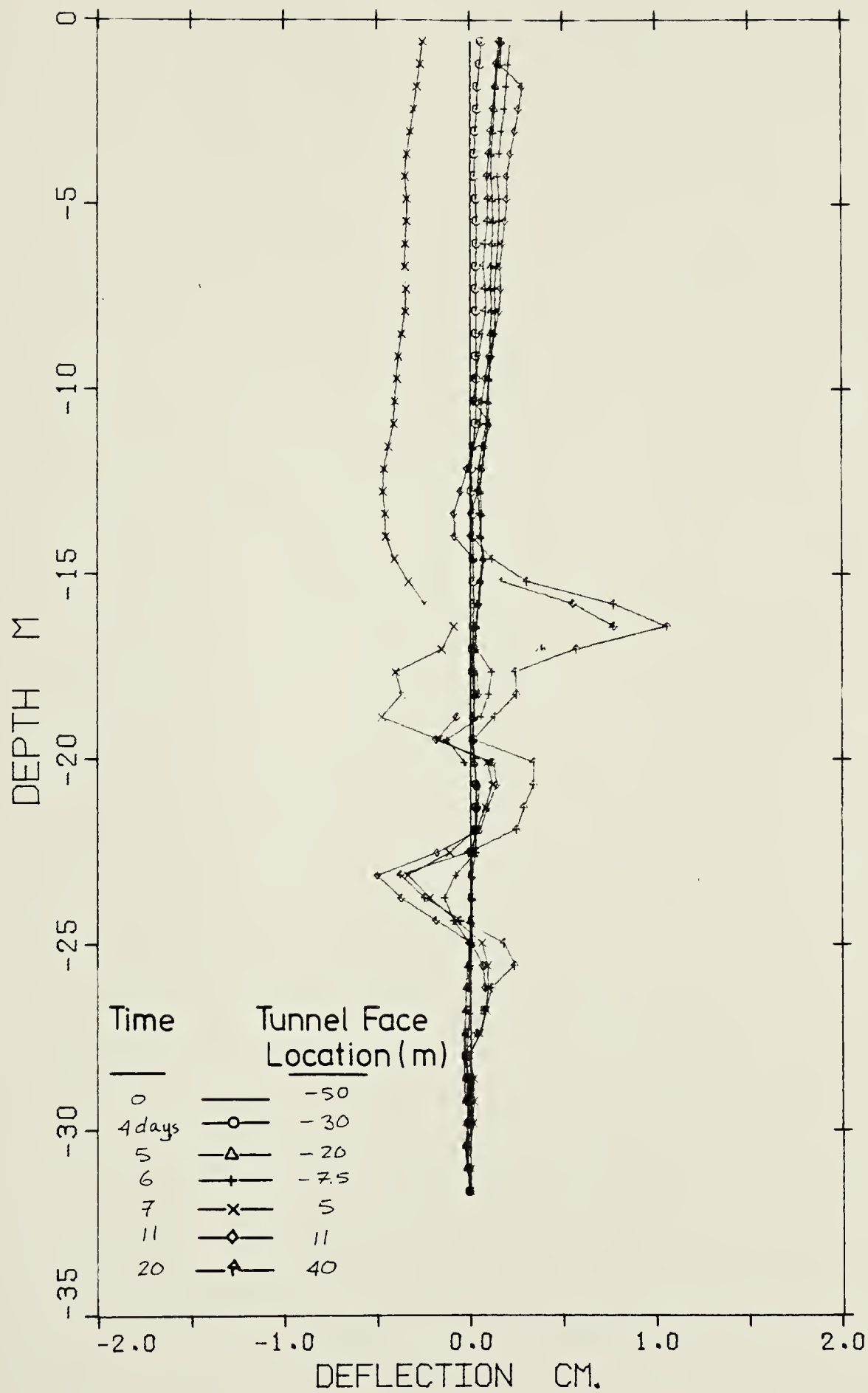
SLOPE INDICATOR #3-3A



SLOPE INDICATOR #3-3B



SLOPE INDICATOR #3-4A



SLOPE INDICATOR #3-4B

B30307